Understanding the combined effects of spruce beetle outbreaks and climate change on Rocky Mountains vegetation through ecological modeling

Adrianna C. Foster
Charlottesville, VA

Environmental Sciences B.A., University of Virginia, 2012

A Dissertation presented to the Graduate Faculty
of the University of Virginia in Candidacy for the Degree of
Doctor of Philosophy

Department of Environmental Sciences

University of Virginia
August, 2016

_____

_____

_____

_____

Abstract

Mean annual temperatures in the western United States have increased in the last few decades, and during the 21st century, it is predicted that this warming trend will continue. In the subalpine zone of the Rocky Mountains, this warming is also predicted to increase the frequency and severity of spruce beetle outbreaks. Climate change itself may also affect vegetation within the Rocky Mountains, potentially leading to shifts in species compositions. These forests are a crucial part of the US's carbon budget, thus it is important to analyze how climate change and bark beetles in conjunction will affect the biomass and species composition of vegetation in the subalpine zone. UVAFME is an individual-based gap model that simulates the biomass and species composition of a forested landscape through time. UVAFME is first calibrated and parameterized to the southern Rocky Mountain landscape using data on species composition, climate, and site conditions. Species-specific parameter inputs for the 11 major Rocky Mountain species are derived from the scientific literature. The model is then quantitatively and qualitatively validated at two Rocky Mountain sites in Wyoming and Colorado. Results show that UVAFME accurately simulates the vegetation dynamics along an elevation gradient. UVAFME output on size structure (stems ha^{-1} size $class^{-1}$) and species-specific biomass (tonnes C ha^{-1}) is comparable to forest inventory data at those locations. A climate sensitivity test is performed in which temperature is first increased linearly by 2°C over 100 years, stabilized for 200 years, cooled back to present climate values over 100 years, and again stabilized for 200 years. This test was conducted to determine what effect elevated temperatures may have on vegetation zonation, and how lasting the changes may be. Results show that elevated temperatures within the southern Rocky Mountains may lead to persistent decreases in biomass and changes in forest composition as species migrate upslope. Without the effect of disturbances,

long-term output from the subalpine zone at the southern WY site shows periodic behavior between Engelmann spruce and subalpine fir, indicating that periodicities in forested ecosystems may be more common than previously thought. UVAFME is then updated with a spruce beetle subroutine created for this study that calculates the probability for beetle infestation of each tree on a plot. This probability is based on site characteristics, such as mean spruce size and plot-level basal area; climate factors, such as temperature; and individual tree characteristics, such as tree size, stress level, and proximity to other infested trees. To determine the net effect of both climate and beetle infestation on subalpine vegetation, UVAFME is then run with multiple scenarios that combine beetle infestation with current or altered climate at sites across the Wyoming and Colorado Rocky Mountains. Climate change projections are from the NCAR Community Earth System Model output for the A1B and A2 IPCC scenarios. These results are compared among the different scenarios. Output from these tests show that the combination of spruce beetle infestations and increasing temperatures will cause a greater loss of Engelmann spruce biomass than either climate change or beetle infestation alone. The combination of spruce beetles and climate change additionally results in a further increase in the dominance of lower-elevation species, such as lodgepole pine, ponderosa pine, and Douglas-fir. These results are an important step in understanding the possible futures for the vegetation of the subalpine zone in the Rocky Mountains.

Table of Contents

List of Figures

List of Tables

Acknowledgements

This project started as a collaboration with Jose Negron at the US Forest Service. I am extremely grateful for his help and advice throughout this process, including opening his home to me on stays in Ft. Collins, giving transport and field expertise during forays across Wyoming and Colorado, and providing inventory data and valuable contacts at Colorado State and the USFS Rocky Mountain Research Station. I am also grateful to Kate Dwire and Paula Fornwalt at the US Forest Service, and Jason Sibold at Colorado State University for valuable inventory data used in Chapter 3 of this work. I would also like to thank Jonathan Walter, who originally put me in contact with Jose and Jason, thus providing the impetus for this project. I am also very grateful for the advice and expertise given by Katherine Holcomb at UVA's Advanced Research Computing Services (ARCS), without whom I may very well still be trapped in an infinite loop of Fortran coding issues.

I would like to especially thank Jacquelyn Shuman for her continual guidance and mentoring throughout my graduate career. I am deeply indebted to Jackie for her advice regarding model testing and application, manuscript and proposal writing, and how to succeed in graduate school and the Great Beyond of my future career. She additionally provided incredibly valuable contacts for future collaborations as well as general encouragement and words of wisdom. I owe a great deal of my current and future successes to her support.

I would not have been able to complete this project without the unflagging support of my partner Nicholas Vercruysse. Whether it was a forum for bouncing ideas around at 2am, a shoulder to cry on after seemingly countless failures and rejections, or a willingness to read and/or listen to my papers and presentations countless times, Nich has been a pillar of

dependability in the rough waters of graduate school. I would also like to thank my parents David and Catherine Foster, who have always supported and encouraged me in my endeavors.

I am particularly grateful to my advisor Herman H. Shugart for invaluable support and motivation. Hank's funding and the collaborative and constructive environment he provided with his lab allowed for great professional development and success during my time as his graduate student. I would also like to thank Robert Smith for help with figure preparation in Chapter 4. I am also thankful to Atticus Stovall and Ksenia Brazhnik in the Shugart Lab, and to my committee Howard Epstein, Paolo D'Odorico, and Barry Condron of the University of Virginia for their support and guidance. This work was funded by the University of Virginia and grants from the VA Space Grant Consortium Graduate Fellowship (project title "Understanding spruce beetle outbreak dynamics and their response to climate change through remote sensing and ecological modeling") and the National Fish and Wildlife Foundation (grant number: 0106.12.032847).

Chapter 1. Introduction

Disturbances such as insect outbreaks are integral in shaping the structure and composition of forested landscapes. These outbreaks are capable of causing widespread tree mortality (Veblen et al. 1991). Subsequent changes in species dominance and composition, forest structure, and biogeochemical processes interact to affect the forest at multiple temporal and spatial scales (Ludwig et al. 1978, Delcourt et al. 1982, Holling 1992, Shugart and Woodward 2011) (Fig.1.1). At the micro-scale (on the order of centimeters and days), individual trees respond to insect outbreaks through various defense mechanisms (Raffa et al. 2008). At the meso-scale (on the order of kilometers and years), whole stands of trees may be affected and even killed by these insect outbreaks, causing reduction in photosynthesis and transpiration, increases in decomposition of leaf litter, and alteration of the energy budget of these stands (Holling 1992, Edburg et al. 2012). At the macro-scale (on the order of several hundred kilometers and several centuries), post-outbreak tree regrowth proceeds, causing shifts in species dominance as subdominant, non-host trees are able to increase growth rate following mortality of host trees (Shugart 1984, Veblen et al. 1991) (Fig. 1.2). The success of insect outbreaks may also be scale-dependent. While local environmental factors may affect small patches of insects and

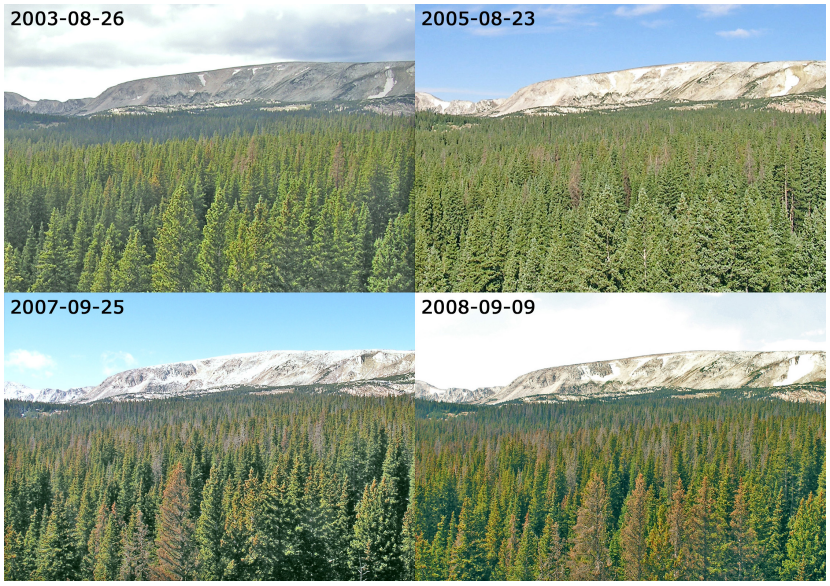

Figure 1.1. Progression of a spruce beetle outbreak in southern Wyoming. Infestation levels go from single trees, to whole stands, to much of the landscape. Photo credit: John Frank 2013.

their ability to infest host trees, landscape-scale changes in climate or vegetation will affect whether or not widespread outbreaks progress (DeRose and Long 2012).

Climate and vegetation also interact across several spatial and temporal scales. The terrestrial biota is able to mediate and even control variability in climate over small to moderate time and space scales (Holling 1992). This mediation may come in the form of stomatal closure during drought conditions or differential allocation to above- and belowground tissues to manage resource limitation (Katul et al. 2012). Over longer time and space scales, climate change may cause shifts in the species composition of a landscape as species migrate into their optimal climate zones (Shugart and Woodward 2011). These shifts may also feed back to climate if they are accompanied by a change in albedo or surface roughness of the forest associated with a change in species dominance.

Figure 1.2. Results of a large-scale spruce beetle outbreak in southern Wyoming.

In the mountains of the western United States and Canada, there are several insect species that cause significant damage to Rocky Mountain forests. The mountain pine beetle (*Dendroctonus ponderosae* (Kirby)) and the spruce beetle (*Dendroctonus rufipennis* (Kirby)) are two such insects that infest *Pinus* and *Picea* species, respectively. These bark beetles are native to the Rocky Mountains, though they may be exhibiting range expansion dynamics akin to exotic, invasive species (de la Giroday et al. 2012). Under outbreak conditions, they are capable

of causing widespread damage and mortality to their host trees (Meddens et al. 2012). While much work has been done in studying the causes and consequences of mountain pine beetle outbreaks (Aukema et al. 2006, Wulder et al. 2006, Chapman et al. 2012, Pelz and Smith 2012, Hansen 2013, Meddens and Hicke 2014), there is still much that is not known about the ecology and outbreak dynamics of the congeneric spruce beetle (DeRose and Long 2012). In recent years, damage from spruce beetle outbreaks within the subalpine zone of the Rocky Mountains has become more and more significant (Veblen et al. 1994), and outbreak intensity and frequency are predicted to increase with climate change (Bentz et al. 2010). These factors suggest the need for a better understanding of spruce beetle ecology, and how the spruce beetle – subalpine system will respond to climate change. With this knowledge, this system can be managed appropriately and the potential future impact on western landscapes can be projected. As such, this project utilizes an individual tree-based model to investigate: **(1)** *the effect of climate change alone on the successional trajectories, biomass, and stand structure of vegetation within the subalpine zone and the broader southern Rocky Mountains region*; **(2)** *current post-insect outbreak successional trajectories and the effect of spruce beetles on biomass and stand structure;* and **(3)** *how these successional trajectories and forest dynamics may change under various climate change and insect outbreak scenarios*.

Several studies have predicted that with increasing temperatures and drought conditions from climate change, the frequency and severity of spruce beetle outbreaks will increase (Hansen et al. 2001, 2011, Berg et al. 2006, Bentz et al. 2010, Sherriff et al. 2011, DeRose and Long 2012). These studies have looked at spruce beetle biology and phenology as well as environmental and climate factors that have triggered outbreaks. With future climate change, *Picea* species will be more susceptible to beetle attacks due to drought and temperature stress

(McKenzie et al. 2009, Nelson et al. 2014). Thus, overall subalpine systems are likely to be more vulnerable to spruce beetle outbreaks. Gap models have been successful at investigating the response of trees to temperature and disturbance, and in predicting shifts in species dominance due to changes in climate (Lasch and Lindner 1995, Bugmann 2001, Shuman and Shugart 2009). As such, ecological modeling is used in this project to determine how subalpine forests will respond to climate change with and without beetle outbreaks. The effect of climate change on spruce beetle outbreak dynamics and their associated effects on forests will also be tested using ecological modeling. This work informs how the carbon storage and species composition of US Rocky Mountain forests may change in the future. It also helps predict vulnerability of these systems to current and future spruce beetle outbreaks. As these forests are a crucial part of the US's carbon budget (Schimel et al. 2002) this work is of importance both at a local and a regional scale.

Background

The climate – insect – vegetation system

The infestation success of bark beetles greatly depends on their population levels (Holling 1992). Young, healthy trees can fend off attacks from low levels of bark beetles through the use of resin (Hadley and Veblen 1993, Keeling and Bohlmann 2006, Raffa et al. 2008). In these cases, unsuccessful beetles are trapped in the resin pitched out by the host tree, and the tree survives. However, a "mass attack" of many beetles on a tree will overwhelm the tree's defenses, and the tree will be killed (Christiansen et al. 1987, Raffa et al. 2008, Meddens et al. 2012). The growth of these insect populations can accelerate very quickly when environmental and climate conditions are favorable, leading to explosive outbreaks in population size, increased mass attacks on trees, and subsequent widespread tree mortality.

As ectotherms, unable to regulate their own internal temperatures, insects are particularly sensitive to changes in ambient temperatures (Powell and Bentz 2009). Warmer temperatures have been shown to accelerate larval growth and increase overwintering survival, thus increasing insect population levels (Bentz et al. 2010, Hansen et al. 2011). With increasing temperatures due to greenhouse gas emissions, insect population thresholds are likely to be reached more often, leading to increased outbreak frequency and severity (Bentz et al. 2010).

Insect outbreaks often result in landscape-scale mortality, which can change the structure, composition, and biogeochemical cycling of forests. Insect outbreaks modify the structure of forests by killing large, dominant trees, leading to the release of subdominant trees and establishment of new seedlings (Roe and Amman 1970, Shugart 1984, Romme et al. 1986, Coates et al. 2009, Hawkins et al. 2012). These outbreaks also often result in an increase in leaf litter and eventually coarse woody debris as the trees die (Meddens et al. 2012, Edburg et al. 2012). This will affect nutrient cycling as large amounts of litter are added to the soil, and may also change the albedo of the forest floor. Bark beetles with one or only a few host species will also greatly impact the species composition of a forest, as the species dominance will shift away from the insect's host species. In subalpine landscapes, which already have low tree diversity (Burns and Honkala 1990), this shift could greatly affect the stability and ecosystem processes of these forests (Knops et al. 1999). When these landscapes are affected by the spruce beetle, the shift in dominance is likely to be from Engelmann spruce to subalpine fir, as subalpine fir generally codominates with Engelmann spruce (Veblen 1986). However, subdominant spruce may also be released following large-scale mortality of larger spruce trees.

Bark beetle infestations reduce stomatal conductance because beetles often carry blue stain fungus (Paine et al. 1997), which infect the host trees and disrupt water flow (Edburg et al.

2012). This reduction in stomatal conductance reduces canopy transpiration (Katul et al. 2012) and thus alters the water and energy balance of the forest prior to tree mortality (Bewley et al. 2010). In one spruce beetle outbreak, canopy evapotranspiration decreased by 20% within a month of initial spruce beetle infestation (Frank et al. 2014).

Bark beetle outbreaks also alter the carbon balance of a system (Kurz et al. 2008, Edburg et al. 2012). Large-scale outbreaks may shift forests that are normally net carbon sinks to net carbon sources through an increase in decomposition of woody debris and leaf litter, and due to widespread tree mortality. In a study by Brown et al. (2012) it was found that a mountain pine beetle outbreak in British Columbia, Canada in 2006, resulted in an NEP of -81 gC m^{-2} immediately after the outbreak. Additionally, it was predicted by Kurz et al. (2008) that another ongoing outbreak in this same area should result in a net C loss of 270 MtC from 2000 to 2020. Ghimire et al. (2015) found that biomass lost to recent bark beetle outbreaks across the western US ranged from 5 to 15 Mt C yr^{-1} from 2000 to 2009. When the host of the insects is a tree species used for commercial lumber, as is with Engelmann spruce (Alexander 1987), outbreaks result in an economic loss in addition to an ecological one.

Changes in forest characteristics and processes have the possibility to affect and interact with other disturbances, such as landslides, avalanches, and fires (Veblen et al. 1994, Jorgensen and Jenkins 2011, Jenkins et al. 2012). While low-level fires may increase a stand's susceptibility to beetles through weakening of host tree defenses (Geiszler et al. 1984, Rasmussen et al. 1996, Hood and Bentz 2007), forests that have just experienced a large-scale fire are less susceptible to bark beetle outbreaks as there is less "fuel" for the insects (Bebi et al. 2003). Avalanches and landslides in forested areas prevent beetle outbreaks for the same reason (Veblen et al. 1994). However, loss of slope stability following major mortality events from

beetle outbreaks may enhance the occurrence of landslides and avalanches (Dale et al. 2001). Additionally, immediately following a beetle outbreak, the increase in leaf litter and woody debris on the ground may increase the risk for fire (Jenkins et al. 2012). It is clear that insect outbreaks are not only capable of causing habitat loss and loss of commercial timber, but that they can also initiate other dangerous and costly disturbances.

The spruce beetle

The spruce beetle (*Dendroctonus rufipennis* (Kirby)) is an important mortality agent of Engelmann spruce (*Picea engelmannii* Parry ex Engelm.) in the subalpine forests of the US Rocky Mountains (Bebi et al. 2003, Bentz et al. 2010). Historically, fire has been the most important natural disturbance in the area, but tree mortality due to spruce beetle infestations has recently become as, if not more, important for shaping forest structure and function (Veblen et al. 1991, 1994, DeRose and Long 2012) (Fig. 1.3). Spruce beetle outbreaks have caused widespread tree mortality across the northwestern United States and

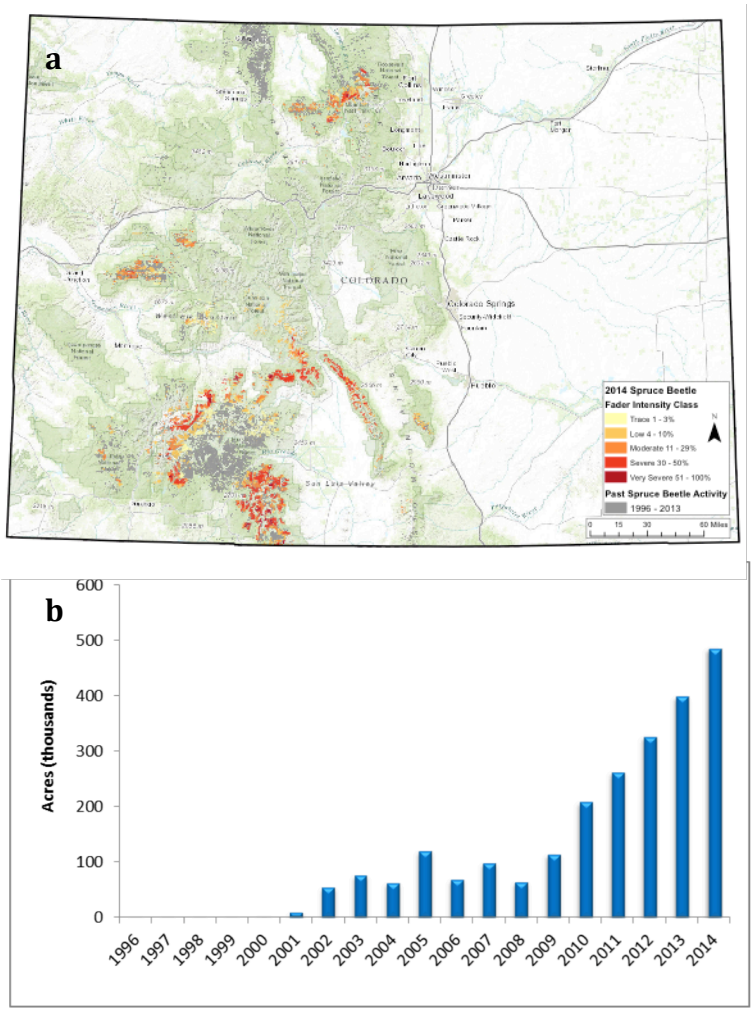

Figure 1.3. (a) Extent of spruce beetle outbreaks in Colorado and (b) annual acres affected by the spruce beetle in CO, from USFS (2015).

Canada. In a Colorado outbreak lasting from 1939 to 1952, spruce beetles affected over 290,000 ha of the landscape (Veblen et al. 1991, Anderson et al. 2010), and an ongoing outbreak in Colorado has affected over 156,000 ha between 2009 and 2014 (USFS 2015). With increasing temperatures due to climate change, the frequency and severity of spruce beetle outbreaks are predicted to continue increasing, further endangering the future of western subalpine forests (Bentz et al. 2010, DeRose and Long 2012).

Spruce beetles infest Engelmann spruce by boring into the bark in late spring or early summer, whereupon they mate and lay eggs in the phloem of infested trees (Schmid and Frye 1977). Beetle eggs hatch by mid-October and the larvae begin to feed on the phloem within the constructed galleries and emerge as adults after they have fully developed (Hansen et al. 2011). Under normal temperature conditions, spruce beetles have a semivoltine life cycle, and take two years to fully develop. Under these conditions, beetle larvae enter diapause during their first winter within their hosts (Schmid and Frye 1977). During this "pause" in development, beetle larvae are more protected from the cold winter temperatures that can occur in subalpine systems. Once temperatures are again favorable, diapause ends and larval development continues. Larvae reach adult stage prior to their second winter, and the adults spend their second winter within their hosts before emerging the following summer to infest new hosts (Schmid and Frye 1977, Hansen et al. 2011).

Anomalously warm summer temperatures accelerate the growth of larvae and warmer winter temperatures may prevent diapause from occurring (Hansen et al. 2001). This increase in growth rate allows the beetles to reach adult stages prior to their first winter, and to emerge the following summer, one year sooner than they would under normal temperature conditions. This univoltine life cycle (one generation of beetles per year) accelerates the population growth of

spruce beetles, and thus increases the probability of mass attacks and subsequent outbreaks (Hansen et al. 2001, Bentz et al. 2010). In a study by Hansen et al. (2011) it was found that spruce beetle larvae kept at 12°C or lower underwent diapause and did not shift to a univoltine life cycle. Larvae kept above 18°C, however, did not enter diapause and were able to develop fast enough to shift to a univoltine life cycle. Additionally, larvae moved from warmer temperatures to below 12°C also entered diapause if they were moved within 10 days after their final instar (instar IV). It has been shown that female beetles from univoltine generations do not differ in their egg production from that of semivoltine females (Hansen and Bentz 2003). The density of the surviving brood of univoltine females also does not differ from that of semivoltine females. Thus, with the same number of beetles emerging every year, rather than every other year, atypically warm temperatures will act to push spruce beetle population levels towards outbreak thresholds. Warmer temperatures also increase overwintering survival, further elevating beetle population levels (Berg et al. 2006).

Spruce beetles also have associated parasites and predators. The northern three-toed woodpecker (*Picoides tridactylus* (Baird)), the hairy woodpecker (*P. villosus* (Anthony)), and the downy woodpecker (*P. pubescens* (Hartlaub)) are all predators of the spruce beetle, the three-toed woodpecker being the most important (Schmid and Frye 1977). These three woodpeckers feed on the boles, trunks, and branches, respectively, of spruce trees and are capable of destroying up to 55% of spruce beetle larvae. Feeding by these woodpeckers is greatest from December through March (Schmid and Frye 1977). *Coeloides dendroctoni* (Cushman) is a parasitic wasp that infests spruce beetle larvae. Their impact on spruce beetle broods is variable, but is usually low. Other parasites have been found (*Roptrocerus eccoptogastri* (Ratzeburg) and

Cecidostiba burkey (Crawford)), but not much is known about their impact on spruce beetle larvae (Schmid and Frye 1977).

Ecology of Engelmann spruce and subalpine ecosystems

Engelmann spruce is the principal host of the spruce beetle in the southern Rocky Mountains. It is an evergreen species distributed throughout the western United States and parts of Canada (Schmid and Frye 1977, Burns and Honkala 1990). It can tolerate the extreme temperature ranges (below -40°C to above 30°C) and high elevations of subalpine forests, but it is sensitive to fire and windthrow (Veblen et al. 1994). Fire in subalpine ecosystems is infrequent, generally with a return period of 300 years, and is often stand-replacing (Veblen et al. 1994).

Young, healthy spruce will be able to fend off attacks from small numbers of beetles, however, a mass attack of spruce beetles, especially on older or more stressed trees, will be enough to overcome the trees' defenses (Raffa et al. 2008). This stress can come in the form of low nutrient availability, drought, or stress from other disturbances such as fire and wind. Because of this, spruce beetles will preferentially attack older, larger trees (>30 cm DBH) (DeRose and Long 2012). These trees will be more likely to succumb to beetle attacks and will provide ample food for developing larvae. Spruce beetles damage their host trees by eating the cambium and phloem within the trunk, interrupting the flow of nutrients and water. Spruce beetles also carry blue stain fungus, which infects attacked trees and disrupts water flow, ultimately killing the trees (Schmid and Frye 1977). During an infestation, Engelmann spruce leaves remain green and photosynthesizing (albeit only slightly) for two or more years after the initial infestation (Schmid and Frye 1977, Frank et al. 2014). Engelmann spruce trees killed by beetle infestations are standing dead, and thus do not create a very large gap in the forest. This

process results in the increased growth rate of subcanopy spruce and subalpine fir, rather than establishment of new seedlings following a spruce beetle outbreak (Veblen et al. 1994). Thus, along with younger Engelmann spruce, suppressed subalpine fir experience increased growth rate following a spruce beetle outbreak.

There are many factors that influence the probability of a spruce beetle outbreak. Studies have shown that suitable weather (i.e. warm, dry summers), as well as amount of woody debris play crucial roles in shifting an endemic spruce beetle population only feeding on a few trees and logs, to an epidemic one capable of causing mass mortality of trees (Berg et al. 2006, Jorgensen and Jenkins 2011, DeRose and Long 2012). Warm and dry summers contribute to the shift to a one-year life cycle and also increase beetle survivorship (Hansen et al. 2011), which will lead to increases in population levels and subsequent increases in the probability for outbreak (Anderson et al. 2010, Sherriff et al. 2011). Smaller, endemic spruce beetle populations infest fallen logs and other coarse woody debris. Blowdown and logging increase the amount of this debris and can accelerate beetle population growth (Wichmann and Ravn 2001, Jorgensen and Jenkins 2011). As beetle population levels rise, the probability of mass attack on individual trees also increases, further increasing the likelihood of a widespread outbreak (Berg et al. 2006).

The availability and location of susceptible spruce trees will influence whether an outbreak occurs, as well as how the outbreak spreads (Schmid and Frye 1976, Berg et al. 2006, DeRose and Long 2012, O'Connor et al. 2015). As such, the heterogeneity of the forest landscape and the spatial extent of spruce stands affect the spread of spruce beetle infestations. In a large, homogenous forest dominated by mostly old, susceptible Engelmann spruce, beetles will be able to spread at a greater rate than in a forest with only small, disparate patches of susceptible spruce (DeRose and Long 2012, O'Connor et al. 2015). Spatial scale is also

important to consider for determining when a spruce beetle outbreak will occur and how it will spread across the landscape. Small-scale effects, such as the presence of woody debris, help to increase small pockets of active beetles, whereas large-scale changes in environmental or climate conditions help to facilitate a synchronized, large-scale outbreak (Sherriff et al. 2011, DeRose and Long 2012).

Climate change

Mean annual temperatures in the western United States have already increased 2°C since 1950 and this warming trend is predicted to continue (Meehl et al. 2012). With this increase in ambient temperatures, more spruce beetles may switch to a one-year life cycle, allowing more populations to grow to outbreak levels (Bentz et al. 2010). If this warming is accompanied by drought in the west, water-stressed trees will be even more susceptible to beetle attacks (Cobb et al. 1997, Berg et al. 2006). Additionally, climate change in the western US is likely to bring about longer fire seasons, which will lead to increases in fire weather and extent of burning (Jolly et al. 2015). Jolly et al. (2015) investigated recent global wildfire frequency and found that the greatest increase has occurred in the northern Rocky Mountains, and Rogers et al. (2015) found that mesic, high biomass forests (such as those of the subalpine zone) are highly vulnerable to the combination of increasing temperatures and fire frequency.

It is difficult to predict how vegetation will respond to climate change, alone and with concurrent disturbances. Stress complexes, i.e. biotic and abiotic stressors that combine to decrease the vigor and sustainability of forests (McKenzie et al. 2009), already exist across the Rocky Mountains landscape. However, climate change is leading to new and more severe stressors, and will undoubtedly continue to do so. Climate change creates shifts in the optimal ranges of tree species, which may lead to the migration of these species. This migration changes

the species composition of a landscape, and may also change its albedo. In complex terrain like that of the Rocky Mountains, tree species at the top of the mountain (such as Engelmann spruce) may not have anywhere to migrate come changes in climate (Bell et al. 2014). Because of this complication, it is important to analyze how climate change alone will affect vegetation. With the addition of the response of spruce beetles to climate change, and the subsequent effects on Rocky Mountains vegetation, the future of subalpine forests in the western US can be predicted.

Objectives

Study sites

I will utilize four sites (Fig. 1.4) within the southern Rocky Mountains to investigate climate – vegetation – insect interactions within western subalpine forests. The Glacier Lakes Ecosystems Experimental Site (GLEES), in southern Wyoming is managed by the US Forest Service and has long-term data on forest characteristics. This site will be used as an initial test site for model verification and validation. Wolf Creek Pass, in the San Juan Mountains of southern Colorado also contains forest inventory plots, which will be used for model validation. Model simulations involving climate and insect infestations will be run at all four sites. These sites are all located in the subalpine zone, and consist of Engelmann spruce, subalpine fir (*Abies lasiocarpa*), lodgepole pine (*Pinus contorta*),

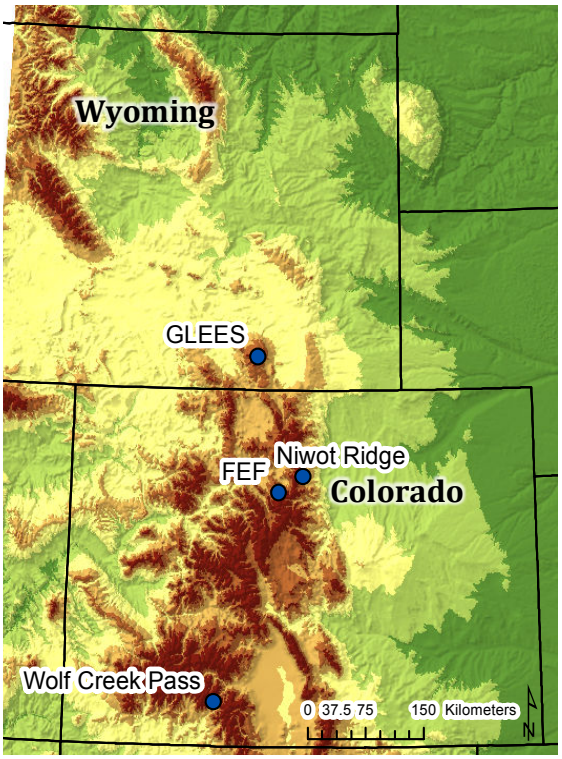

Fig. 1.4. Map of study sites to be used in this project.

quaking aspen (*Populus tremuloides*), Douglas-fir (*Pseudotsuga menziesii*), and limber pine (*Pinus flexilis*) (Musselman et al. 1994, Wooldridge et al. 1996, Stottlemyer and Troendle 2001, Monson et al. 2005, Sacks et al. 2006).

Objective 1: Parameterize and validate the individual-based gap model UVAFME to the Rocky Mountains sites and conduct an initial climate sensitivity test.

Disturbance type and frequency are important factors in shaping the heterogeneity and mosaic nature of forests (Shugart 1984). At the scale of an individual plot, disturbances such as fire, windthrow, or insect infestation may kill a dominant tree, allowing subdominant trees and seedlings better access to resources (Shugart 1998). This release from environmental stressors causes rapid growth of seedlings and subcanopy trees within the "gap" made by the fallen dominant tree. Eventually, a single tree again dominates the gap, and the cycle starts anew. Over the scale of a whole landscape, these gap dynamics create a mosaic forest structure with different patches of the forest at different successional stages. The distribution of tree species and tree ages within a landscape can have profound effects on the physical structure as well as the carbon storage and cycling of a forest (Shugart 1998). Species-specific disturbances, such as spruce beetle outbreaks, have an outsized impact on species composition, as they preferentially affect one or a few tree species. These species composition and biomass changes can also cause climate feedbacks through alteration of the carbon and energy budget of an ecosystem or through changes in surface roughness and albedo (Bonan 1989).

It is difficult to study how these interactions will play out, especially when also considering climate change. Ecological models are valuable tools for understanding how these processes will interact and affect the species composition and biomass of forests, both spatially and temporally. Individual-based models, which focus on the individual trees themselves, can be

used to scale up these interactions from small patches to a larger landscape. Coupling these models to global climate change models can also serve to understand how these interactions may change in the future. Chapters 3 will cover Objective 1 and will begin to answer the first question of this work regarding climate change's effect on Rocky Mountains vegetation.

The University of Virginia Forest Model Enhanced (UVAFME) is an extension of the individual-based model FAREAST (Yan and Shugart 2005). UVAFME is an individual tree-based gap model that follows the annual growth, establishment, and death of individual trees on independent patches of a landscape. Each patch is equivalent to the size of influence of a dominant tree crown (500 m^2), and the average of several hundred of these patches simulates the average biomass and species composition of a forest landscape through time. This model can also be run with climate input from General Circulation Models (GCMs) to simulate the effect of climate change on forest dynamics. Yan and Shugart (2005) tested the ability of the model to simulate forest composition along an elevation gradient in China using Chinese forest inventory data from different regions, and they also analyzed forest types at 31 sites in eastern Russia. Further validation of the model following application to point locations across all of boreal Russia for a range of forest types showed that it captures natural biomass accumulation rates for the Russian forest without recalibration (Shuman et al. 2014). In all of these tests, climate was found to have a strong role in driving species composition and biomass (Shuman and Shugart 2009, Shuman et al. 2015).

UVAFME will be parameterized to field sites in Wyoming and Colorado by using data on species composition, climate, and other site parameters from the US Forest Service. Species-specific parameters for each tree species will be derived from Burns and Honkala (1990) and other relevant scientific literature (Baker 1949, Daubenmire 1978, Peet 1981, Alexander 1987,

Sibold et al. 2007). As UVAFME was developed for use in boreal Eurasia, code modifications may be necessary in order to update the model to the Rocky Mountains landscape. The success of these updates and parameterization will be verified using inventory data and by running it along an altitudinal gradient. The distribution of tree species within the Rocky Mountains is highly dependent on elevation (Peet 1981). While Engelmann spruce-subalpine fir stands tend to dominate at the highest elevations (2400 m and higher), lodgepole pine dominates at relatively high elevations (2000 to 3000 m) and where fire has recently occurred (Daubenmire 1978). The mid-elevations are comprised of a Douglas-fir zone, and a ponderosa pine (*Pinus ponderosa*) zone below it (2000 to 2700 m). Pinyon pine (*Pinus edulis*) and juniper (*Juniperus scopulorum*) woodlands occur at the lowest elevations (1700 to 2000 m) (Daubenmire 1943). By testing the ability of UVAFME to replicate this change in species composition with elevation, this study will evaluate its capacity to properly simulate forest dynamics within the Rocky Mountains.

Once the model is successfully validated, it will be run with altered climate to determine the effect of climate change on subalpine vegetation and the Rocky Mountains landscape in general. This will be conducted as a temperature sensitivity analysis in which the modeled temperature is set to increase linearly by a certain amount over a certain number of years. After climate has stabilized at the new values for a few hundred years, the temperature will then be brought back down to present levels to determine how persistent the vegetation changes due to climate may be. The output of species composition and biomass from this model run will be compared to output at current conditions. UVAFME will be run with this climate change scenario along an elevation gradient to evaluate the effect of climate change on species zonation in the Rocky Mountains. This information will be used to determine how sensitive subalpine systems and the overall Rocky Mountains landscape are to increasing temperatures.

Objective 2: Run UVAFME without disturbances over long time scales in the subalpine zone to determine the long-term forest dynamics within the system.

The study of long-term forest dynamics, and the internal and external factors that drive them, is an essential part of understanding the role of species change within landscape ecology and forest management (Tansley 1935). Given the long life of many tree species, there are inherent challenges in using existing field data to discern patterns of change in many forest systems (Bugmann 2001). Additionally, the presence of disturbances on the landscape often hinders the study of purely endogenous, or internal, forest dynamics. Through ecological modeling, one has the capacity to examine forest processes over centuries without the intrusion of natural disturbances, allowing for the internal properties of ecosystems to be investigated.

A field study within the Colorado subalpine zone found evidence for periodic phenomena between Engelmann spruce and subalpine fir (Aplet et al. 1988). Cyclic phenomena have been the focus of many studies in stressed conifer forests (Reiners and Lang 1979, Shugart 1984, Sprugel 1984, Moloney 1986). In these systems, suppressed seedlings are released following the synchronous death of canopy trees (Sprugel 1984, Moloney 1986). These cycles occur over hundreds of years, and thus studying them in the field is difficult, if not impossible in some cases. This difficulty further highlights the advantages of vegetation modeling studies.

I will use UVAFME to simulate forest dynamics over time at the high-elevation, subalpine site in southern Wyoming (Fig. 1.4). The model will be run at this location for periods of 3,000 years to simulate long-term forest dynamics at the site. These model runs will be conducted under three different scenarios: (1) subalpine fir as the only available species; (2) Engelmann spruce only; and (3) with both subalpine fir and Engelmann spruce available. These different scenarios will allow me to determine tree demography for both species and for the

forest as a whole. Finally, model output will be compared to field data from similar high-elevation conifer sites, including that of the Aplet et al. (1988) study. Chapter 4 will cover Objective 2 and will serve to further our understanding of fundamental vegetation dynamics in this region by identifying underlying patterns, which may help to discern the response of this system to future change.

Objective 3: Develop a spruce beetle subroutine and run it under different climate change and bark beetle scenarios to understand the response of subalpine vegetation to climate change and concurrent spruce beetle outbreaks.

In order to model how spruce beetles affect the landscape, a subroutine for spruce beetle infestation will be developed and added to UVAFME. This subroutine will calculate the probability for spruce beetle-induced tree mortality (p_{beetle}) based on several environmental and climate factors. Assuming that larger populations of spruce beetles cause an increased likelihood of a mass attack and subsequent infestation, this probability will increase based on temperature and other environmental conditions that increase spruce beetle populations. The specific environmental thresholds will be generated using data on spruce beetle climate sensitivity from Hansen et al. (2011) and the results of other studies on bark beetle outbreaks (Schmid and Frye 1976, Berg et al. 2006, Seidl et al. 2008, Bentz et al. 2010, Sherriff et al. 2011, DeRose and Long 2012).

As beetles preferentially attack larger and more stressed trees, p_{beetle} will also increase with spruce size and stress (in the form of reduced growth rate and damage from other disturbances). The growth subroutine of UVAFME annually updates each simulated tree's diameter at breast height (DBH) and other characteristics based on environmental conditions and

species-specific parameters (Yan and Shugart 2005). These tree characteristics will be used to determine susceptibility to spruce attack.

Propagation of spruce beetles from tree to tree requires spatially interactive modeling. Currently, UVAFME is not spatially interactive; this will be modified so that spruce beetle infestation can be spread between adjacent trees. In this way, if a modeled tree is infested, any spruce trees next to it will have a higher chance of also being infested.

Finally, in order to understand how outbreaks will respond to predicted climate change scenarios, the updated UVAFME model will be run with altered climate with input from a GCM. Four different scenarios will be conducted using these methods: (1) current climate and no beetle disturbance (as in Chapter 3); (2) current climate with beetle disturbance; (3) climate change and no beetle disturbance (as in Chapter 3); and (4) climate change with beetle disturbance. The biomass and species composition will be compared across all runs. This information will be used to determine how much of an impact the spruce beetle – climate change interaction may have on western subalpine forests.

Project Impacts and Significance

The subalpine zone of the southern Rocky Mountains is particularly vulnerable to the interacting effects of insects, climate, and vegetation. In addition to being a significant portion of the US carbon budget, this ecosystem contributes significantly to commercial timber and water resources, wildlife habitat, and forage for livestock. It is also important for summer and winter recreational activities, and is a source of great scenic beauty (Alexander 1987). During an outbreak, spruce beetles are capable of producing widespread mortality of Engelmann spruce, leading to altered carbon dynamics, energy and water fluxes, and species composition. It is thus an inherent and important component of the dynamics of subalpine forests. Despite their

destructive potential, when compared to the dynamics and effects of the mountain pine beetle, relatively little is known about the impacts of spruce beetle outbreaks on western landscapes. Insect pests like the spruce beetle, which have long outbreaks at moderate intervals, and a spreading level of contagion, are predicted to have a great effect on the forested landscape in conjunction with climate change (Holling 1992). It is therefore imperative that more is understood about how spruce beetle outbreak frequency and intensity will respond to climate change. This proposed work seeks to close this knowledge gap through the use of ecological modeling. By pairing an individual-based model with climate change models, the complicated interactions of climate, spruce beetle outbreaks, and vegetative response can be simulated. These results can be used to predict the future biomass and community composition of US subalpine forests.

References

Alexander, R. 1987. Ecology, silviculture, and management of the Engelmann spruce - subalpine fir type in the central and southern Rocky Mountains. USDA Forest Service, Agricultural Handbook No. 659:155.

Anderson, R. S., S. J. Smith, A. M. Lynch, and B. W. Geils. 2010. The pollen record of a 20th century spruce beetle (Dendroctonus rufipennis) outbreak in a Colorado subalpine forest, USA. Forest Ecology and Management 260:448–455.

Aplet, G. H., R. D. Laven, and F. W. Smith. 1988. Patterns of community dynamics in Colorado Engelmann spruce-subalpine fir forests. Ecology 69:312–319.

Aukema, B. H., A. L. Carroll, J. Zhu, K. F. Raffa, T. A. Sickley, and S. W. Taylor. 2006. Landscape level analysis of mountain pine beetle in British Columbia, Canada: spatiotemporal development and spatial synchrony within the present outbreak. Ecography 29:427–441.

Baker, F. S. 1949. A revised tolerance table. Journal of Forestry 47:179–181.

Bebi, P., D. Kulakowski, and T. T. Veblen. 2003. Interactions between fire and spruce beetles in a subalpine Rocky Mountain forest landscape. Ecology 84:362–371.

Bell, D. M., J. B. Bradford, and W. K. Lauenroth. 2014. Mountain landscapes offer few opportunities for high-elevation tree species migration. Global Change Biology 20:1441–1451.

Bentz, B. J., J. Régnière, C. J. Fettig, E. M. Hansen, J. L. Hayes, J. A. Hicke, R. G. Kelsey, J. F. Negrón, and S. J. Seybold. 2010. Climate Change and Bark Beetles of the Western United States and Canada: Direct and Indirect Effects. BioScience 60:602–613.

Berg, E. E., J. D. Henry, C. L. Fastie, A. D. De Volder, and S. M. Matsuoka. 2006. Spruce beetle outbreaks on the Kenai Peninsula, Alaska, and Kluane National Park and Reseve, Yukon Territory: Relationship to summer temperatures and regional differences in disturbance regimes. Forest Ecology and Management 227:219–232.

Bewley, D., Y. Alila, and A. Varhola. 2010. Variability of snow water equivalent and snow energetics across a large catchment subject to Mountain Pine Beetle infestation and rapid salvage logging. Journal of Hydrology 388:464–479.

Bonan, B. G. 1989. A computer model of the solar radiation, soil moisture, and soil thermal regimes in boreal forests. Ecological Modelling 45:275–306.

Brown, M. G., T. A. Black, Z. Nesic, A. L. Fredeen, V. N. Foord, D. L. Spittlehouse, R. Bowler, P. J. Burton, J. A. Trofymow, N. J. Grant, and D. Lessard. 2012. The carbon balance of two lodgepole pine stands recovering from mountain pine beetle attack in British Columbia. Agricultural and Forest Meteorology 153:82–93.

Bugmann, H. 2001. A review of forest gap models. Climatic Change 51:259–305.

Burns, R. M., and B. H. Honkala. 1990. Silvics of North America: 1. Conifers; 2. Hardwoods. Agricultural Handbook 654. U.S. Department of Agriculture, Forest Service, Washington, DC. vol. 2 877 p.

Chapman, T. B., T. T. Veblen, and T. Schoennagel. 2012. Spatiotemporal patterns of mountain pine beetle activity in the southern Rocky Mountains. Ecology 93:2175–2185.

Christiansen, E., R. H. Waring, and A. A. Berryman. 1987. Resistance of conifers to bark beetle attack: searching for general relationships. Forest Ecology and Management 22:89–106.

Coates, K. D., T. Glover, B. Henderson, and others. 2009. Abundance of secondary structure in lodgepole pine stands affected by the mountain pine beetle in the Cariboo-Chilcotin. Pacific Forestry Centre.

Cobb, N. S., S. Mopper, C. A. Gehring, M. Caouette, K. M. Christensen, and T. G. Whitham. 1997. Increased moth herbivory associated with environmental stress of pinyon pine at local and regional levels. Oecologia 109:389–397.

Dale, V. H., L. A. Joyce, S. Mcnulty, R. P. Neilson, M. P. Ayres, M. D. Flannigan, P. J. Hanson, L. C. Irland, A. E. Lugo, C. J. Peterson, D. Simberloff, F. J. Swanson, B. J. Stocks, and B. Michael Wotton. 2001. Climate Change and Forest Disturbances. BioScience 51:723.

Daubenmire, R. F. 1943. Vegetational zonation in the Rocky Mountains. The Botanical Review 9:325–393.

Daubenmire, R. F. 1978. Plant Geography With Special Reference to North America. Academic Press, New York, NY.

Delcourt, H. R., P. A. Delcourt, and T. Webb. 1982. Dynamic plant ecology: the spectrum of vegetational change in space and time. Quaternary Science Reviews 1:153–175.

DeRose, R. J., and J. N. Long. 2012. Factors Influencing the Spatial and Temporal Dynamics of Engelmann Spruce Mortality during a Spruce Beetle Outbreak on the Markagunt Plateau, Utah. Forest Science 58:1–14.

Edburg, S. L., J. A. Hicke, P. D. Brooks, E. G. Pendall, B. E. Ewers, U. Norton, D. Gochis, E. D. Gutmann, and A. J. Meddens. 2012. Cascading impacts of bark beetle-caused tree mortality on coupled biogeophysical and biogeochemical processes. Frontiers in Ecology and the Environment 10:416–424.

Frank, J. M., W. J. Massman, B. E. Ewers, L. S. Huckaby, and J. F. Negrón. 2014. Ecosystem CO_2 /H_2O fluxes are explained by hydraulically limited gas exchange during tree mortality from spruce bark beetles: CO_2 /H_2O FLUX EXPLAINED FROM DISTURBANCE. Journal of Geophysical Research: Biogeosciences 119:1195–1215.

Geiszler, D. R., D. R. Gara, and W. R. Littke. 1984. Bark beetle infestations of lodgespole pine following a fire in south central Oregon. Zitschrift fur Angewandte Entomologie 98:389–394.

Ghimire, B., C. A. Williams, G. J. Collatz, M. Vanderhoof, J. Rogan, D. Kulakowski, and J. G. Masek. 2015. Large carbon release legacy from bark beetle outbreaks across Western United States. Global Change Biology 21:3087–3101.

de la Giroday, H.-M. C., A. L. Carroll, and B. H. Aukema. 2012. Breach of the northern Rocky Mountain geoclimatic barrier: initiation of range expansion by the mountain pine beetle: Range expansion by the mountain pine beetle. Journal of Biogeography 39:1112–1123.

Hadley, K. S., and T. T. Veblen. 1993. Stand response to western spruce budworm and Douglas-fir bark beetle outbreaks, Colorado Front Range. Canadian Journal of Forest Research 23:479–491.

Hansen, E. M. 2013. Forest Development and Carbon Dynamics After Mountain Pine Beetle Outbreaks. Forest Science 60.

Hansen, E. M., and B. J. Bentz. 2003. Comparison of reproductive capacity among univoltine, semivoltine, and re-emerged parent spruce beetles (Coleoptera: Scolytidae). The Canadian Entomologist 135:697–712.

Hansen, E. M., B. J. Bentz, J. A. Powell, D. R. Gray, and J. C. Vandygriff. 2011. Prepupal diapause and instar IV developmental rates of the spruce beetle, Dendroctonus rufipennis (Coleoptera: Curculionidae, Scolytinae). Journal of Insect Physiology 57:1347–1357.

Hansen, E. M., B. J. Bentz, and D. L. Turner. 2001. Physiological basis for flexible voltinism in the spruce beetle (Coleoptera: Scolytidae). The Canadian Entomologist 133:805–817.

Hawkins, C. D. B., A. Dhar, N. A. Balliet, and K. D. Runzer. 2012. Residual mature trees and secondary stand structure after mountain pine beetle attack in central British Columbia. Forest Ecology and Management 277:107–115.

Holling, C. S. 1992. The role of forest insects in structuring the boreal landscape. *in* H. H. Shugart, R. Leemans, and G. B. Bonan, editors. A Systems Analysis of the Global Boreal Forest. Cambridge University Press, New York, NY.

Hood, S., and B. Bentz. 2007. Predicting postfire Douglas-fir beetle attacks and tree mortality in the northern Rocky Mountains. Canadian Journal of Forest Research 37:1058–1069.

Jenkins, M. J., W. G. Page, E. G. Hebertson, and M. E. Alexander. 2012. Fuels and fire behavior dynamics in bark beetle-attacked forests in Western North America and implications for fire management. Forest Ecology and Management 275:23–34.

Jolly, W. M., M. A. Cochrane, P. H. Freeborn, Z. A. Holden, T. J. Brown, G. J. Williamson, and D. M. J. S. Bowman. 2015. Climate-induced variations in global wildfire danger from 1979 to 2013. Nature Communications 6:7537.

Jorgensen, C. A., and M. J. Jenkins. 2011. Fuel complex alterations associated with spruce beetle-induced tree mortality in Intermountain spruce/fir forests. Forest Science 57:232–240.

Katul, G. G., R. Oren, S. Manzoni, C. Higgins, and M. B. Parlange. 2012. Evapotranspiration: A process driving mass transport and energy exchange in the soil-plant-atmosphere-climate system. Reviews of Geophysics 50.

Keeling, C. I., and J. Bohlmann. 2006. Genes, enzymes and chemicals of terpenoid diversity in the constitutive and induced defence of conifers against insects and pathogens. New Phytologist 170:657–675.

Knops, J. M., D. Tilman, d N. Haddad, S. Naeem, C. E. Mitchell, J. Haarstad, M. E. Ritchie, K. M. Howe, P. B. Reich, E. Siemann, and others. 1999. Effects of plant species richness on invasion dynamics, disease outbreaks, insect abundances and diversity. Ecology Letters 2:286–293.

Kurz, W. A., C. C. Dymond, G. Stinson, G. J. Rampley, E. T. Neilson, A. L. Carroll, T. Ebata, and L. Safranyik. 2008. Mountain pine beetle and forest carbon feedback to climate change. Nature 452:987–990.

Lasch, P., and M. Lindner. 1995. Application of Two Forest Succession Models at Sites in North East Germany. Journal of Biogeography 22:485.

Ludwig, D., D. D. Jones, and C. S. Holling. 1978. Qualitative Analysis of Insect Outbreak Systems: The Spruce Budworm and Forest. The Journal of Animal Ecology 47:315.

McKenzie, D., D. L. Peterson, and J. J. Littell. 2009. Chapter 15 Global Warming and Stress Complexes in Forests of Western North America. Pages 319–337 Developments in Environmental Science. Elsevier.

Meddens, A. J. H., and J. A. Hicke. 2014. Spatial and temporal patterns of Landsat-based detection of tree mortality caused by mountain pine beetle outbreak in Colorado, USA. Forest Ecology and Management 322:78–88.

Meddens, A. J., J. A. Hicke, and C. A. Ferguson. 2012. Spatiotemporal patterns of observed bark beetle-caused tree mortality in British Columbia and the western United States. Ecological Applications 22:1876–1891.

Meehl, G. A., J. M. Arblaster, and G. Branstator. 2012. Mechanisms contributing to the warming hole and consequent US east-west differential of heat extremes. Journal of Climate 25:6394–6408.

Moloney, K. A. 1986. Wave and nonwave regeneration processes in a subalpine Abies balsamea forest. Canadian Journal of Botany 64:341–349.

Monson, R. K., J. P. Sparks, T. N. Rosenstiel, L. E. Scott-Denton, T. E. Huxman, P. C. Harley, A. A. Turnipseed, S. P. Burns, B. Backlund, and J. Hu. 2005. Climatic influences on net ecosystem CO2 exchange during the transition from wintertime carbon source to springtime carbon sink in a high-elevation, subalpine forest. Oecologia 146:130–147.

Musselman, R. C., D. G. Fox, A. W. Schoettle, and C. M. Regan. 1994. The Glacier Lakes Ecosystem Experiments Site. U.S. Department of Agriculture, Forest Service, Rocky Mountain Forest and Range Experiment Station:94.

Nelson, K. N., M. E. Rocca, M. Diskin, C. F. Aoki, and W. H. Romme. 2014. Predictors of bark beetle activity and scale-dependent spatial heterogeneity change during the course of an outbreak in a subalpine forest. Landscape Ecology 29:97–109.

O'Connor, C. D., A. M. Lynch, D. A. Falk, and T. W. Swetnam. 2015. Post-fire forest dynamics and climate variability affect spatial and temporal properties of spruce beetle outbreaks on a Sky Island mountain range. Forest Ecology and Management 336:148–162.

Paine, T. D., K. F. Raffa, and T. C. Harrington. 1997. Interactions among Scolytid bark beetles, their assocaited fungi, and live host conifers. Annual Review of Entymology 42:179–206.

Peet, R. K. 1981. Forest vegetation of the Colorado front range. Vegetatio 45:3–75.

Pelz, K. A., and F. W. Smith. 2012. Thirty year change in lodgepole and lodgepole/mixed conifer forest structure following 1980s mountain pine beetle outbreak in western Colorado, USA. Forest Ecology and Management 280:93–102.

Powell, J. A., and B. J. Bentz. 2009. Connecting phenological predictions with population growth rates for mountain pine beetle, an outbreak insect. Landscape Ecology 24:657–672.

Raffa, K. F., B. H. Aukema, B. J. Bentz, A. L. Carroll, J. A. Hicke, M. G. Turner, and W. H. Romme. 2008. Cross-scale Drivers of Natural Disturbances Prone to Anthropogenic Amplification: The Dynamics of Bark Beetle Eruptions. BioScience 58:501.

Rasmussen, L. A., G. D. Amman, J. C. Vandygriff, R. D. Oakes, A. S. Munson, and K. E. Gibson. 1996. Bark beetle and wood borer infestation in the greater Yellowstone area during four postfire years. USDA Forest Service Research Paper INT-RP-487. Intermountain Research Station, Ogden, UT.

Reiners, W. A., and G. E. Lang. 1979. Vegetational Patterns and Processes in the Balsam Fir Zone, White Mountains New Hampshire. Ecology 60:403.

Roe, A. L., and G. D. Amman. 1970. Mountain pine beetle in lodgepole pine forests.

Rogers, B. M., D. Bachelet, R. J. Drapek, B. E. Law, R. P. Neilson, and J. R. Wells. 2015. Drivers of Future Ecosystem Change in the US Pacific Northwest: The Role of Climate, Fire, and Nitrogen. Global Vegetation Dynamics: Concepts and Applications in the MC1 Model 214:91.

Romme, W. ., D. H. Knight, and J. B. Yavitt. 1986. Mountain pine beetle outbreaks in the Rocky Mountains: regulators of primary production? The American Naturalist 127:484–494.

Sacks, W. J., D. S. Schimel, R. K. Monson, and B. H. Braswell. 2006. Model-data synthesis of diurnal and seasonal CO2 fluxes at Niwot Ridge, Colorado. Global Change Biology 12:240–259.

Schimel, D. S., T. G. F. Kittel, S. Running, R. Monson, A. Turnipseed, and D. Anderson. 2002. Carbon sequestration studied in western US mountains. EOS Transactions, American Geophysical Union 83:445–456.

Schmid, J. M., and R. H. Frye. 1976. Stand ratings for spruce beetles. US Dept. of Agriculture, Forest Service, Rocky Mountain Forest and Range Experiment Station.

Schmid, J. M., and R. H. Frye. 1977. Spruce beetle in the Rockies.

Seidl, R., W. Rammer, D. Jäger, and M. J. Lexer. 2008. Impact of bark beetle (Ips typographus L.) disturbance on timber production and carbon sequestration in different management strategies under climate change. Forest Ecology and Management 256:209–220.

Sherriff, R. L., E. E. Berg, and A. E. Miller. 2011. Climate variability and spruce beetle (Dendroctonus rufipennis) outbreaks in south-central and southwest Alaska. Ecology 92:1459–1470.

Shugart, H. H. 1984. A Theory of Forest Dynamics: The Ecological Implications of Forest Succession Models. Springer Science & Business Media, New York, NY.

Shugart, H. H. 1998. Terrestrial Ecosystems in Changing Environments. Cambridge University Press, Cambridge, UK.

Shugart, H. H., and F. I. Woodward. 2011. Global Change and the Terrestrial Biosphere. Wiley-Blackwell, Sussex, UK.

Shuman, J. K., and H. H. Shugart. 2009. Evaluating the sensitivity of Eurasian forest biomass to climate change using a dynamic vegetation model. Environmental Research Letters 4:045024.

Shuman, J. K., H. H. Shugart, and O. N. Krankina. 2014. Testing individual-based models of forest dynamics: Issues and an example from the boreal forests of Russia. Ecological Modelling 293:102–110.

Shuman, J. K., N. Tchebakova, E. Parfenova, A. Soja, H. H. Shugart, E. Ershov, and H. Holcomb. 2015. Forest forecasting with vegetation models across Russia. Canadian Journal of Forest Research 45:175–184.

Sibold, J. S., T. T. Veblen, K. Chipko, L. Lawson, E. Mathis, and J. Scott. 2007. Influences of secondary disturbances on lodgepole pine stand development in Rocky Mountain National Park. Ecological Applications 17:1638–1655.

Sprugel, D. G. 1984. Density, Biomass, Productivity, and Nutrient-Cycling Changes During Stand Development in Wave-Regenerated Balsam Fir Forests. Ecological Monographs 54:165.

Stottlemyer, R., and C. A. Troendle. 2001. Effect of canopy removal on snowpack quantity and quality, Fraser Experimental Forest, Colorado. Journal of Hydrology 245:165–176.

Tansley, A. G. 1935. The use and abuse of vegetational concepts and terms. Ecology 16:284–307.

USFS. 2015. Aerial survey highlights for Colorado 2014. http://www.fs.usda.gov/detail/r2/forest-grasslandhealth/?cid=stelprd3827262.

Veblen, T. T. 1986. Age and Size Structure of Subalpine Forests in the Colorado Front Range. Bulletin of the Torrey Botanical Club 113:225.

Veblen, T. T., K. S. Hadley, E. M. Nel, T. Kitzberger, M. Reid, and R. Villalba. 1994. Disturbance Regime and Disturbance Interactions in a Rocky Mountain Subalpine Forest. The Journal of Ecology 82:125.

Veblen, T. T., K. S. Hadley, M. S. Reid, and A. J. Rebertus. 1991. The Response of Subalpine Forests to Spruce Beetle Outbreak in Colorado. Ecology 72:213.

Wichmann, L., and H. P. Ravn. 2001. The spread of Ips typographus (L.)(Coleoptera, Scolytidae) attacks following heavy windthrow in Denmark, analysed using GIS. Forest Ecology and Management 148:31–39.

Wooldridge, G. L., R. C. Musselman, R. A. Sommerfield, D. G. Fox, and B. H. Connell. 1996. Mean wind patterns and snow depths in an alpine-subalpine ecosystem as measured by damage to coniferous trees. Journal of Applied Ecology 33:100–108.

Wulder, M. A., J. C. White, B. Bentz, M. F. Alvarez, and N. C. Coops. 2006. Estimating the probability of mountain pine beetle red-attack damage. Remote Sensing of Environment 101:150–166.

Yan, X., and H. H. Shugart. 2005. FAREAST: a forest gap model to simulate dynamics and patterns of eastern Eurasian forests: Simulation of eastern Eurasian forests. Journal of Biogeography 32:1641–1658.

Chapter 2. The University of Virginia Forest Model Enhanced: Model Description, Updates, and Parameterization

Individual-based gap models, which simulate the establishment, growth, and death of individual trees on patches of a landscape, have the capability to simulate and track detailed forest dynamics through time (Shugart 1998). These models simulate the annual diameter

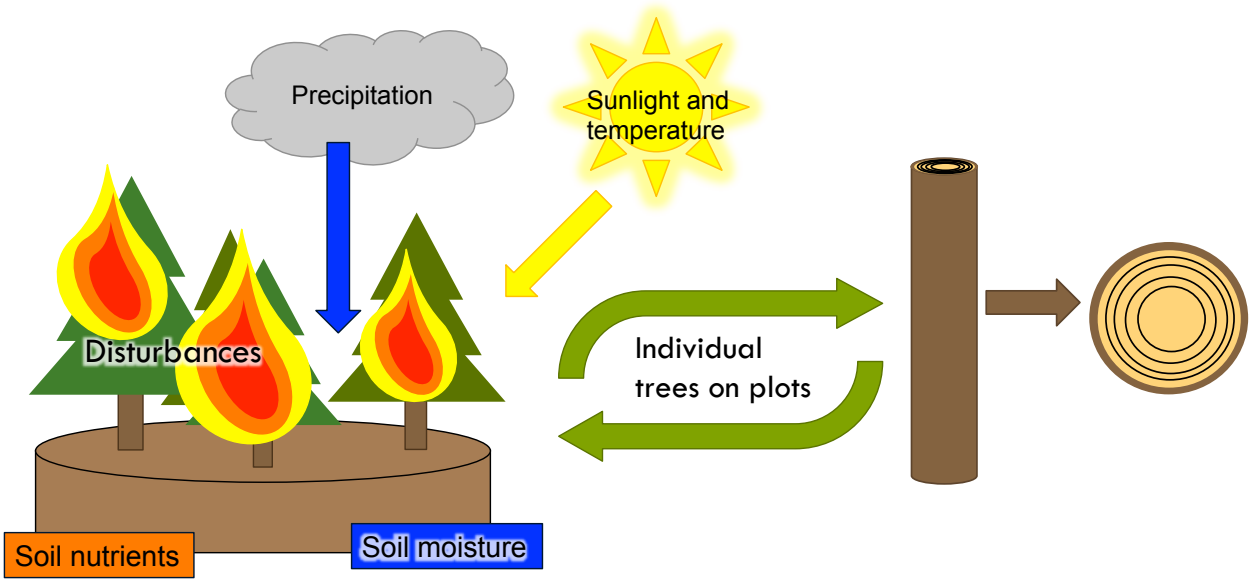

Figure 2.1. Schematic of how individual tree-based models function. Environmental variables such as climate, site and soil characteristics, and disturbances determine the diameter increment growth of each tree on a plot each year.

increment growth for individual trees on patches, or "gaps," about the size of influence of a dominant tree crown (Bugmann 2001, Shugart and Woodward 2011). This annual growth is generally based on climate and soil processes, light, various stressors, and tree size (Fig. 2.1). Trees compete with one another through shading and appropriation of resources. Simulated trees die due to decreased growth, and new trees establish in their place based on site, climate, and light conditions (Shugart and Woodward 2011).

Gap models are valuable tools for studying forest dynamics because they simulate small-scale annual processes, such as tree diameter increment growth and competition, which can be

aggregated to larger spatial scales (i.e. multiple hectares) and for extended time scales (i.e. hundreds of years of simulation) (Fig. 2.2). Thus, gap models can simulate emergent properties of forest ecosystems that arise from multiple interacting processes at different time and space scales.

In this study, the individual-based gap model University of Virginia Forest Model Enhanced (UVAFME) is used to simulate forest dynamics over time within the southern Rocky Mountains landscape.

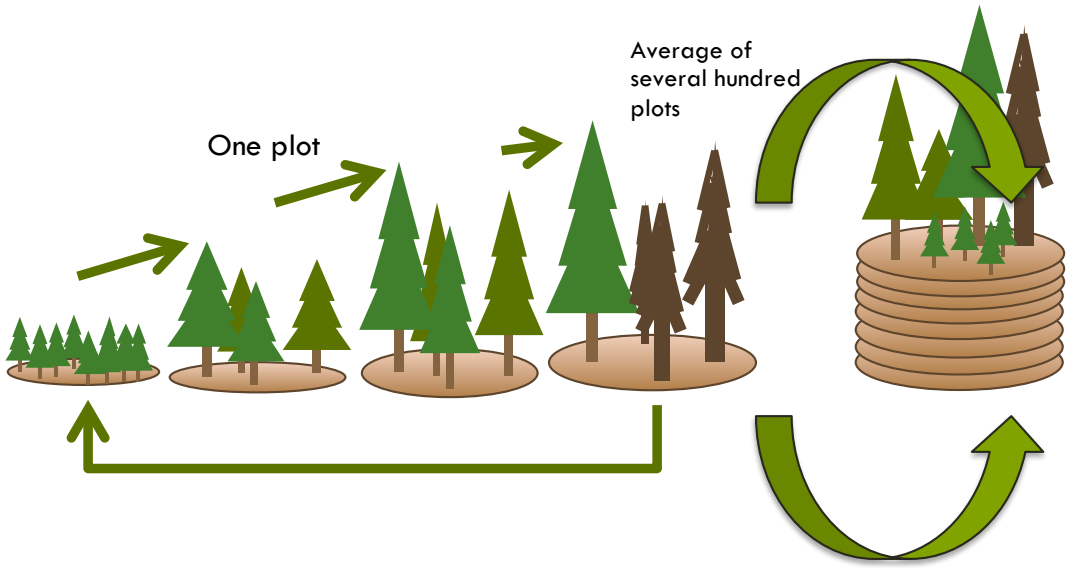

Figure 2.2. Forest dynamics simulated by individual-based models at the plot scale are aggregated over several hundred plots to represent forest dynamics at the landscape scale.

Model Description

The University of Virginia Forest Model Enhanced (UVAFME) is an object-oriented extension of the individual-based gap model FAREAST. Detailed descriptions of the parameters and functioning of UVAFME can be found in the Appendix of this work. FAREAST was originally developed by Yan and Shugart (2005) for use in boreal Eurasia and has been successfully applied and tested within this region. Yan & Shugart tested the FAREAST model's

ability to simulate forest composition and zonation along an elevation gradient on Changbai Mountain in China, and subsequently tested its ability to simulate different forest types at 31 sites across eastern Russia (Yan and Shugart 2005). Forest composition and biomass output from both tests showed agreement with forest inventory data, demonstrating the model's ability to simulate forest compositional dynamics at both the local and regional scales. Additional model validation against 44 well-studied locations across all of Russia showed that results capture natural biomass accumulation rates without recalibration, with appropriate responsiveness to local site and climate variability, and demonstrate strong correlations to inventoried forest biomass (Shuman et al. 2014, 2015). Model output also compared favorably to the bioclimatic envelope model RuBCLiM when applied at 31,000 sites across Russia (Shuman et al. 2015).

As a gap model, UVAFME computes the annual growth, death, and establishment of each tree on independent patches, which together comprise a forested landscape. Each patch is about the size of influence of a dominant tree crown (500 m^2). The annual output of each simulated patch resembles a sample area with a tally of the diameter and species of each tree on the plot. Several hundred such simulated patches are averaged to produce an expected mean biomass and species composition of a forested landscape through time.

The species composition and biomass of each plot, and as such of the whole landscape, are affected by competition between individual trees for resources. Competition between trees is simulated through species- and tree size-specific differences in shade, drought, nutrient, and temperature tolerances. Throughout the simulation, changes in species' seedling banks and to individual tree processes (i.e. growth, regeneration, and biomass accumulation) are functions of changes in the vertical light profile, temperature, moisture, and nutrients. Species-specific input parameters determine the annual optimal diameter increment growth of each simulated tree as a

function of tree size. This optimal increment growth is then modified according to the environment (i.e. light, temperature, and resource availabilities interacting with species-specific tolerances). In the individual-tree competition, different species and tree sizes have resource-specific advantages over others. Competition thus occurs both between conspecific individuals as well as between individuals of differing species. The probability of a tree dying is based on growth-related stress, and new trees regenerate based on resource availability and species-specific resource requirements. Soil conditions for each plot, such as soil water content, soil carbon, and plant available nitrogen, are then computed annually using a coupled three soil-layer water, carbon, and nitrogen submodel, driven by climate, environmental conditions, and available nutrients. UVAFME also simulates tree mortality from stress or old age and tree response to disturbances by fire and windthrow.

Inputs to UVAFME include climate information (mean monthly temperature minima and maxima and precipitation), site and soil information (such as elevation, slope, organic and A layer carbon and nitrogen contents, and organic and A layer field capacities) and species-specific parameters such as drought, temperature, shade, and nutrient tolerances, maximum height, and maximum diameter at breast height (DBH). UVAFME output includes the species, DBH, and height of each tree on each plot, making it directly comparable to forest inventory data. Output from UVAFME can then be aggregated to derive forest characteristics such as biomass (tonnes C ha^{-1}), basal area (m^2 ha^{-1}), size structure (stems size $class^{-1}$ ha^{-1}), species composition and dominance, LAI, and DBH and height distributions. Thus, output from UVAFME can be used to make inferences about the effects of various management, climate, or disturbance scenarios on vegetation composition and structure.

Model Updates

Several modifications were made to UVAFME to update it to the Rocky Mountains region. UVAFME simulates soil moisture and soil decomposition processes through a coupled three-layer (organic, A, and B layers) soil bucket model. Inputs to the soil layers come in the form of precipitation and potential evapotranspiration (PET) from the climate subroutine, and carbon and nitrogen inputs from the tree growth and death subroutines. UVAFME then simulates soil moisture, C, and N in each soil layer based on these inputs and input soil characteristics (i.e. field capacity, wilting point, slope, etc.). A simple snowmelt submodel (Eq. 2.1) was implemented within the soil subroutine of this version of UVAFME using degree-day method equations from Singh et al. (2000) in order to simulate accumulation and melting of snow. If the air temperature is below 5°C, precipitation for that day is assumed to be snow, and is accumulated in the snowpack. If the temperature is above the base temperature (t_b, generally set to 0°C), the thaw for that day (M, in mm) is calculated as:

$$M = c_m(t_a - t_b) \quad (2.1)$$

where c_m is the melt factor (mm degree-day Celsius^{-1}), based on site characteristics (DeWalle et al. 2002), and t_a is the mean air temperature (°C). This meltwater is then transferred to the soil water pool for further soil moisture modeling. Additionally, errors associated with the previous version of the soil moisture routine (e.g. incorrect ordering of the three different soil layers, misuse of "dummy" vs. "actual" subroutine arguments, and lack of checks for negative/positive values) were corrected. A check for the initialization (i.e. at year 0) of soil moisture values was also added such that the soil moisture would not be initialized to values above a site's field capacity. The addition of snowpack accumulation and snowmelt within UVAFME allows for better representation of soil moisture dynamics within the Rocky

Mountains subalpine zone, where most of the precipitation falls as snow in the fall and winter, and melts in spring and summer (Serreze et al., 1999).

To better track vegetation response to changing climate conditions, the original equation for the effect of growing degree-days (GDD) on tree growth was modified from a parabolic response curve (Eq. 2.2) to an asymptotic response curve (Eq. 2.3).

$$f_{temp} = \begin{cases} 0, & GDD \leq DD_{min} \\ 0, & GDD \geq DD_{max} \\ \left(\frac{GDD - DD_{min}}{DD_{opt} - DD_{min}}^{a}\right)\left(\frac{DD_{max} - GDD}{DD_{max} - DD_{opt}}^{b}\right), & DD_{min} < GDD < DD_{max} \end{cases} \quad (2.2)$$

$$f_{temp} = \begin{cases} 0, & GDD \leq DD_{min} \\ 1, & GDD \geq DD_{opt} \\ \left(\frac{GDD - DD_{min}}{DD_{opt} - DD_{min}}^{a}\right)\left(\frac{DD_{max} - GDD}{DD_{max} - DD_{opt}}^{b}\right), & DD_{min} < GDD < DD_{opt} \end{cases} \quad (2.3)$$

where f_{temp} is the effect of GDD on tree growth, GDD is the annual growing degree day sum that year, DD_{min}, DD_{opt}, and DD_{max} are the minimum, optimum, and maximum tolerable growing degree day sums, $a = (DD_{opt} - DD_{min})/(DD_{max} - DD_{min})$, and $b = (DD_{max} - DD_{opt})/(DD_{max} - DD_{min})$.

This change means that trees are negatively affected by growing degree-days below their optimum tolerable GDD, but unaffected by growing degree-days above DD_{opt}. The parabolic temperature response curve (Eq. 2.2) has been criticized for predicting extremely low growth at species' warmest range limits, in contrast to empirical studies, which often find that, in the absence of drought, trees grow quite well at their warmer range limits (Korzukhin et al. 1989, Loehle 2000, Bugmann 2001). By using an asymptotic temperature response curve, simulated trees that are experiencing high temperatures are only negatively affected by potential increases in drought stress and tree – tree competition. The switch from parabolic to asymptotic allows for

a move away from a "climate envelope" approach to species distribution modeling, and allows for testing of species responses to increasing temperatures often associated with climate change, without a need to assume trees cannot grow at temperatures above their normal range.

FAREAST originally used the multiplicative method (Eq. 2.4) to aggregate the different growth-limiting factors (i.e. shade, drought, temperature, and nutrient stress, all 0 to 1 in scale) to create an overall growth-limiting factor. In this method, each factor is multiplied together and the final growth-limiting factor is used to reduce annual optimal diameter increment growth, based on allometric equations, to an actual increment growth for that year.

$$f_{growth} = f_{shade} \cdot f_{drought} \cdot f_{temp} \cdot f_{nutrient} \quad (2.4)$$

$$f_{growth} = \min (f_{shade}, f_{drought}, f_{temp}, f_{nutrient}) \quad (2.5)$$

The multiplicative method has been criticized for resulting in growth rates that are far too low (Bugmann 2001). A key issue with this method is that the more growth-limiting factors considered, the harsher the environment becomes with respect to annual tree growth. As did Pastor and Post (1986) in their model LINKAGES, the growth-limitation in this version of UVAFME is calculated using a Liebig's Law of the Minimum approach. Here, the smallest of the stress-specific growth factors is chosen as the overall growth-limiting factor (Eq. 2.5), meaning that an individual tree's growth is hindered by only the most limiting environmental factor. This method is more representative of tree response to stressors, especially in the Rocky Mountains region, where many of the species have adapted to the harsh climate and conditions of the high elevations (Daubenmire 1978).

The number of years a tree can experience extremely low diameter increment growth (i.e. less than 0.03 cm) without potential stress-related mortality was also modified to accommodate

the harsh conditions of the Rocky Mountains landscape. In the previous version of UVAFME, trees that experienced DBH growth less than a certain growth threshold in any given year had the possibility for stress-related mortality that same year, with a probability based on their species-specific stress tolerance, ranging from a 31 to 43% chance for mortality. UVAFME was updated to include a counter for low growth ($mort\_count$), which is 0 when a tree has diameter increment growth above the growth threshold, and increases by 1 each year the tree has low growth. This counter is also set back to 0 if a tree has growth higher than the growth threshold, even if in the previous year it had low growth. In this new version, only trees that have a mortality counter of 3 or higher have the possibility for stress-related mortality. This addition resulted in higher biomass in model simulations in the Rocky Mountains, mostly for subdominant species.

The effect of fire disturbance on tree mortality and tree regeneration within the Rocky Mountains depends on tree species as well as tree size (Ryan and Reinhardt 1988). Wildfire significantly affects species composition and size structure within the Rocky Mountains landscape (Veblen et al. 1994, Sibold et al. 2007) and is an important feature of modeling forest dynamics in this region. The fire module for UVAFME was updated so that the size- and species-level effects of fire on tree mortality and regeneration could be simulated. Previously, any fire disturbance would kill all trees on a plot. In this new module, fire kills trees based on their size and their species-specific bark thickness coefficient, and affects the regeneration of trees based on their species-specific fire regeneration parameter. Fire in UVAFME is stochastic and based on the site-specific fire return interval. With fire occurrence, UVAFME first calculates the intensity level of the fire (f_{cat}) using a normally distributed random number between 0.0 and 12.0, with a site-specific mean corresponding to the site's average fire intensity. Low-level,

surface fires have a fire category between 0.0 and 4.0, mid-level fires have a fire category between 5.0 and 8.0, and high-level, crown fires have a fire category between 9.0 and 12.0. UVAFME then calculates which trees will die and which will survive. The model first calculates the scorch height of the fire (Eq. 2.6) and percent of crown volume scorched (Eq. 2.7) of each tree based on equations from Keane et al. (2011) and Van Wagner (1973).

$$SH = \frac{a \cdot FI^{1.1667}}{(T_{kill} - T_{amb})[b \cdot FI + c \cdot U^3]^{0.5}} \quad (2.6)$$

$$CK = 100 \frac{CS(2CL - CS)}{CL^2} \quad (2.7)$$

where SH is the scorch height of the fire (m), CK is the percent crown volume scorched (%), CL is the crown length (m), CS is the scorch length (m), and FI is the fire intensity (kW m^{-1}, calculated as $FI = 1000 f_{cat}$). The empirical parameters a (0.74183 m $°C^{-1}$), b (0.025574 (kW m^{-1}) $^{4/3}$), and c (0.021433 km^{-1} hr (kW m^{-1})$^{7/9}$), are based on values from Keane et al. (2011), as are the values for the ambient fire temperature (T_{amb}, 20°C) and lethal fire temperature (T_{kill}, 60°C). The exponent in the numerator of the equation for scorch height (Eq. 2.6) is from Van Wagner (1973), based on a two-thirds power law relationship between scorch height and fire intensity. Wind speed (U, km hr^{-1}) is a randomly generated value between 0 and 32.0, based on the default value in Reinhardt and Crookston (2003).

All trees less than 12.7 cm in diameter die regardless of fire intensity or bark thickness, based on Bonan (1989). Trees larger than 12.7 cm may die based on percent scorch volume (CK), bark thickness, and tree diameter. Species-specific bark thickness coefficients (b_{thick}, cm

bark cm DBH^{-1}) are adapted from values in Keane et al. (2011). The probability for tree mortality (Eq. 2.8), based on the fire mortality from Ryan and Reinhardt (1988), is calculated as:

$$p_{fire} = \frac{1}{1+e^{[-1.941+6.32(1-e^{-b_{thick}DBH})-0.00053CK^2]}} \quad (2.8)$$

where p_{fire} is the probability of mortality due to cambial death and percent of crown scorch. These equations have been successfully used to predict crown scorch and fire mortality within forests of the western United States (Ryan and Reinhardt 1988, Reinhardt and Crookston 2003, Hood et al. 2007, Keane et al. 2011) and are a valuable addition to UVAFME's disturbance submodels.

The seedbank for each species is also updated based on species-specific fire regeneration tolerance (1-6; 1 being the most tolerant, and 6 being the least tolerant). If the fire category (f_{cat}) is 11.0 or higher, a five-year wait occurs before new seedlings and saplings can regenerate. Otherwise, each species' seedbank is multiplied by the variable f_{fire}, which ranges from 0.001 to 100.0, depending on the species' regeneration tolerance to fire. Thus, fire increases the seedbank of species that have a high regeneration tolerance to fire, and decreases the seedbank of species that have a low regeneration tolerance to fire. More information on the updated fire submodel can be found in the Appendix.

Study Sites

This project focuses on the climate response of the broader southern Rocky Mountains region (Bassman et al. 2003) as well as specific forest dynamics at four subalpine sites in the Wyoming and Colorado Rocky Mountains (Fig. 2.3). These specific sites are the USDA Forest Service, Rocky Mountain Research Station Glacier Lakes Ecosystem Experimental Site

(GLEES), Niwot Ridge/US NR1, USDA Forest Service's Fraser Experimental Forest (FEF), and Wolf Creek Pass. GLEES is located east of the continental divide in the Snowy Range, near Centennial WY (41°22'30"N, 106°15'30"W, 3200 to 3500 m). It is dominated by Engelmann spruce (*Picea engelmannii*) and subalpine fir (*Abies lasiocarpa*), with some lodgepole pine (*Pinus contorta*) and limber pine (*P. flexilis*) (Regan et al. 1997). Average annual precipitation is about 100 cm, and mean annual temperature is about -0.5°C. Niwot Ridge is located 50 miles west of Boulder, CO at 40°1'58.44"N, 105°32'45.60"W. It is situated on the eastern slope of the Colorado Front Range at elevations from 3020 to 3810 m. Annual precipitation is about 70 cm and mean annual temperature is about 2.7°C. The vegetation at this site is also typical of a subalpine forest in this region, dominated by subalpine fir, Engelmann spruce, and lodgepole pine (Sacks et al. 2006). Fraser Experimental Forest is located on the west slope of the continental divide, at 39°50'50"N, 105°54'42"W and at elevations from 2700 to 3400 m. Average precipitation at this site is about 50 cm and average temperature is about 1°C (Elder, 2006, 2005). Vegetation at this site consists of Engelmann spruce, subalpine fir, and lodgepole pine (Stottlemyer and Troendle 2001). Wolf Creek is also

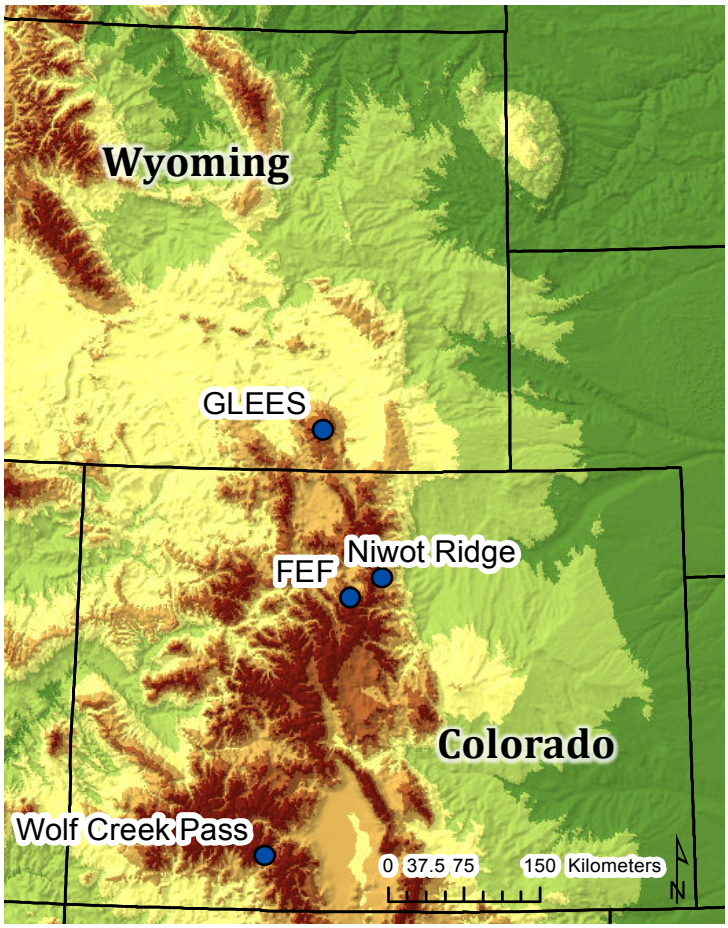

Figure 2.3. Map of study sites.

west of the continental divide and is located in the San Juan Mountains, in southern Colorado at 37°29’24”N, 106°50’24” and at elevations from 2800 to 3600 m. Average precipitation at Wolf Creek is about 110 cm and average temperature is about 1.5°C. Vegetation at this site is comprised of Engelmann spruce, subalpine fir, quaking aspen (*Populus tremuloides*), and Douglas-fir (*Pseudotsuga menziesii*).

Model Parameterization

UVAFME was parameterized to the southern Rocky Mountains with climate, site, soil, and species information from the US Forest Service, the National Climatic Data Center (NCDC) and the SNOTEL Network (Elder 2005, 2006, Menne et al. 2012a, 2012b, NCDC 2015), Burns and Honkala (1990), and other scientific literature. Daily precipitation and temperature conditions for the four sites used in simulations by UVAFME are derived from statistical distributions of mean monthly precipitation and temperature for years ranging from 1976 to 2016 for an average of 29 years. Precipitation is also used to update soil water content on a daily basis. Species-specific parameter inputs for eleven major species found in the greater Rocky Mountains landscape (*Juniperus scopulorum*, *Pinus edulis*, *P. contorta*, *P. ponderosa, P. flexilis*, *Pseudotsuga menziesii*, *Populus tremuloides*, *P. angustifolia Abies lasiocarpa*, *Picea engelmannii,* and *P. pungens*; (Peet 1981, Burns and Honkala 1990)) such as maximum age, DBH, and height; stress tolerance levels; and temperature thresholds, are derived from Burns and Honkala (1990) (see Table 2.1). These inputs are used to determine species establishment and growth at different locations.

The inputs for month-specific environmental lapse rates (i.e. change in temperature with elevation) were developed using mean monthly temperature for years ranging from 1967 to 2014 for an average of 26 years at 15 sites across the Rocky Mountains and at elevations ranging from

1690 to 3414 m. These data were used to create an average change in temperature with elevation (°C km^{-1}) for each month. Change in precipitation with elevation (mm km^{-1}) was derived from Marr (1961). These values are comparable to lapse rates found in other studies (Daubenmire, 1943; Peet, 1981), and are used to run UVAFME at different elevations within the Rocky Mountains. Species-specific growing degree day (GDD, i.e. annual sum of mean daily temperatures above 5°C) tolerances were also developed using this lapse rate and information from Peet (1981) and Marr (1961) on the elevation zones of southern Rocky Mountains species. For example, Engelmann spruce (*Picea engelmannii*) is documented as surviving at elevations between 2438 and 3353 m (CSFS, 2016). The derived lapse rates and the temperature data across all 15 weather stations were utilized to create an average minimum and maximum GDD for Engelmann spruce in the southern Rockies.

NDS	0.6	0.5	0.8	0.5	0.7	0.6	0.8	0.5	0.31	0.31	0.7
NDE	0.6	0.5	0.8	0.5	0.7	0.6	0.8	0.56	0.78	0.78	0.7
seed	1	1	1	1	1	1	1	1	100	100	1
invader	1	1	1	1	0.5	0.5	1	0.5	1	1	1
old	1	1	1	1	1	1	1	1	2	1	2

H_{max} (m)	s	g	ρ_w	l_c	DD_{mi}	DD_{opt}	DD_{ma}	shade	drought	nutrient	b_{thick}	fire regen	stress
30	1.03	1.041	0.43	0.5	200	500	1665	1	5	3	0.015	6	2
15	0.69	0.455	0.46	0.5	800	1900	3200	4	1	1	0.015	4	2
40	1.0	0.689	0.45	0.5	250	600	1665	2	4	1	0.022	5	1
38	0.52	0.55	0.45	0.5	600	1550	2300	3	3	3	0.022	3	3
27	0.58	1.19	0.45	0.5	450	900	2500	4	3	1	0.055	1	1
10.7	0.46	0.256	0.45	0.5	800	1900	3200	5	2	1	0.03	3	2
40	0.56	0.579	0.45	0.5	800	1600	2500	3	3	1	0.063	1	2
15	0.33	0.157	0.46	0.5	300	1600	3000	3	3	3	0.03	2	1
22	0.61	0.986	0.42	0.316	350	1500	2200	5	3	2	0.014	1	4
18	0.47	0.82	0.42	0.316	600	1550	2500	5	5	2	0.014	3	3
49	0.66	1.054	0.48	0.5	700	1400	2300	3	3	1	0.063	2	2

Species Name	AGE_{max}	DBH_{max} (cm)
Abies lasiocarpa	250	61
Juniperus scopulorum	300	43
Picea engelmanii	500	95
Picea pungens	600	150
Pinus contorta	400	46
Pinus edulis	400	46
Pinus ponderosa	600	127
Pinus flexilis	900	90
Populus tremuloides	200	75
Populus angustifolia	200	76
Pseudotsuga menziesii	400	152

Table 2.1. Relevant parameter input for the eleven species used in UVAFME simulations. AGE_{max}, DBH_{max}, and H_{max} are the species-specific maximum age (yr), diameter at breast height (cm), and height (m); *s* and *g* are growth parameters; DD_{min}, DD_{opt}, and DD_{max}, are the minimum, optimum, and maximum growing degree days for the species; *shade* is the relative shade tolerance of the species, from 1 to 5, 5 being the least tolerant; *drought* is the relative drought tolerance of the species, from 1 to 6, 6 being the least tolerant; *nutrient* is the relative nutrient availability tolerance of the species, from 1 to 3, 3 being the least tolerant, b_{thick} is the bark thickness parameter (cm bark cm DBH^{-1}); *fire regen* is the relative response of regeneration to fire, from 1 to 6, 6 being the least tolerant; *stress* is the relative stress tolerance of the species, from 1 to 5, 5 being the least tolerant; *old* is the likelihood of that species surviving to its maximum age, from 1 to 3, 3 being the lowest probability; *invader* is the probability of seeds "invading" from nearby locations, with wind-dispersed seeds generally having a probability of 1; *seed* is the seed numbers from inside the plot, and is related to seed and dispersal type (i.e. cones = 1, samaras/maple keys = 10, wind-dispersed = 100); *NDE* is the coefficient for annual reduction of the seed bank, 0 to 1; and *NDS* is the coefficient for annual reduction of seedlings, 0 to 1.

References

Bassman, J. H., J. D. Johnson, L. Fins, and J. P. Dobrowolski. 2003. Rocky Mountain ecosystems: diversity, complexity and interactions. Tree Physiology 23:1081–1089.

Bonan, B. G. 1989. A computer model of the solar radiation, soil moisture, and soil thermal regimes in boreal forests. Ecological Modelling 45:275–306.

Bugmann, H. 2001. A review of forest gap models. Climatic Change 51:259–305.

Burns, R. M., and B. H. Honkala. 1990. Silvics of North America: 1. Conifers; 2. Hardwoods. Agricultural Handbook 654. U.S. Department of Agriculture, Forest Service, Washington, DC. vol. 2 877 p.

CSFS, C. S. F. S. 2016. Colorado's Major Tree Species: Characteristics and Descriptions. https://csfs.colostate.edu/colorado-trees/colorados-major-tree-species/.

Daubenmire, R. F. 1943. Vegetational zonation in the Rocky Mountains. The Botanical Review 9:325–393.

Daubenmire, R. F. 1978. Plant Geography With Special Reference to North America. Academic Press, New York, NY.

DeWalle, D. R., Z. Henderson, and A. Rango. 2002. Spatial and temporal variations in snowmelt degree-day factors computed from snotel data in the upper Rio Grande Basin. Western Snow Conference 2002:73–81.

Elder, K. 2005. Fraser Experimental Forest Headquarters Station daily precipitation data: 1976-2003. Fort Collins, CO: U.S. Department of Agriculture, Forest Service, Rocky Mountain Research Station.

Elder, K. 2006. Fraser Experimental Forest Headquarters station horly temperature data: 1976-2003. Fort Collins, CO: U.S. Department of Agriculture, Forest Service, Rocky Mountain Research Station.

Hood, S. M., C. W. McHugh, K. C. Ryan, E. Reinhardt, and S. L. Smith. 2007. Evaluation of a post-fire tree mortality model for western USA conifers. International Journal of Wildland Fire 16:679–689.

Keane, R. E., R. A. Loehman, and L. M. Holsinger. 2011. The FireBGCv2 Landscape Fire Succession Model: A research simulation platform for exploring fire and vegetation dynamics. USDA Forest Service General Technical Report RMRS-GTR-55:145.

Korzukhin, M. D., A. E. Rubinina, G. B. Bonan, A. M. Solomon, and M. Y. Antonovsky. 1989. The Silvics of Some East European and Siberian Boreal Forest Tree Species. WP-89-56, International Institute for Applied Systems Analysis, Laxenburg, Austria.

Loehle, C. 2000. Forest ecotone response to climate change: sensitivity to temperature response functional forms. Canadian journal of forest research 30:1632–1645.

Marr, J. W. 1961. Ecosystems of the east slope of the Front Range in Colorado. University of Colorado Press.

Menne, M. J., I. Durre, B. Korzeniewski, S. McNeal, K. Thomas, X. Yin, S. Anthony, R. Ray, R. S. Vose, B. E. Gleason, and T. G. Houston. 2012a. Global Historical Climatology Network Daily (GHCN-Daily), Version 3.22. NOAA National Climatic Data Center.

Menne, M. J., I. Durre, R. S. Vose, B. E. Gleason, and T. G. Houston. 2012b. An overview of the Global Historical Climatology Network-Daily Database. Journal of Atmospheric and Oceanic Technology 29:897–910.

NCDC, N. N. C. for E. I. 2015. Climate Data Online: Dataset Discovery. http://www.ncdc.noaa.gov/cdo-web/datasets.

Pastor, J., and W. M. Post. 1986. Influence of climate, soil moisture, and succession on forest carbon and nitrogen cycles. Biogeochemistry 2:3–27.

Peet, R. K. 1981. Forest vegetation of the Colorado front range. Vegetatio 45:3–75.

Regan, C. M., R. C. Musselman, and J. D. Haines. 1997. Vegetation of the Glacier Lakes Ecosystem Experiments Site. Page 36. USDA Forest Service, Rocky Mountain Research Station, Fort Collins, CO.

Reinhardt, E., and N. Crookston, editors. 2003. The fire and fuels extension to the forest vegetation simulator. Gen. Tech. Rep. RMRS-GTR-116. Ogden, UT: Department of Agriculture, Forest Service, Rocky Mountain Research Station:209.

Ryan, K. C., and E. D. Reinhardt. 1988. Predicting Postfire Mortality of Seven Western Conifers. Canadian Journal of Forest Research 18:1291–1297.

Sacks, W. J., D. S. Schimel, R. K. Monson, and B. H. Braswell. 2006. Model-data synthesis of diurnal and seasonal CO2 fluxes at Niwot Ridge, Colorado. Global Change Biology 12:240–259.

Shugart, H. H. 1998. Terrestrial Ecosystems in Changing Environments. Cambridge University Press, Cambridge, UK.

Shugart, H. H., and F. I. Woodward. 2011. Global Change and the Terrestrial Biosphere. Wiley-Blackwell, Sussex, UK.

Shuman, J. K., H. H. Shugart, and O. N. Krankina. 2014. Testing individual-based models of forest dynamics: Issues and an example from the boreal forests of Russia. Ecological Modelling 293:102–110.

Shuman, J. K., N. Tchebakova, E. Parfenova, A. Soja, H. H. Shugart, E. Ershov, and H. Holcomb. 2015. Forest forecasting with vegetation models across Russia. Canadian Journal of Forest Research 45:175–184.

Sibold, J. S., T. T. Veblen, K. Chipko, L. Lawson, E. Mathis, and J. Scott. 2007. Influences of secondary disturbances on lodgepole pine stand development in Rocky Mountain National Park. Ecological Applications 17:1638–1655.

Singh, P., N. Kumar, and M. Arora. 2000. Degree-day factors for snow and ice for Dokriani Glacier, Garhwal Himalayas. Journal of Hydrology 234:1–11.

Stottlemyer, R., and C. A. Troendle. 2001. Effect of canopy removal on snowpack quantity and quality, Fraser Experimental Forest, Colorado. Journal of Hydrology 245:165–176.

Van Wagner, C. E. 1973. Height of crown scorch in forest fires. Canadian Journal of Forest Research 3:373–378.

Veblen, T. T., K. S. Hadley, E. M. Nel, T. Kitzberger, M. Reid, and R. Villalba. 1994. Disturbance Regime and Disturbance Interactions in a Rocky Mountain Subalpine Forest. The Journal of Ecology 82:125.

Yan, X., and H. H. Shugart. 2005. FAREAST: a forest gap model to simulate dynamics and patterns of eastern Eurasian forests: Simulation of eastern Eurasian forests. Journal of Biogeography 32:1641–1658.

Chapter 3. Validation and Application of a Forest Gap Model to the Southern Rocky Mountains Region

Introduction

Forests in the Rocky Mountains are a crucial part of the North American carbon budget (Schimel et al. 2002), but increases in disturbances such as insect outbreaks and fire, in conjunction with climate change, threaten their vitality (Joyce et al. 2014). Mean annual temperatures in the western United States have increased by 2°C since 1950 (Meehl et al. 2012), and the higher elevations are warming faster than the rest of the landscape (Wang et al. 2014). It is predicted that this warming trend will continue, and that by the end of this century, nearly 50% of the western US landscape will have climate profiles with no current analog within that region (Rehfeldt et al. 2006, Bentz et al. 2010).

Water-limited systems, such as much of the western US, are vulnerable to drought resulting from warmer temperatures (Hicke et al. 2002). Recently, there have been large-scale die-off events related to rising temperatures and water stress in western forests (Anderegg et al. 2012, Hicke and Zeppel 2013, Joyce et al. 2014, McDowell and Allen 2015). A severe drought in northern New Mexico in the 1950s resulted in widespread mortality of ponderosa pine (*Pinus ponderosa*) and a shift upwards in the transition zone between pinyon pine (*P. edulis*)-juniper (*Juniperus spp.*) woodland and ponderosa pine forest (Allen and Breshears 1998), and a regional-scale drought from 2002 to 2003 within the western US resulted in high mortality of pinyon pine (Breshears et al. 2005). Trees are more vulnerable to drought at higher temperatures (Adams et al. 2009). Thus, even if the frequency of prolonged low-precipitation intervals across the Rocky Mountains does not increase in the future, higher temperatures could lead to drought effects through increased water demand, which may then lead to higher tree mortality.

Vegetation patterns of the Rocky Mountains are strongly driven by climate, particularly by elevation gradients in temperature and moisture (Peet 1981, Korner 1998, Bugmann 2001a). Disturbances are also dominant and integral components of the Rocky Mountains that affect the species composition, size-structure, and stand age of vegetation (Hadley and Veblen 1993, Veblen et al. 1994, Sibold et al. 2007). Major disturbances include fire, windthrow, and insect outbreaks (Peet 1981), which can affect and interact with each other (Veblen et al. 1994, Rasmussen et al. 1996, Dale et al. 2001, Jenkins et al. 2012). Climate change is predicted to result in an increase in the frequency and severity of disturbances within the Rocky Mountains (Dale et al. 2001, Bentz et al. 2010), further influencing the future of western forests.

It is difficult to predict how vegetation will respond to climate change alone and with concurrent disturbances. Plants are able to respond to changing climate at multiple spatial and temporal scales. Over short time and space scales, plants may respond to water stress through stomatal closure, leading to lower transpiration and canopy conductance (Katul et al. 2012). While elevated atmospheric CO_2 may increase plant water use efficiency (Neilson et al. 2005), this drought-ameliorating effect may be dampened by nutrient limitation (Smith and Dukes 2013). Over longer time and space scales, changing climate may lead to shifts in species' optimal ranges (Shugart and Woodward 2011). Increased disturbances could accelerate these shifts by opening up canopies for different species to dominate the region (McKenzie et al. 2009). However, within the complex terrain of the Rocky Mountains, these shifts may be hindered by lack of available space for upward migration (Bell et al. 2014).

The complex interactions between climate, vegetation, and disturbances in this region make parsing the relative effects of these drivers difficult. Gap models are based on the forest dynamics involved in the competitive aftermath of the death of a large, dominant tree (Watt

1947, Shugart 1984) and are able to simulate small-scale tree responses to their environment, climate and disturbances, tree to tree competition, as well as larger-scale successional dynamics (Shugart and Woodward 2011). For these reasons, they have been successfully used to study the response of forests to shifting climate and disturbance regimes (Lasch and Lindner 1995, Bugmann 2001b, Keane et al. 2001, Shuman and Shugart 2009). Since the creation of the original gap model, JABOWA (Botkin et al. 1972), others like it have been developed, each with its own set of governing processes and assumptions (Bugmann and Solomon 2000, Bugmann 2001b). In general, the relatively simple equations and moderate number of parameters of forest gap models make them adaptable to a wide range of forest types (Waldrop et al. 1986). However, model validation is necessary to ensure the model is performing well in a given location and climate.

The goals of this study are to evaluate the performance of the individual-based gap model UVAFME within the southern Rocky Mountains and to determine how changing climate may affect the vegetation within this region. After the tests on UVAFME's performance, a temperature sensitivity test is conducted to investigate how species zonation and species-specific biomass within the region may respond to increasing temperatures. In this sensitivity test, temperature is also cooled back to present values after a period of stabilization at the elevated values. This cooling is conducted to determine how persistent the response to climate change might be and whether vegetation of the southern Rockies might be able to recover from elevated temperatures if the climate were to return to its current state. This type of temperature sensitivity test has not been conducted in this region as of yet, and is only possible with an individual tree-based model such as UVAFME, capable of capturing the interactions between climate, vegetation, and disturbances at multiple spatiotemporal scales.

Methods

Study sites and inventory data

Four subalpine sites in the Wyoming and Colorado Rocky Mountains were used for this study (Fig. 3.1): the Glacier Lakes Ecosystem Experimental Site (GLEES), Niwot Ridge, Fraser Experimental Forest, and Wolf Creek Pass. Site descriptions for each of these sites can be found in Chapter 2 of this work. Forest inventory data on species, diameter at breast height (DBH), and tree status (i.e. alive, dead, infested, etc.) for each tree were collected at GLEES by the US Forest Service between 1989 and 1991 and between 2010 and 2012, at plot sizes ranging from 100 to 200 m^2 (J. Negron, *pers. comm*). Inventory data in the form of species, DBH, and status were also collected at Wolf Creek Pass by researchers at Colorado State University in 2015 in 400 m^2 plots (J. Sibold, *pers. comm.*). These inventory data were used in this study used to quantitatively validate model performance at these two sites. For the GLEES data, if plots had been sampled during both inventory periods, only the data from the latest sampling date were used. There was no available inventory data for either Niwot Ridge or Fraser Experimental Forest, and thus model output at

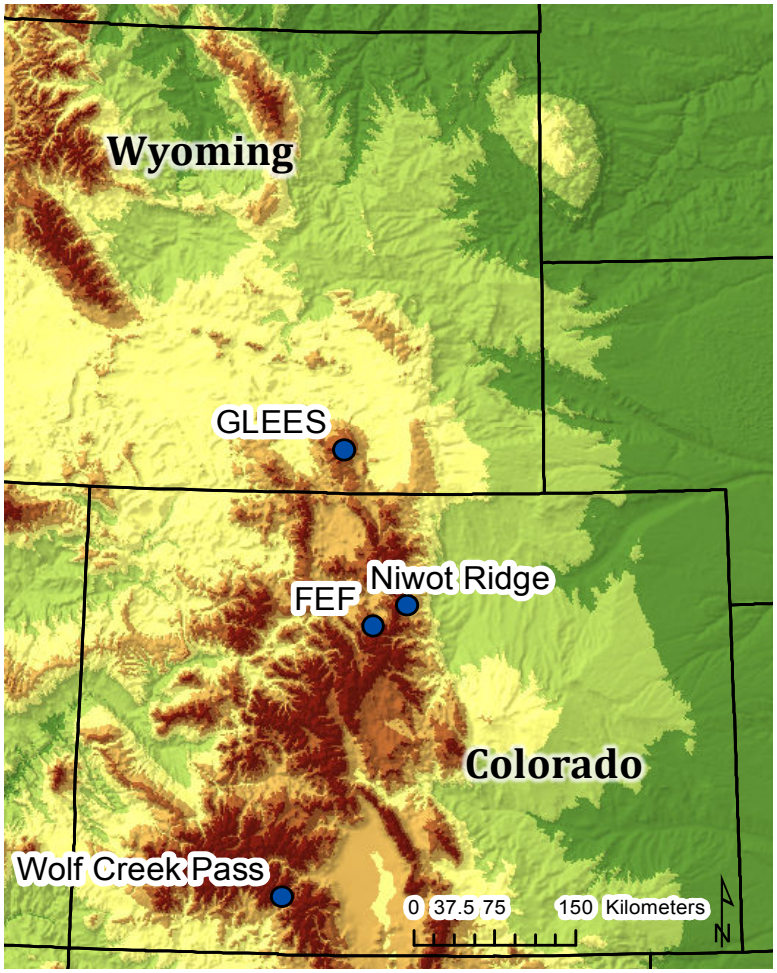

Figure 3.1. Map of study sites.

those sites were compared to qualitative descriptions of species composition and successional trajectories for the region.

Model validation

To determine whether the updated UVAFME accurately simulates forest dynamics of the Rocky Mountains, several tests of the model's performance were conducted. The model was first run at successive elevations at both GLEES and Wolf Creek to determine whether UVAFME could predict the expected change in species composition with elevation present in the southern Rockies. Results from elevation tests at GLEES and Wolf Creek represent zonation for the northern and southern extent of the study region, respectively. Even though in reality the specific locations at which the elevation tests were run are not comprised of the full elevation range used and may not include all species present, this study was focused on determining how well UVAFME is able to predict the general species zonation within the region (Daubenmire 1943, Marr 1961, Peet 1981). In these tests, UVAFME was run from 1600 m to 3600 m at 100 m intervals.

Model evaluation involves both model verification, in which the model is tested against a set of observations that were used during parameterization, and model validation, in which model output is compared to an independent set of observations, not used to structure or parameterize the model (Shuman et al. 2014). Model calibration was performed during the verification phase, with small changes in parameter values and internal processes (for example, increasing the number of years a tree can survive at extremely low diameter increment growth) at two elevations (2400 and 3400 m) at GLEES prior to conducting the validation elevation tests. Other than at these two elevations at this location, all additional validation tests are independent of observational data. At each of the 20 elevations, and at both sites, 200 independent plots were

run in a Monte Carlo-style simulation from bare ground for 500 years. Model output at year 500 averaged over all 200 plots reflects the average expected species composition for a mature forest landscape at that elevation. These tests were conducted both without any disturbances on the landscape (at GLEES) and with disturbances by fire and windthrow (GLEES and Wolf Creek). The eleven major tree species found in the southern Rocky Mountains were allowed to grow at each elevation except for pinyon pine (*P. edulis*) at GLEES and lodgepole pine (*P. contorta*) at Wolf Creek, as the geographical ranges of these species do not intersect with these sites. In this test, only the internal mechanics of UVAFME determined which species prospered and dominated at each elevation zone as well as which species failed to grow at a particular elevation. The resultant species zonations thus arose from the resource requirements and climate tolerances of each species as well as competition among trees of different species. The pattern of species composition (based on biomass at year 500) with elevation was then compared to descriptions of zonation expected in a typical mountainside in the southern Rocky Mountains (Marr 1961, Peet 1981).

UVAFME-simulated biomass and size structure were also compared to forest inventory data from GLEES and Wolf Creek. *T*-tests (for biomass) and linear regressions (for size structure) were conducted to determine if model-derived data was significantly different from inventory data on forest structure and composition. In these tests, only species present in a particular site's inventory data were allowed to grow at that site so as to incorporate the influence of the land use and disturbance history on species presence at each site. For these validation tests, at both Wolf Creek and GLEES, the model was again run with 200 independent plots for 500 years. Within the inventory data, species-specific aboveground biomass (tonnes C) for each tree above 3 cm DBH was calculated using updated diameter – biomass equations from Chojnacky et

al. (2014). These data were then aggregated to create species-specific biomass (tonnes C ha^{-1}) for each inventory plot. The current version of UVAFME does not contain disturbances by bark beetles. Information on the bark beetle infestation status of each tree on each plot was collected along with the inventory data, and trees denoted as "beetle killed" were included in the biomass and size structure calculations for each site. There was no plot-specific data on stand age for either site, and so it was assumed that the forests at each location were at a mature, quasi-equilibrium state. Hence, model output at 500 years was compared to the inventory data.

As a final model test, UVAFME was run at all four test sites (Fig. 3.1) for 500 years on 200 independent plots, to determine if successional dynamics and the time series of species-specific biomass changes over time predicted by UVAFME correspond to what is reported for the subalpine zone in the region. Similarly, only species present in the inventory data and site descriptions for a site were allowed to grow at that location.

Climate change test

A temperature sensitivity test was conducted at GLEES to determine what effect climate change might have on the general species zonation of the southern Rocky Mountains region, and how persistent this effect might be. The model was run for 1100 years, using 200 independent plots, from 1600 m to 3600 m at 100 m intervals, as in the elevation validation tests. In these climate change simulations, the model was run with current climate conditions until year 500. At year 500 a 2°C linear increase in temperature was employed over 100 years (i.e. 0.02°C/year), after which climate was allowed to stabilize at these new values for 200 years. At year 800, a 2°C linear decrease in temperature was employed over 100 years, back to current historical values. This climate was then allowed to stabilize for another 200 years. This 2°C increase was chosen as a conservative estimate for climate change. It was conducted to determine how the

biomass and species composition may change with increasing temperatures, and whether the vegetation could transition back to its current state if temperatures were to cool again. Change in precipitation was not included in these simulations, thus any increase in drought-related stress would be due to increasing evaporative demand at the current levels of water availability.

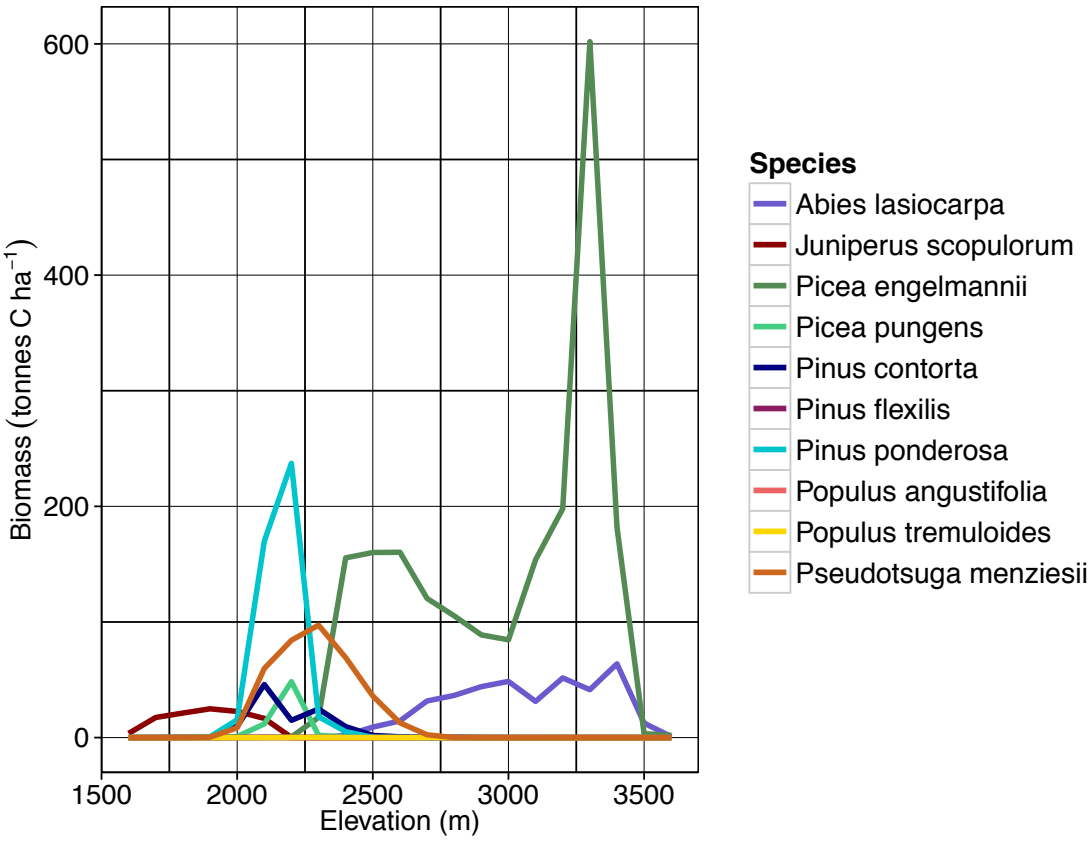

Figure 3.2. UVAFME-simulated biomass (tonnes C ha^{-1}) at year 500 of ten Rocky Mountain species at different elevations at GLEES without disturbances. UVAFME was run every 100 m from 1600 m to 3600 m.

Results and Discussion

Validation

UVAFME-output on species composition with elevation for the simulations including disturbances (Figs. 3.3) is comparable to what is expected for a typical mountainside in the southern Rocky Mountains (Daubenmire 1943, Marr 1961, Peet 1981). A pinyon pine (*P. edulis*)

and/or juniper (*J. scopulorum*) woodland exists at the lower elevations, giving way to a conspicuous ponderosa pine (*P. ponderosa*) belt at about 2000 m. Douglas-fir prospers between about 2000 and 2700 m at the northern site (GLEES), and up to 3000 m at the southern site (Wolf Creek). Ponderosa pine also has a wider range at Wolf Creek than it does at GLEES. Finally, a subalpine zone, dominated by subalpine fir (*A. lasiocarpa*) and Engelmann spruce (*P. engelmannii*), exists at elevations above 3000 m at GLEES and Wolf Creek. GLEES also contains a lodgepole pine (*P. contorta*)-dominated zone between 2700 m and 3000 m, whereas at Wolf Creek lodgepole pine is present, but not dominant, from about 2500 to 3500 m. GLEES also contains a zone with Engelmann spruce, subalpine fir, and lodgepole pine (*P. contorta*) between 2700 m and 3000 m. In reality, GLEES and Wolf Creek are subalpine sites with elevations that range from a minimum of 3200 and 2800 m, to a maximum of 3500 and 3600 m, respectively. By using the climate and site data from each location along with the calculated lapse rates, this study is able to explore dynamics for hypothetical forests at lower elevations.

The results of the elevation tests at GLEES with (Fig. 3.3a) and without (Fig. 3.2) disturbances are similar, but with some striking differences. The non-disturbance test conducted at GLEES resulted in very high biomass in the subalpine zone (2600 to 3600 m), and an underrepresentation of lodgepole pine. The inclusion of windthrow (higher in the subalpine zone) and fire disturbance (higher probability, but lower intensity, in the montane zone; 2200 to 2500 m) resulted in lower biomass of Engelmann spruce, and slightly higher biomass of ponderosa pine and lodgepole pine. Most notably, lodgepole pine biomass increased considerably with disturbances and its distribution shifted upslope relative to the test without disturbances (Figs. 3.2, 3.3a). Lodgepole pine is disturbance-adapted, recolonizing quickly after

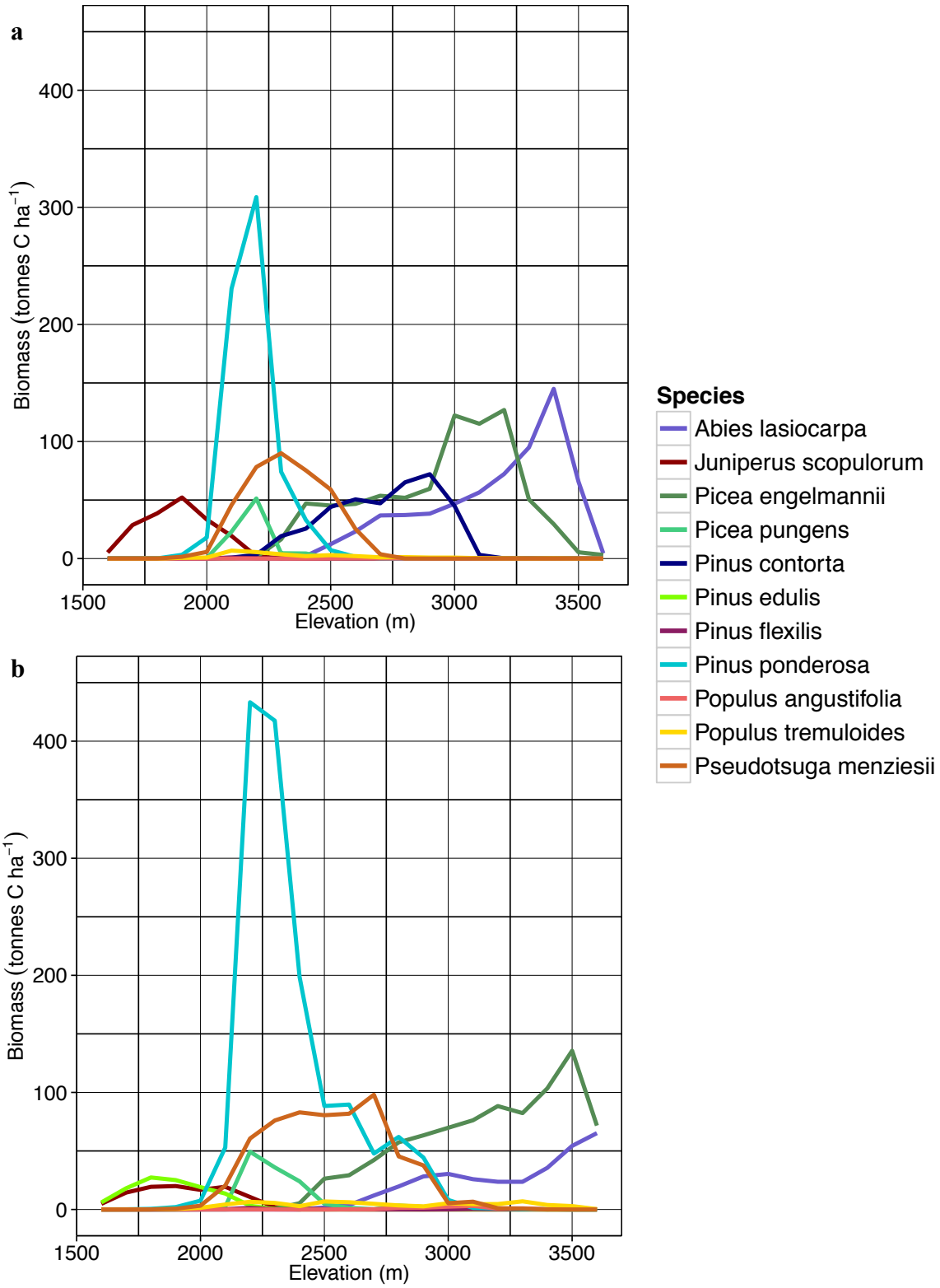

Figure 3.3. UVAFME-simulated biomass (tonnes C ha^{-1}) at year 500 of eleven Rocky Mountain species at different elevations at (a) GLEES and (b) Wolf Creek. UVAFME was run every 100 m from 1600 m to 3600 m with species- and size-specific effects of fire and windthrow.

wildfire (Sibold et al. 2007), and so it follows that the addition of fire disturbance would increase its dominance. These results are similar to findings by Bugmann (2001a); the addition of disturbances in model runs of ForClim in the Colorado Front Range resulted in higher dominance of lodgepole pine as well as ponderosa pine. It is clear that disturbances are important factors to include in forest gap models, especially in the Rocky Mountains, where disturbances are fundamental drivers of forest dynamics. Simulations with UVAFME in Chapter 5 of this work will include disturbances by the spruce beetle (*Dendroctonus rufipennis*), which infests Engelmann spruce in the subalpine zone and greatly affects forest composition and structure (Bentz et al. 2010).

The differences between the elevation tests with disturbance at GLEES and at Wolf Creek are chiefly in the subalpine zone. Whereas the biomass dominance of lodgepole pine, Engelmann spruce, and subalpine fir are shown as three distinct peaks at GLEES, the biomass of

Table 3.1. Results of t-tests comparing UVAFME-simulated biomass at year 500 and inventory-derived biomass at GLEES and Wolf Creek for the subalpine zone at 3115 and 3100 m.

Site	Species	Modeled Biomass (tonnes C ha^{-1})	Inventory Biomass (tonnes C ha^{-1})	*t*-statistic	p-value
GLEES	*Picea engelmannii*	145.97	153.76	-0.36	0.718
	Abies lasiocarpa	51.09	33.16	4.69	<0.001
	Other	3.60	0.57	3.77	<0.001
	Total	200.66	187.49	0.61	0.543
Wolf Creek Pass	*Picea engelmannii*	84.02	93.55	-1.04	0.301
	Abies lasiocarpa	21.70	11.16	4.33	<0.001
	Populus tremuloides	8.17	1.76	6.12	<0.001
	Pseudotsuga menziesii	2.18	3.17	-0.59	0.558
	Total	116.07	109.65	0.76	0.449

Engelmann spruce and subalpine fir at Wolf Creek is more evenly distributed between 2700 and 3400 m (Fig. 3.3). This difference is likely due to the climate differences between the two sites. Wolf Creek is considerably warmer and wetter than is GLEES, potentially leading to less decline

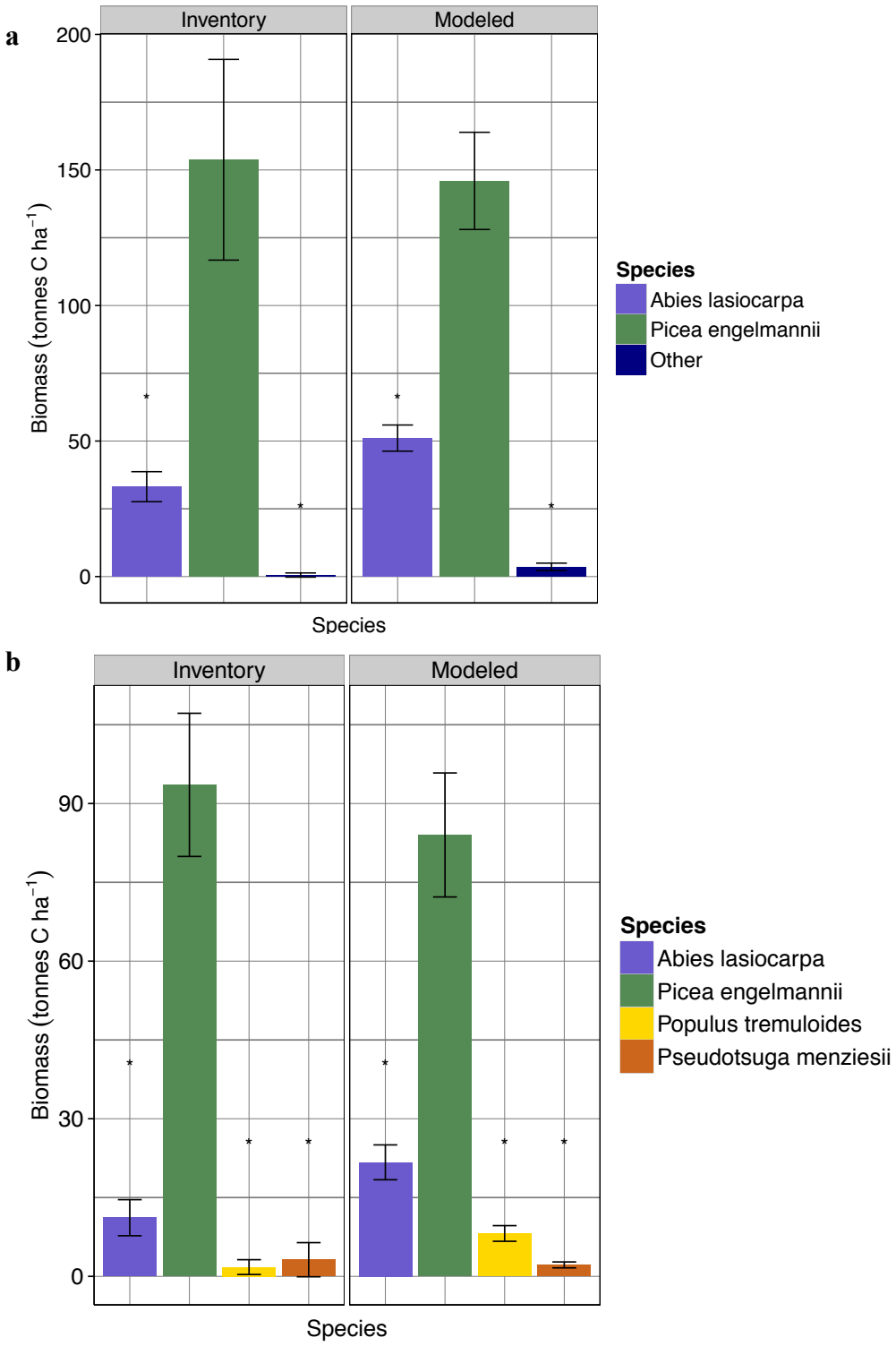

Figure 3.4. UVAFME-simulated biomass (tonnes C ha^{-1}) at year 500 compared with inventory biomass for (a) GLEES (3115 m) and (b) Wolf Creek (3100 m). Error bars correspond to 95% confidence intervals and stars indicate significant differences ($p < 0.05$) between modeled and inventory biomass.

in subalpine fir and Engelmann spruce at high elevations. There is also a higher level of Douglas-fir biomass above 2600 m at Wolf Creek, which could be due to its warmer, wetter climate. These differences between model output for each elevation test indicate that UVAFME is sensitive to site-level differences in site and climate characteristics, while still maintaining realistic representations of species-specific tolerances and tree competition.

Local-scale model output on species-specific biomass within the subalpine zone at both GLEES (3115 m) and Wolf Creek (3100 m) compared fairly well with inventory data at those locations (Fig. 3.4). There was no statistically significant difference between simulated and measured Engelmann spruce biomass at either test site (Table 3.1). While the measured and simulated biomass values of most of the subdominant species at each site did statistically differ, in general UVAFME performed well at predicting the relative dominance of each species. Total biomass at each site was not significantly different between modeled and simulated values (Table 3.1).

UVAFME also performed well at predicting the tree size class distribution at GLEES and Wolf Creek for trees with a DBH larger than 20 cm at Wolf Creek and for all size classes at GLEES (Fig. 3.5). At GLEES, a linear regression of modeled vs. measured stem count had no significant difference from an intercept of zero ($t = 0.221$, $p = 0.83$) and a slope of 1 (95% confidence interval: 0.67, 1.33). At Wolf Creek, the linear regression had no significant difference from a zero intercept ($t = 1.893$, $p = 0.09$), however the slope was significantly different from 1 (95% confidence interval: 0.08, 0.37). The simulated stem count in the smaller size classes (below a DBH of 20 cm) at Wolf Creek was larger than the measured stem count, leading a slope lower than 1 in the linear regression. However, UVAFME-simulated stem counts

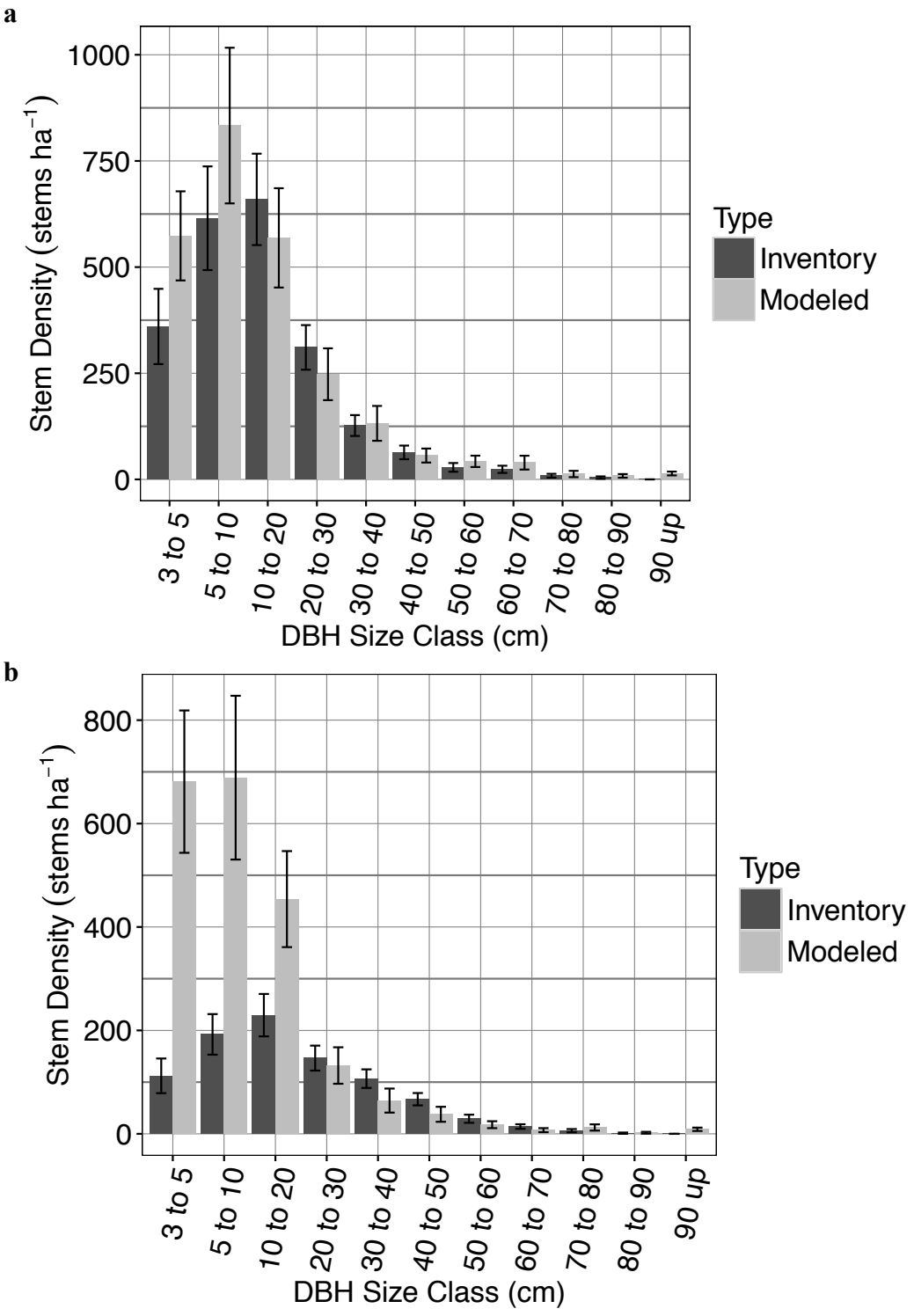

Figure 3.5. UVAFME-simulated total stem count (trees ha^{-1}) for different size classes (cm DBH) at year 500 compared with inventory-derived stem count for (a) GLEES (3115 m) and (b) Wolf Creek (3100 m). Error bars correspond to 95% confidence intervals.

in the middle and upper size classes (for a DBH of 20 cm to above 90 cm) were comparable to measured values at both locations (Fig. 3.5).

It is not clear why there were differences between modeled and measured values in the smaller tree size classes and in the biomass of the subdominant species. Tree establishment in high elevation ecosystems such as the subalpine zone are highly influenced by local-scale conditions (Elliott and Kipfmueller 2010). It is thus possible that small-scale differences in climate or site conditions, not captured by this generalized method of parameterization, would result in differences in the abundance of small stems and in the proportion of subdominant species, which are generally present as small, subcanopy trees. Additionally, the 200 independent plots used in UVAFME are 500 m^2 each. Plot sizes for the inventory data (100 to 200 m^2 at GLEES and 400 m^2 at Wolf Creek), however, are smaller, which could potentially lead to differences in modeled and measured size structure.

A time series of model-simulated biomass at all four locations is typical of the subalpine zone in the region (Daubenmire 1978, Veblen 1986, Aplet et al. 1988). In the first one hundred years, Engelmann spruce and subalpine fir coexist, with Engelmann spruce eventually attaining dominance by year 200 (Fig. 3.6). At Fraser Forest and Niwot Ridge (Fig. 3.6b, c), which have relatively drier climates than GLEES and Wolf Creek, there is a higher occurrence of lodgepole pine, which is common on xeric sites (Veblen 1986). Total biomass is comparable across all sites.

The validation tests presented in this study were conducted with prior testing at two elevations (2400 and 3400 m) at only one site (GLEES); the model was not “tuned” in order to achieve higher accuracy at GLEES or the additional sites. Accurate simulation of species zonation (Fig. 3.3) requires that the model’s internal logic and parameterization reflect actual

forest dynamics in the region. The results of the elevation tests (Fig. 3.2, 3.3) demonstrate UVAFME's ability to simulate tree – tree competition for resources and species-specific environmental responses in the Rocky Mountains, as well as the species-specific responses to

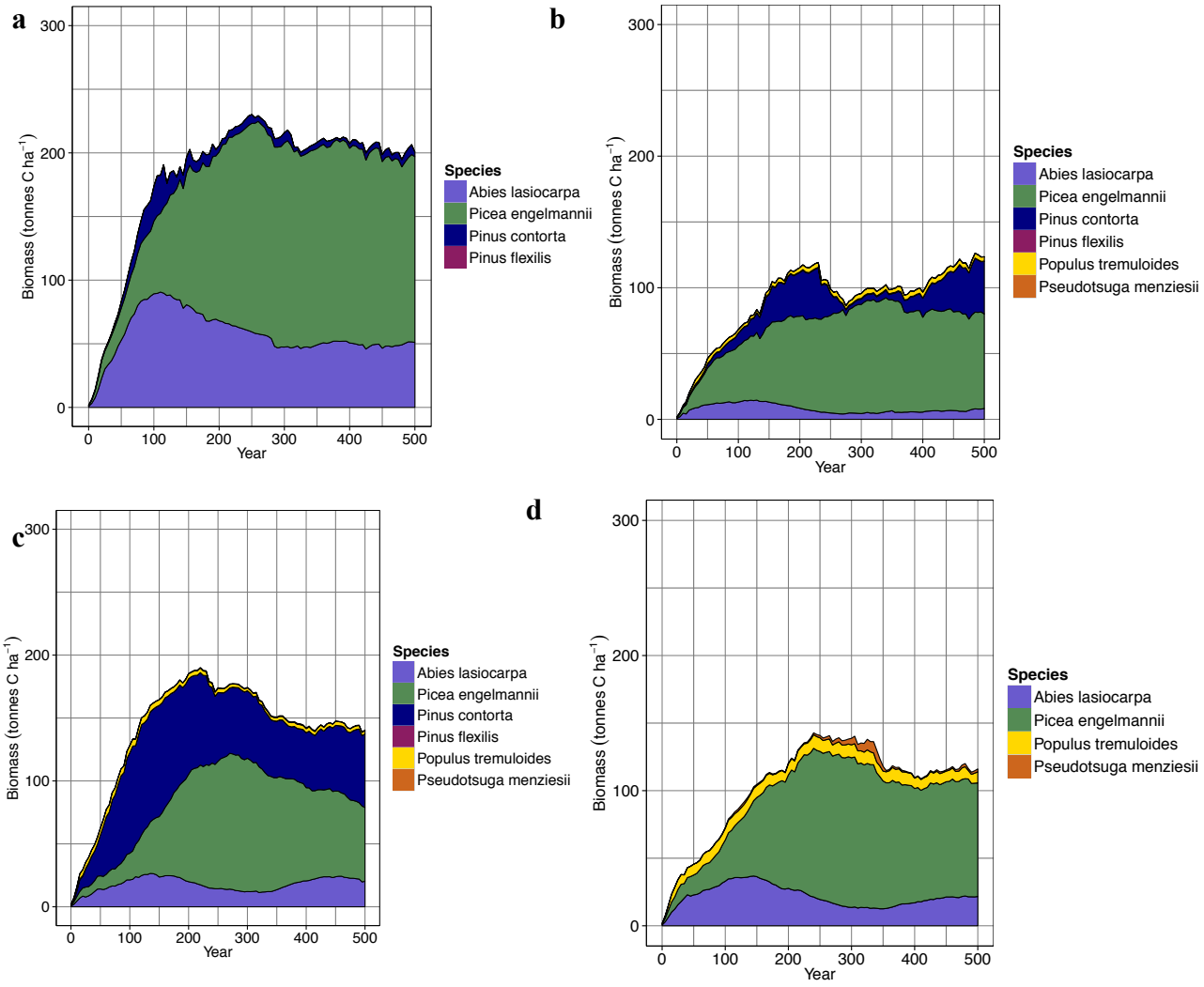

Figure 3.6. Model-simulated biomass (tonnes C ha^{-1}) at (a) GLEES (3115 m), (b) Fraser Forest (2900 m), (c) Niwot Ridge (3020 m), and (d) Wolf Creek (3100 m).

fire disturbance. The quantitative validation tests (Fig. 3.4, 3.5; Table 3.1) show that UVAFME can simulate tree response to local-scale environmental conditions and can predict site-specific biomass, species composition, and size structure. The model can also simulate the expected

successional dynamics within the subalpine zone, even at disparate locations within the Rocky Mountains, each with their own set of climate conditions, site characteristics, and species composition (Fig. 3.6). The input parameters on climate and soil conditions and species presence for these sites varied, but UVAFME was not reformatted across the sites, demonstrating its broad applicability within the study area. Because UVAFME can reliably model species distributions and forest dynamics under current climate conditions in the Rocky Mountains, it has potential as a useful tool for predicting the response of vegetation within this region to changing climate.

Climate change

There were considerable differences in the species zonation between current climate conditions at GLEES (Fig. 3.7a) and those conditions with elevated temperatures (Fig. 3.7b). The ponderosa pine (*P. ponderosa*) zone shifted upslope and decreased in biomass due to increased temperatures. The juniper (*J. scopulorum*) woodland also shifted upwards in elevation, and declined in biomass between 1600 and 1900 m. Douglas-fir (*P. menziesii*) also shifted upwards in elevation, encroaching on the original subalpine zone. Lodgepole pine (*P. contorta*) and subalpine fir (*A. lasiocarpa*) biomass were considerably reduced throughout their original range, and the dominance of Engelmann spruce (*P. engelmannii*) shifted upwards.

By year 1100 (once temperature had returned to current values) only some of the landscape had recovered to what it had been under current climate conditions (Fig. 3.7c). Time series results which tracked the climate response at specific elevations show that the ponderosa pine zone regained the biomass it had lost due to increasing temperatures, although it did not shift back downwards in elevation (Fig 3.8a, b). The juniper woodland regrew at the lower elevations, though it retained dominance at higher elevations than it had before climate change was implemented (Fig. 3.8a). Douglas-fir retreated from the original subalpine zone, however

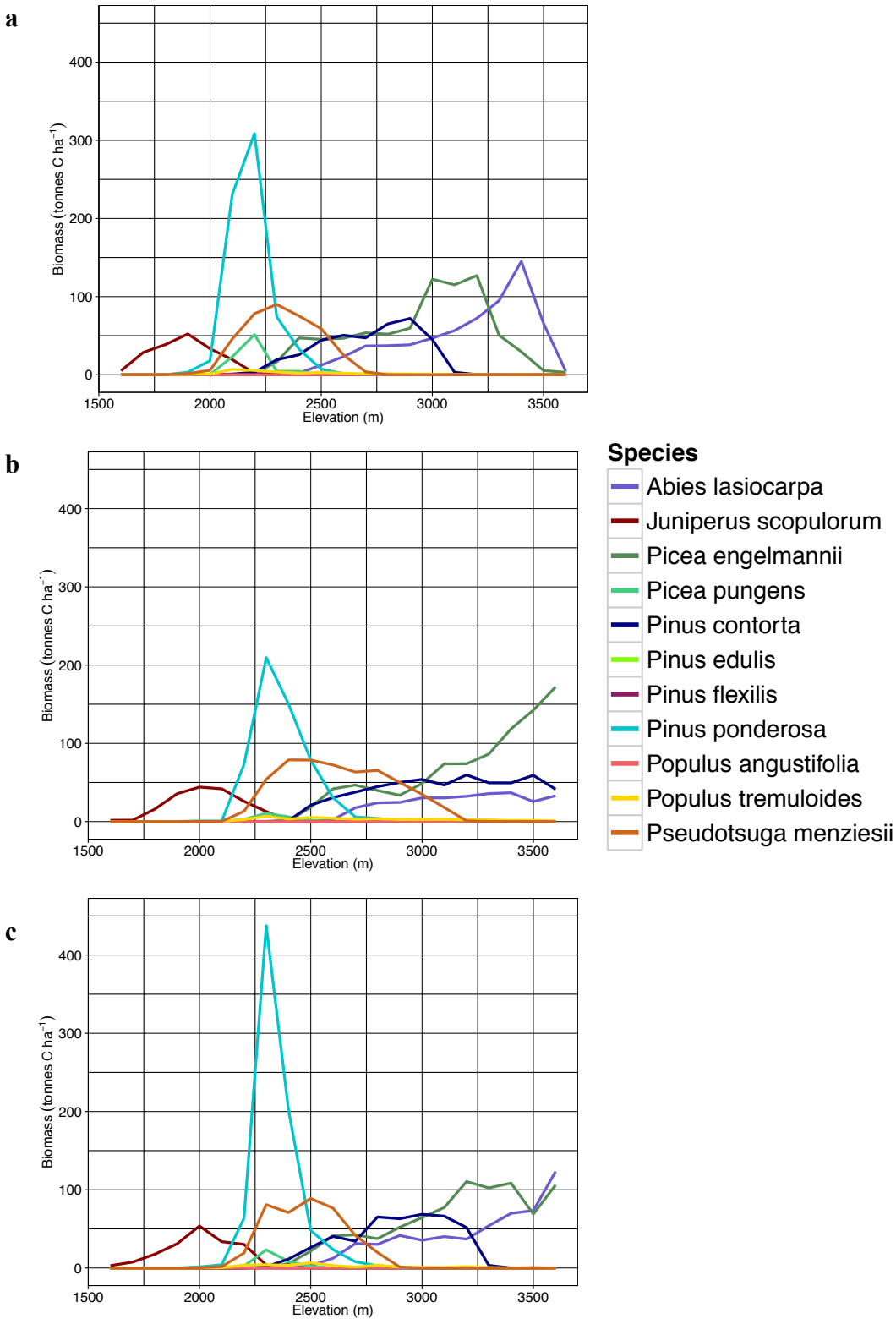

Figure 3.7. UVAFME-simulated biomass (tonnes C ha^{-1}) of ten Rocky Mountain species at different elevations at GLEES at (a) year 500 with present climate, (b) year 800 after 200 years at 2°C warmer temperatures, and (c) year 1100 after 200 years at 2°C cooling back to current climate.

while the general species mix of the subalpine zone was restored after climate cooled again (Fig. 3.8c), lodgepole pine, subalpine fir, and Engelmann spruce were not completely restored to their original biomass values (Fig. 3.7c, 3.8c). Even though in general, the overall landscape of the Rocky Mountains at year 1100 (Fig. 3.7c) looks similar to that at year 500 (Fig. 3.7a), snapshots of individual elevations show substantial and persistent changes due to the applied climate change scheme (Fig. 3.8).

The decline in juniper biomass and the shift upwards in the transition zone between ponderosa pine and juniper under increasing temperatures (Fig. 3.7a, 3.7b) has also been documented in field studies of sites undergoing climate stress (Allen and Breshears 1998, Breshears et al. 2005). Bell et al. (2014) predicted changes in climatic suitability over the next century within the western US and found that ponderosa pine is likely to shift upslope due to its relative drought tolerance and current proximity to areas that will remain suitable. Even though ponderosa pine is drought tolerant (Zhang et al. 1997) it has been subject to drought-related mortality, as in the Allen and Breshears (1988) study, and in the climate change test shown here it declined in biomass due to increasing temperatures. Ponderosa pine also failed to regain dominance in the lower elevations (Fig. 3.8a), even after climate had cooled to original levels and stabilized for 200 years. In contrast, ponderosa pine actually increased in biomass within its new climate-induced range at an elevation of 2100 to 2700 m after climate cooling had occurred (Fig. 3.7c). This increase in dominance was evident in the upper limits of the species' range (2500 m, Fig. 3.8b). Originally at this location it had very low biomass. The small increase in temperature that was employed gave ponderosa pine a competitive advantage over the other species, and combined with the presence of stand-replacing disturbances, allowed it to increase in dominance, a shift that was persistent even after climate had cooled. While these changes may

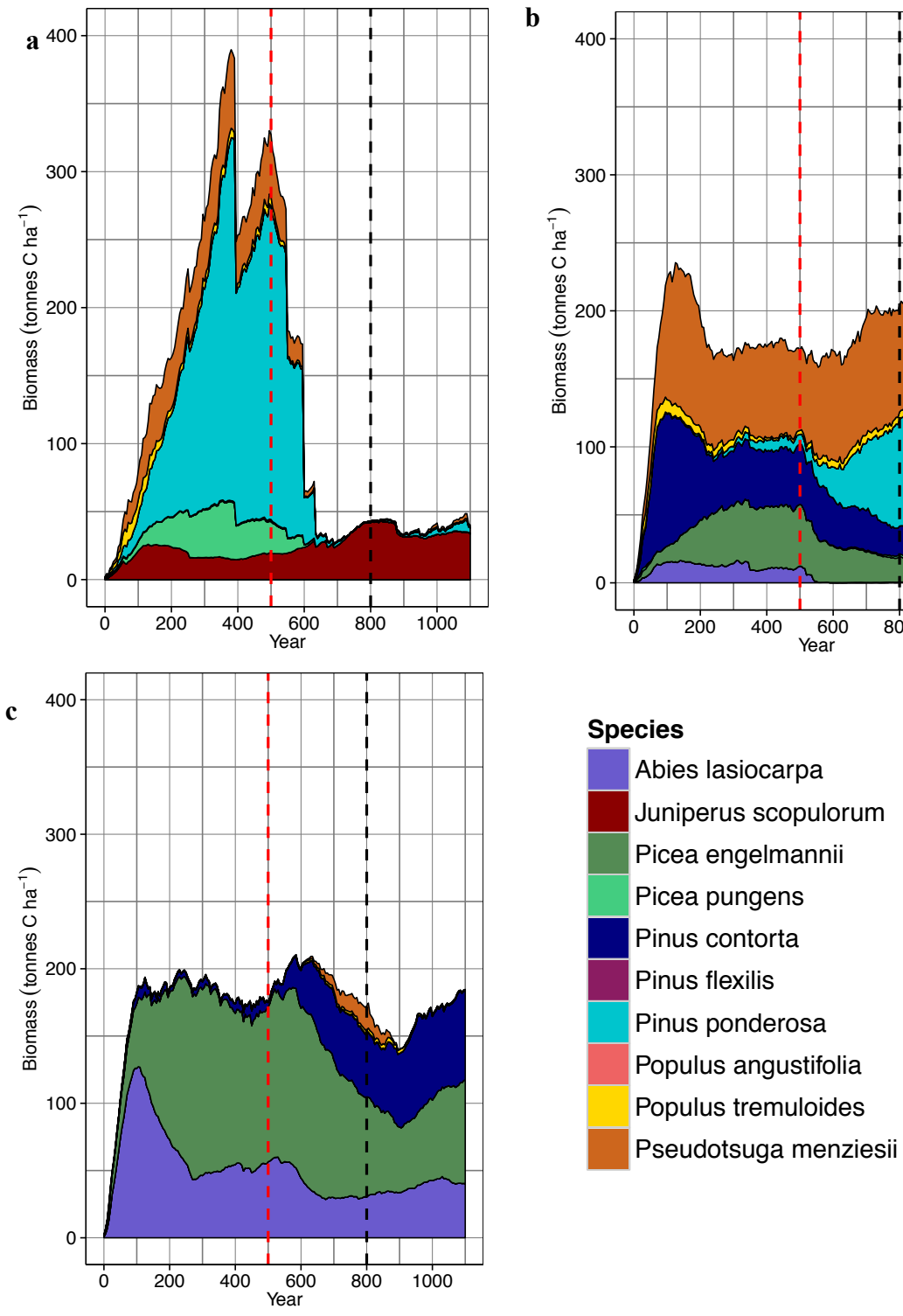

Figure 3.8. Model-simulated biomass (tonnes C ha^{-1}) at GLEES under the climate change scenario at (a) 2100 m, (b) 2500 m, and (c) 3100 m. The red dashed line corresponds to year 500 and the start of a 2°C increase in temperature over 100 years; the black dashed line corresponds to the start of a 2°C cooling over 100 years.

have disappeared given a longer stabilization period, within the time period of one or two centuries, the effects of only a 2°C increase had noticeable effects on the biomass and distribution of species within the montane zone.

The subalpine zone also experienced significant changes due to elevated temperatures (Fig. 3.7b). Subalpine fir and Engelmann spruce declined in biomass within their original elevation zones, potentially due to competition with lodgepole pine and Douglas-fir (Fig. 3.8b), which both shifted upslope with increasing temperatures. This increase in Douglas-fir and decrease of Engelmann spruce with climate change has also been seen in other modeling studies within the western US (Notaro et al. 2012, Temperli et al. 2015). Even after climate had cooled again (Fig 3.7c), the vegetation of the subalpine zone was still fairly different from that of present climate conditions (Fig. 3.7a); neither Engelmann spruce nor subalpine fir regained the biomass they lost in the 3000 to 3400 m zone, though subalpine fir did start to increase again at the highest elevations. It is important to note that the increase in Engelmann spruce dominance with increasing temperatures at 3400 m and above is only possible for mountains that reach those elevations. If the test had restricted elevations to the area from 1600 to 3100 m or so, much of the subalpine zone would have been lost under elevated temperatures to Douglas-fir, which does not typically exist at high elevations (Daubenmire 1943). Bell et al. (2014) predicted that climate suitability in mountain ecosystems will likely decline for species in their current ranges as well as in nearby areas where they may be able to migrate. They found that there may be significant reduction in climatically suitable areas for high elevation species, and that there will not be adequate geographical area to offset the loss of habitat.

These predictions of potential future biomass and species composition can be used to determine the possible futures of the Rocky Mountains landscape. A critical piece of the Rocky

Mountains climate change puzzle that was not included in this sensitivity test was increasing disturbances. Disturbances by fire and insect outbreak are predicted to increase in frequency and severity with climate change (Dale et al. 2001, Bentz et al. 2010, Jolly et al. 2015). Annual wildfire suppression in the last ten years has cost the US upwards of $1.7 billion (Jolly et al. 2015) and outbreaks of the mountain pine beetle (*Dendroctonus ponderosae*) and spruce beetle (*D. rufipennis*) have affected over 1.9 million ha since 1996 in Colorado alone (USFS 2015). Given that the inclusion of fire and wind disturbances in the elevation tests presented here resulted in significant differences in biomass and species composition compared to that without disturbances (Fig. 3.2, 3.3a) it is likely that an increase in the frequency or severity of disturbances in combination with changes in climate would lead to even further changes in the vegetation of the Rocky Mountains. The tests presented here did not include changes to precipitation, thus any increase in drought-related stress that occurred within these climate simulations would have been due to increasing atmospheric demand at current levels of water availability. With the temperature sensitivity test presented here as a guide (Fig. 3.7; Fig. 3.8), it is possible that further increases in tree mortality and changes in species composition may occur if there is a concurrent increase in the frequency of prolonged low-precipitation intervals in this region. These changes may lead to even higher dominance of ponderosa pine and Douglas-fir in the upper elevations and a further reduction in subalpine species.

The updates made to the calculation of the effect of temperature (in the form of GDD) on tree growth (see Chapter 2) move UVAFME further away from climate envelope or niche-based models. Niche-based models generally use data on species distributions and their relationship with environmental or climatic predictors to project future species composition (Morin and Thuiller 2009). Unlike process-based models (such as UVAFME), envelope models do not

consider between-tree competition, individual tree mortality and growth, or phenotypic plasticity. With such rigid controls on where and how certain species grow, niche-based models tend to predict stronger levels of mortality under changing climate than do process-based models (Morin and Thuiller 2009). The fact that UVAFME did predict tree mortality and species shifts in this simulation, even without the restriction of tree growth at higher temperatures, points to the importance of individual tree competition. Forest gap models like UVAFME, which explicitly consider the responses and interactions of individual trees are thus valuable tools for projecting the future of vegetation under changing climate and disturbance regimes. UVAFME, whose original version was broadly applied across boreal Russia, has been updated to better reflect forest dynamics and their response to climate and fire disturbance within the southern Rocky Mountains. The validation tests presented here show that the model can be used to accurately simulate biomass, species composition, and stand structure at various sites within the Wyoming and Colorado Rocky Mountains. UVAFME is a valuable new model that can be used to study the variations in stand age, species composition, size structure, and biomass given different climate and disturbance conditions. It can also be used to test different forest management schemes, such as thinning to reduce competition and increase overall biomass, which may be used to mitigate the effects of climate change. Additionally, due to the tree-level modeling within UVAFME, model output can compare directly to inventory and high-resolution remote sensing data, allowing for unique methods of model initialization and validation, and model-data intercomparisons.

Conclusions

High elevation ecotones are highly controlled by climate, and can be seen as "barometers" for climatic change (Loehle 2000, Malanson et al. 2007). Within the Rocky

Mountains, many factors, including natural disturbances, the harsh conditions of the landscape, and species zonation, make predicting vegetation response to climate change difficult. Forest gap models have been successfully used to study vegetation response to climate and disturbances across a wide variety of ecosystems (Kercher and Axelrod 1984, Bonan 1989, Huth and Ditzer 2000, Bugmann 2001a). UVAFME has been significantly updated from its original version (FAREAST; Yan and Shugart (2005)) with improved handling of climate and moisture dynamics, and a new fire disturbance routine. This new version was tested across four sites in the southern Rocky Mountains. The model accurately simulates the forest structure and dynamics of the subalpine zone as well as the greater Rocky Mountain landscape. This study has shown that as little as a 2°C increase in ambient temperature is likely to significantly affect the vegetation of the Rocky Mountains, leading to changes in species dominance, shifts upslope in forest ecotones, and decreases in biomass. These changes are also likely to be fairly persistent at many elevations. This 2°C increase coincides with the outcomes of the UN Climate Change Conference in Paris in December 2015, in which the key result was the agreement to keep global average temperature change below 2°C. While I cannot speak to the efficacy of this plan, it is clear that even this level of climate change may have significant negative impacts on vegetation, and the Rocky Mountains landscape in particular. The changes brought on by only a 2°C increase are also likely to be persistent, at least for one to two centuries. The use of individual-based gap models to project the future of forest landscapes will continue to increase in value in the coming years. Ultimately, I hope that UVAFME will be used to project the many complicated and varied scenarios that are a potential for vegetation of the western US as well as other forest ecosystems.

References

Adams, H. D., M. Guardiola-Claramonte, G. A. Barron-Gafford, J. C. Villegas, D. D. Breshears, C. B. Zou, P. A. Troch, and T. E. Huxman. 2009. Temperature sensitivity of drought-induced tree mortality portends increased regional die-off under global change-type drought. Proceedings of the National Academy of Sciences 106:7063–7066.

Allen, C. D., and D. D. Breshears. 1998. Drought-induced shift of a forest-woodland ecotone: rapid landscape response to climate variation. Proceedings of the National Academy of Sciences 95:14839–14842.

Anderegg, W. R. L., J. M. Kane, and L. D. . Anderegg. 2012. Consequences of widespread tree mortality triggered by drought and temperature stress. Nature Climate Change.

Aplet, G. H., R. D. Laven, and F. W. Smith. 1988. Patterns of community dynamics in Colorado Engelmann spruce-subalpine fir forests. Ecology 69:312–319.

Bell, D. M., J. B. Bradford, and W. K. Lauenroth. 2014. Mountain landscapes offer few opportunities for high-elevation tree species migration. Global Change Biology 20:1441–1451.

Bentz, B. J., J. Régnière, C. J. Fettig, E. M. Hansen, J. L. Hayes, J. A. Hicke, R. G. Kelsey, J. F. Negrón, and S. J. Seybold. 2010. Climate Change and Bark Beetles of the Western United States and Canada: Direct and Indirect Effects. BioScience 60:602–613.

Bonan, B. G. 1989. A computer model of the solar radiation, soil moisture, and soil thermal regimes in boreal forests. Ecological Modelling 45:275–306.

Botkin, D. B., J. F. Janak, and J. R. Wallis. 1972. Some Ecological Consequences of a Computer Model of Forest Growth. The Journal of Ecology 60:849.

Breshears, D. D., N. S. Cobb, P. M. Rich, K. P. Price, C. D. Allen, R. G. Balice, W. H. Romme, J. H. Kastens, M. L. Floyd, J. Belnap, J. J. Anderson, O. B. Myers, and C. W. Meyer. 2005. Regional vegetation die-off in response to global-change-type drought. Proceedings of the National Academy of Sciences 102:15144–15148.

Bugmann, H. 2001a. A comparitive analysis of forest dynamics in the Swiss Alps and the Colorado Front Range. Forest Ecology and Management 145:43–55.

Bugmann, H. 2001b. A review of forest gap models. Climatic Change 51:259–305.

Bugmann, H. K. ., and A. M. Solomon. 2000. Explaining forest composition and biomass across multiple biogeographical regions. Ecological Applications 10:95–114.

Chojnacky, D. C., L. S. Heath, and J. C. Jenkins. 2014. Updated generalized biomass equations for North American tree species. Forestry 87:129–151.

Dale, V. H., L. A. Joyce, S. Mcnulty, R. P. Neilson, M. P. Ayres, M. D. Flannigan, P. J. Hanson, L. C. Irland, A. E. Lugo, C. J. Peterson, D. Simberloff, F. J. Swanson, B. J. Stocks, and B. Michael Wotton. 2001. Climate Change and Forest Disturbances. BioScience 51:723.

Daubenmire, R. F. 1943. Vegetational zonation in the Rocky Mountains. The Botanical Review 9:325–393.

Daubenmire, R. F. 1978. Plant Geography With Special Reference to North America. Academic Press, New York, NY.

Elliott, G. P., and K. F. Kipfmueller. 2010. Multi-scale Influences of Slope Aspect and Spatial Pattern on Ecotonal Dynamics at Upper Treeline in the Southern Rocky Mountains, U.S.A. Arctic, Antarctic, and Alpine Research 42:45–56.

Hadley, K. S., and T. T. Veblen. 1993. Stand response to western spruce budworm and Douglas-fir bark beetle outbreaks, Colorado Front Range. Canadian Journal of Forest Research 23:479–491.

Hicke, J. A., G. P. Asner, J. T. Randerson, C. Tucker, S. Los, R. Birdsey, J. C. Jenkins, and C. Field. 2002. Trends in North American net primary productivity derived from satellite observations. Global Biogeochemical Cycles 16.

Hicke, J. A., and M. J. Zeppel. 2013. Climate-driven tree mortality: insights from the piñon pine die-off in the United States. New Phytologist 200:301–303.

Huth, A., and T. Ditzer. 2000. Simulation of the growth of a lowland Dipterocarp rain forest with FORMIX3. Ecological Modelling 134:1–25.

Jenkins, M. J., W. G. Page, E. G. Hebertson, and M. E. Alexander. 2012. Fuels and fire behavior dynamics in bark beetle-attacked forests in Western North America and implications for fire management. Forest Ecology and Management 275:23–34.

Jolly, W. M., M. A. Cochrane, P. H. Freeborn, Z. A. Holden, T. J. Brown, G. J. Williamson, and D. M. J. S. Bowman. 2015. Climate-induced variations in global wildfire danger from 1979 to 2013. Nature Communications 6:7537.

Joyce, L. A., S. W. Running, D. D. Breshears, V. H. Dale, R. W. Malmsheimer, R. N. Sampson, B. Sohngen, and C. W. Woodall. 2014. Ch. 7: Forests. Pages 175–194 Climate Change Impacts in the United States: The Third National Climate Assessment. U.S. Global Change Research Program.

Katul, G. G., R. Oren, S. Manzoni, C. Higgins, and M. B. Parlange. 2012. Evapotranspiration: A process driving mass transport and energy exchange in the soil-plant-atmosphere-climate system. Reviews of Geophysics 50.

Keane, R. E., M. Austin, C. Field, A. Huth, M. J. Lexer, D. Peters, A. Solomon, and P. Wyckoff. 2001. Tree mortality in gap models: application to climate change. Climatic Change 51:509–540.

Kercher, J. R., and M. C. Axelrod. 1984. A Process Model of Fire Ecology and Succession in a Mixed-Conifer Forest. Ecology 65:1725.

Korner, C. 1998. A re-assessment of high elevation treeline positions and their explanation. Oecologia 115:445–459.

Lasch, P., and M. Lindner. 1995. Application of Two Forest Succession Models at Sites in North East Germany. Journal of Biogeography 22:485.

Loehle, C. 2000. Forest ecotone response to climate change: sensitivity to temperature response functional forms. Canadian journal of forest research 30:1632–1645.

Malanson, G. P., D. R. Butler, D. B. Fagre, S. J. Walsh, D. F. Tomback, L. D. Daniels, L. M. Resler, W. K. Smith, D. J. Weiss, D. L. Peterson, A. G. Bunn, C. A. Hiemstra, D. Liptzin, P. S. Bourgeron, Z. Shen, and C. I. Millar. 2007. Alpine treeline of western North America: linking organism-to-landscape dynamics. Physical Geography 28:378–396.

Marr, J. W. 1961. Ecosystems of the east slope of the Front Range in Colorado. University of Colorado Press.

McDowell, N. G., and C. D. Allen. 2015. Darcy's law predicts widespread forest mortality under climate warming. Nature Climate Change 5:669–672.

McKenzie, D., D. L. Peterson, and J. J. Littell. 2009. Chapter 15 Global Warming and Stress Complexes in Forests of Western North America. Pages 319–337 Developments in Environmental Science. Elsevier.

Meehl, G. A., J. M. Arblaster, and G. Branstator. 2012. Mechanisms contributing to the warming hole and consequent US east-west differential of heat extremes. Journal of Climate 25:6394–6408.

Morin, X., and W. Thuiller. 2009. Comparing niche-and process-based models to reduce prediction uncertainty in species range shifts under climate change. Ecology 90:1301–1313.

Neilson, R. P., L. F. Pitelka, A. M. Solomon, R. Nathan, G. F. Midgley, J. M. V. Fragoso, H. Lischke, and K. Thompson. 2005. Forecasting regional to global plant migration in response to climate change. BioScience 55:749–759.

Notaro, M., A. Mauss, and J. W. Williams. 2012. Projected vegetation changes for the American Southwest: combined dynamics modeling and bioclimatic-envelope approach. Ecological Applications 22:1365–1388.

Peet, R. K. 1981. Forest vegetation of the Colorado front range. Vegetatio 45:3–75.

Rasmussen, L. A., G. D. Amman, J. C. Vandygriff, R. D. Oakes, A. S. Munson, and K. E. Gibson. 1996. Bark beetle and wood borer infestation in the greater Yellowstone area during four postfire years. USDA Forest Service Research Paper INT-RP-487. Intermountain Research Station, Ogden, UT.

Rehfeldt, G. E., N. L. Crookston, M. V. Warwell, and J. S. Evans. 2006. Empirical analyses of plant-climate relationships for the western United States. International Journal of Plant Sciences 167:1123–1150.

Schimel, D. S., T. G. F. Kittel, S. Running, R. Monson, A. Turnipseed, and D. Anderson. 2002. Carbon sequestration studied in western US mountains. EOS Transactions, American Geophysical Union 83:445–456.

Shugart, H. H. 1984. A Theory of Forest Dynamics: The Ecological Implications of Forest Succession Models. Springer Science & Business Media, New York, NY.

Shugart, H. H., and F. I. Woodward. 2011. Global Change and the Terrestrial Biosphere. Wiley-Blackwell, Sussex, UK.

Shuman, J. K., and H. H. Shugart. 2009. Evaluating the sensitivity of Eurasian forest biomass to climate change using a dynamic vegetation model. Environmental Research Letters 4:045024.

Shuman, J. K., H. H. Shugart, and O. N. Krankina. 2014. Testing individual-based models of forest dynamics: Issues and an example from the boreal forests of Russia. Ecological Modelling 293:102–110.

Sibold, J. S., T. T. Veblen, K. Chipko, L. Lawson, E. Mathis, and J. Scott. 2007. Influences of secondary disturbances on lodgepole pine stand development in Rocky Mountain National Park. Ecological Applications 17:1638–1655.

Smith, N. G., and J. S. Dukes. 2013. Plant respiration and photosynthesis in global-scale models: incorporating acclimation to temperature and CO2. Global Change Biology 19:45–63.

Temperli, C., T. T. Veblen, S. J. Hart, D. Kulakowski, and A. J. Tepley. 2015. Interactions among spruce beetle disturbance, climate change and forest dynamics captured by a forest landscape model. Ecosphere 6.

USFS. 2015. Aerial survey highlights for Colorado 2014. http://www.fs.usda.gov/detail/r2/forest-grasslandhealth/?cid=stelprd3827262.

Veblen, T. T. 1986. Age and Size Structure of Subalpine Forests in the Colorado Front Range. Bulletin of the Torrey Botanical Club 113:225.

Veblen, T. T., K. S. Hadley, E. M. Nel, T. Kitzberger, M. Reid, and R. Villalba. 1994. Disturbance Regime and Disturbance Interactions in a Rocky Mountain Subalpine Forest. The Journal of Ecology 82:125.

Waldrop, T. A., E. R. Buckner, H. H. Shugart, and C. E. McGee. 1986. FORCAT: A single tree model of stand development following clearcutting on the Cumberland Plateau. Forest Science 32:297–317.

Wang, Q., X. Fan, and M. Wang. 2014. Recent warming amplification over high elevation regions across globe. Climate Dynamics 43:87–101.

Watt, A. S. 1947. Pattern and process in the plant community. The Journal of Ecology:1–22.

Zhang, J. W., Z. Feng, B. M. Cregg, and C. M. Schumann. 1997. Carbon isotopic composition, gas exchange, and growth of three populations of ponderosa pine differing in drought tolerance. Tree physiology 17:461–466.

Chapter 4: Model-based Evidence for Cyclic Phenomena in a High-Elevation, Two-Species Forest

Introduction

In the 1935 paper in which A.G. Tansley used the word "ecosystem" for the first time in print, he also distinguished between autogenic succession, in which dynamic change is brought about by feedbacks among plants and their habitat, and allogenic succession, in which the changes are the result of external factors. Most modern ecologists, as did Tansley in 1935, see ecosystem dynamics arising from a mixture of autogenic and allogenic factors. In the dynamics of a system, the part of the system response that arises from interactions among internal components often features feedbacks that can produce periodic sinusoidal variation. These embedded natural periodicities can reveal which frequencies in the external drivers of the system might excite increases in oscillations or instability in the system.

In forests, disturbances such as fire, wind, and insect outbreaks are the exogenous factors that most obviously excite ecosystem dynamics. "Space for time substitution" procedures are often applied to document long-term forest dynamics, through the study of ecosystem responses to equivalent disturbances on arguably similar ecosystems. The century-scale dynamics of forests make direct observation of their responses to exogenous factors quite difficult. This is doubly true for the endogenous dynamics of forests and their expected internal periodicities, as these cycles and waves of periodic variation can occur over hundreds of years. Hence, *in situ* studies on cyclical phenomena are difficult, if not impossible, especially if their cyclic nature is not visually obvious or spatially coordinated. Reconstructions can be developed using dendrochronology or pollen records, but even these methods are limited by the spatial and temporal extent of the data (Bugmann 2001). These limitations on direct observation implicate

ecological models as a tool to investigate cyclic phenomena that result from exogenous and endogenous factors, and provide insight into which factors drive the cyclic behavior.

Several studies have provided clues of strongly cyclical internal forest dynamics. Watt (1947) in his classic "pattern and process" paradigm viewed forests and other ecosystems as mosaics with small-scale cyclical dynamics at the scale of a large dominant plant. Cyclic patterns in forests, those with a spatial aspect and those with only a temporal aspect, are seen as evidence for this underlying cyclic nature (Shugart and Woodward 2011). Indeed, Watt produced several examples of cyclic patterns in shrubs and herbaceous plants in stressful conditions in the Cairngorms of Scotland. Cyclical patterns of growth - dieback - regeneration cycles have been observed in other forests, notably in the 'ohi'a (*Metrosideros polymorpha*) forests of Hawaii (Boehmer et al. 2013), the *Scalescia* forests of the Galapagos Islands (Itow 1988), various New Zealand forests (Jane and Green 1983), as well as others. The general pattern that is observed is one of exogenous factors, such as drought, producing episodic collapses of forest stands depending on endogenous preconditions, usually for large numbers of older or senescent trees. This cycle of a similar cohort of trees becoming dominant and subsequently dying all at once continues, generally with species-specific frequencies (McGee 1984, Shugart 1984, Sprugel 1984).

There has been a long history of documenting and studying cyclic phenomena in stressed conifer forests (Reiners and Lang 1979, Sprugel and Bormann 1981, Shugart 1984, Sprugel 1984, Moloney 1986). Balsam fir (*Abies balsamea*) in the subalpine forests of the northeastern U.S. exhibits a temporal and spatial wave regeneration pattern in which suppressed seedlings are released following the synchronous death of canopy trees, forming spatially coordinated waves of dead and regenerating trees (Sprugel 1984, Moloney 1986). This synchrony has been

attributed to windthrow damage and environmental stress of exposed, older trees (Reiners and Lang 1979). A similar pattern also occurs in the high-elevation conifer forests of Japan (Kohyama 1983, Sato and Iwasa 1993, Sato 1994). The objective of this study is to apply an individual-based forest gap model to investigate the presence of periodicities in the internal forest dynamics of a high-elevation conifer forest in the Rocky Mountains of the western US.

In this chapter, the individual-based gap model University of Virginia Forest Model Enhanced (UVAFME) is used to simulate forest dynamics over time at a high-elevation, subalpine forest in southern Wyoming. It has been shown that the subalpine zone in this area may exhibit some cyclic phenomena (Aplet et al. 1988), however the temporal extent of that study was limited by the age of the oldest tree on the stand. Using UVAFME, forest dynamics over thousands of years were simulated to explore cyclic behavior at both the plot and landscape scale at this subalpine site.

Methods

Study site

The Glacier Lakes Ecosystem Experimental Site (GLEES) is located in the Snowy Range of the Rocky Mountains at 41°22’30”N and 106°15’30”W at elevations from 3200 to 3500 m. GLEES is in the Medicine Bow National Forest managed by the USDA Forest Service. Average annual precipitation at the site is about 100 cm (Musselman et al. 1994), mean July temperature is 24°C, and mean January temperature is -9°C. The climate and site conditions are in general extremely harsh for tree growth, and the forest is strongly influenced by climate. Subalpine fir (*Abies lasiocarpa*) and Engelmann spruce (*Picea engelmannii*) dominate the site (Wooldridge et al. 1996). Both species are characterized as very shade tolerant, but subalpine fir is slightly more tolerant than is Engelmann spruce (Alexander 1987, Burns and Honkala 1990).

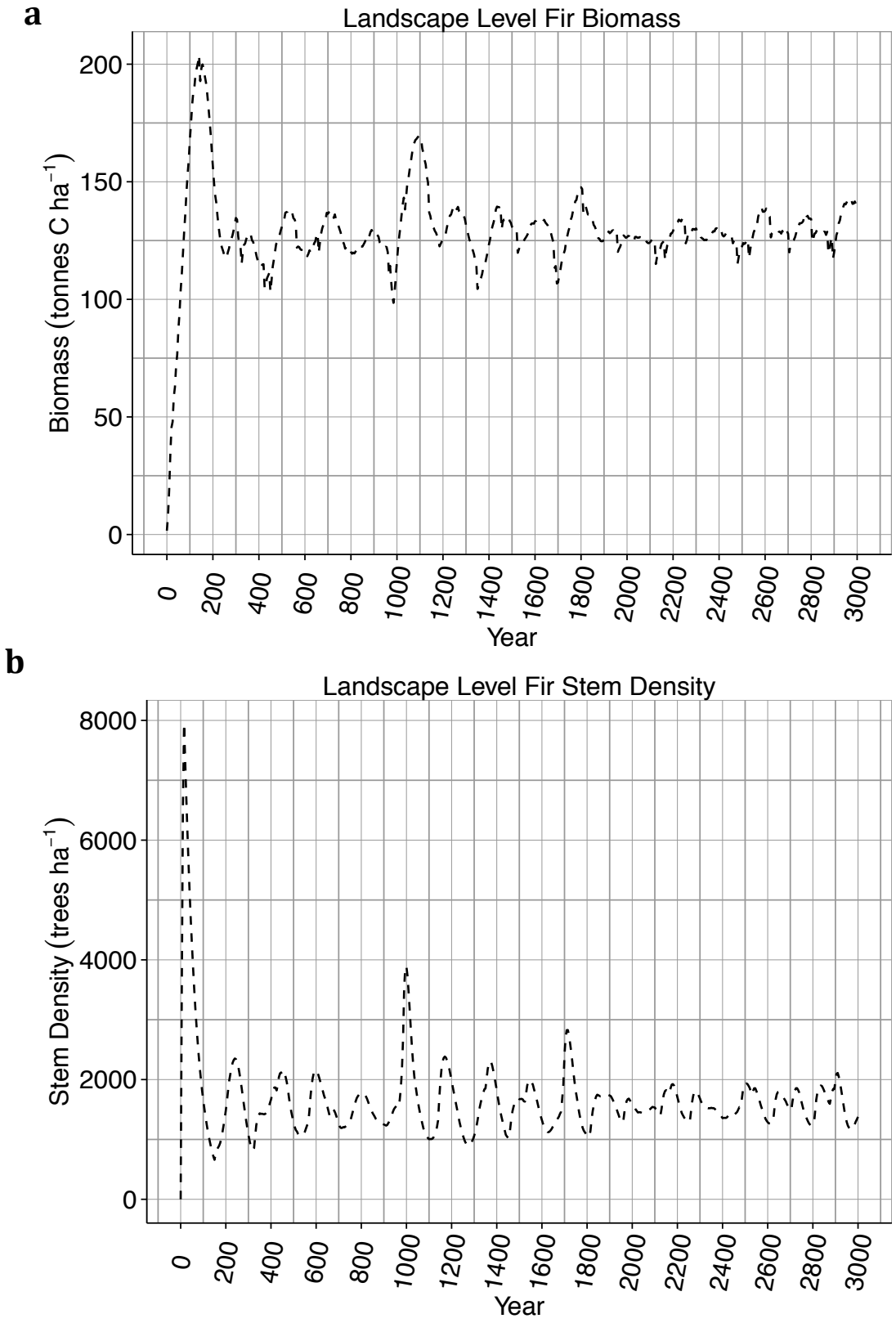

Figure 4.1 (a) Biomass and (b) stem count for modeled stands of exclusively fir (*Abies lasiocarpa*).

Model simulation of subalpine zone

UVAFME-simulated dynamics were inspected in detail in the subalpine (3400 m) location, where subalpine fir (*A. lasiocarpa*) and Engelmann spruce (*P. engelmannii*) are expected to occur. To determine tree demography for both species and for the forest as a whole, the model was run under three different scenarios: (1) subalpine fir as the only available species; (2) Engelmann spruce only; and (3) with both subalpine fir and Engelmann spruce available. For each model simulation run, 200 independent, 500 m^2 (0.05 ha) plots are simulated from bare ground to year 3,000. The same soil and climate conditions influence each plot in a simulation run. The resultant Monte Carlo simulation produces a statistical sample of a larger forested landscape (Bormann and Likens 1979, Bugmann et al. 1996). Again, disturbances were not used so that endogenous factors could be clearly studied.

Results

The 3,000-year simulations of the subalpine zone show cyclic phenomena that vary with the species mixture. For the first model scenario (exclusively subalpine fir) fir pulsates with a period of about 200 years (Fig. 4.1a, b). This cyclic pattern occurs in both the stem count (Fig. 4.1b) and biomass responses (Fig.4.1a). In the second model scenario, Engelmann spruce shows a periodicity of about 300 years (Fig. 4.2a, b). With possible interspecies competition in the third model scenario, both Engelmann spruce and subalpine fir have a frequency of about 300 years (Fig. 4.3, 4.4). This cyclic pattern occurs at the plot level (Fig. 4.3b, 4.4b) and at the landscape level (Fig. 4.3a, 4.4a).

To more clearly visualize the synchrony found in these cyclic patterns, the simulated biomass curves were detrended by subtracting the best-fit linear model through each species'

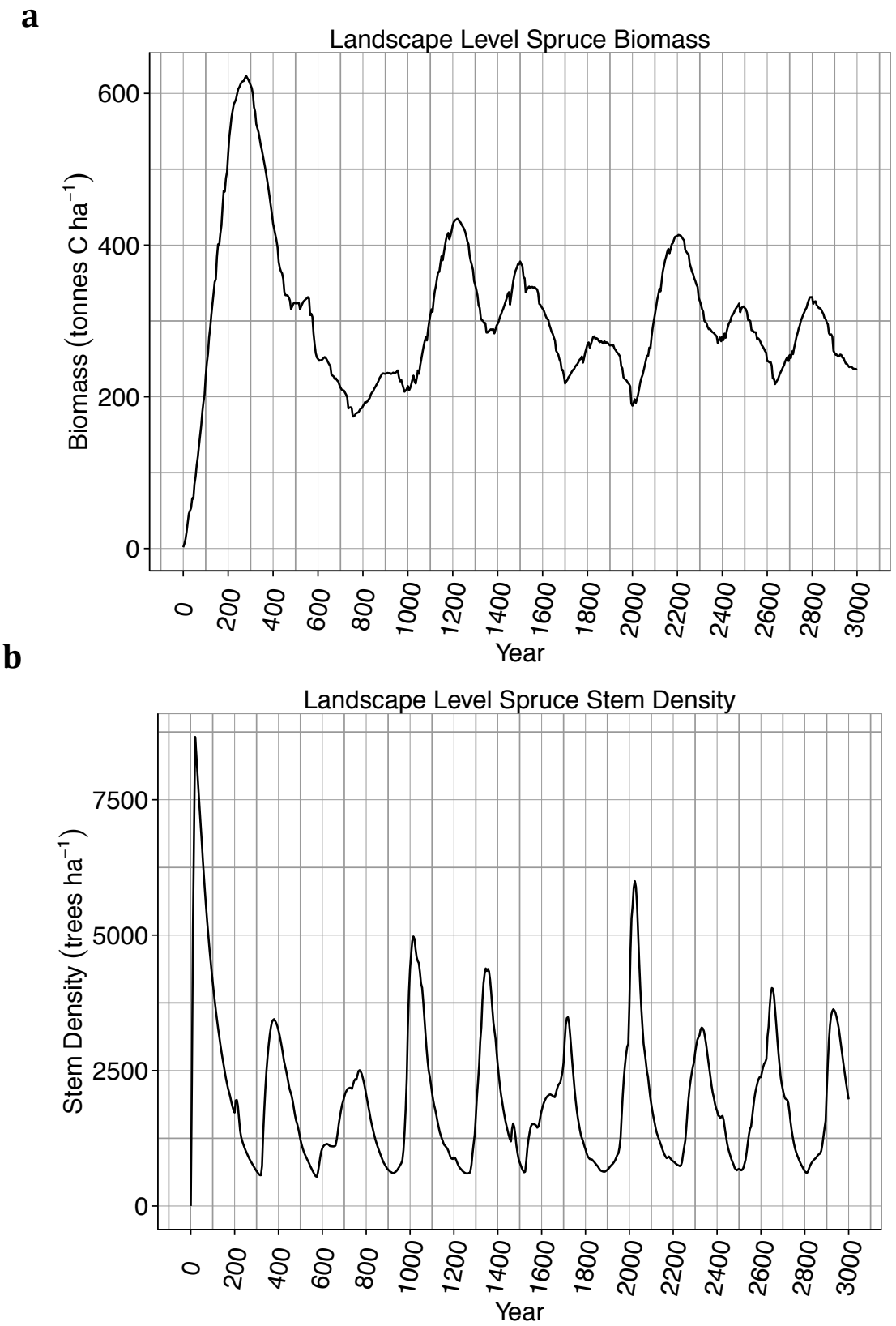

Figure 4.2 (a) Biomass and (b) stem count for modeled stands of exclusively Engelmann spruce (*Picea engelmannii*).

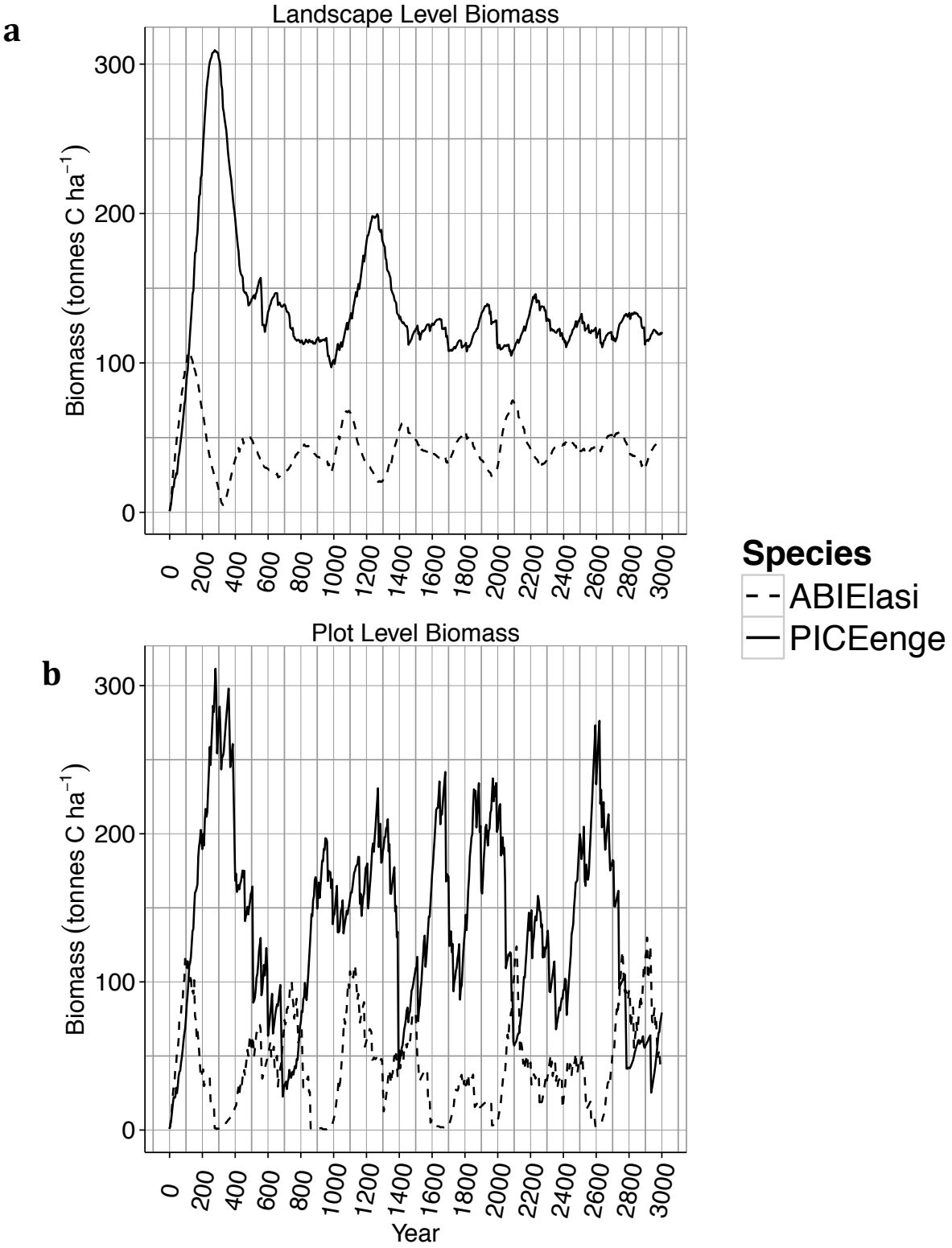

Figure 4.3 Biomass for a subalpine system (*A. lasiocarpa* and *P. engelmannii*) over 3000 years. Graph (a) is landscape-level output of biomass (tonnes C ha^{-1}), averaged over 200 plots. Graph (b) is plot-level output of biomass.

biomass dynamics. These landscape-scale biomass curves clearly show that these species are almost exactly out of phase with each other; the peak of one species' biomass occurs at the trough of the other's (Fig. 4.5).

Discussion

Several investigators have demonstrated evidence for long-term periodicities in forest ecosystems, despite the logistic challenges inherent in making such direct observations. McGee (1984) used dendrochronological analyses to investigate a synchronized canopy dieback of century-old trees during a drought in a diverse uncut forest in East Tennessee to find large canopy trees demonstrating semi-synchronized mortality in two species. Mueller-Dombois (1986) reviews many examples of synchronized diebacks for a range of forest ecosystems at widespread locations. Green (1981) conducted a time series analysis on several 2,000-year-old pollen cores from Everitt Lake, Nova Scotia, and found that there was a periodicity in the pollen data for many of the tree species, including fir, spruce, and pine, with periodicities ranging from 100 to 600 years. In a detailed reconstruction of *Pinus sylvestris* forest demographics, Zyabchenko (1982) found that *P. sylvestris* stands in the high-latitude forests of western Russia exhibit a cyclic pattern with a frequency of about 300 years. Space-for-time substitution studies on fir dynamics of Japan and the northeastern U.S. offer a clear visual example of cyclic phenomena that have a spatial component (i.e. fir waves) (Sprugel 1984, Moloney 1986, Sato and Iwasa 1993). These observations suggest that the underlying periodicities in forest ecosystems, such as those described in this study, are more common that it may seem (Platt and Denman 1975). These endogenous periodicities are usually obscured at the human time scale by disturbances to the system (i.e. hurricanes, logging, etc.).

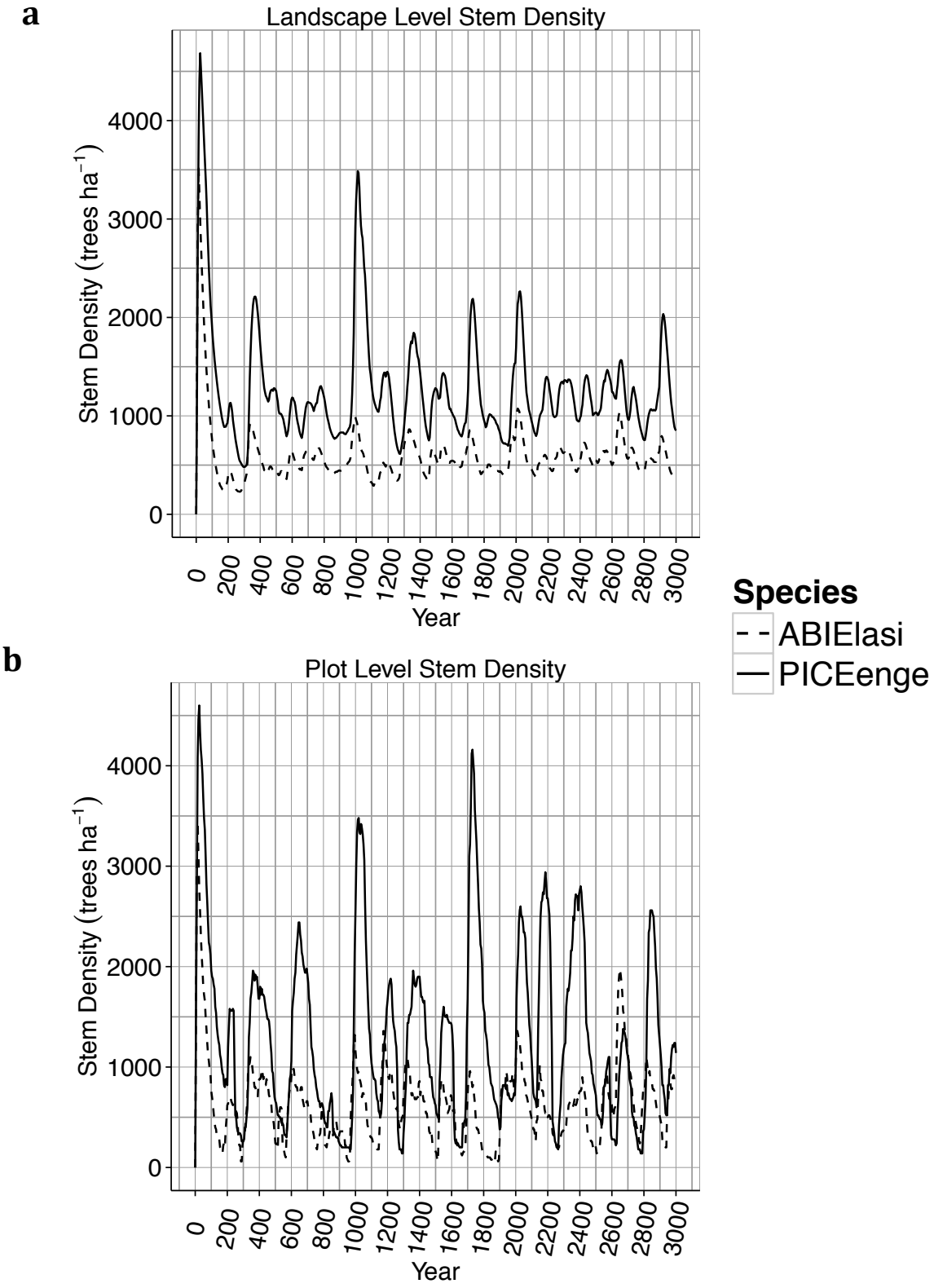

Figure 4.4 Stem count for a subalpine system (*A. lasiocarpa* and *P. engelmannii*) over 3000 years. Graph (a) is landscape-level output of stem count (trees ha^{-1}), averaged over 200 plots. Graph (b) is plot-level output of stem count.

Ecological modeling provides a unique opportunity for studying the endogenous properties of ecosystems, without the intrusion of exogenous factors. In individual-based gap models, periodic phenomena are emergent properties of local-scale forest dynamics. Periodicities in the dynamic responses of ecosystems are of interest because of the internal dynamics that they imply. This is particularly so when these dynamics arise as the consequences of internal interactions, or through autogenic succession. Fir (*Abies* spp.) waves are a rich example in forest ecosystems because they seem to be a chronosequence of the cyclical underlying patterns of change originally discussed by Watt (1947) for forests and other systems. While *Abies lasiocarpa* in this model-based analysis is not known for wave regeneration, this study indicates that without the intrusion of disturbance, it could also produce a wave-like pattern. Though UVAFME is not spatially explicit, the fact that it produces cyclic phenomena in fir and spruce without spatial coordination and without regeneration by exogenous intrusions, points to an underlying periodicity within the system. These internal periodicities, when organized by external environmental drivers as in Sprugel's (1984) classic study, could produce the spatially coordinated fir waves seen in the northeastern US and Japan,

Based on the ~180º out-of-phase periodicity in the biomass peaks of spruce and fir in these simulations (Fig. 4.3a, 4.5), the cycles seen in the model resemble some sort of reciprocal replacement between the two tree species. There have been many recorded instances of reciprocal replacement in which the seedlings and saplings of one tree species are unable to regenerate under adults of the same species (Jones 1945, Schaeffer and Moreau 1958, Grubb 1977). This phenomenon has been attributed to a difference in an environmental factor experienced by the adult trees relative to that experienced by young trees. Light represents such a

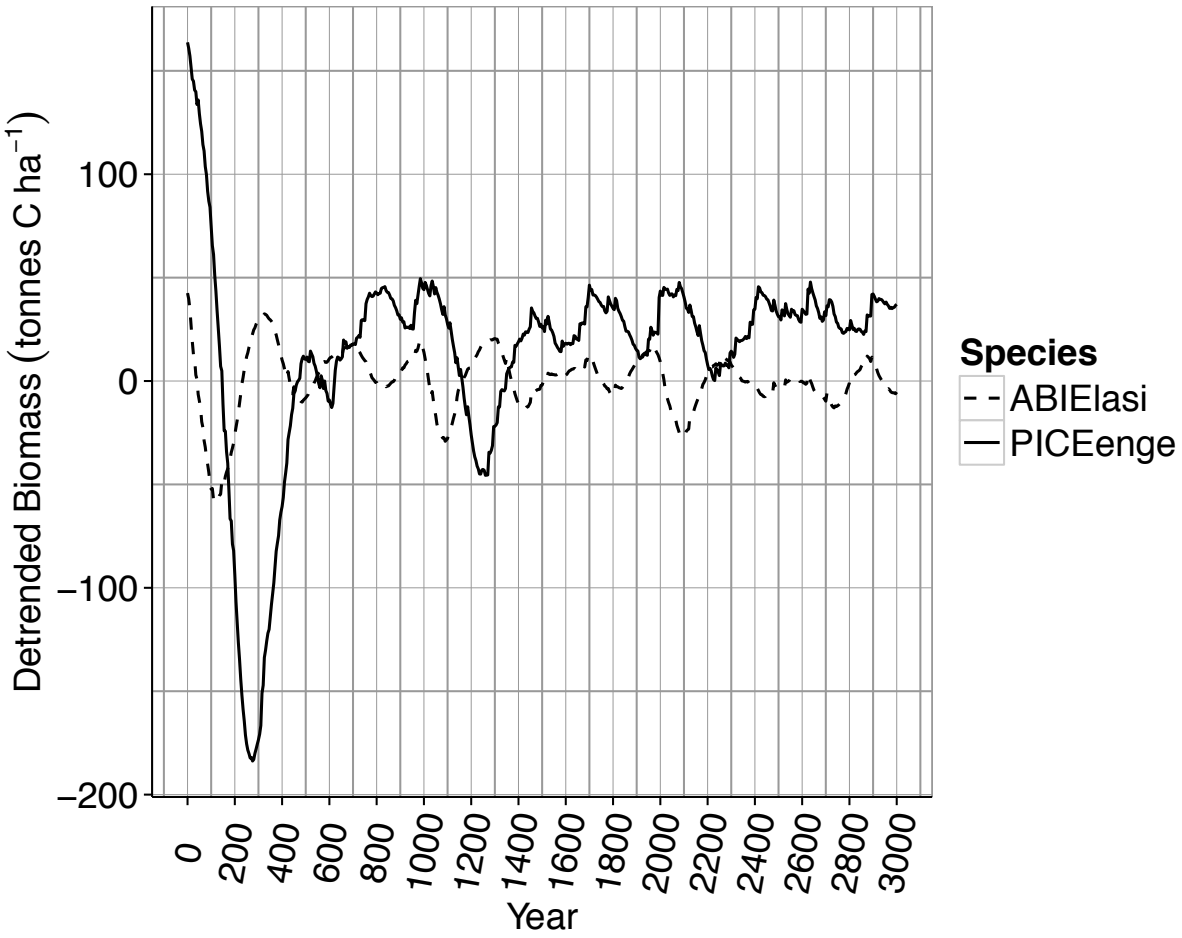

Figure 4.5. Detrended biomass for the output from the third modeling scenario (*A. lasiocarpa* and *P. engelmannii*) over 3,000 years

potential factor. When two shade tolerant species co-dominate, they may repeatedly replace each other on the landscape.

For example, in American beech (*Fagus grandifolia*)- sugar maple (*Acer saccharum*) forests (Woods 1979, Woods and Whittaker 1981), both shade tolerant species co-dominate the forest. In old growth stands of these species, beech and maple saplings tend to occur in areas that are closer to a canopy tree of the opposite species (Woods and Whittaker 1981). A study by Forcier (1975) found that the negative association between young trees and adult trees of the same species was a large driver of cyclical dynamics between yellow birch (*Betula*

alleghaniensis), sugar maple, and beech in a New Hampshire forest. While the dynamics seen in this study superficially resemble reciprocal replacement, with detailed inspection of the simulated stem count, reciprocal replacement does not seem to be the cause of the cyclic pattern in the subalpine zone. Both spruce and fir go through rapid regeneration at the same time on the individually simulated small plots, and not one after the other (Fig. 4.4a, b), as would be expected for reciprocal replacement.

Cyclic behavior of forests has already been seen in other individual-based models (Emanuel et al. 1978, Tharp 1978, Shugart 1984). For example, using a model-based analysis, Pastor et al. (1987) showed cyclic dynamics between spruce and birch in boreal North America arising from nitrogen limitation interacting with forest demography. Emanuel et al. (1978) found that the biomass output generated from the FORET model in an eastern U.S. hardwood forest had a strong cyclical component, with a frequency of about 200 years. The addition of a formerly dominant species (American chestnut, *Castanea dentata*) changed the frequency of the biomass cycle. A similar change in frequency is seen in the simulations of the subalpine zone of the Rocky Mountains in this study (Fig. 4.1, 4.3). By itself, subalpine fir exhibits a strong periodicity of about 200 years (Fig. 4.1), but with the addition of Engelmann spruce, which dominates subalpine fir, the periodicity of stem count and biomass changes to 300 years (Fig. 4.3, 4.4).

From the biomass and stem counts in three scenarios investigated, the cyclic pattern apparently results from the differences in the size and growth rate of fir and spruce. At the plot level (Fig. 4.3b, 4.4b), with the initial forest establishment on a plot at year 0, subalpine fir outcompetes the slower-growing Engelmann spruce. While subalpine fir grows very quickly initially, its rate of diameter increase drops rapidly at around year 100. In contrast, Engelmann spruce grows more slowly throughout its lifetime, and generally lives much longer than does

subalpine fir (Burns and Honkala 1990, Veblen et al. 1991). When the dominant age class of subalpine fir slows in growth around year 200 of the simulation, Engelmann spruce overtakes subalpine fir and becomes the dominant species (Fig. 4.3b). As the older subalpine fir begin to die, neither new fir nor spruce can regenerate under the dense canopy of adult spruce trees, which typically have a higher maximum diameter and height than subalpine fir (Burns and Honkala 1990). These growth characteristics of spruce and fir are manifested in the model through the species-specific parameters AGE_{max} , DBH_{max}, and H_{max} (see Table 2.1). The diameter increment growth for each year (G, cm) is based on these parameters, and is calculated in part from the growth equation of Botkin et al. (1972):

$$G = \frac{4H_{max}}{AGE_{max}}\left\{\ln\left(2(2DBH_{max}-1)+\frac{a}{2}\ln\left(\frac{\frac{9}{4}+\frac{a}{2}}{4DBH^{2}{}_{max}+2aDBH_{max}-a}\right)\right.\right.$$
$$\left.\left.-\frac{a+\frac{a^2}{2}}{\sqrt{a^2+4a}}\ln\left[\frac{\left(3+a-\sqrt{a^2+4a}\right)\left(4DBH_{max}+a+\sqrt{a^2+4a}\right)}{\left(3+a+\sqrt{a^2+4a}\right)\left(4DBH_{max}+a-\sqrt{a^2+4a}\right)}\right]\right\}$$

where DBH_{max} is the species-specific maximum diameter at breast height for the tree (cm), H_{max} is the maximum height (cm), AGE_{max} is the maximum age (years), and $a = (1 - 1.37)/H_{max}$. Through this equation, the increment growth for each tree slows as it ages, according to its own species-specific parameters. These input parameters can be found in Table 2.1 in Chapter 2, and were derived chiefly from Burns and Honkala (1990).

Once Engelmann spruce becomes dominant, those few dominant trees are large enough to suppress all seedlings. Eventually at around year 300, the old canopy spruce trees begin to senesce and are increasingly susceptible to environmental stress. In this window, a series of

unfortunate events in the form of multiple bad years kill the canopy spruce. Suppressed trees in the subcanopy and understory are released. Fir, due to its higher growth rate, is able to outperform the young spruce and the cycle repeats (see Figure 4.7 for a simplified drawing of this cycle).

The plot level output from this study also corresponds with what has been seen in some field studies on forest demographics in stressed conifer systems (Zyabchenko 1982, Aplet et al. 1988). Zyabchenko (1982) conducted an intensive field campaign on *Pinus sylvestris* stands in the high-latitude forests of western Russia featuring massive and detailed volumes of data collection from over 24 plots in order to reconstruct basal area, biovolume (m^3 C ha^{-1}) and average accumulation of biovolume, stems per hectare, and average DBH and height for a 650-year chronosequence. Through this rigorous investigation (in which over 1700 trees were cut down and over 1900 saplings were cored), it was found that *P. sylvestris* exhibits a cyclic canopy breakup and explosive increases in regeneration, with a periodicity of about 300 years (Fig. 4.6a, b). These data closely resemble the output from UVAFME for the subalpine zone (Fig. 4.3a, 4.6c). This type of forest dynamics analysis from *in situ* data is only feasible using such comprehensive and exhaustive field methods. Ecological modeling allows us to examine these phenomena without such labor-intensive, time-consuming methods.

Aplet et al. (1988) created a 600-year chronosequence of changes in age structure of an Engelmann spruce-subalpine fir forest in Colorado using field and dendrochronological data from five stands, and through this chronosequence, a cyclic spruce-fir basal area pattern emerged. They theorized that there were four phases of spruce-fir dynamics: colonization, in which both spruce and fir seedlings regenerate on the stand; spruce exclusion, in which spruce are initially inhibited by fir; spruce reinitiation, in which spruce outcompete fir; and second

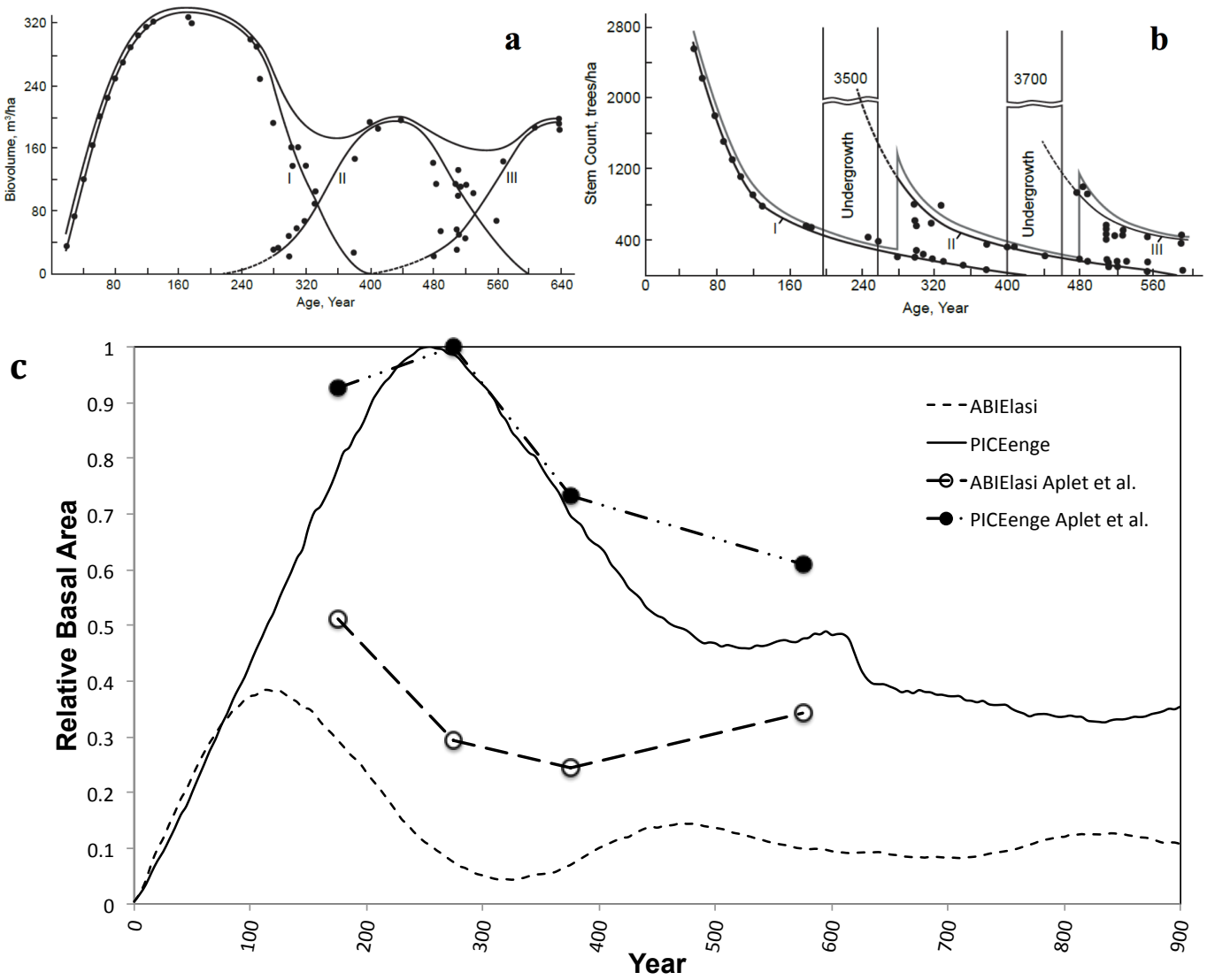

Figure 4.6. Internal wave dynamics in cold systems. (a) Biovolume ($m^3C\ ha^{-1}$) of *Pinus sylvestris* (redrawn from Zyabchenko 1982). The I, II, and III notations indicate cohorts of trees, i.e. individual generations; (b) stem count (trees ha^{-1}) of *P. sylvestris* in western Russia (redrawn from Zyabchenko 1982); c) relative basal area from the third modeling scenario for fir (dashed line) and spruce (solid line) from year 0 to year 900 alongside relative basal area data from Aplet *et al.* (1988) for fir (open circles) and spruce (solid circles).

generation spruce-fir forest, the final phase of the spruce-fir dynamics, in which the basal area of spruce and fir stabilize. The UVAFME output from bare ground to year 500 for the third model scenario (the competitive scenario of spruce and fir; Fig. 4.3a) corresponds to the basal area pattern from Aplet et al. (1988) (Fig. 4.6c) and to the first three theorized phases. While the fits between the two data sets are not perfect, the changes in the basal area trend match well. The

study by Aplet et al. (1988) did not have field data past year 575, so it is not certain how the respective basal areas of spruce and fir may have changed. The UVAFME output suggests that without disturbance, the periodic cycle of spruce and fir may continue into the future.

The results of this current study only use endogenous mortality due to tree stress or low growth. Disturbance by fire, wind, and insects are not included in these simulations. These types of disturbances are integral parts of the subalpine landscape, however the potential underlying periodicities of the system were better visualized with disturbances "turned off." Without random disturbance, secondary succession starts at the same time for all 200 plots, which sets in motion the cyclical pattern of both species. This repeating cycle can be seen at both the plot scale (Fig. 4.3b, 4.4b), and at the landscape scale (Fig. 4.3a, 4.4a), indicating that most of the 200 plots in the model are fairly in sync. This is likely occurring due to the strong influence of climate on this site and the absence of disturbance in the model. The subalpine zone is literally the edge of these trees' tolerance zones. On mountains that extend past 3600 meters or so, the trees turn stunted and hunch over into "*Krummholz*" forms, beaten down by icy wind and cold. With no disturbances in the model, these trees are so influenced by climate that they are synchronized when the combination of tree senescence and the occurrence of a run of stressful years kill most of the dominant old trees on most of the plots. One expects that under normal conditions in the field, disturbances like fire, windthrow and insect outbreaks disrupt this endogenous pattern by "resetting" the internal cycle on different plots. This produces a landscape comprised of plots that may be at a different stage at any one time, a quasi-equilibrium forest landscape mosaic (Bormann and Likens 1979, Shugart 1984).

This study has implications for an alternate subalpine landscape under an alternate climate regime. Most of the plot-scale cycle is relatively predictable. Once spruce and fir

regenerate at the same time, spruce will eventually outcompete fir, suppress fir and spruce seedlings, and then eventually release both species through synchronous mortality. This self-

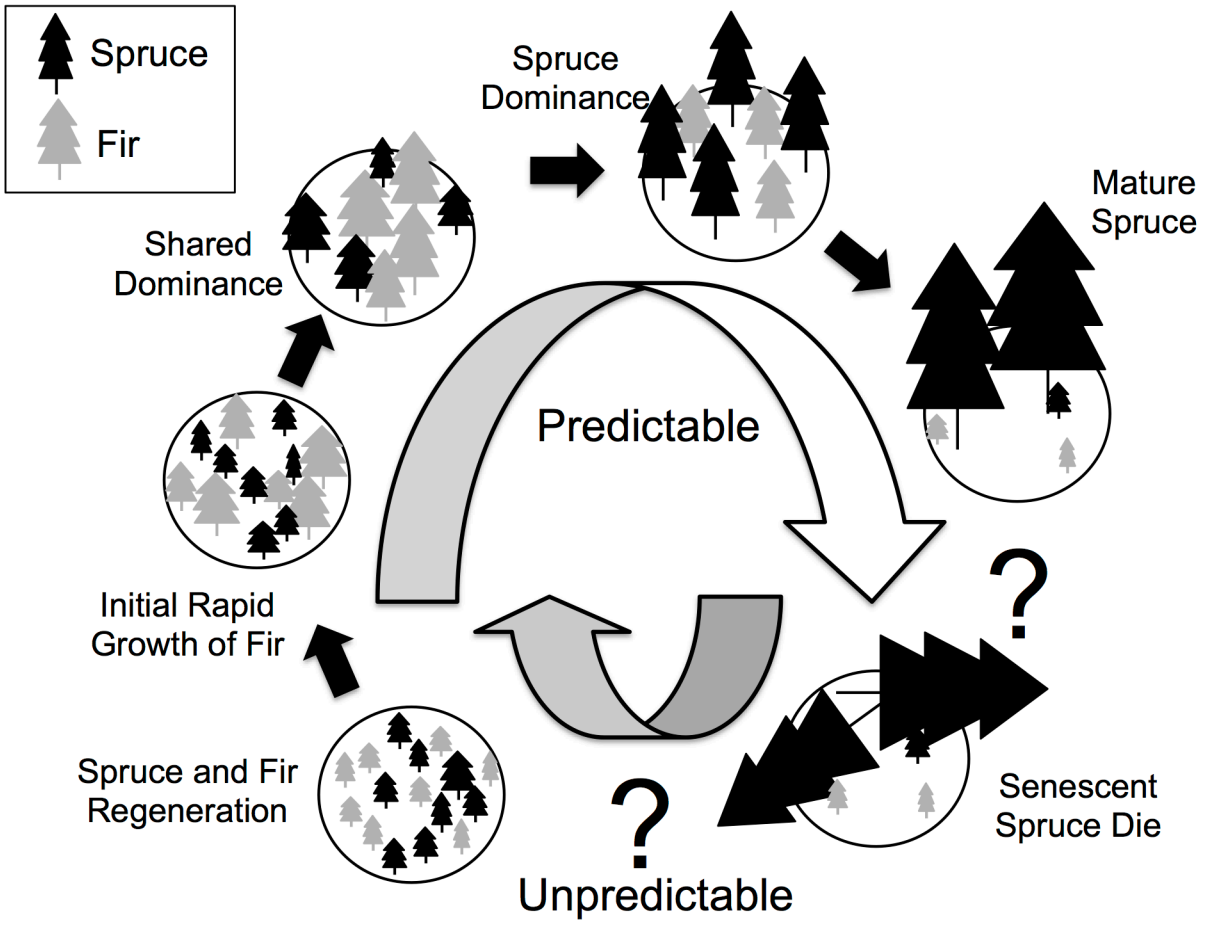

Figure 4.7. Cyclic phenomena in a spruce-fir forest.

perpetuating cycle creates the conditions (i.e. simultaneous spruce and fir regeneration) for it to continue into the future. There is only a small "window of opportunity" in between spruce mortality and the spruce/fir regeneration for the pattern to go in a different direction (Shugart et al. 1986). If, for example, fir were to establish in greater numbers than spruce, fir may successfully suppress and eventually overtake spruce as the dominant species on the stand. This small window of opportunity introduces the ability for changes in climate to drastically alter the dynamics of the subalpine zone (Fig. 4.7).

In a study by Elliott (2011), it was found that while factors affecting successful regeneration were strong drivers of forest dynamics in the subalpine zone, climate has the ability to change these driving factors. With climate change, tree species may become more vulnerable to drought and warmer temperatures (Anderegg et al. 2012), and Engelmann spruce seedlings are known to be generally intolerant to high temperatures (Seidel 1986). Additionally, increases in spruce beetle (*Dendroctonus rufipennis*) outbreaks may further reduce Engelmann spruce dominance at the plot scale (Berg et al. 2006). The greater stem density of fir may then allow it to quickly overtake the temperature intolerant, beetle-sensitive spruce. These changes in species dominance at the plot level may then scale up to changes in species dominance across the subalpine landscape.

Conclusions

Periodic phenomena in forest ecosystems have been variously studied using pollen records, dendrochronological reconstructions, space-for-time substitutions, and intensive and long-term forest sampling campaigns. In order to study these cyclic phenomena, which often have periodicities of hundreds of years, long-term data sets that are unmarred by disturbance events are a necessity. It is no small wonder that studies of this nature are few and far between. Using field methods alone, it would be nearly impossible to find more than a few forest stands older than about 500 years, especially in the western United States, where stand-replacing disturbance events are an integral component of the ecosystem. Ecological modeling provides a tool to study autogenic succession and the forest dynamics resulting from endogenous factors, without the need for long-term inventory or reconstruction data. With thousands-of-years model output, and the ability to “turn off” stand-replacing disturbances, the long-term, internal dynamics of forest ecosystems can be studied. This study has shown, through the use of the

individual-based gap model UVAFME, that the subalpine zone of the Rocky Mountains may contain internal cyclic phenomena, with a periodicity of about 300 years. Without disturbance, this cycle of fir initiation, eventual spruce dominance, spruce dieback, and spruce/fir regeneration, is self-perpetuating, as long as the initial conditions of spruce/fir regeneration are present. If the initial conditions were to change, due to climate change or a shift in disturbance frequency, the cycle may go in a new, different direction. Shifts in patterns and processes at the plot (i.e. less than 1 ha) scale have the ability to effect changes at the landscape and regional scales. It is clear that processes such as the cyclic phenomena described here are important, not just from a theoretical perspective, but also in terms of how the greater Rocky Mountain landscape may change in the context of regional shifts in climate and disturbance.

References

Alexander, R. 1987. Ecology, silviculture, and management of the Engelmann spruce - subalpine fir type in the central and southern Rocky Mountains. USDA Forest Service, Agricultural Handbook No. 659:155.

Anderegg, W. R. L., J. M. Kane, and L. D. . Anderegg. 2012. Consequences of widespread tree mortality triggered by drought and temperature stress. Nature Climate Change.

Aplet, G. H., R. D. Laven, and F. W. Smith. 1988. Patterns of community dynamics in Colorado Engelmann spruce-subalpine fir forests. Ecology 69:312–319.

Berg, E. E., J. D. Henry, C. L. Fastie, A. D. De Volder, and S. M. Matsuoka. 2006. Spruce beetle outbreaks on the Kenai Peninsula, Alaska, and Kluane National Park and Reseve, Yukon Territory: Relationship to summer temperatures and regional differences in disturbance regimes. Forest Ecology and Management 227:219–232.

Boehmer, H. J., H. H. Wagner, J. D. Jacobi, G. C. Gerrish, and D. Mueller-Dombois. 2013. Rebuilding after collapse: evidence for long-term cohort dynamics in the native Hawaiian rain forest. Journal of Vegetation Science 24:639–650.

Bormann, F. H., and G. E. Likens. 1979. Pattern and process in a forested ecosystem. Springer-Verlag, New York, NY.

Botkin, D. B., J. F. Janak, and J. R. Wallis. 1972. Some Ecological Consequences of a Computer Model of Forest Growth. The Journal of Ecology 60:849.

Bugmann, H. 2001. A review of forest gap models. Climatic Change 51:259–305.

Bugmann, H., A. Fischlin, and F. Kienast. 1996. Model convergence and state variable update in forest gap models. Ecological Modelling 89:197–208.

Burns, R. M., and B. H. Honkala. 1990. Silvics of North America: 1. Conifers; 2. Hardwoods. Agricultural Handbook 654. U.S. Department of Agriculture, Forest Service, Washington, DC. vol. 2 877 p.

Elliott, G. P. 2011. Influences of 20th-century warming at the upper tree line contingent on local-scale interactions: evidence from a latitudinal gradient in the Rocky Mountains, USA: Climate-pattern interactions at the tree line. Global Ecology and Biogeography 20:46–57.

Emanuel, W. R., D. C. West, and H. H. Shugart. 1978. Spectral analysis of forest model time series. Ecological Modelling 4:313–326.

Forcier, L. K. 1975. Reproductive strategies and the co-occurrence of climax tree species. Science 189:808–810.

Green, D. G. 1981. Time Series and Postglacial Forest Ecology. Quaternary Research 15:265–277.

Grubb, P. J. 1977. The maintenance of species-richness in plant communities: the importance of the regeneration niche. Biol. Rev 52:107–145.

Itow, S. 1988. Population structure, stand-level dieback and recovery of Scalesia pedunculata forest in the Galápagos Islands. Ecological Research 3:333–339.

Jane, G. T., and T. G. A. Green. 1983. Episodic forest mortality in the Kaimai Ranges, North Island, New Zealand. New Zealand journal of botany 21:21–31.

Jones, E. W. 1945. The structure and reproduction of the virgin forest of the North Temperate zone. New Phytologist 44:130–148.

Kohyama, T. 1983. Studies on the Abies population of Mt. Shimagare II. Reproductive and life history traits. Botanical Magazine of Tokyo 95:130–148.

McGee, C. E. 1984. Heavy mortality and succession in a virgin mixed mesophytic forest. USDA Forest Service Research Paper SO-209, Southern Forest Experiment Station, New Orleanse, LA.

Moloney, K. A. 1986. Wave and nonwave regeneration processes in a subalpine Abies balsamea forest. Canadian Journal of Botany 64:341–349.

Mueller-Dombois, D. 1986. Perspectives for an etiology of stand-level dieback. Annual Review of Ecology and Systematics 17:221–243.

Musselman, R. C., D. G. Fox, A. W. Schoettle, and C. M. Regan. 1994. The Glacier Lakes Ecosystem Experiments Site. U.S. Department of Agriculture, Forest Service, Rocky Mountain Forest and Range Experiment Station:94.

Pastor, J., R. H. Gardner, V. H. Dale, and W. M. Post. 1987. Successional changes in nitrogen availability as a potential factor contributing to spruce declines in boreal North America. Canadian Journal of Forest Research 17:1394–1400.

Platt, T., and K. L. Denman. 1975. Spectral analysis in ecology. Annual review of Ecology and Systematics:189–210.

Reiners, W. A., and G. E. Lang. 1979. Vegetational Patterns and Processes in the Balsam Fir Zone, White Mountains New Hampshire. Ecology 60:403.

Sato, K., and Y. Iwasa. 1993. Modeling of Wave Regeneration in Subalpine Abies Forests: Population Dynamics with Spatial Structure. Ecology 74:1538.

Sato, T. 1994. Stand structure and dynamics of wave-type Abies sachalinensis costal forest. Ecological Research 9:77–84.

Schaeffer, R., and R. Moreau. 1958. L'alternance des essences. Society For. France Compte Bull. 29:1–12, 76–84, 277–298.

Seidel, K. W. 1986. Tolerance of seedlings of ponderosa pine, Douglas fir, grand fir, and Engelmann spruce for high temperatures. Northwest Science 60:7.

Shugart, H. H. 1984. A Theory of Forest Dynamics: The Ecological Implications of Forest Succession Models. Springer Science & Business Media, New York, NY.

Shugart, H. H., M. J. Antonovsky, P. G. Jarvis, and A. P. Sanford. 1986. CO2, climatic change, and forest ecosystems: assessing the response of global forests to the direct effects of increasing CO2 and climatic change. Pages 475–521 *in* B. Bolin, B. R. Doos, J. Jager, and R. A. Warrick, editors. The greenhouse effect, climate change, and ecosystems (SCOPE 29). John Wiley, New York, NY.

Shugart, H. H., and F. I. Woodward. 2011. Global Change and the Terrestrial Biosphere. Wiley-Blackwell, Sussex, UK.

Sprugel, D. G. 1984. Density, Biomass, Productivity, and Nutrient-Cycling Changes During Stand Development in Wave-Regenerated Balsam Fir Forests. Ecological Monographs 54:165.

Sprugel, D. G., and F. H. Bormann. 1981. Natural disturbance and the steady state in high-altitude balsam fir forests. Science 211:390–393.

Tansley, A. G. 1935. The use and abuse of vegetational concepts and terms. Ecology 16:284–307.

Tharp, M. L. 1978. Modeling major perturbations on a forest ecosystem. M.S. Thesis, University of Tennessee, Knoxville, TN.

Veblen, T. T., K. S. Hadley, M. S. Reid, and A. J. Rebertus. 1991. The Response of Subalpine Forests to Spruce Beetle Outbreak in Colorado. Ecology 72:213.

Watt, A. S. 1947. Pattern and process in the plant community. The Journal of Ecology:1–22.

Woods, K. D. 1979. Reciprocal Replacement and the Maintenance of Codominance in a Beech-Maple Forest. Oikos 33:31.

Woods, K. D., and R. H. Whittaker. 1981. Canopy-understory interaction and the internal dynamics of mature hardwood and hemlock-hardwood forests. Pages 305–323 *in* D. C. West, H. H. Shugart, and D. B. Botkin, editors. Forest succession: concepts and applications. Springer-Verlag, New York, Ny.

Wooldridge, G. L., R. C. Musselman, R. A. Sommerfield, D. G. Fox, and B. H. Connell. 1996. Mean wind patterns and snow depths in an alpine-subalpine ecosystem as measured by damage to coniferous trees. Journal of Applied Ecology 33:100–108.

Zyabchenko, S. S. 1982. Age dynamics of scotch pine forests in the European North. Lesovedenie 2:3–10.

Chapter 5. Modeling the interactive effects of spruce beetle infestation and climate on subalpine vegetation

Introduction

Disturbances such as fire, windthrow, and insect outbreaks are principal drivers of the vegetation dynamics within the Rocky Mountains and can interact to affect forest composition and dynamics as well as ecosystem processes and biogeochemical cycling (Veblen et al. 1991, 1994, Goetz et al. 2012, Edburg et al. 2012, Hansen 2013, Frank et al. 2014, O'Halloran et al. 2014). Outbreaks of the spruce beetle (*Dendroctonus rufipennis* (Kirby)), which infests Engelmann spruce (*Picea engelmannii* (Parry ex Engelm.)) in subalpine forests, have increased in recent years (USFS 2015), leading to widespread mortality and carbon losses throughout the western US and Canada (Berg et al. 2006, Bentz et al. 2009). Many factors have been attributed to these recent outbreaks, including the availability of vast, contiguous areas of large-diameter spruce (DeRose et al. 2013, Hart et al. 2015b), higher incidents of drought (Hebertson and Jenkins 2008, DeRose and Long 2012a, Hart et al. 2014a), and increases in ambient temperatures (Sherriff et al. 2011, DeRose et al. 2013). The frequency and severity of spruce beetle outbreaks, as well as wildfire, are predicted to increase further with climate change (Westerling et al. 2006, Bentz et al. 2010), potentially leading to elevated drought- and disturbance-related mortality, and shifts in species zonation. The future of subalpine forests is thus becoming progressively unclear as climate change and disturbances act in concert to alter their structure, composition, and internal dynamics (Fettig et al. 2013).

Within the Rocky Mountains, fire, windthrow, and bark beetle outbreaks can act as moderate, or non-stand-replacing disturbances (Veblen et al. 1991, Kulakowski and Veblen 2002, Sibold et al. 2007), which have the capacity to modify the structural and biological diversity of forest

stands, rather than simply "leveling" the forest to initiate secondary succession (Bond-Lamberty et al. 2015). This differential effect on tree size and species allows for unique interactions between the different types of disturbances. For example, wildfire can reduce stand susceptibility to all but the most extreme windthrow events through increases in the prevalence of smaller, more wind resistant stems (Kulakowski and Veblen 2002). Moderate windthrow and low intensity fires can increase stand susceptibility to insect outbreaks through tree damage and increases in coarse woody debris (Schmid and Frye 1977, Geiszler et al. 1984, Christiansen et al. 1987, Rasmussen et al. 1996, Hood and Bentz 2007, Fettig et al. 2008, Mezei et al. 2014). In contrast, high-intensity fires decrease the probability for insect outbreak through decreases in the availability of suitable host tree material (Veblen et al. 1994, Bebi et al. 2003, Kulakowski and Veblen 2006). Bark beetles can also interact with wildfire, and are capable of increasing the probability for active crown fires in the early stages of an outbreak through increases in dry, flammable fuels (Hicke et al. 2012, Jenkins et al. 2012).

It is clear that the interactions between disturbances and vegetation are complicated and nonlinear. With the addition of climate change effects on disturbances as well as vegetation, even more complications arise. Vegetation, wildfire, and insects respond to small-scale changes in weather, such as seasonal droughts, as well as larger-scale changes in climate, such as El Niño events or more directional climate change (Veblen et al. 2000, Sherriff et al. 2011). During droughts or periods of elevated atmospheric demand, trees' defenses are compromised through loss of carbohydrate reserves (Fettig et al. 2013), whereas population growth of bark beetles is accelerated by increasing summer and winter temperatures (Veblen et al. 1991, Hansen et al. 2001a, 2011). Thus drought and warmer temperatures act together to increase forest vulnerability to insect outbreak. However, as bark beetles require adequate host material to mate and

reproduce, climate change may result in a decrease in insect outbreak simply through reduction in suitable hosts (DeRose et al. 2013).

Spruce beetle populations typically exist at low, endemic levels, with periods of high, epidemic levels due to climate, disturbance, or forest structure-related triggers (DeRose et al. 2013). During endemic periods spruce beetles colonize downed spruce logs and may attack older or larger trees, though the success of these attacks is mediated by the health and ability of the tree to defend itself and the number of beetles attacking the tree (Schmid and Frye 1977, Raffa et al. 2008). Trees with high vigor may fend off infestations by exuding resin and allelochemicals, trapping and killing their attackers and their brood. A "mass attack" of many beetles, however, overwhelms trees' efforts, leading to successful infestations and subsequent tree mortality (Raffa et al. 2008). Weather and environmental factors that increase spruce beetle population levels (i.e. a high amount of coarse woody debris, high density and proportion of spruce, or droughts) often allow for more successful mass attacks that build into widespread outbreaks (Schmid and Frye 1976, Berg et al. 2006, DeRose and Long 2012b). Over the course of a spruce beetle outbreak, however, the factors and conditions necessary for infestation tend to become less and less important as spruce beetle populations rise. For example, a study by Wallin and Raffa (2004) found that while individual beetles strongly avoid trees with a high concentration of allelochemicals, this avoidance decreases as the number of beetles present increases. Additionally, DeRose & Long (2012b) found that as outbreak phase progresses and beetle population pressure escalates, host selection factors (i.e. spruce DBH and density, etc.) correlate less and less with the number of attacked trees.

Spruce beetle growth response to ambient temperatures has also been shown to influence population growth and outbreak success, especially in recent years (Sherriff et al. 2011, DeRose

and Long 2012b). Spruce beetles have a differential life cycle depending on ambient temperatures. Under low or normal temperature conditions, spruce beetle larvae take two full years to develop into adults, whereas anomalously warm temperatures allow larvae to fully develop in only one year (Hansen et al. 2001a). This flexible voltinism results in higher populations under univoltine (one-year) life cycles compared to semivoltine (two-year) life cycles, especially considering that there is no difference between egg production and survivorship of univoltine and semivoltine broods (Hansen and Bentz 2003). It is predicted that with increasing ambient temperatures from greenhouse gas emissions more and more spruce beetles will switch from a semivoltine to a univoltine life cycle (Bentz et al. 2010). This switch in life cycles will lead to more beetles emerging and reproducing every year rather than every other year, potentially allowing for exponential population growth compared to that of solely semivoltine beetles (Hansen et al. 2001b). Higher beetle populations will allow for more frequent mass attacks on spruce trees, and potentially more frequent and widespread outbreaks, though these outbreaks may be impeded by declining spruce biomass.

Due to the complex interactions between climate, vegetation, and disturbances, which occur at multiple spatial and temporal scales, it is difficult to determine what the ultimate response of spruce beetles, and subsequently subalpine vegetation, will be to various climate change scenarios. Plausible outcomes include an enhancing effect between spruce beetle infestations and climate, leading to greater spruce mortality than would be expected from simply the addition of climate and beetle-related mortalities, as well as a dampening effect of climate on infestations due to declining spruce hosts. Some combination of these interactions may also occur, and it is likely to change over time and with stand characteristics. Thus, to predict the relative and combined effects of shifting climate and disturbance regimes, individual tree and

individual stand interactions between climate, vegetation, and various disturbances must be considered. Individual-based models simulate individual tree response to competition and external forces and can also be scaled up to understand landscape-scale dynamics and emergent properties of landscapes. As such, they are a valuable tool for answering such questions about the future of forested ecosystems and are uniquely capable of capturing the interactive dynamics between various vegetation drivers. In this chapter, a spruce beetle submodel is developed and implemented in the individual-based gap model UVAFME. Model simulations are conducted at sites within the southern Rocky Mountains with different combinations of spruce beetle presence and climate change to determine the relative and combined effects of beetle disturbance and changing climate on subalpine vegetation. These results advance our understanding of the possible futures for the southern Rocky Mountains subalpine zone and form a baseline for further study on potential climate and disturbance mitigation techniques.

Methods

Windthrow and fire submodel updates

Windthrow in UVAFME is stochastic and is based on a site-specific return interval. Previously, when windthrow occurred on a plot in UVAFME, it would immediately kill all trees on the plot, regardless of size. Studies have shown that windthrow differentially affects trees of varying sizes, with larger trees having a higher probability of windthrow mortality than smaller, more wind resistant trees (Foster 1988, Everham and Brokaw 1996, Canham et al. 2001, Kulakowski and Veblen 2002, Rich et al. 2007). The windthrow submodel in UVAFME was updated to reflect these dynamics using equations (Eq. 5.1, 5.2) based on a study by Rich et al. (2007).

$$L_{wind} = 0.75 \ln (DBH_{tree}) \quad (5.1)$$

$$p_{wind} = \frac{1.0}{1.0+e^{-L_{wind}}} \quad (5.2)$$

where DBH_{tree} is the diameter at breast height (cm) of a simulated tree, and p_{wind} is the probability of that tree dying from the windthrow event. This updated windthrow submodel allows for more a realistic simulation of the effect of windthrow on forest structure within the southern Rockies and will also allow for better interaction between fire, windthrow, and bark beetles. The fire submodel was also updated such that the fire probability of a site (based on a site-specific return interval) increases with increasing site aridity, defined as the ratio of precipitation to potential evapotranspiration ($arid = \frac{p}{PET}$) as in Feng and Fu (2013). A base aridity ($arid_{base}$) for each site is calculated using the first 100 years of climate simulation, and this base aridity is compared against each subsequent year's aridity. If the aridity in any subsequent year is lower (i.e. drier) than the site's base aridity, the fire probability for that site that year is modified using the percentage difference between the base aridity and that year's aridity:

$$f'_{prob} = f_{prob} + f_{prob}\left(\frac{arid_{base}-arid}{arid_{base}}\right) \quad (5.3)$$

Using this modification, the probability of fire occurring can increase along with increasing evaporative demand, either due to lower precipitation or higher temperatures. This interaction between fire and climate has been widely predicted for various regions, including the western US (Dale et al. 2001, Joyce et al. 2014, Rogers et al. 2015, Jolly et al. 2015). With the addition of changing climate's effect on fire in UVAFME, the combined effect of changing climate, increasing fire, and potentially increasing insect infestations can be evaluated.

Spruce beetle submodel

The probability of spruce beetle infestation in any given Engelmann spruce tree is based on three factor types, each operating at different scales: climate factors, which affect infestation probability at the site and plot level; plot characteristics, which affect infestation probability at the plot level; and tree characteristics, which affect each tree individually. The climate factors were derived from studies on the phenology of spruce beetles and what influences their shift from a semivoltine to a univoltine life cycle (Hansen et al. 2001b, 2011, Sherriff et al. 2011). Based on a detailed spruce beetle phenology study by Hansen et al. (2001b), calculations were included to determine whether the beetle population on each plot has a semivoltine (two-year) or univoltine (one-year) life cycle. This calculation is based on the cumulative hours above 17°C during the period of 40 to 90 days prior to the beetles' peak flight. Peak flight is set to June 10 based on Dyer (1975) and Schmid and Frye (1977). In order to calculate cumulative hours, modeled daily minimum (T_{min}, °C) and maximum (T_{max}, °C) temperatures are converted into hourly temperatures via a sinusoidal formula from Reicosky et al. (1989). This formulation is based on inputs of daily minimum and maximum temperatures as well as sunrise time. Hourly temperature (T_H, °C) is calculated as:

$$T_H = \begin{cases} T_{av} + \left(\frac{T_{max}-T_{min}}{2}\right)\cos\left(\frac{\pi H'}{10.0+H_{rise}}\right), & 0 \le H < H_{rise} \; and \; 14 < H \le 24 \\ T_{av} - \left(\frac{T_{max}-T_{min}}{2}\right)\cos\left(\frac{\pi(H-H_{rise})}{14.0-H_{rise}}\right), & H_{rise} \le H \le 14 \end{cases} \quad (5.4)$$

where T_{av} is average daily temperature, defined as $T_{av} = (T_{max} + T_{min})/2$, H_{rise} is the hour of sunrise, and H' is defined as $H' = H + 10$ when $H < H_{rise}$, and $H' = H + 14.0$ when $H > 14.0$ (Fig. 5.1). This equation is then used to accumulate the number of hours above 17°C (H_{17}) during 40 to 90 days prior to peak spruce beetle flight, defined as March 12 through May 1 in

these simulations. Cumulative hours above 17°C is equal across all plots within an individual site, but may change from year to year and from site to site. The probability of any one plot

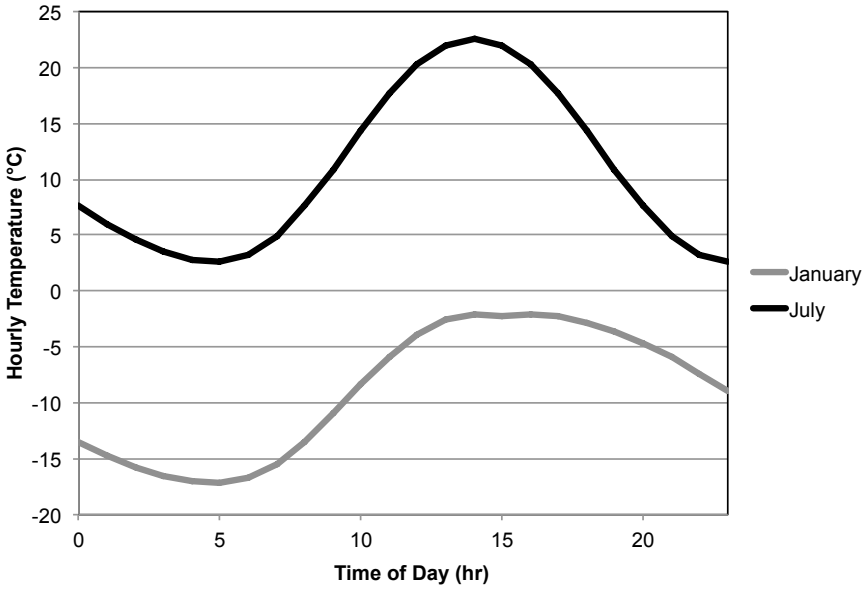

Figure 5.1. Example of hourly temperature calculated based on Equation 5.4 for a typical day in January (T_{min} = -17.22, T_{max}= -2.14) and July (T_{min} = 2.63, T_{max}= 22.63) in the southern Rocky Mountains.

having beetles with a univoltine life cycle (p_{uv}; Eq. 5.5, 5.6), from Hansen et al. (2001), is then calculated and is used to influence the infestation probability of each individual tree on that plot.

$$L_{H_{17}} = -3.954 + 0.01944H_{17} \quad (5.5)$$

$$p_{uv} = \frac{1.0}{1.0+e^{-L_{H_{17}}}} \quad (5.6)$$

Plot-level factors are calculated each year based on individual plot characteristics, and thus will vary between the simulated plots at a given site. These plot-level factors are based on spruce beetle susceptibility stand ratings from Schmid and Frye (1976). As in their stand rating system, this model uses average DBH of live spruce above 25.4 cm DBH, plot-level basal area

(including all species), and percent of spruce in the canopy as factors for determining plot-wide susceptibility to spruce beetle attacks. Depending on the value of each of the three factors, each plot receives three factor ratings from 1 to 3 (Table 5.1), and the ratings from each individual factor are added together to produce an overall stand rating (possible values being 3 to 9). The overall stand rating is then used to calculate the probability for spruce beetle infestation in each tree due solely to plot characteristics (f_{stand}, 0 to 1; Eq. 5.7).

$$f_{stand} = 0.75 \ln(f_{DBH} + f_{BA} + f_{can}) - 0.8 \quad (5.7)$$

This overall stand rating is then modified based on recent windthrow events to account for the high influence of blowdown on bark beetle outbreaks (Christiansen et al. 1987, Wichmann and Ravn 2001, Mezei et al. 2014). Following a windthrow event, the overall stand infestation probability is increased by 0.3 for the first three years, 0.2 from four to six years, and 0.1 from five to nine years. Because spruce beetle populations can utilize downed spruce trees (from windthrow or other mortality factors) for reproduction at low levels (Schmid and Frye 1977), plot-wide susceptibility is also influenced based on the amount of coarse woody debris on the plot available for spruce beetle colonization. Spruce trees larger than 25.4 cm DBH that die from either windthrow, age, or low growth are added to a pool of coarse woody debris (CWD_{spruce}, tonnes C ha^{-1}). A plot-wide woody debris factor (f_{CWD}, 0 to 1) is then calculated, which increases linearly with increasing spruce woody debris:

Table 5.1. Values of plot factors associated with each factor rating used to calculate overall plot-wide probability of spruce beetle infestation (from Schmid and Frye 1976).

	Plot Factor Value		
Susceptibility Rating	Basal area of stand (m^2 ha^{-1})	Mean DBH of live Engelmann spruce over 24.5 cm DBH (cm)	Percent Engelmann spruce in canopy (%)
Low (1)	< 22.95	< 30.48	< 50.0
Medium (2)	22.95 to 34.43	30.48 to 40.64	50.0 to 65.0
High (3)	≥ 34.43	≥ 40.64	≥ 65.0

$$f_{CWD} = \min\left(\left(\frac{CWD_{spruce}}{CWD_{base}}\right), 1.0\right) \quad (5.8)$$

where equation CWD_{spruce} is the amount of spruce coarse woody debris on the plot, and CWD_{base} is a maximum amount of spruce CWD, set to 300 tonnes C ha^{-1} (Temperli et al. 2013).

Tree-level factors that affect the probability of spruce beetle infestation include individual tree size (f_{tDBH}), stress level (f_{stress}), and scorch volume of recent fires (f_{scorch}). Under normal conditions, trees that are smaller than 30 cm DBH are not susceptible to spruce beetle attack (DeRose and Long 2012b). Under epidemic conditions (i.e. greater than 15 m^2 ha^{-1} of basal area killed per year) trees as small as 10 cm DBH may be killed by spruce beetles (Peet 1981, Veblen et al. 1994, DeRose and Long 2012b). Otherwise, based on information from relevant literature on bark beetle infestations (Furniss et al. 1979, Negron 1998, Hood and Bentz 2007, Zolubas et al. 2009, Mezei et al. 2014) and inventory data from the US Forest Service, infestation probability due to tree size (f_{tDBH}, 0 to 1) increases linearly with increasing tree diameter (Eq. 5.9).

$$f_{tDBH} = \min(0.011 DBH_{tree}, 1.0) \quad (5.9)$$

Many studies have shown that prolonged stress and associated low tree vigor, due to drought, age, or other factors, increases a tree's susceptibility to bark beetle attacks (Kalkstein 1976, Waring and Pitman 1980, Larsson et al. 1983, Christiansen et al. 1987, Mattson and Haack 1987, Malmstrom and Raffa 2000, McKenzie et al. 2009). In this model, tree stress is quantified as prolonged low diameter increment growth (i.e. less than 0.03 cm per year). Probability of spruce beetle infestation due to stress level (f_{stress}, 0 to 1) increases by 0.1 each year the tree in question has diameter growth below 0.03 cm, and is reset to 0 if the tree has higher than 0.03 cm growth in any given year. Damage due to fire has also been cited as a potential precursor to bark beetle attack (Geiszler et al. 1984, Christiansen et al. 1987, Rasmussen et al. 1996, Hood and

Bentz 2007). UVAFME calculates fire damage by percent crown volume scorched (CK, %) based on fire dynamics equations from Keane et al. (2011) and Van Wagner (1973). In this spruce beetle model, susceptibility to beetle infestation based on fire damage (f_{scorch}, 0 to 1) is equal to the percent crown volume scorched from fires.

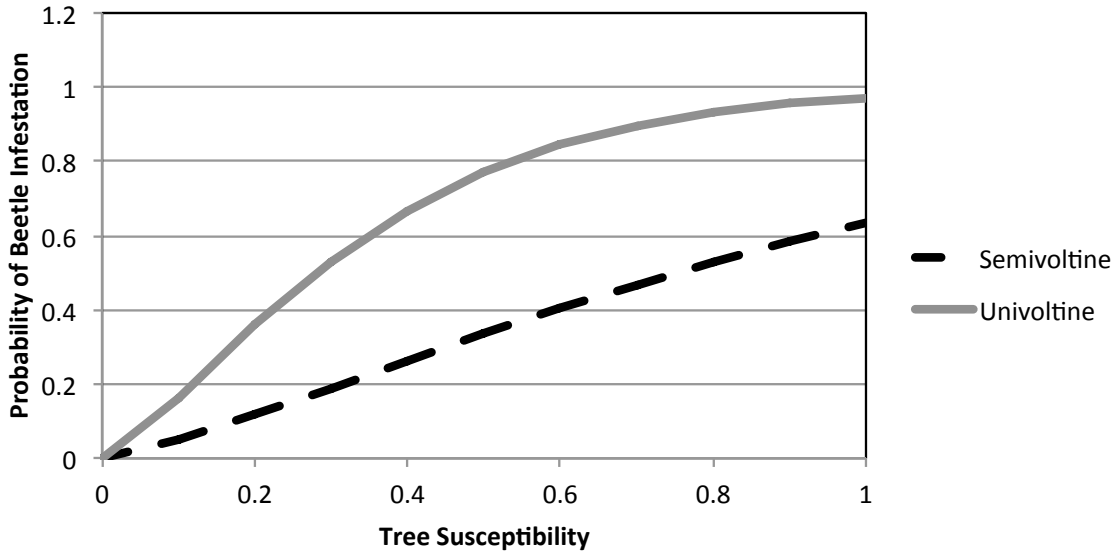

Figure 5.2. Probability of beetle infestation (p_{beetle}) increases with increasing tree susceptibility (f_{tree}) and with the presence of univoltine beetles (Eq. 5.11).

As with the individual plot-level factors, these tree-level factors are combined, along with the overall plot-wide factors, to produce an overall tree-level susceptibility to spruce beetles (f_{tree}, 0 to 1; Eq. 5.10).

$$f_{tree} = \min\big((0.3f_{stand} + 0.25f_{tDBH} + 0.2f_{stress} + 0.1f_{scorch} + 0.4f_{CWD}), 1.0\big) \quad (5.10)$$

This susceptibility is used to calculate the final tree-level probability for spruce beetle infestation (Eq. 5.11, Fig. 5.2):

$$p_{beetle} = 1.0 - e^{(-2.0{f_{tree}}^{1.3})^{gen}} \quad (5.11)$$

where gen is equal to 1.8 if the plot in question has univoltine beetles (based on Eq. 5.6) and 0.5 if it does not. Equation 5.11 was adapted from a bark beetle modeling study by Seidl et al. (2007) on the European spruce bark beetle in Norway spruce forests.

Once a tree becomes infested in this spruce beetle submodel, it ceases growth (Frank et al. 2014), and loses its needles after two years (Schmid and Frye 1977). Finally, after five years of being infested, the tree is marked as dead and is added to the soil layers for decomposition. A study by Hart et al. (2014b) found that proximity to infested spruce trees was an important factor in determining infestation probability. Thus, within this spruce beetle submodel, during the time when a tree is infested and still on a plot it increases the infestation probability of directly (by 0.3) and diagonally (by 0.1) adjacent spruce trees. This spatial interactivity between spruce trees required the conversion of UVAFME's 1D list of trees to a 2D grid of trees.

Model simulations

All model simulations were conducted at each of the four sites within the subalpine zone of the southern Rocky Mountains (Fig. 5.3). Detailed descriptions of these sites can be found in Chapter 2 of this work. To determine the response of subalpine vegetation to climate change, spruce beetles, and their interaction, several model simulations were run involving four different beetle/climate scenarios at each site: (1) a control run with current climate and no spruce beetle disturbance; (2) current climate with spruce beetle disturbance; (3) climate change without beetle disturbance; and (4) climate change with concurrent beetle disturbance. For each of these simulations, the model was run with 200 independent, 500 m^2 plots. Range maps were used to determine which of the eleven major southern Rocky Mountains species were eligible for colonization and growth at each site (Little 1971). For the current climate simulations (scenarios 1 and 2), UVAFME was run from bare ground for 800 years, at which point the forest should

reach a stable, quasi-equilibrium status. For the climate change simulations (scenarios 3 and 4), UVAFME was run from bare ground until year 500 under current climate conditions, after which 100 years of climate change were initiated. Climate and vegetation were then allowed to stabilize at the new values until year 800. In either beetle scenario (scenarios 2 and 4), beetle infestation was initiated at year 400.

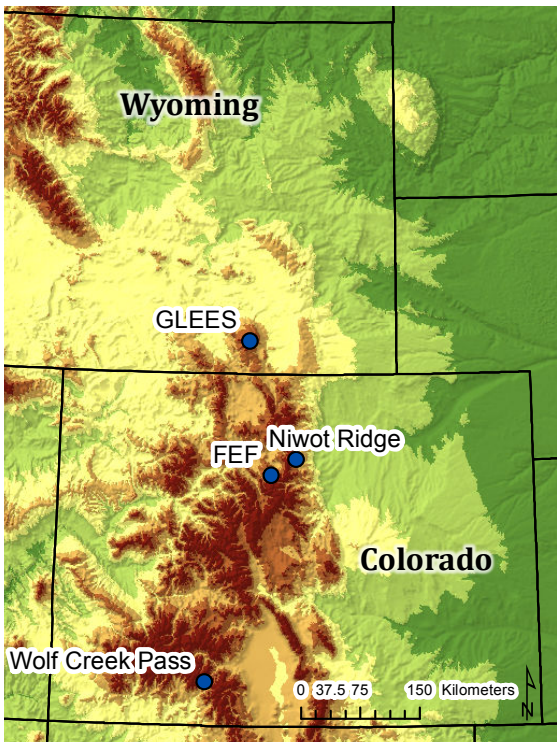

Figure 5.3. Map of study sites.

Climate input, in the form of changing monthly minimum and maximum temperature and monthly precipitation, was derived from output from the NCAR's Community Earth System Model (CESM) for the A1B and A2 IPCC climate change scenarios. The A1B scenario resulted in an increase in summer and winter temperatures of about 3°C, and relatively no change in precipitation. The A2 scenario resulted in an increase in winter temperatures of about 4°C, an increase in summer temperatures of about 7°C, and relatively no change in precipitation. After this 100-year period of climate change, vegetation was allowed to stabilize for 200 more years at the new temperature and precipitation values. The size structure and species-specific biomass output were then compared for all scenarios at all four sites. Additionally, two elevation tests were conducted as in Chapter 3 (1600 to 3600 m, 100 m intervals) with (1) beetle infestation under current climate, and (2) beetle infestation under the A1B scenario, to determine how species zonation may change with the combined effect of spruce beetles and climate change.

Results and Discussion

The response of subalpine vegetation to spruce beetles under current climate varied across all four sites, with GLEES and Wolf Creek having the steepest declines in Engelmann spruce (*Picea engelmannii*) biomass following the introduction of beetles (Fig. 5.4b, 5.5b), and Fraser Experimental Forest having only a slight decline in spruce biomass (Fig. 5.Bb). Graphs of biomass over time for the control and solely beetle disturbance simulations (as well as other beetle/climate change simulations not presented in this section) for Niwot Ridge and Fraser Experimental Forest can be found in the supplementary material of this chapter. Across all four sites, the addition of spruce beetle infestation under current climate scenarios resulted in about a 70% loss of spruce biomass at year 800 (at the end of the simulations) relative to year 800 biomass without beetles (Fig. 5.6). In contrast, there was only a small increase in the biomass of non-host species (i.e. *Abies lasiocarpa*, *Pinus contorta*, etc.) between the control and beetle simulations (Fig. 5.8, 5.9). Additionally, there was a difference in the size structure of Engelmann spruce between the two simulations (Fig. 5.10). The beetle disturbance simulation had virtually no large spruce stems (above 40 cm DBH); it also had a much higher proportion of small spruce stems (below 10 cm DBH) than did the control simulation. Thus, spruce beetle infestations resulted in a shift towards smaller trees and an increase in subdominant spruce trees in addition to an increase in non-host species.

These biomass dynamics are comparable to what has been found in various field studies. Derderian et al. (2016) found that a recent spruce beetle infestation in northern CO resulted in a decline in Engelmann spruce biomass of about 70%, very little increase in subalpine fir biomass (~2%), and a strong increase in the stem production of both spruce (~50%) and fir (~80%). Another study investigated the effects of the 1940s spruce beetle outbreak across sites in central-

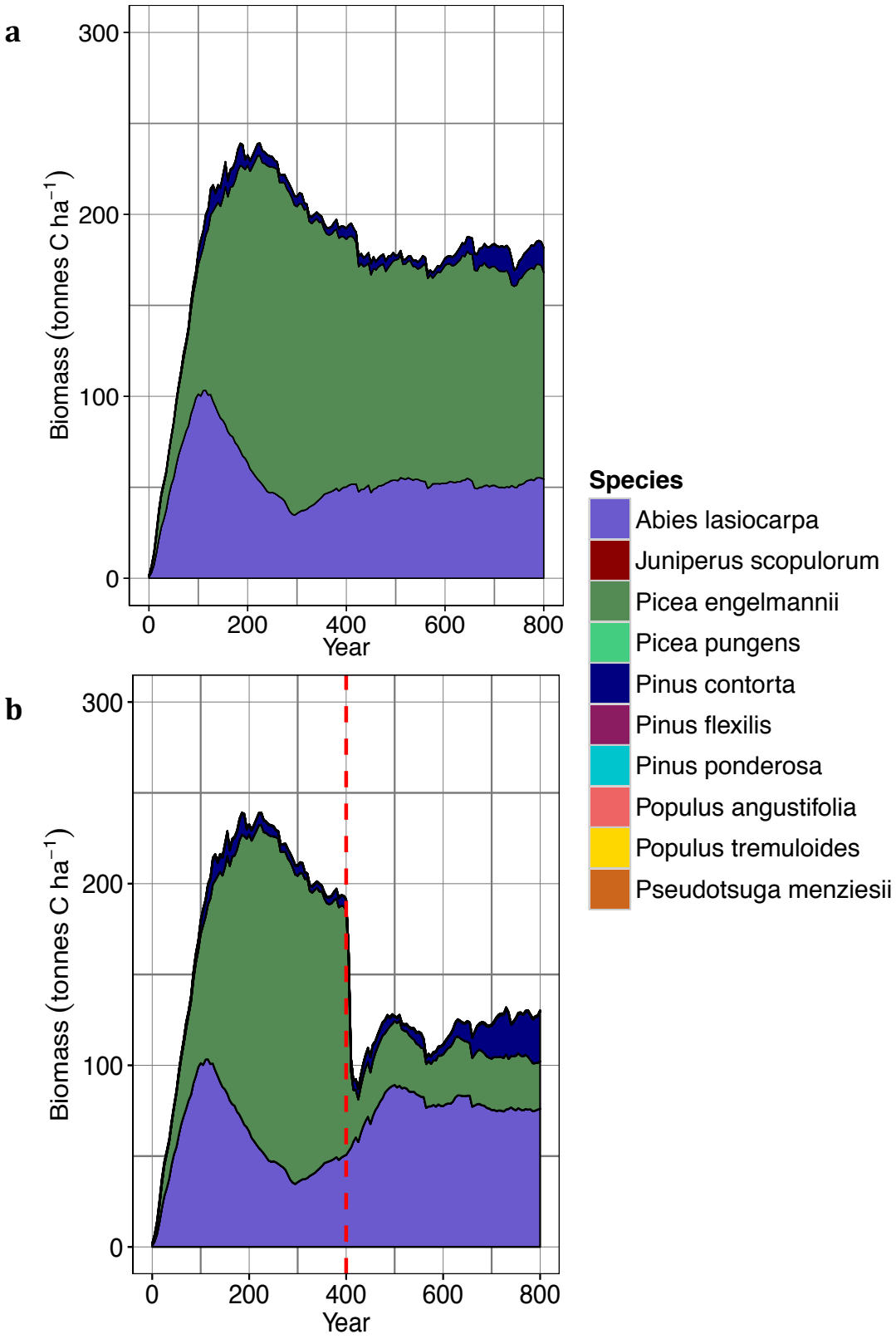

Figure 5.4. Time scale output of species-specific biomass (tonnes C ha^{-1}) under current climate conditions at GLEES for the (a) control and (b) solely beetle disturbance simulations. In the solely beetle disturbance simulation beetles were introduced at year 400 (red dashed line).

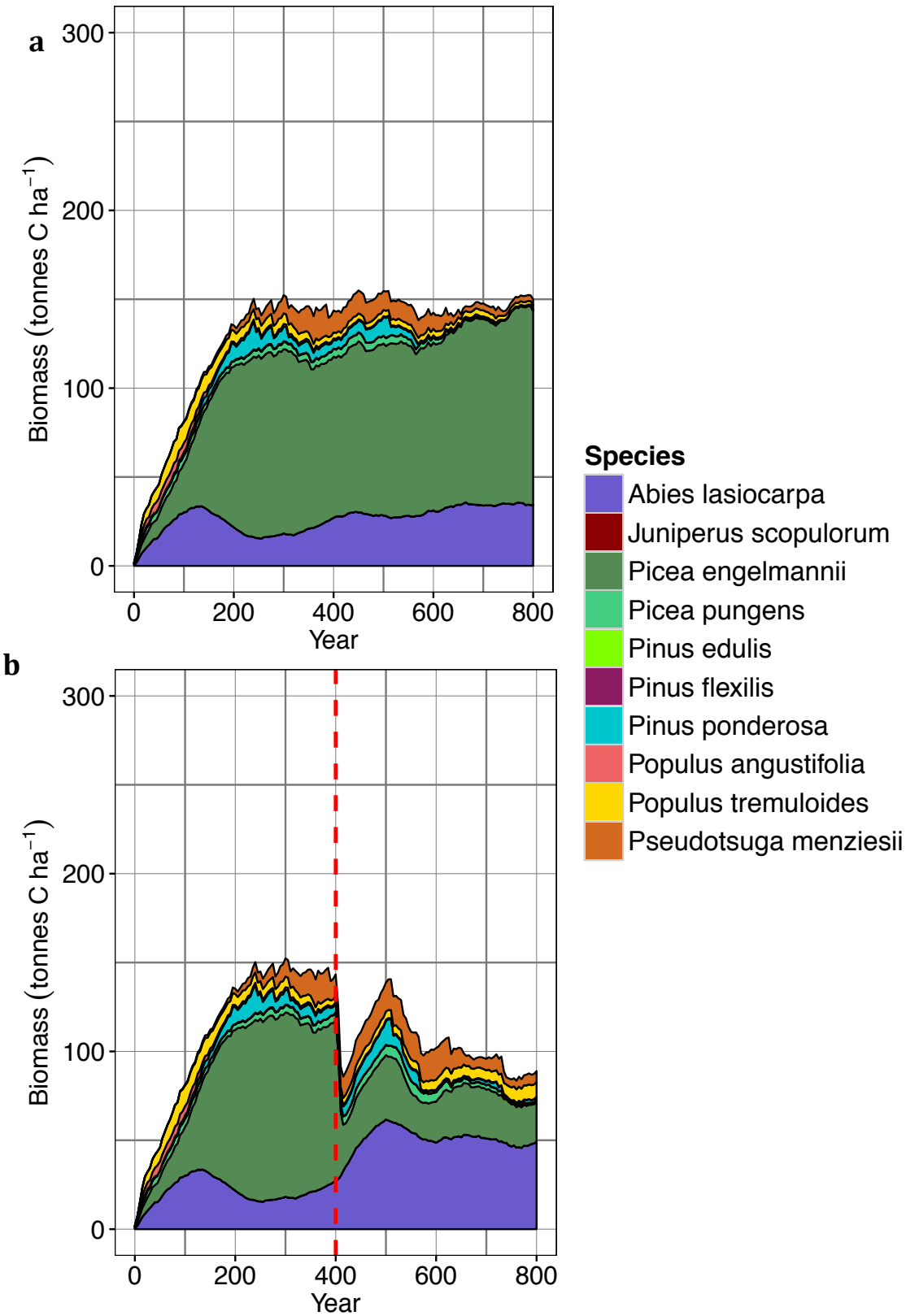

Figure 5.5. Time scale output of species-specific biomass (tonnes C ha^{-1}) under current climate conditions at Wolf Creek for the (a) control and (b) solely beetle disturbance simulations. In the solely beetle disturbance simulation beetles were introduced at year 400 (red dashed line).

western and northwestern CO and also found that the growth rates of both subcanopy spruce and fir increased for several decades following infestation (Veblen et al. 1991). From these field studies (Veblen et al. 1991, Derderian et al. 2016) and from the simulations presented here it is clear that spruce beetles can have a large impact on forest stand structure, an important effect that can be simulated using individual-based models which capture changes in size structure across stands.

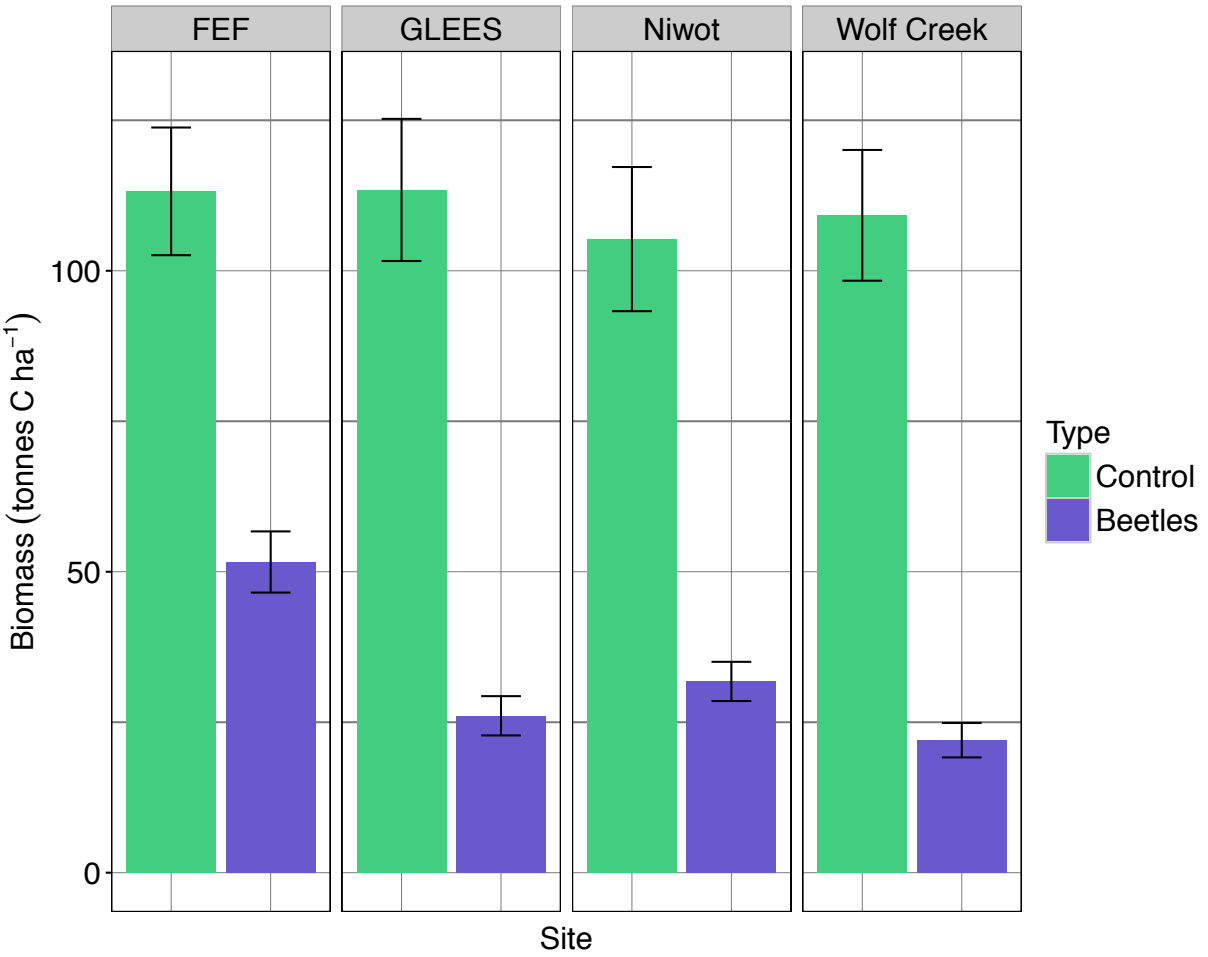

Figure 5.6. Biomass (tonnes C ha^{-1}) at year 800 of Engelmann spruce (*Picea engelmanni*) at all four subalpine sites for the control simulation (i.e. no beetle disturbance, current climate) and the solely beetle disturbance simulation (i.e. beetle disturbance, current climate) along with 95% confidence intervals.

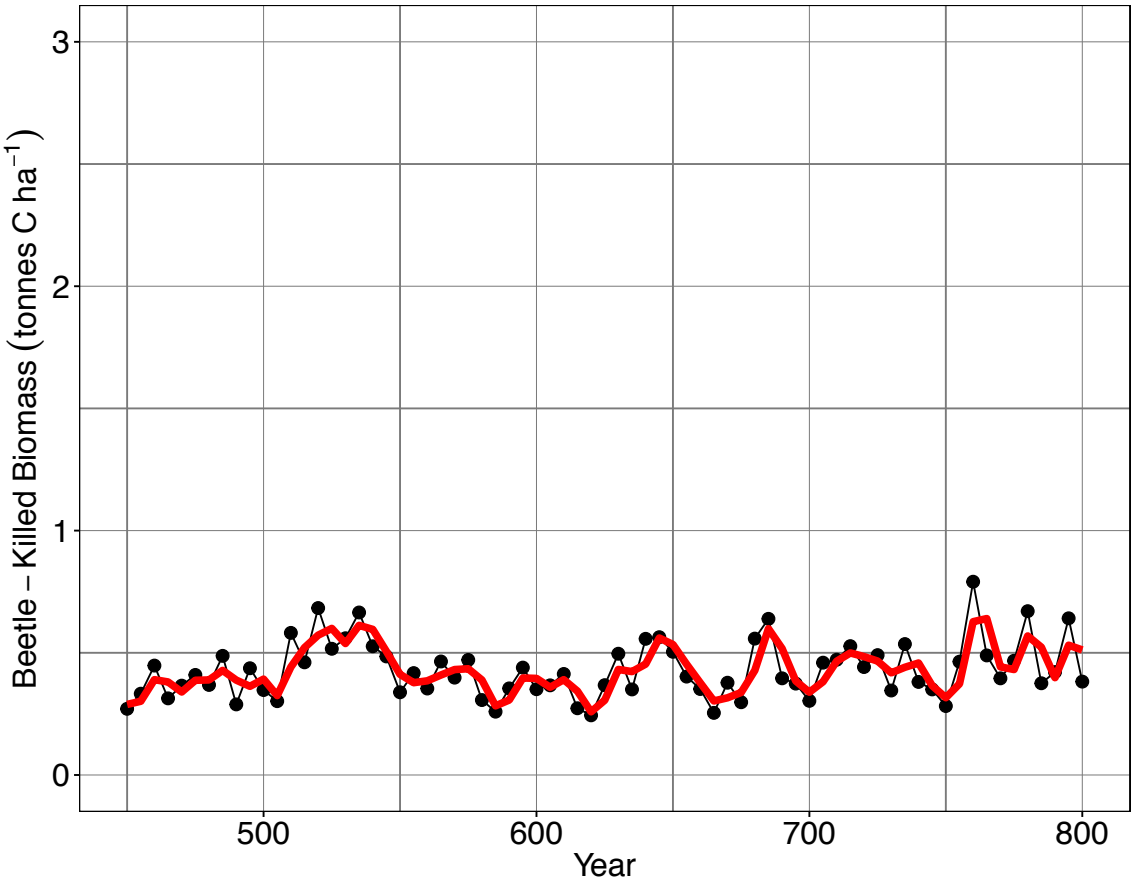

Figure 5.7. Spruce beetle-killed biomass (tonnes C ha^{-1}) over time at GLEES from year 450 to year 800 for the solely beetle disturbance simulation. The red line corresponds to a 10-year running average.

At most of the sites, and especially at GLEES, the addition of spruce beetles resulted in a fluctuation over time in spruce biomass (Fig. 5.4b), which corresponded to a fluctuation in spruce beetle-killed biomass over time (Fig. 5.7). A 10-year running average shows that beetle-killed biomass had a periodicity of about 30 to 50 years. This periodicity is comparable to periodicities in spruce beetle outbreaks found by recent field studies, with outbreaks occurring about every 50 years in Alaska (Berg et al. 2006), about every 100 years in British Columbia and northwestern CO (Veblen et al. 1994, Zhang et al. 1999), and about every 40 to 60 years in the Colorado Front Range (Hart et al. 2014a). What may be occurring in these simulations – as well as in the field – is that once spruce beetles have killed most of the large diameter spruce on a

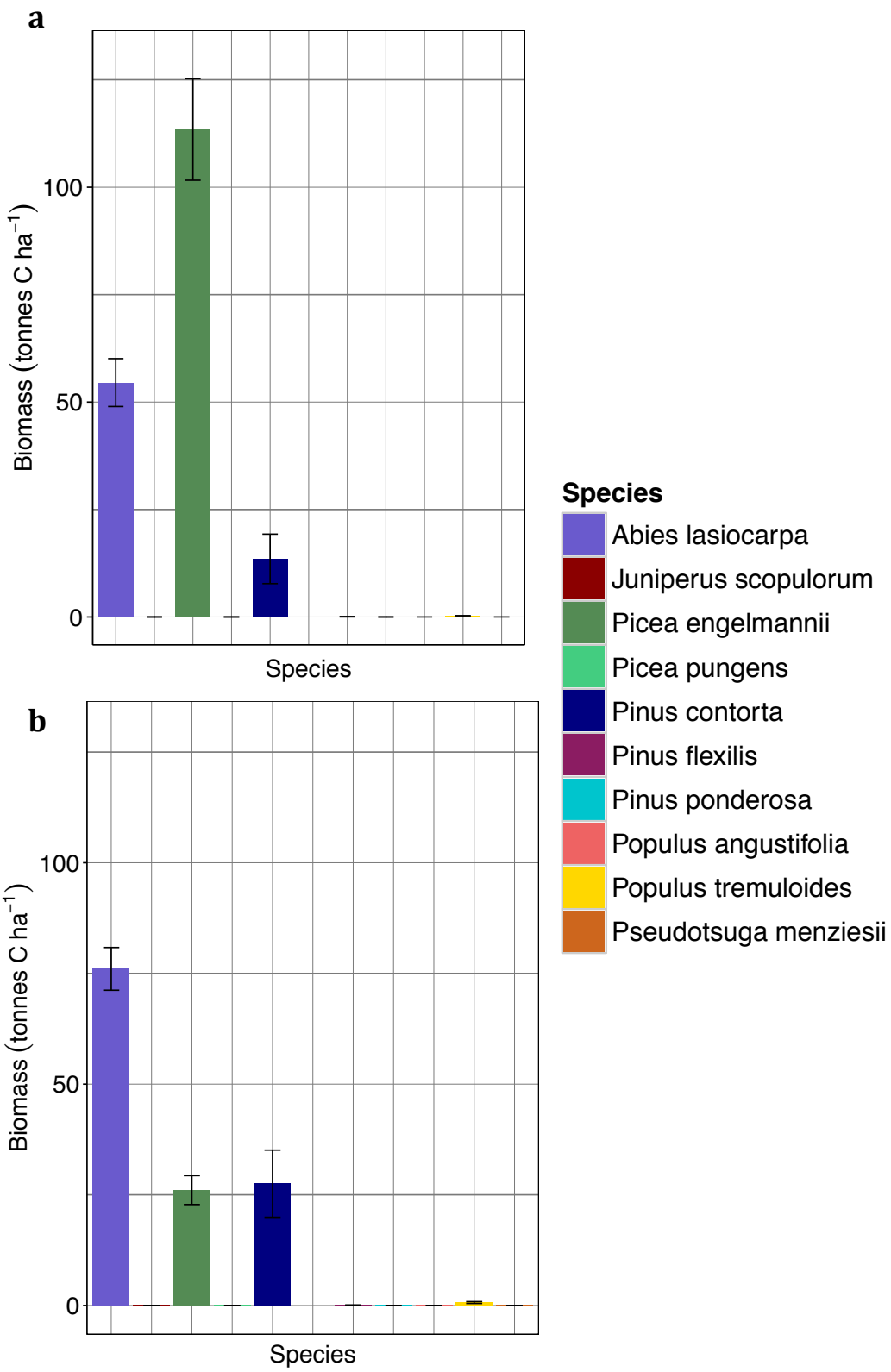

Figure 5.8. Species-specific biomass (tonnes C ha^{-1}) at GLEES at year 800 for (a) the control simulation and (b) the solely beetle disturbance simulation along with 95% confidence intervals.

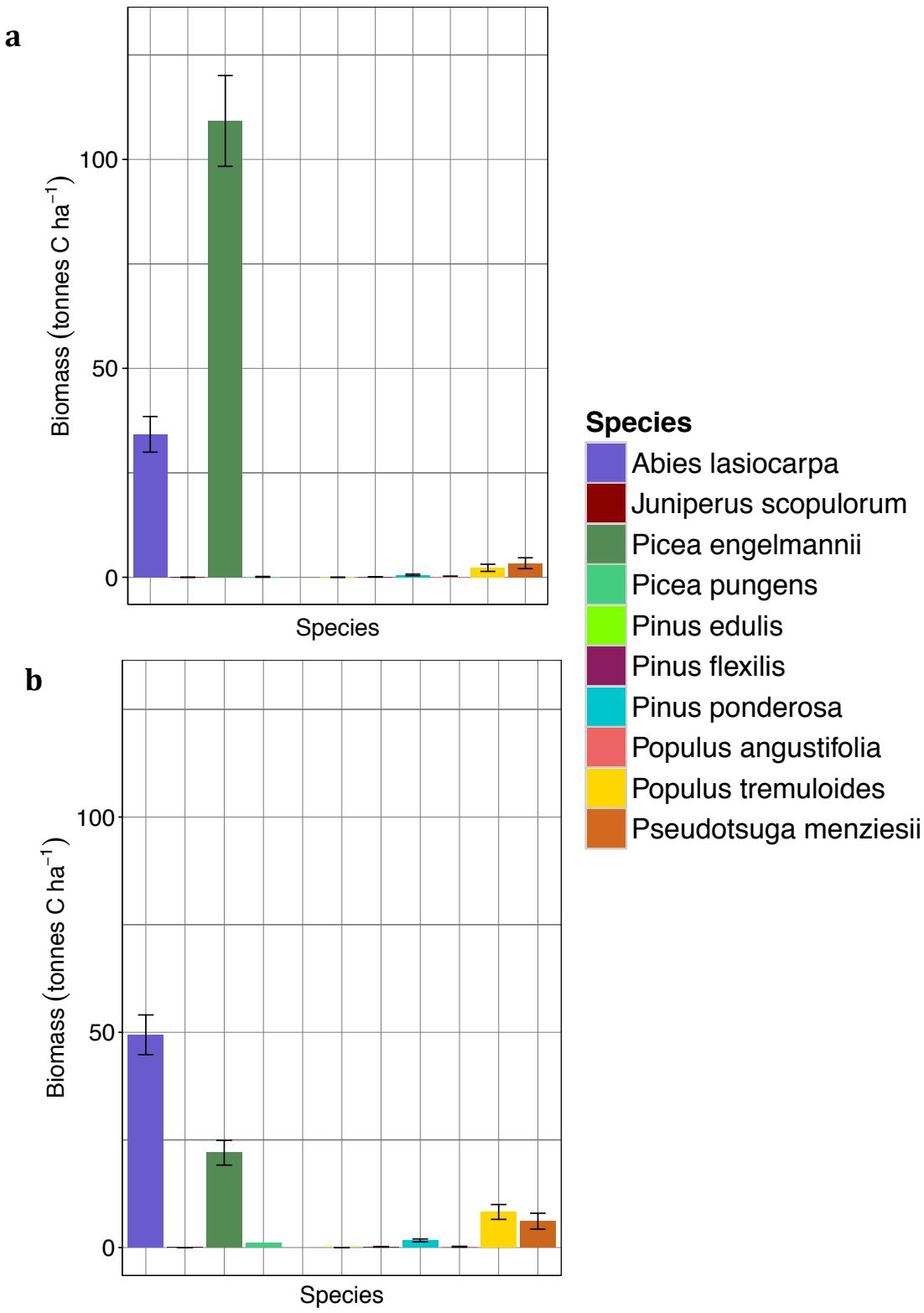

Figure 5.9. Species-specific biomass (tonnes C ha^{-1}) at Wolf Creek at year 800 for (a) the control simulation and (b) the solely beetle disturbance simulation along with 95% confidence intervals.

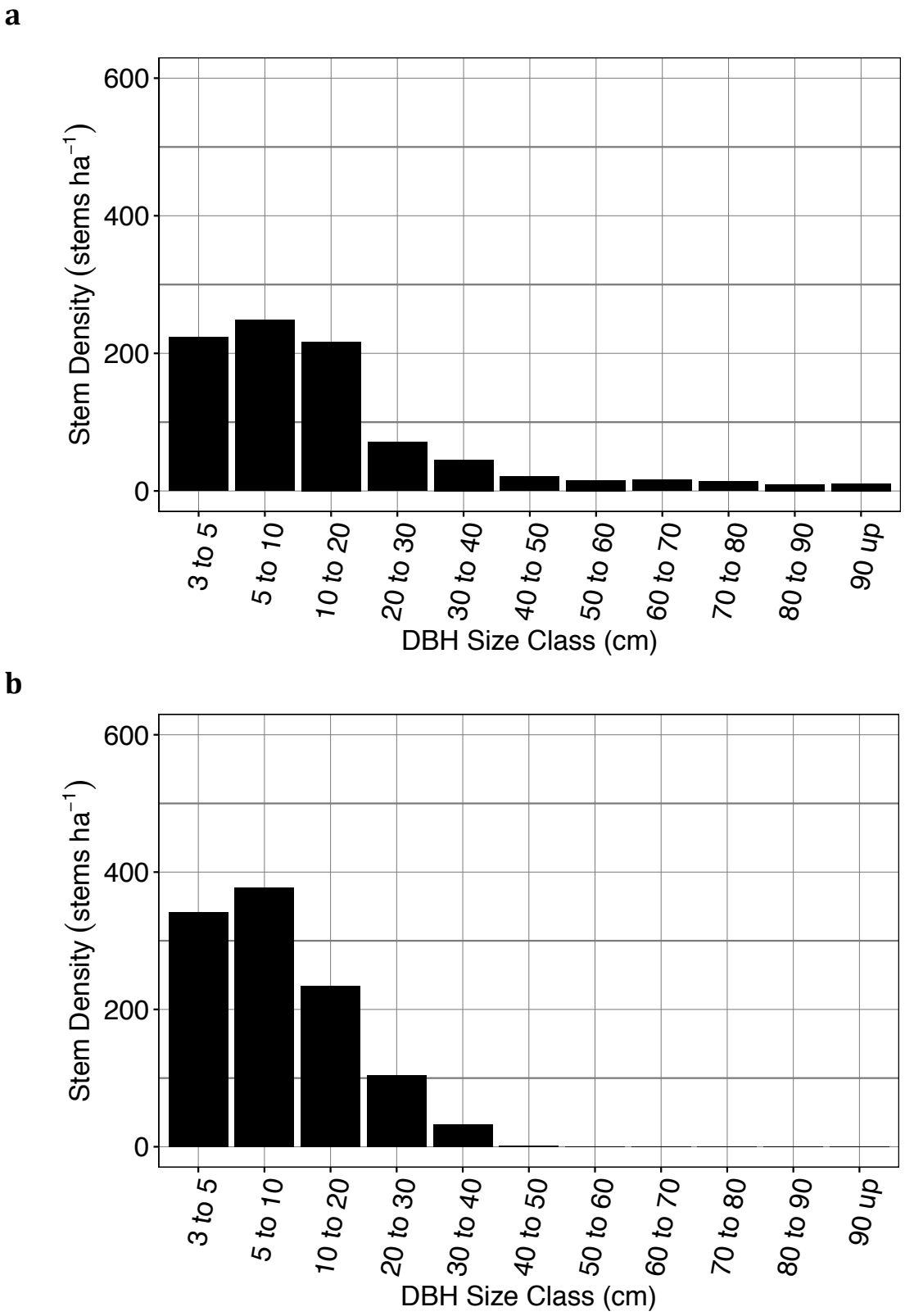

Figure 5.10. Engelmann spruce size structure at year 800 at GLEES for (a) the control simulation, and (b) the solely beetle disturbance simulation.

plot, the only remaining spruce trees are too small to be available for infestation, thus beetle-killed biomass decreases. These subcanopy trees grow, and eventually become large enough to be susceptible to beetle infestation, thus beetle-killed biomass increases. In this way, cycles of increasing and decreasing infestations arise over time.

These infestation cycles may be important to consider when predicting the effects of droughts, El Niño events, or even longer-scale climate effects on Rocky Mountains vegetation. If a severe drought were to occur during a "trough," or endemic period of low infestation rates, it may not have as drastic an effect on Engelmann spruce biomass as it would during or leading up to a "peak," or epidemic period. During endemic periods, there may not be enough large diameter spruce to sustain high populations of spruce beetles, even with the addition of drought stress and lowered tree defenses. During or leading up to epidemic periods, however, there may be many large diameter spruce trees. This availability of large diameter spruce may allow for even more rapid growth of beetle populations following drought, potentially triggering large-scale outbreaks across whole landscapes.

Across all four sites, increasing temperatures resulted in a decline in Engelmann spruce biomass, an increase in more drought-tolerant subalpine species (i.e. *Pinus contorta*), and the introduction of lower-elevation species (i.e. *Pseudotsuga menziesii*, *Pinus ponderosa*). In some cases, climate change was so detrimental as to completely or very nearly completely eradicate all subalpine species (Fig. 5.13, 5.14). Surprisingly, there was little difference in the biomass dynamics of the solely climate change simulations between those using the A1B and those using the A2 IPCC scenarios, even though the A2 scenario had much larger temperature increases (Fig. 5.11 through 5.14).

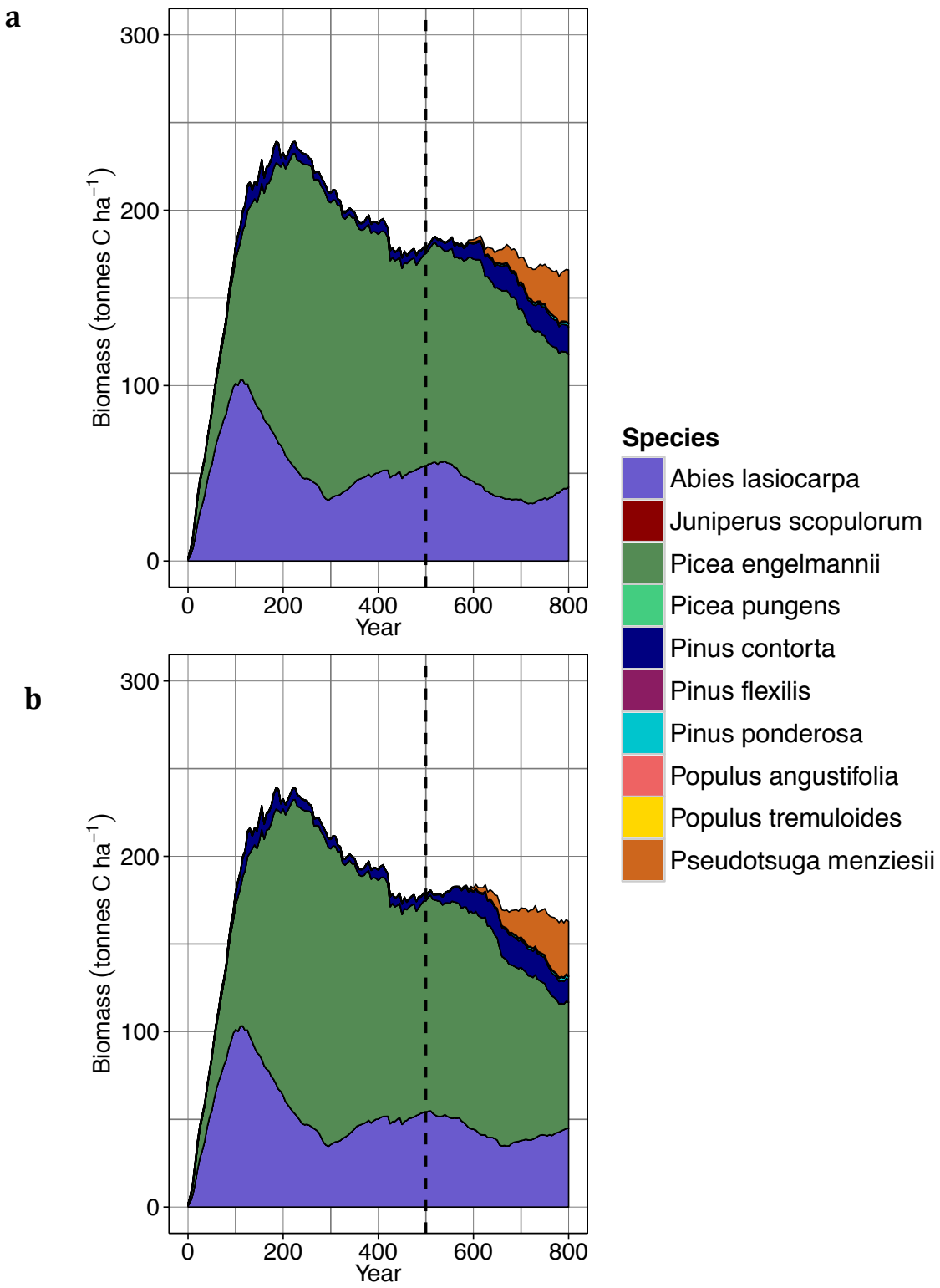

Figure 5.11. Time scale output of species-specific biomass (tonnes C ha^{-1}) with climate change occurring at year 500 (dashed black line) at GLEES for the (a) A1B and (b) A2 IPCC scenarios.

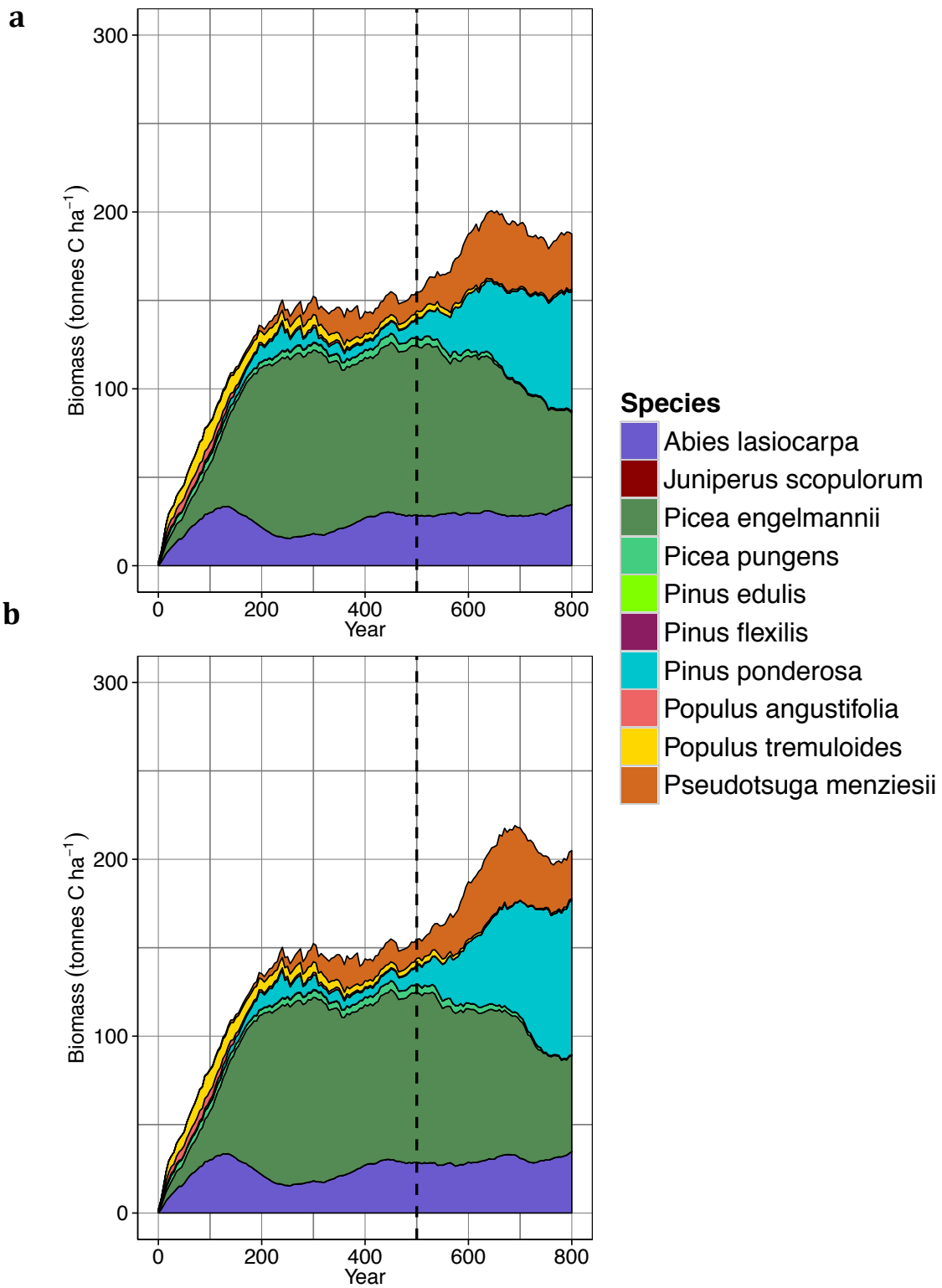

Figure 5.12. Time scale output of species-specific biomass (tonnes C ha^{-1}) with climate change occurring at year 500 (dashed black line) at Wolf Creek for the (a) A1B and (b) A2 IPCC scenarios.

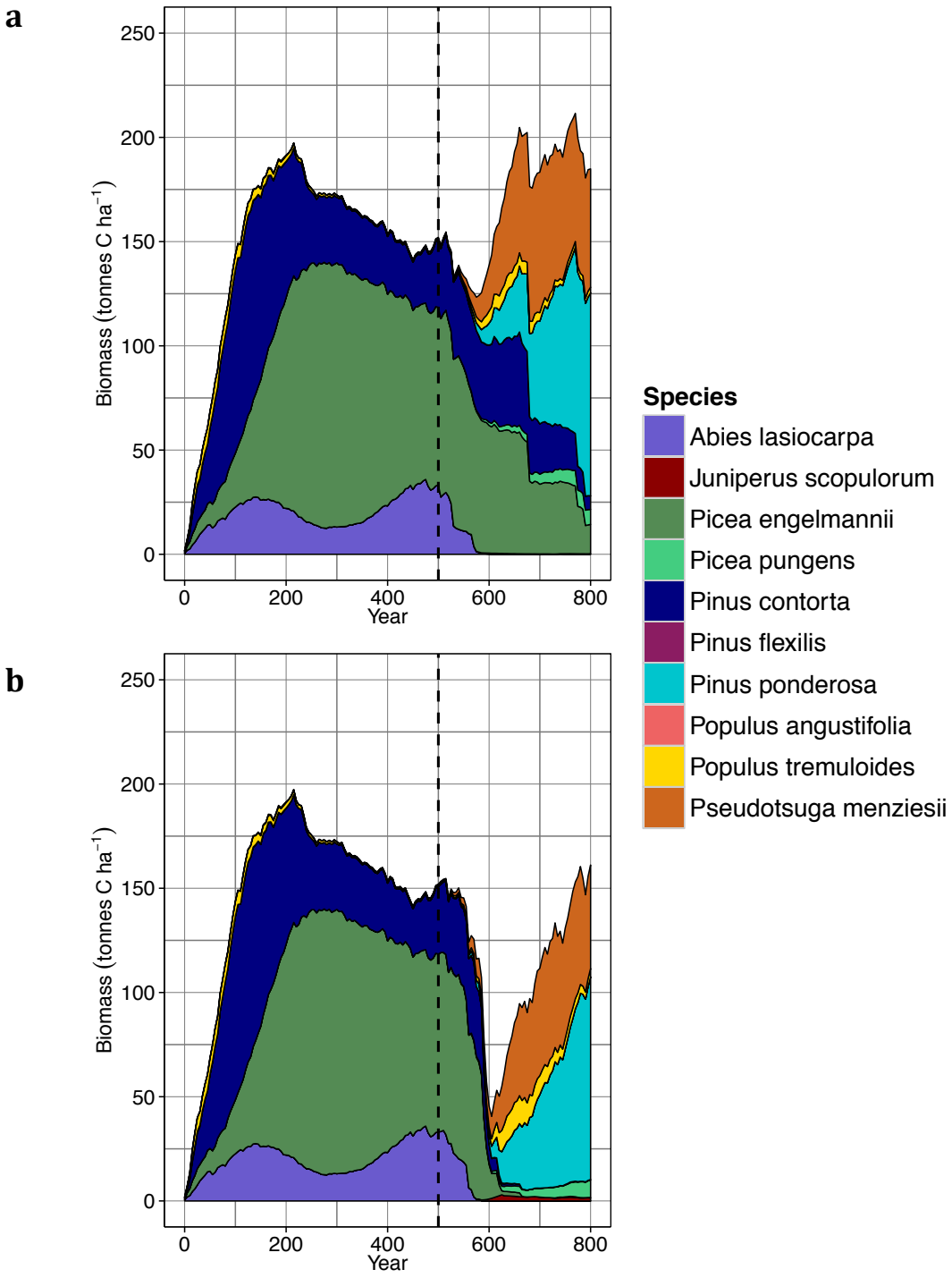

Figure 5.13. Time scale output of species-specific biomass (tonnes C ha^{-1}) with climate change occurring at year 500 (dashed black line) at Niwot Ridge for the (a) A1B and (b) A2 IPCC scenarios.

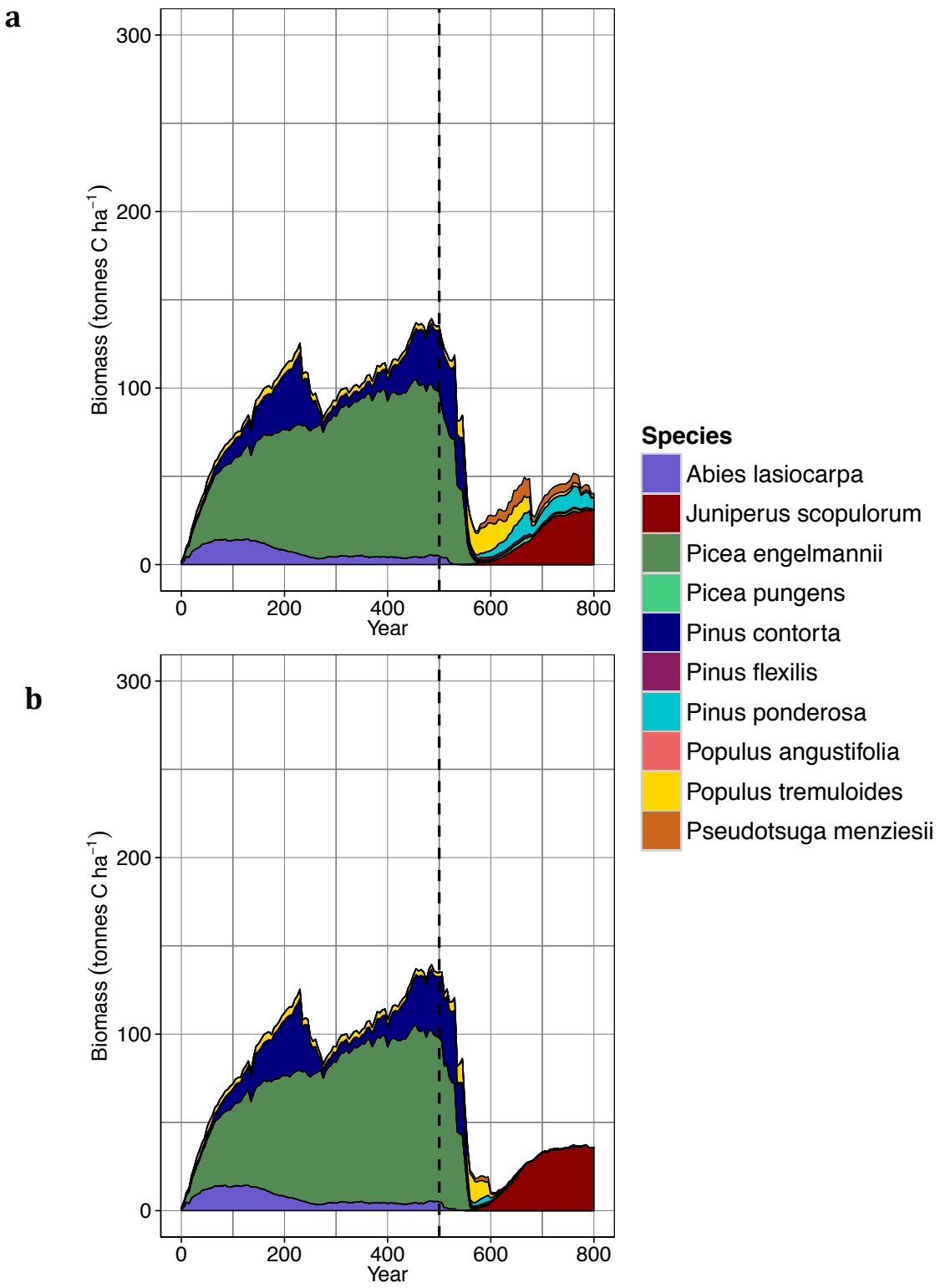

Figure 5.14. Time scale output of specie-specific biomass (tonnes C ha^{-1}) with climate change occurring at year 500 (dashed black line) at Fraser Forest for the (a) A1B and (b) A2 IPCC scenarios.

It is clear from these climate change simulations that local scale factors such as site characteristics and climate play an important role in the response of subalpine vegetation to climate change. Even though the effect of spruce beetles on Engelmann spruce biomass was fairly consistent across all four sites (Fig. 5.6), the effect of climate change was quite variable (Fig. 5.15). Increasing temperatures had only a moderate effect on subalpine biomass at GLEES

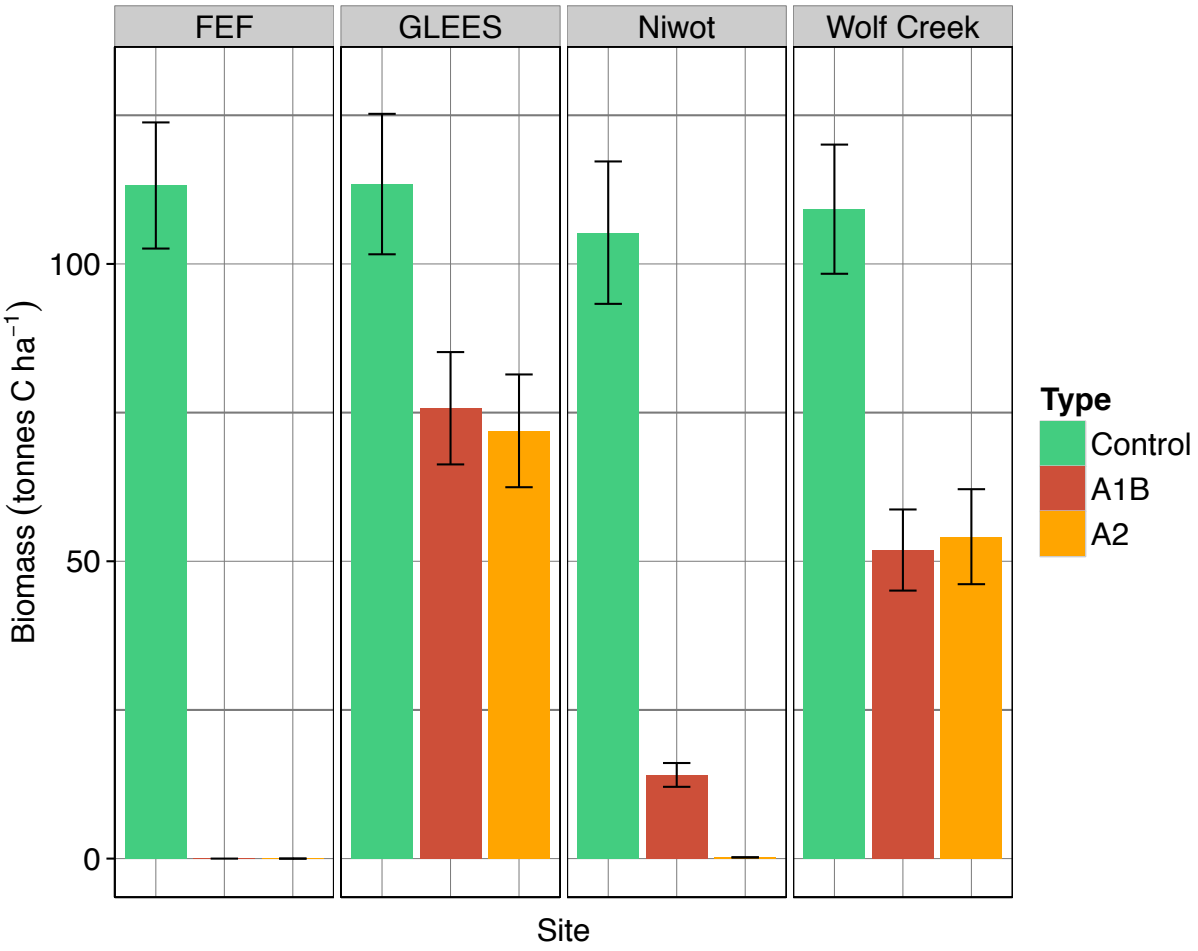

Figure 5.15. Biomass (tonnes C ha^{-1}) at year 800 of Engelmann spruce (*Picea engelmanni*) at all four subalpine sites for the control simulation (i.e. no beetles, current climate), and the A1B and A2 simulations (i.e. no beetles, climate change), along with 95% confidence intervals.

and Wolf Creek (Fig. 5.11, 5.12, 5.15), and was not as detrimental to Engelmann spruce by itself as was beetle infestation (Fig. 5.16). In contrast, climate change was incredibly detrimental to

biomass at both Fraser Experimental Forest and Niwot Ridge (Fig. 5.13, 5.14), which are slightly drier sites (~70 cm and ~50 cm annual precipitation, respectively) compared to GLEES and Wolf Creek (~100 cm and ~110 cm, respectively). This difference in overall climate may be driving the increased effect of elevated temperatures at Niwot Ridge and Fraser Forest. These results indicate that fine-scale patterns in climate, weather, and disturbance regimes should be considered when predicting the future state of vegetation within the Rocky Mountains.

In general, the combination of spruce beetles and climate change resulted in lower Engelmann spruce biomass than did either factor alone, with some site-specific differences (Fig. 5.16). At GLEES, beetle disturbance and climate change resulted in a further decrease in Engelmann spruce biomass as well as the introduction of a new lower elevation species, ponderosa pine (*Pinus ponderosa*) (Fig. 5.17). This shift in species dominance can also be seen in graphs of stand structure from simulations with and without beetle infestation. Without spruce beetle infestation, there were still many large-diameter spruce at year 800, even after climate change effects (Fig. 5.21a). With climate change and spruce beetles, however, there were virtually no large-diameter spruce and a higher number of moderately sized trees of other species (Fig. 5.21b). These results are similar for Wolf Creek Pass (Fig. 5.18), however, at Niwot Ridge and Fraser Experimental Forest climate change produced such a large loss of Engelmann spruce that the addition of spruce beetle infestation had little to no effect on spruce biomass (Fig. 5.19, 5.20).

It seems that beetle infestation not only resulted in loss of spruce biomass, but that it may have also facilitated competition between Engelmann spruce and lower elevation species. A graph of proportion of spruce biomass killed over time by shade stress and beetle disturbance for

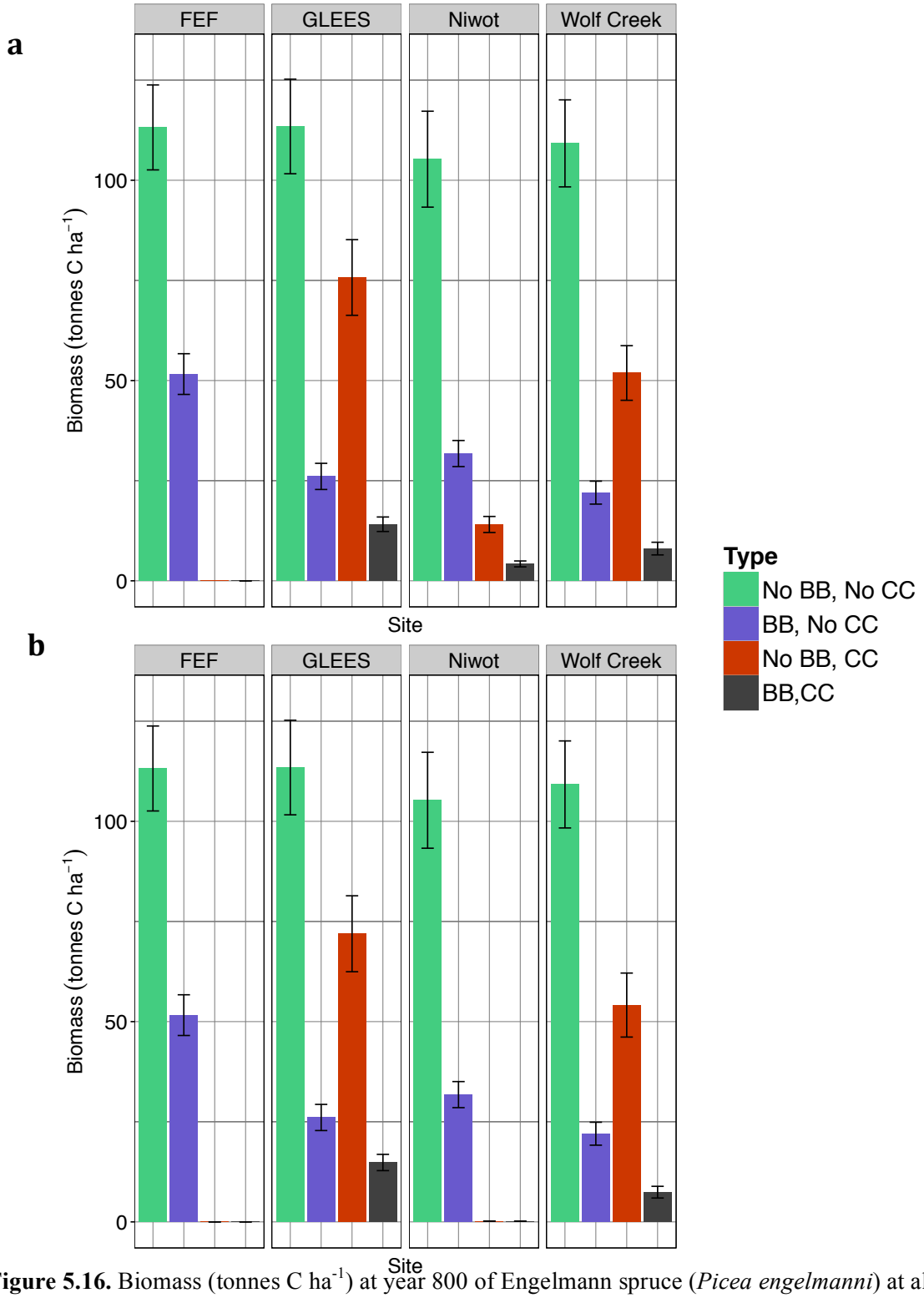

Figure 5.16. Biomass (tonnes C ha^{-1}) at year 800 of Engelmann spruce (*Picea engelmanni*) at all four subalpine sites for the control simulation (i.e. no beetle disturbance, current climate), the solely beetle disturbance simulation (i.e. beetle disturbance, current climate), the solely climate change simulation (i.e. no beetle disturbance, climate change), and the combination of beetle disturbance and climate, along with 95% confidence intervals. Climate simulations for graph (a) use the A1B climate change scenario; simulations for graph (b) use the A2 climate change scenario.

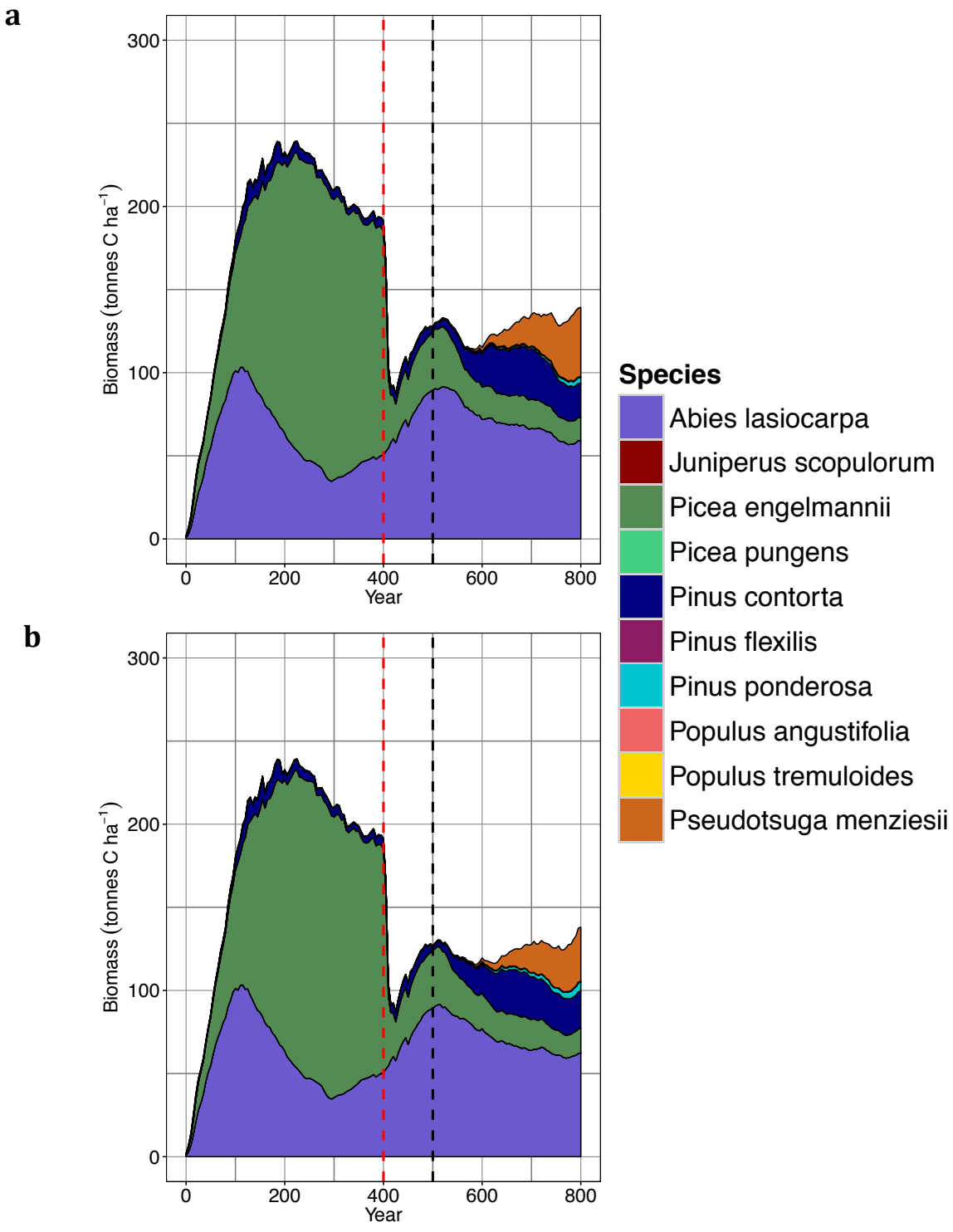

Figure 5.17. Time scale output of species-specific biomass (tonnes C ha^{-1}) with beetle infestation beginning at year 400 (red dashed line) and climate change occurring at year 500 (dashed black line) at GLEES for the (a) A1B and (b) A2 IPCC scenarios.

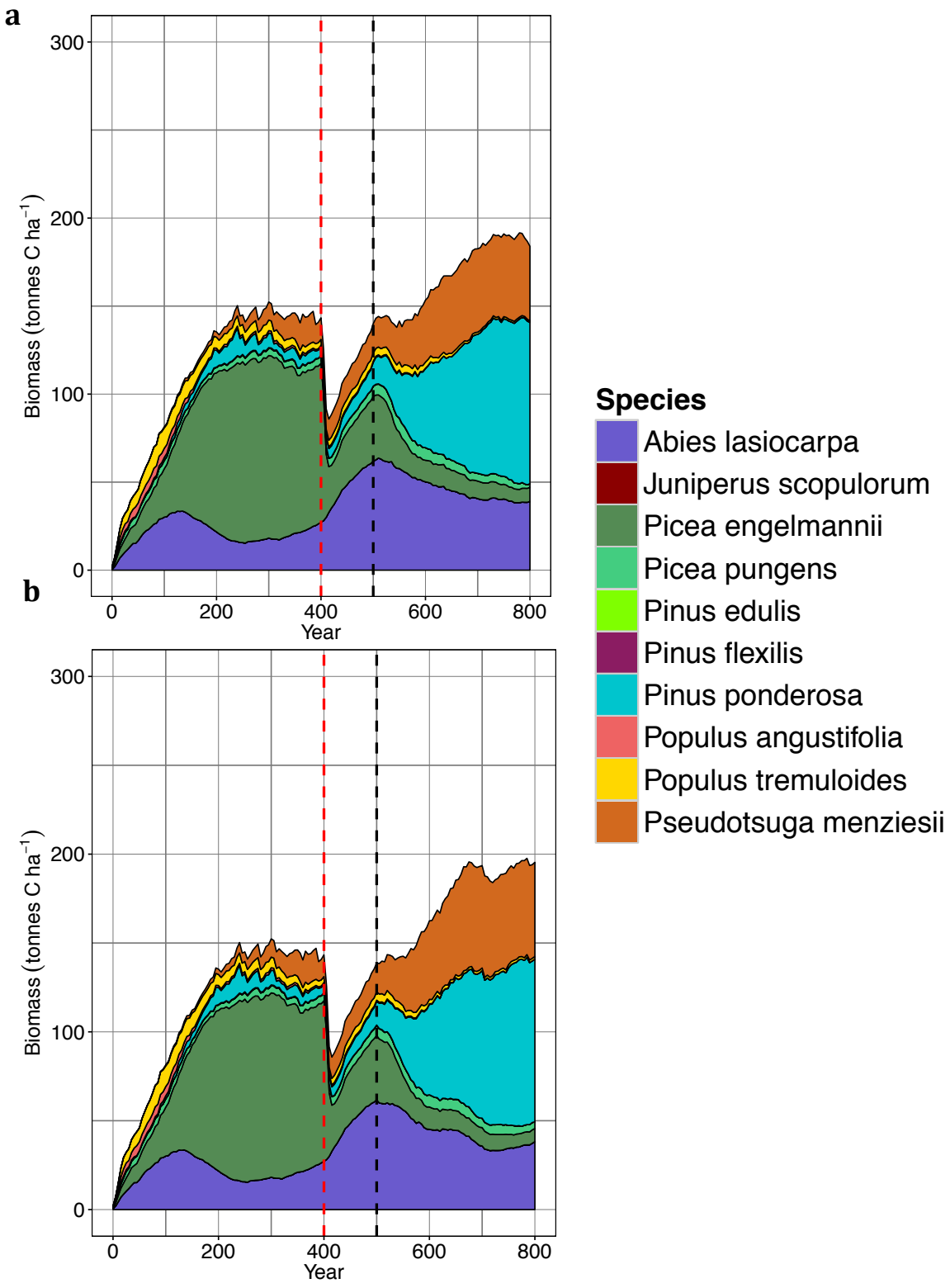

Figure 5.18. Time scale output of species-specific biomass (tonnes C ha^{-1}) with beetle infestation beginning at year 400 (red dashed line) and climate change occurring at year 500 (dashed black line) at Wolf Creek for the (a) A1B and (b) A2 IPCC scenarios.

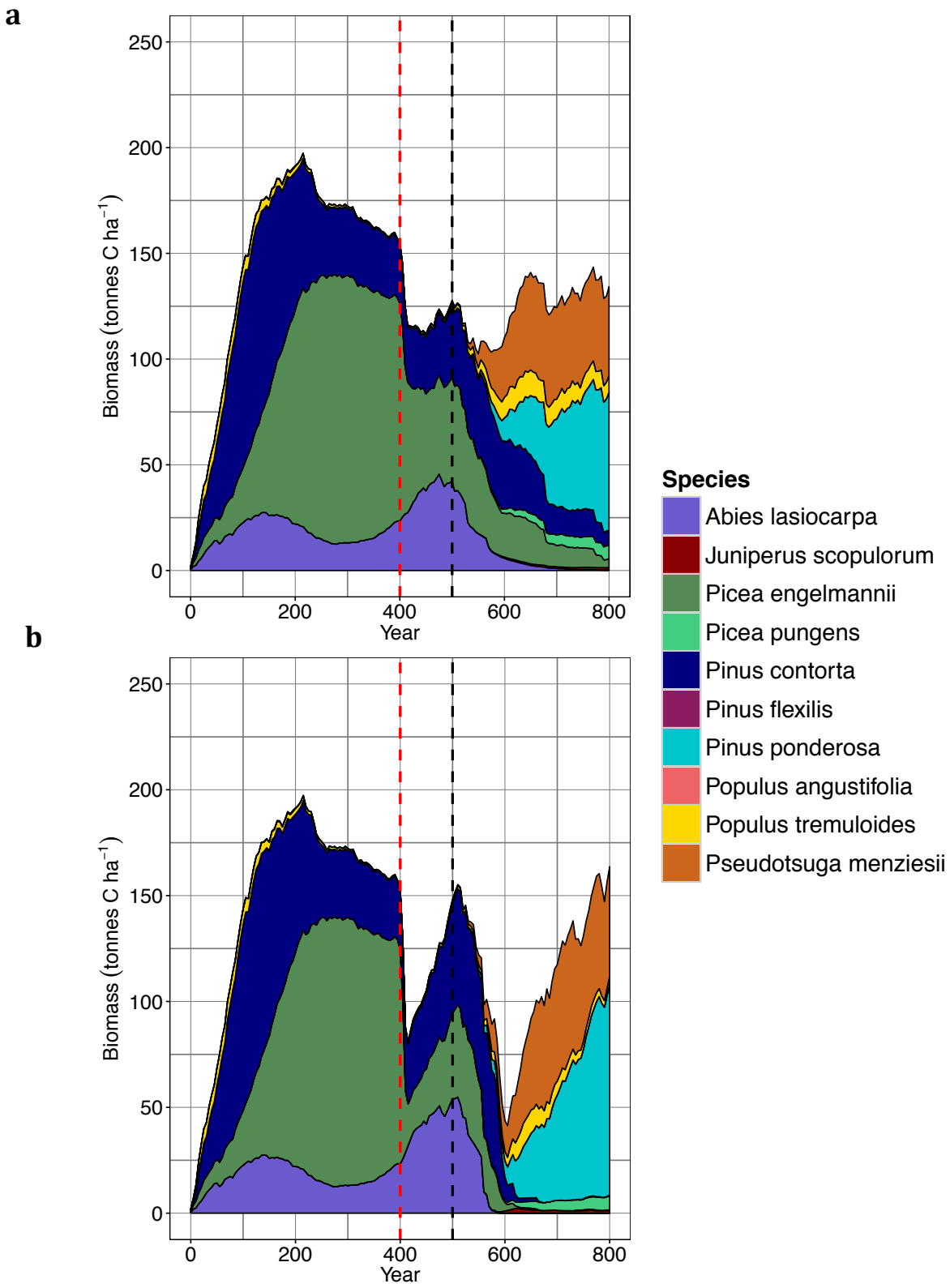

Figure 5.19. Time scale output of species-specific biomass (tonnes C ha^{-1}) with beetle infestation beginning at year 400 (red dashed line) and climate change occurring at year 500 (dashed black line) at Niwot Ridge for the (a) A1B and (b) A2 IPCC scenarios.

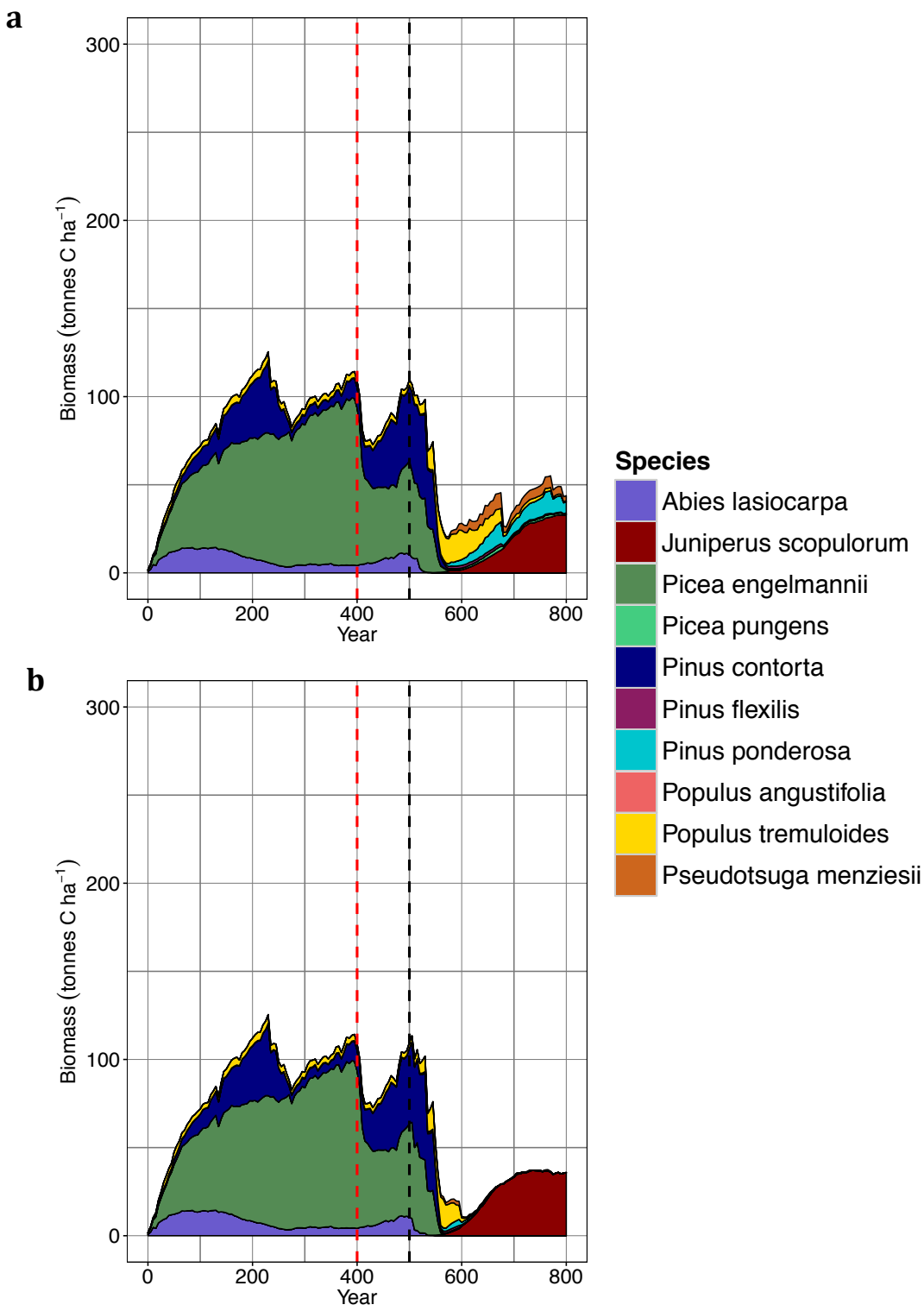

Figure 5.20. Time scale output of species-specific biomass (tonnes C ha^{-1}) with beetle infestation beginning at year 400 (red dashed line) and climate change occurring at year 500 (dashed black line) at Fraser Experimental Forest for the (a) A1B and (b) A2 IPCC scenarios.

the solely beetle disturbance and beetle disturbance with climate change scenarios shows that with the addition of climate change, the spruce mortality from shade stress increased (Fig. 5.22). This increase in shade stress can be seen as an increase in competition for light. Thus, spruce beetle infestation in conjunction with climate change may help to open up the canopy to new, traditionally lower elevation species. These low elevation species, which tend to have faster growth rates than the cold-adapted subalpine species (Burns and Honkala 1990), may then be able to outcompete and crowd out younger spruce trees from ever dominating the stand again.

This increase in lower elevation species at the expense of subalpine species has been documented in other modeling studies (Rehfeldt et al. 2006, Crookston et al. 2010, Notaro et al. 2012, Jiang et al. 2013, Bell et al. 2014, Temperli et al. 2015). Notaro et al. (2012) utilized a dynamic global vegetation model (DGVM) to predict declines in suitable habitat for Engelmann spruce with changing climate, and Rehfeldt et al. (2006) utilized a climate envelope approach to predict a decline in subalpine and alpine forests and an increase in lower elevation forests and grasslands under climate change scenarios. A study utilizing a DGVM coupled with a global climate model also found a decrease in needle leaved evergreen trees and an increase in shrubs and woodland with increasing temperatures (Jiang et al. 2013). The results from UVAFME agree with these past studies and expand on their predictions by providing additional details on potential changes in size structure.

Studies have also shown competition and species interactions to be a key factor in predicting species composition change (Araujo and Luoto 2007, Zhang et al. 2015). A recent longitudinal study of over 27,000 trees found that competition accounted for the most variability

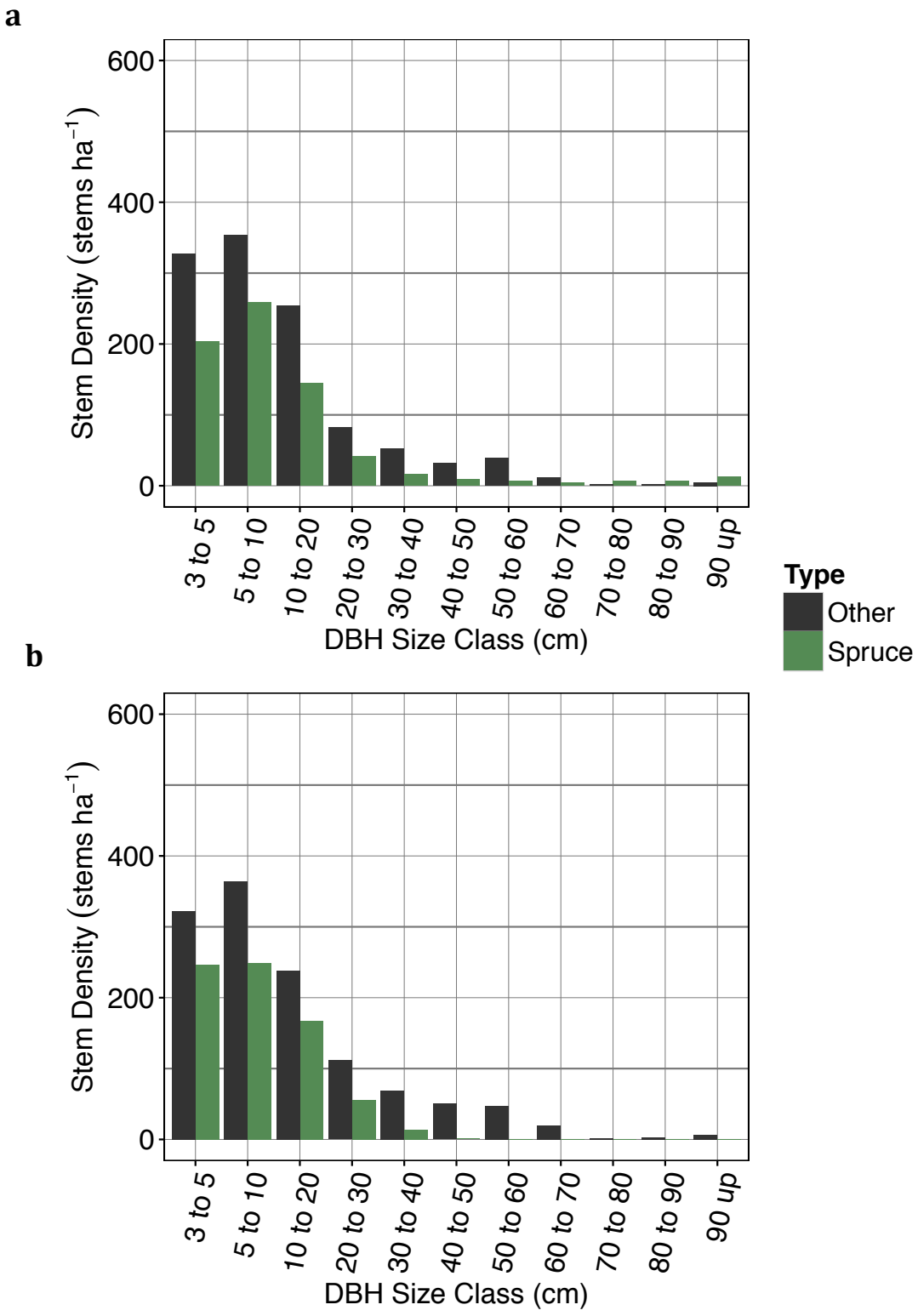

Figure 5.21. Size structure at year 800 at GLEES for Engelmann spruce (green) and all other species (black) for (a) the solely climate change simulation (A1B scenario), and (b) the beetle disturbance plus climate change simulation (A1B scenario).

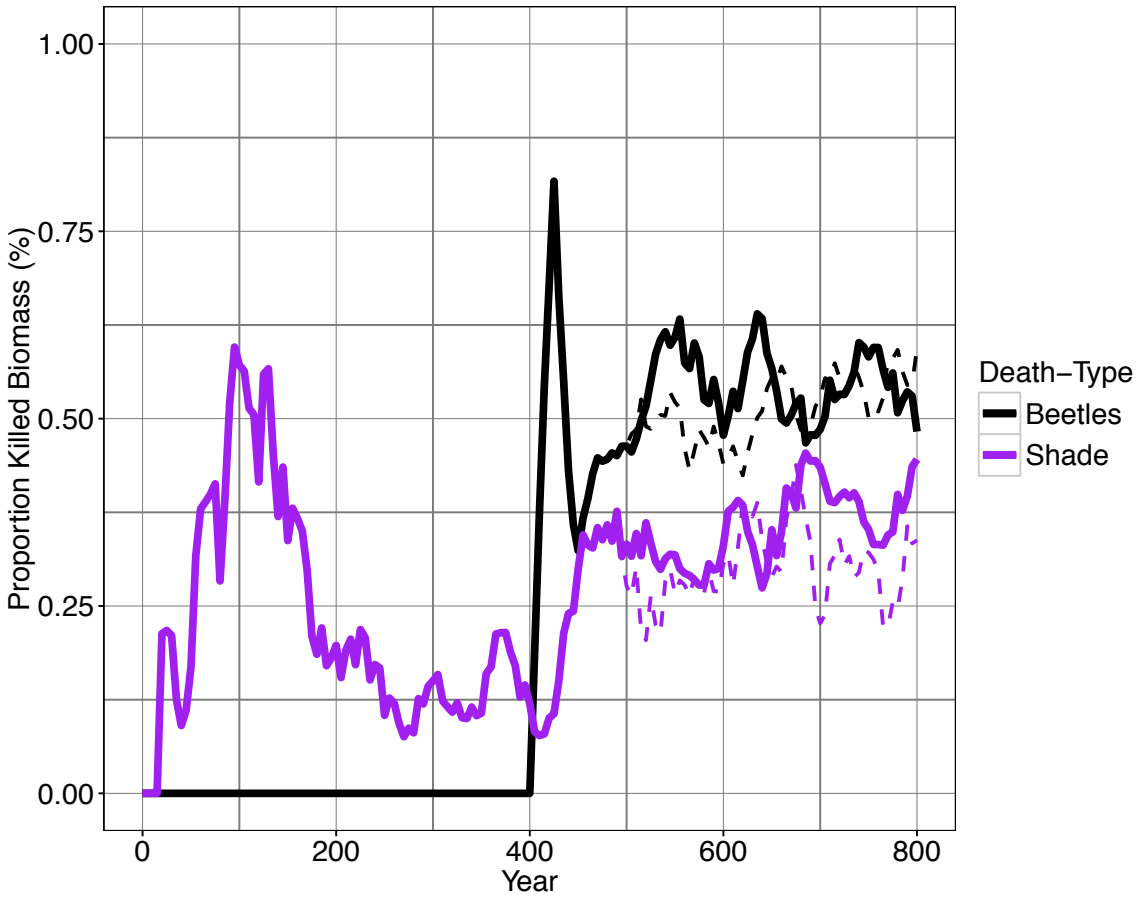

Figure 5.22. Proportion of spruce biomass killed from beetles and shade stress over time at GLEES for the climate change (A1B) plus beetles simulation (solid lines) and the solely beetle simulation (dashed lines).

in growth and mortality (Clark et al. 2011). While inhabitants of the lower elevations may be susceptible to higher moisture stress from increasing temperatures (Allen and Breshears 1998, Breshears et al. 2005), those of the characteristically mesic subalpine zone may be more vulnerable to the negative effects of competition, arising from those very same low elevation species escaping drought. These studies, along with the simulations presented here, spell a grim future for Engelmann spruce. It may be possible for spruce ranges to expand upward or northward (Hanberry and Hansen 2015, Bretfeld et al. 2016), however, this possibility depends

on adequate soil, available space for migration, and future spruce beetle outbreak dynamics (Raffa et al. 2008, Bell et al. 2014).

The relative effects of spruce beetles and climate change varied over time and among the different sites. Graphs of spruce biomass difference between the control run and all other runs show the loss of spruce biomass due to each factor individually and in concert (Fig. 5.24 through 5.27). The "additive" effect is also plotted, which is simply the loss from beetle disturbance

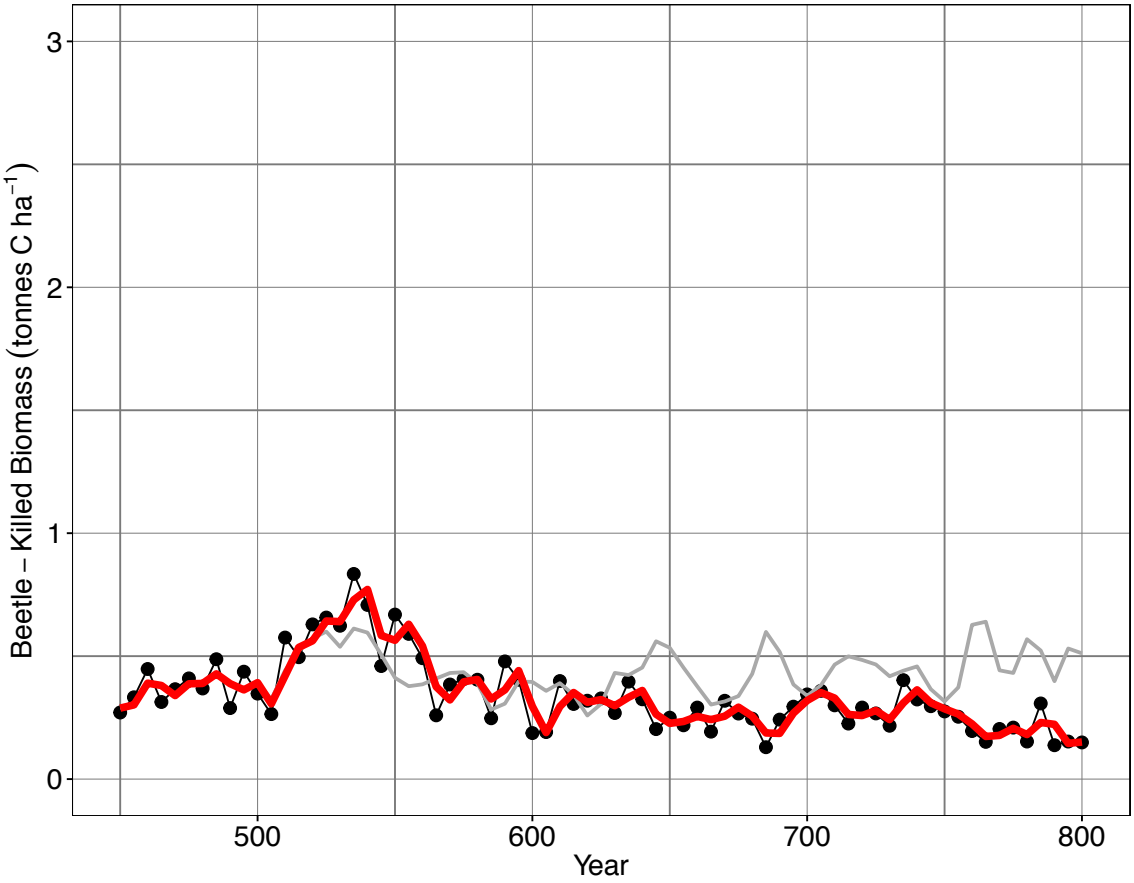

Figure 5.23. Spruce beetle-killed biomass (tonnes C ha^{-1}) over time at GLEES from year 450 to year 800 for the climate change (A1B) plus beetle disturbance simulation (black line). The red line corresponds to a 25-year running average for this simulation. The grey line represents the 10-year average of spruce beetle-killed biomass over time under the beetle disturbance with current climate simulation (see Figure 5.7).

alone plus the loss from climate change alone. It represents what spruce biomass loss would have been if there had been no interaction at all between climate and beetle infestation. When this line

is above the combination (i.e. beetle disturbance with climate change) curve, the spruce loss under the combination scenario is higher than would be expected and there is an enhancing effect between beetle disturbance and climate change. When the additive line is below the combination line, spruce loss is lower than would be expected, and there is a dampening effect between the two factors. At GLEES, beetle disturbance and climate seemed to enhance each other following the initialization of climate change (Fig. 5.24). However, towards the end of the simulation the additive loss was much greater than the combination loss, indicating that as the effects of climate change played out, there may have been an eventual dampening effect. Beetle-killed biomass also declined over time under the combination scenario, and was less periodic than it was without climate change effects (Fig. 5.23). These results are somewhat similar at Wolf Creek, with some enhancement early on following climate change and eventual dampening between climate change and beetles (Fig. 5.25). At Fraser Experimental Forest and Niwot Ridge, climate change was so detrimental to Engelmann spruce biomass that mortality from spruce beetles became almost irrelevant by the end of the simulation (Fig. 5.26, 5.27).

These results are similar to findings by DeRose et al. (2013). They utilized forest inventory data and spruce beetle population metrics to predict future spruce beetle presence across the central and southern Rocky Mountains. Their results showed that while climate data were important, they were far outstripped by the importance of habitat variables like stand basal area and percent Engelmann spruce. As spruce beetles require adequate host material to survive and reproduce, it follows that even with the ability for accelerated population growth under increasing temperatures, flexible voltinism becomes a moot point in the absence of spruce biomass. Thus, from these results it seems that climate change and beetles may initially enhance one another, through facilitation of competition and through increases in beetle population

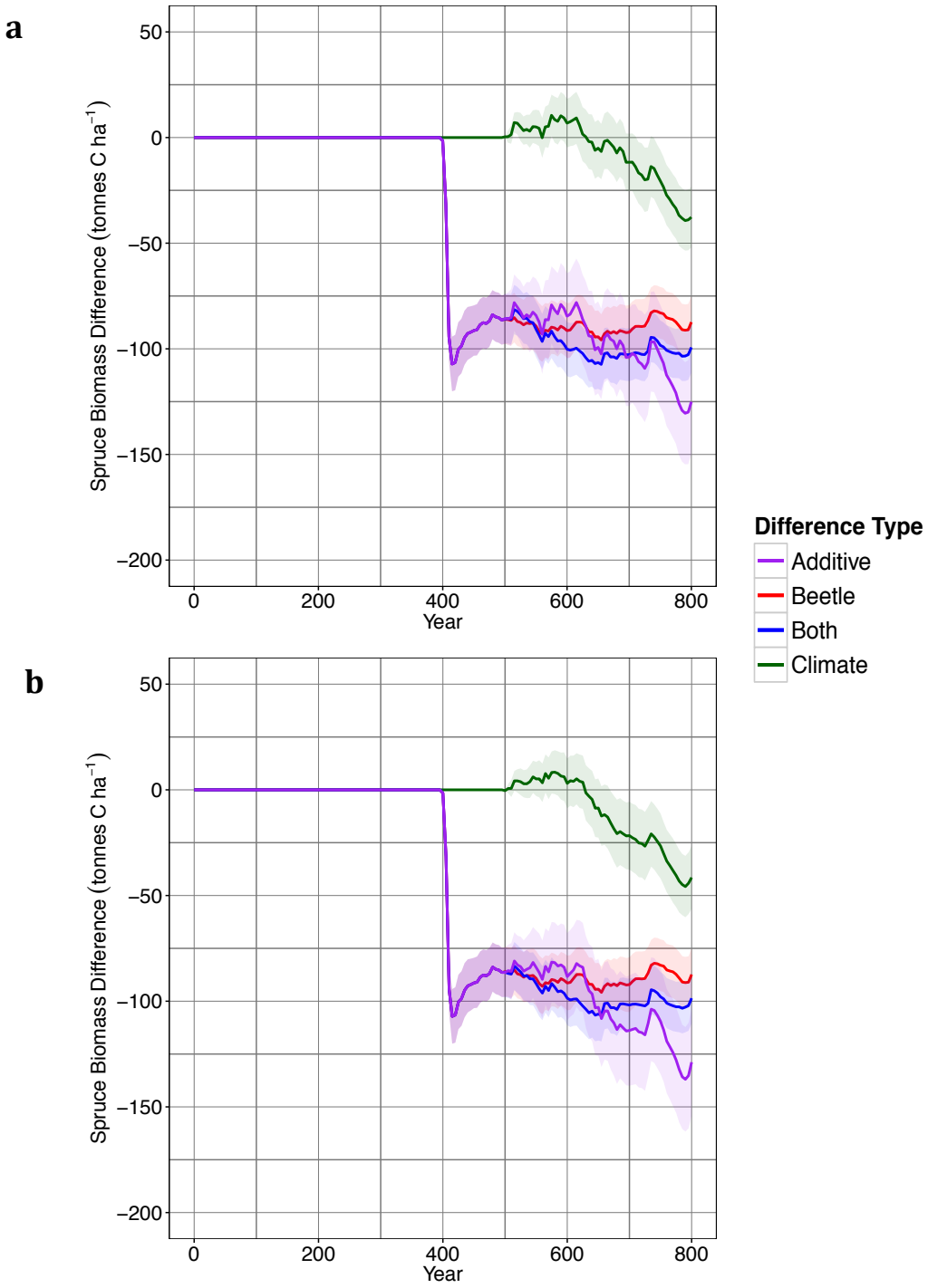

Figure 5.24. Spruce biomass difference (tonnes C ha^{-1}) over time at GLEES between the control simulation and the solely beetle disturbance simulation (red), the solely climate simulation (green), and the combination of climate and beetle disturbance (blue) for the (a) A1B and (b) A2 climate change scenarios. The additive (purple) line is the loss from beetle disturbance alone plus the loss from climate alone. Shading represents 95% confidence intervals.

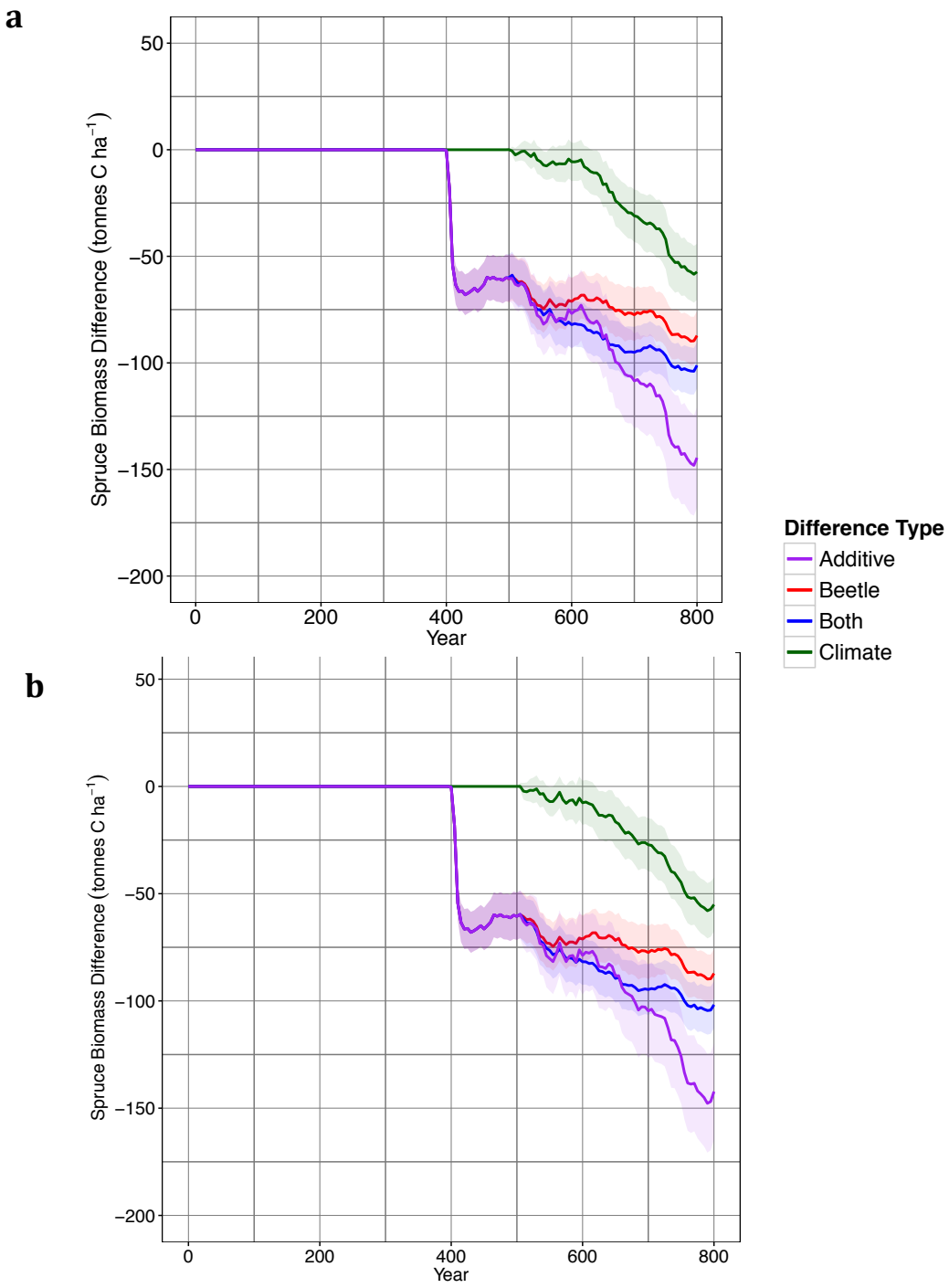

Figure 5.25. Spruce biomass difference (tonnes C ha^{-1}) over time at Wolf Creek between the control simulation and the solely beetle disturbance simulation (red), the solely climate simulation (green), and the combination of climate and beetle disturbance (blue) for the (a) A1B and (b) A2 climate change scenarios. The additive (purple) line is the loss from beetle disturbance alone plus the loss from climate alone. Shading represents 95% confidence intervals.

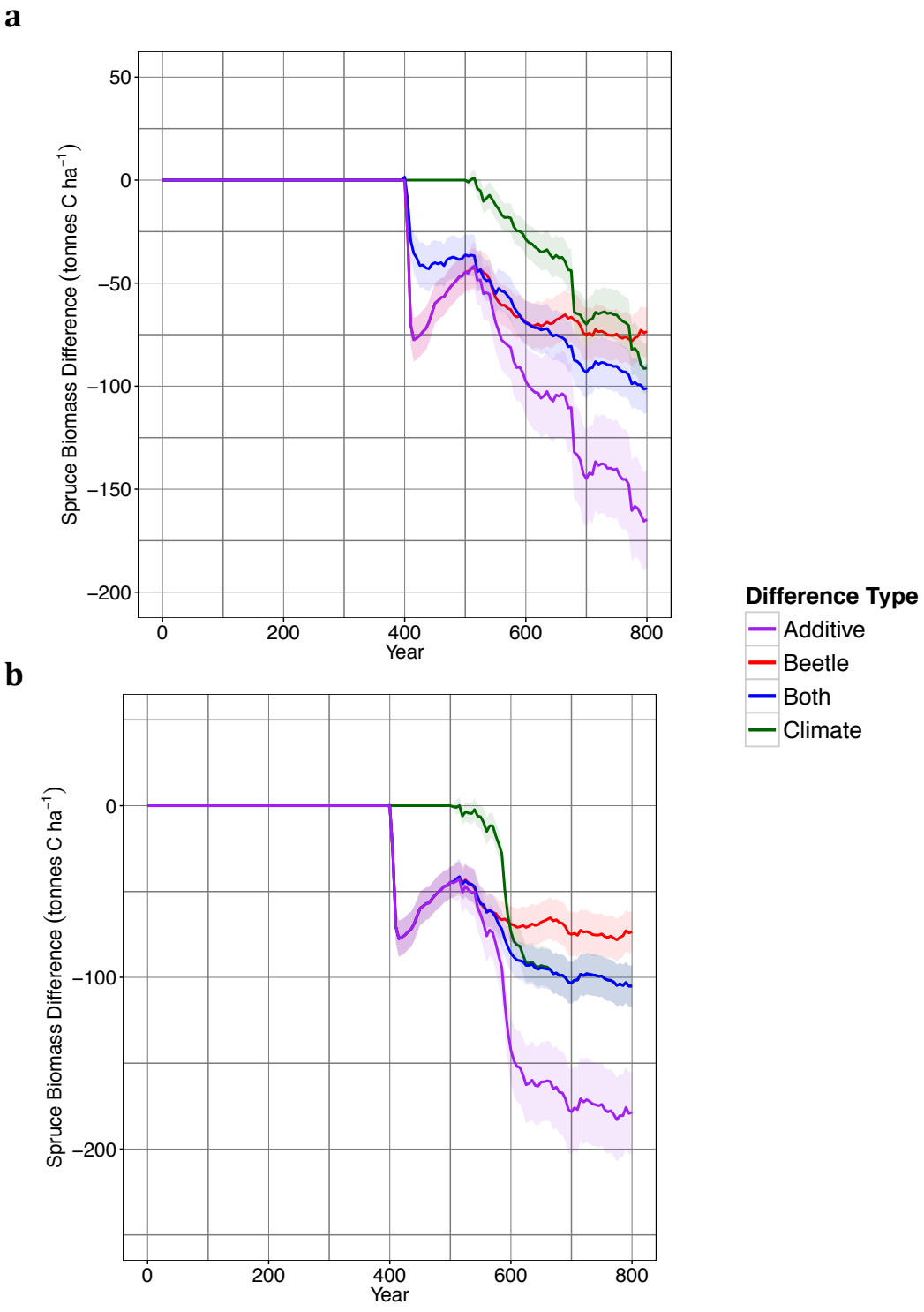

Figure 5.26. Spruce biomass difference (tonnes C ha^{-1}) over time at Niwot Ridge between the control simulation and the solely beetle disturbance simulation (red), the solely climate simulation (green), and the combination of climate and beetle disturbance (blue) for the (a) A1B and (b) A2 climate change scenarios. The additive (purple) line is the loss from beetle disturbance alone plus the loss from climate alone. Shading represents 95% confidence intervals.

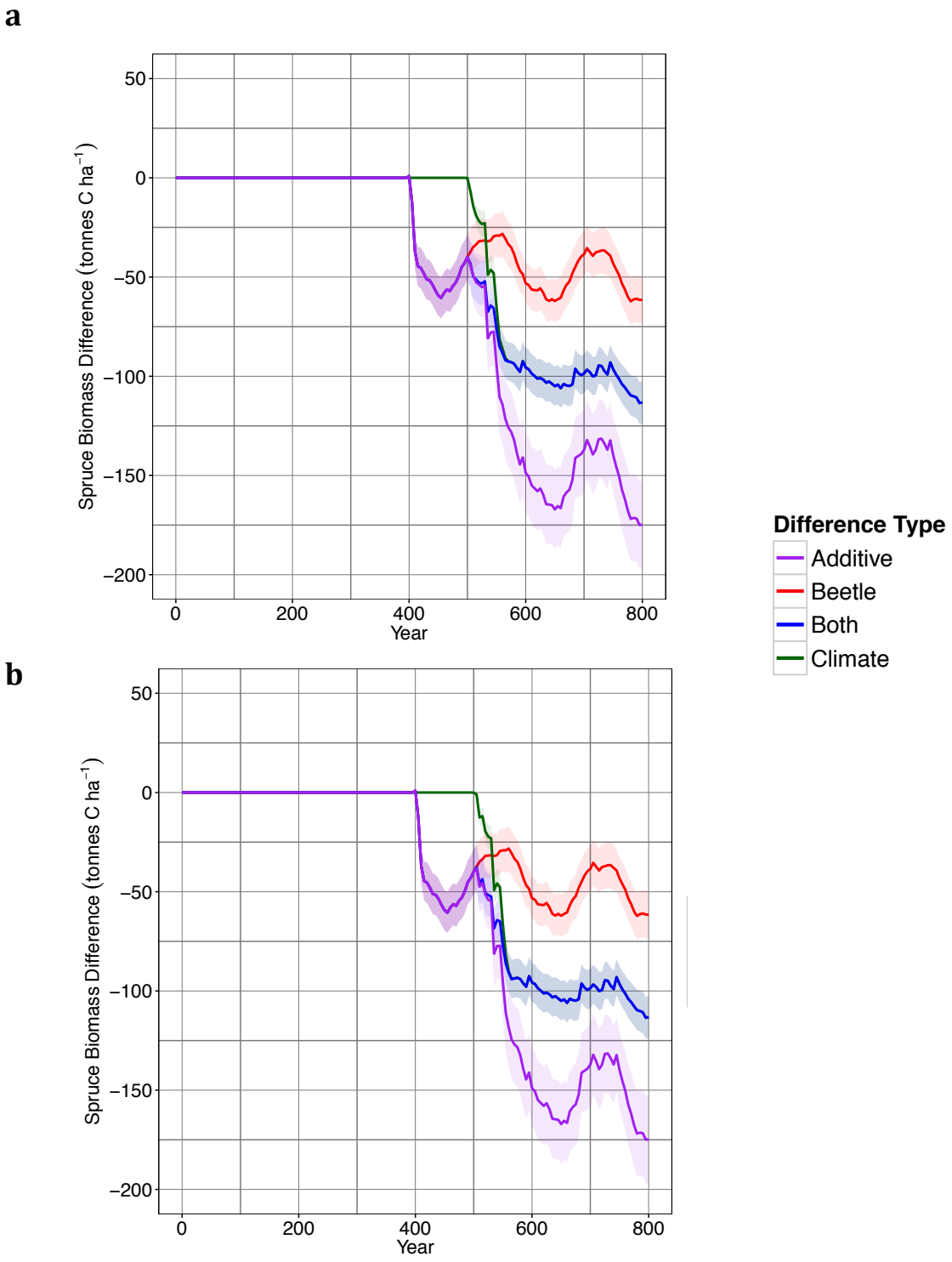

Figure 5.27. Spruce biomass difference (tonnes C ha^{-1}) over time at Fraser Experimental Forest between the control simulation and the solely beetle disturbance simulation (red), the solely climate simulation (green), and the combination of climate and beetle disturbance (blue) for the (a) A1B and (b) A2 climate change scenarios. The additive (purple) line is the loss from beetle disturbance alone plus the loss from climate alone. Shading represents 95% confidence intervals.

growth. However, eventually, due to the high infestation-related mortality of large-diameter spruce and the effective suppression of small-diameter spruce by species like ponderosa pine and Douglas-fir, spruce biomass may decline so much that spruce beetles will become less and less important.

A recent study by Temperli et al. (2015) utilized the landscape model LandClim to investigate the response of subalpine vegetation in northern CO to increasing spruce beetle infestations and climate change. They similarly predicted a reduction in Engelmann spruce and an increase in Douglas-fir and ponderosa pine, however their climate change scenarios were considerably more extreme than the ones utilized here (+4.4°C & -9% precipitation; +5.2°C & +12% precipitation; +7.0°C & -29% precipitation). They also predicted a decline in beetle-related mortality with climate change and an eventual dampening effect (i.e. after 2070) between climate and spruce beetles at high elevations. They additionally found a completely dampening effect between spruce beetle disturbance and climate at low elevations (2200 to 2800 m). LandClim utilizes a cohort-based approach to tree modeling, which assumes that trees within a certain age range are the same size (Temperli et al. 2013, 2015). The spruce beetle infestation model presented here and that of the Temperli et al. (2015) study relied on similar spruce beetle susceptibility metrics. However, the cohort-based modeling of LandClim does not allow for individual tree mortality and was constrained to a plot-wide susceptibility metric to reduce total spruce biomass. Thus, individual tree interactions arising from differences in tree sizes and the facilitation of competition between Engelmann spruce and lower elevation species could not be fully simulated. Furthermore, this lack of individual tree modeling does not allow for complete representation of the effects of and interactions among moderate disturbances such as fire, windthrow, and insects. Although UVAFME and the disturbance submodels presented in this

work have yet to be applied within an ecosystem or landscape modeling framework, which would allow disturbances to progress across vast landscapes, the results presented here can be used to answer compelling questions about the potential fate of the forested landscapes of the Rocky Mountains.

Results from the elevation tests show that with spruce beetles and climate change, Engelmann spruce biomass was considerably reduced throughout its range (Fig. 5.28b). Other subalpine species such as subalpine fir (*Abies lasiocarpa*) and lodgepole pine (*Pinus contorta*) also declined under increasing temperatures, potentially from competition with invading lower elevation species (*Pseudotsuga menziesii* and *Pinus ponderosa*). It is important to note that lodgepole pine and ponderosa pine are principal hosts of the mountain pine beetle (*Dendroctonus ponderosae*), a close relative of the spruce beetle that has recently caused extensive tree mortality throughout the western US (Logan and Powell 2001, Powell and Bentz 2009). Douglas-fir also has an associated bark beetle, the Douglas-fir beetle (*Dendroctonus pseudotsugae*) (Hood and Bentz 2007). Currently, outbreaks of the Douglas-fir beetle are not as severe as outbreaks of the spruce or mountain pine beetles (USFS 2015), however, infestations may increase in the future (Raffa et al. 2008). Infestation by mountain pine beetles and Douglas-fir beetles were not included in these simulations with UVAFME, and thus projections of increased ponderosa pine, lodgepole pine, and Douglas-fir biomass must be taken with these mortality agents in mind.

Another factor not included in these simulations was the influence of spruce beetle infestations on subsequent fire probability and severity. The effect of bark beetle outbreaks on wildfire has been widely debated (Jenkins et al. 2014). Early on, qualitative observations and anecdotal evidence seemed to suggest that the preponderance of dead stems and coarse woody

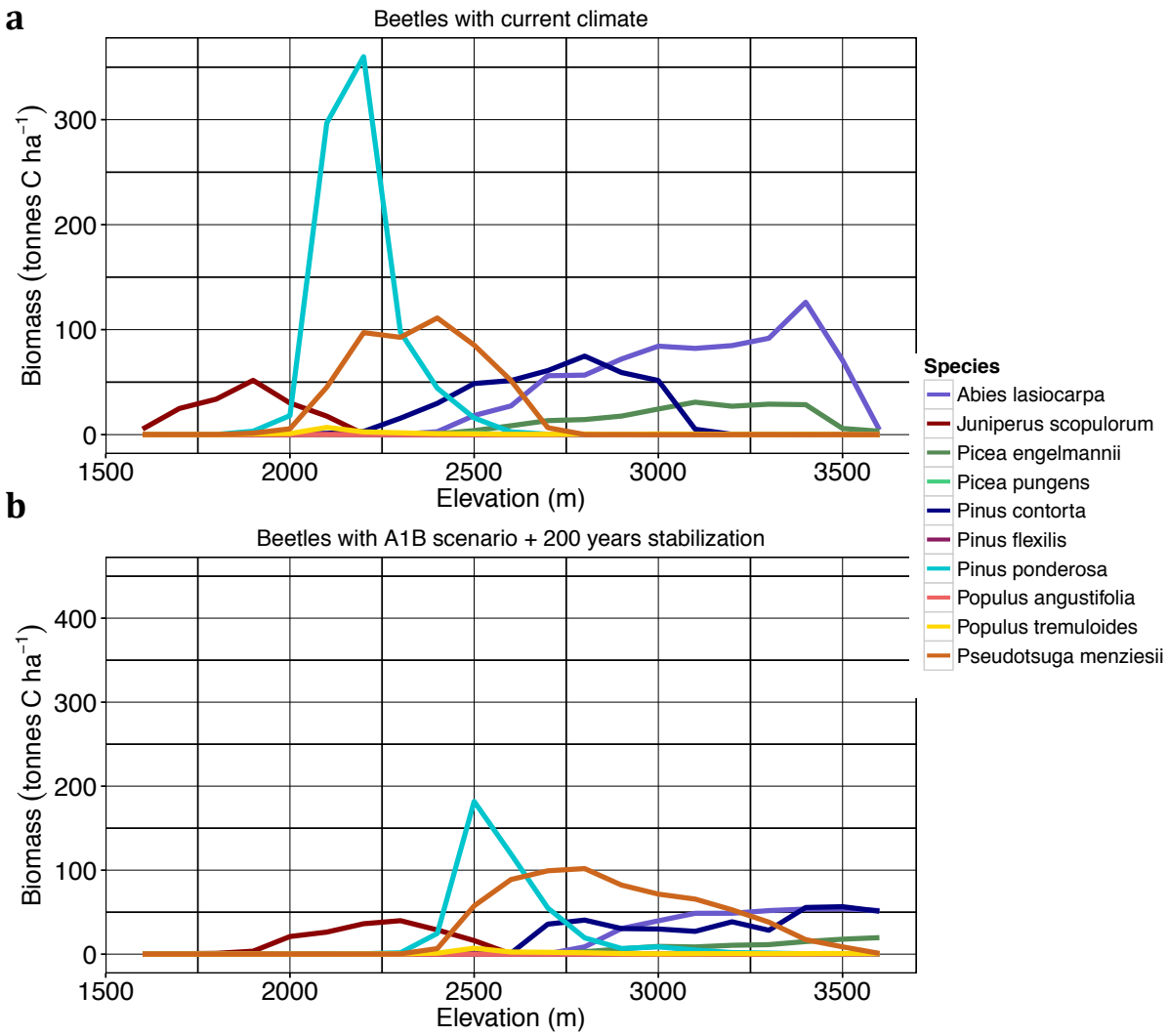

Figure 5.28. Simulated biomass (tonnes C ha^{-1}) of ten Rocky Mountain species at different elevations under (a) current climate conditions with spruce beetle infestation and (b) 200 years after the A1B climate change scenario with spruce beetle infestation.

debris following a bark beetle outbreak increased fire susceptibility, however, recent quantitative evidence suggests that the relationship between insect outbreaks and fire risk is more complex and non-linear (Jenkins et al. 2012, 2014). Studies have shown that recently attacked forest stands (i.e. within one to four years of infestation) have a higher probability for fire ignition and spread due to the decreased moisture level in the leaves and increased levels of flammable defense chemicals of attacked trees (Jolly et al. 2012, Jenkins et al. 2012, 2014). Later on in the

stages of an outbreak, however, the potential for active crown fires has been shown to decline due to decreased surface-to-canopy fuel continuity (Hicke et al. 2012). These interactions also seem to vary with location and climate. A recent study by Hart et al. (2015a) found that increases across the western US in mountain pine beetle outbreak had no affect on total area burned within that region. In contrast, a study by Hansen et al. (2016) found that spruce beetle outbreaks increased fire probability in northern Alaska, an area dominated by both black (highly flammable, beetle resistant) and white (low flammability, beetle mortality prone) spruce. Future work with UVAFME which explicitly models forest fuels and wildland fire dynamics will seek to simulate these additional bark beetle – wildfire interactions. These interactions may be key in predicting forest species composition under a warming, drying, and potentially more flammable landscape (Westerling et al. 2006, Jolly et al. 2015).

Conclusions

The forest dynamics simulated in this study and the climate - vegetation - disturbance interactions that shaped them can only be attained with an individual tree-based model such as UVAFME. Other ecological models have studied the effects of climate and disturbances on vegetation, but have often been limited by the lack of explicit consideration of individual species and individual trees. A recent comparison of 40 terrestrial biosphere models (which simulate ecosystem processes and the distribution of vegetation, generally at the level of plant functional types) found high uncertainty and variability in both the magnitude and sign of annual carbon flux over the Alaskan Arctic, another region strongly driven by climate and disturbances (Fisher et al. 2014). The results presented here demonstrate the importance of tree-level interactions between vegetation, climate, and disturbances. These simulations have shown that although the amount of infested spruce decreases over time under a warming climate, the combination of

spruce beetles and climate change may be more detrimental to spruce biomass than either climate change or spruce beetles alone. Additionally, through species- and tree size-specific modeling, this study predicts that spruce beetle infestations may facilitate competition between Engelmann spruce and invading lower elevation species, further threatening the future of subalpine systems. Subalpine forests are important for their contribution to the US carbon budget, for their influence on slope stability, for commercial timber and water resources, and for their impact on tourism in the region. They are a source of great natural beauty and are home to many charismatic and important wildlife species. The loss of this valued ecosystem would thus carry with it environmental, economic, and social implications.

The effects of spruce beetle infestations, climate, and other disturbances may be mitigated through various forest management techniques such as selective thinning (Hansen et al. 2010). The disturbance submodels developed in this work, along with additional harvest and management submodels, can be used to inform and improve these management techniques, potentially alleviating some of the predicted mortality. The infestation submodel described here can also be applied to the study of other bark beetle species, such as the mountain pine beetle, the Douglas-fir beetle, or *Ips spp.* bark beetles. Outbreaks of these additional bark beetles have similar effects on forest stand structure, and additionally interact with other disturbances and climate (Bentz et al. 2009, 2010). Thus, individual-based modeling will be just as important with these systems. As shifting climate and disturbance regimes continue to alter forest dynamics and interactions between vegetation and vegetation drivers, individual-based modeling will become a valuable tool to investigate the possible futures of Rocky Mountain forests.

Supplementary Material

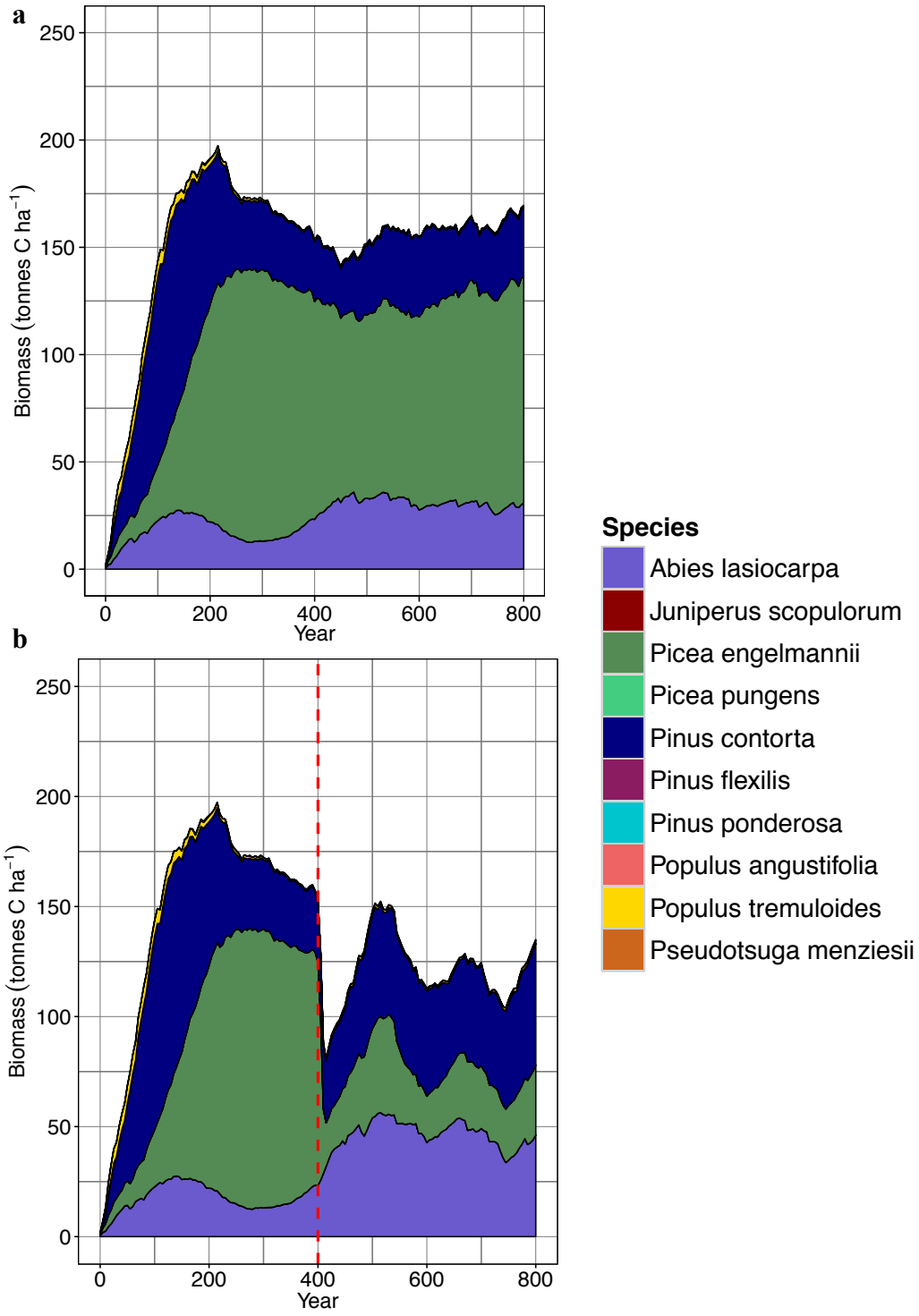

Figure 5.A. Time scale output of species-specific biomass (tonnes C ha^{-1}) under current climate conditions at Niwot Ridge for the (a) control and (b) solely beetle disturbance simulations. In the solely beetle disturbance simulation beetles were introduced at year 400 (red dashed line).

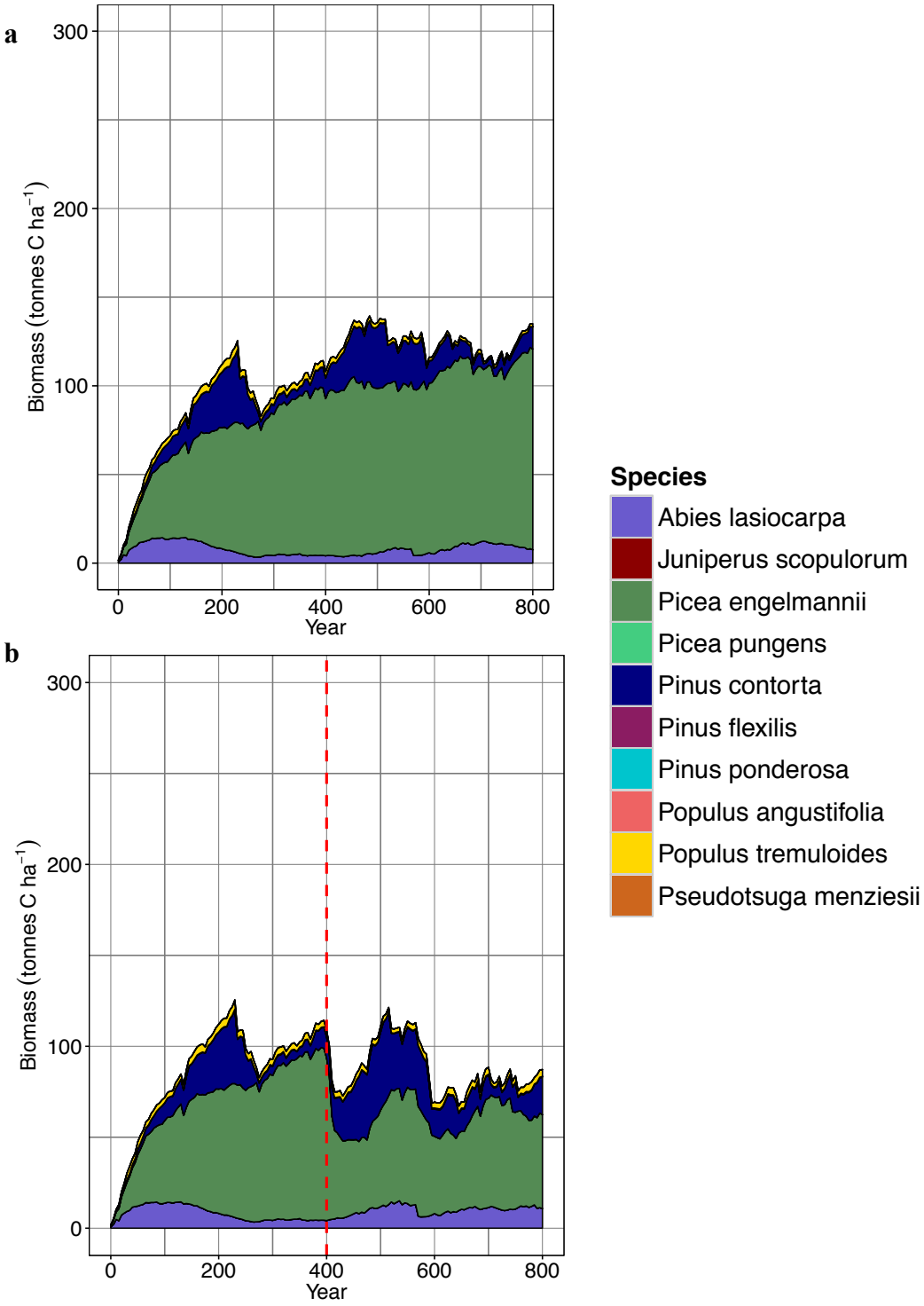

Figure 5.B. Time scale output of species-specific biomass (tonnes C ha^{-1}) under current climate conditions at Fraser Experimental Forest for the (a) control and (b) solely beetle disturbance simulations. In the solely beetle disturbance simulation beetles were introduced at year 400 (red dashed line).

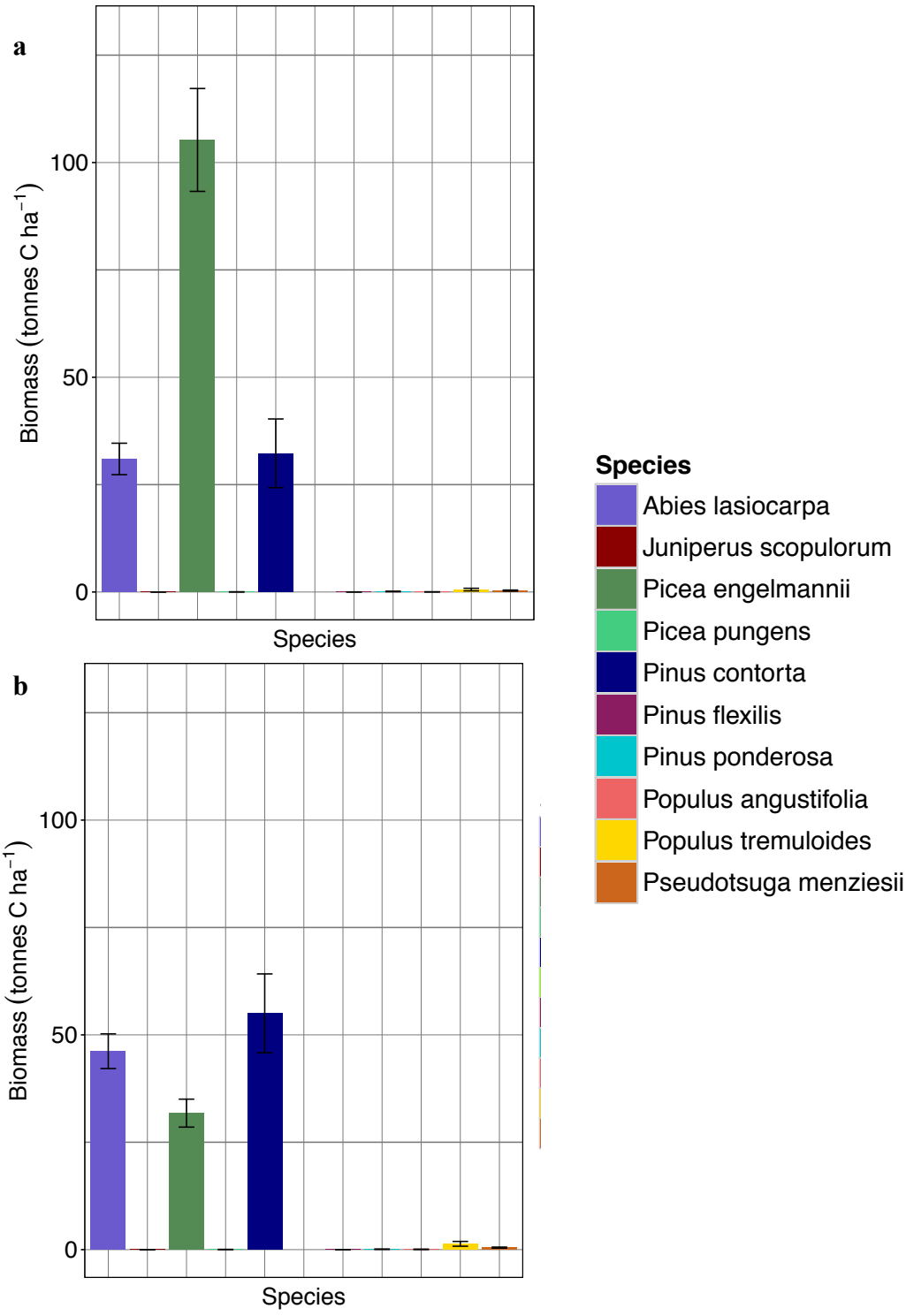

Figure 5.C. Species-specific biomass (tonnes C ha^{-1}) at Niwot Ridge at year 800 for (a) the control simulation and (b) the solely beetle disturbance simulation along with 95% confidence intervals.

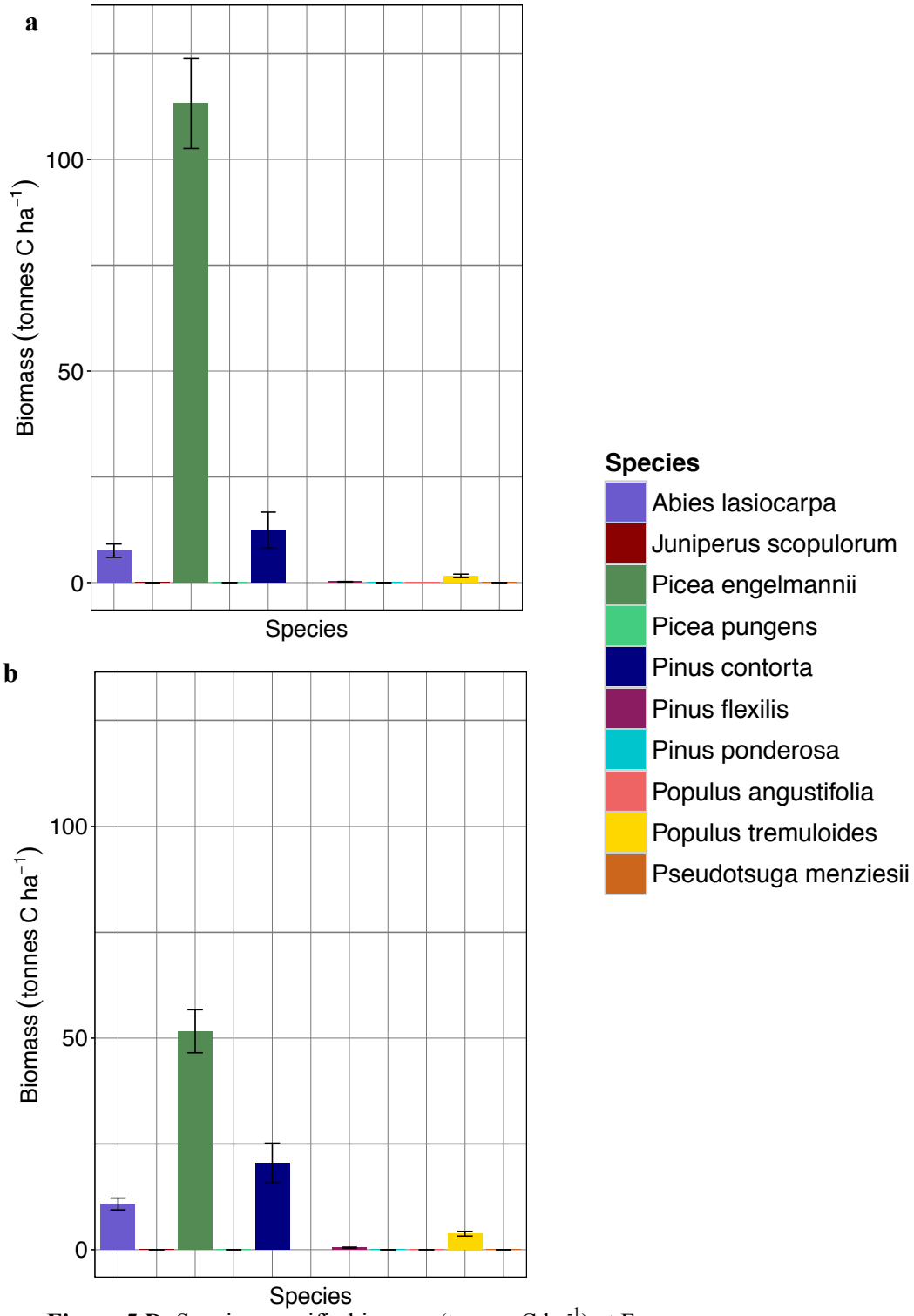

Figure 5.D. Species-specific biomass (tonnes C ha^{-1}) at Fraser Experimental Forest at year 800 for (a) the control simulation and (b) the solely beetle disturbance simulation along with 95% confidence intervals.

References

Allen, C. D., and D. D. Breshears. 1998. Drought-induced shift of a forest-woodland ecotone: rapid landscape response to climate variation. Proceedings of the National Academy of Sciences 95:14839–14842.

Araujo, M. B., and M. Luoto. 2007. The importance of biotic interactions for modelling species distributions under climate change. Global Ecology and Biogeography 16:743–753.

Bebi, P., D. Kulakowski, and T. T. Veblen. 2003. Interactions between fire and spruce beetles in a subalpine Rocky Mountain forest landscape. Ecology 84:362–371.

Bell, D. M., J. B. Bradford, and W. K. Lauenroth. 2014. Mountain landscapes offer few opportunities for high-elevation tree species migration. Global Change Biology 20:1441–1451.

Bentz, B. J., J. Régnière, C. J. Fettig, E. M. Hansen, J. L. Hayes, J. A. Hicke, R. G. Kelsey, J. F. Negrón, and S. J. Seybold. 2010. Climate Change and Bark Beetles of the Western United States and Canada: Direct and Indirect Effects. BioScience 60:602–613.

Bentz, B., J. Logan, J. MacMahon, C. D. Allen, M. Ayres, E. Berg, A. Carroll, M. Hansen, J. Hicke, L. Joyce, and others. 2009. Bark beetle outbreaks in western North America: Causes and consequences. Bark Beetle Symposium, Snowbird Utah.

Berg, E. E., J. D. Henry, C. L. Fastie, A. D. De Volder, and S. M. Matsuoka. 2006. Spruce beetle outbreaks on the Kenai Peninsula, Alaska, and Kluane National Park and Reseve, Yukon Territory: Relationship to summer temperatures and regional differences in disturbance regimes. Forest Ecology and Management 227:219–232.

Bond-Lamberty, B., J. P. Fisk, J. A. Holm, V. Bailey, G. Bohrer, and C. M. Gough. 2015. Moderate forest disturbance as a stringent test for gap and big-leaf models. Biogeosciences 12:513–526.

Breshears, D. D., N. S. Cobb, P. M. Rich, K. P. Price, C. D. Allen, R. G. Balice, W. H. Romme, J. H. Kastens, M. L. Floyd, J. Belnap, J. J. Anderson, O. B. Myers, and C. W. Meyer. 2005. Regional vegetation die-off in response to global-change-type drought. Proceedings of the National Academy of Sciences 102:15144–15148.

Bretfeld, M., S. B. Franklin, and R. K. Peet. 2016. A multiple-scale assessment of long-term aspen persistence and elevation range shifts in the Colorado Front Range. Ecological Monographs.

Burns, R. M., and B. H. Honkala. 1990. Silvics of North America: 1. Conifers; 2. Hardwoods. Agricultural Handbook 654. U.S. Department of Agriculture, Forest Service, Washington, DC. vol. 2 877 p.

Canham, C. D., M. J. Papaik, and E. F. Latty. 2001. Interspecific variation in susceptibilty to wind-throw as a function of tree size and storm severity for northern temperate tree species. Canadian Journal of Forest Research 31:1–10.

Christiansen, E., R. H. Waring, and A. A. Berryman. 1987. Resistance of conifers to bark beetle attack: searching for general relationships. Forest Ecology and Management 22:89–106.

Clark, J. S., D. M. Bell, M. H. Hersh, and L. Nichols. 2011. Climate change vulnerability of forest biodiversity: climate and competition tracking of demographic rates. Global Change Biology 17:1834–1849.

Crookston, N. ., G. E. Rehfeldt, G. E. Dixon, and A. R. Weiskittel. 2010. Addressing climate change in the forest vegetation simulator to assess impacts on landscape forest dynamics. Forest Ecology and Management 260:1198–1211.

Dale, V. H., L. A. Joyce, S. Mcnulty, R. P. Neilson, M. P. Ayres, M. D. Flannigan, P. J. Hanson, L. C. Irland, A. E. Lugo, C. J. Peterson, D. Simberloff, F. J. Swanson, B. J. Stocks, and B. Michael Wotton. 2001. Climate Change and Forest Disturbances. BioScience 51:723.

Derderian, D. ., H. Dang, G. H. Aplet, and D. Binkley. 2016. Bark beetle effects on a seven-century chronosequence of Engelmann spruce and subalpine fir in Colorado, USA. Forest Ecology and Management 361:154–162.

DeRose, R. J., B. J. Bentz, J. N. Long, and J. D. Shaw. 2013. Effect of increasing temperatures on the distribution of spruce beetle in Engelmann spruce forests of the Interior West, USA. Forest Ecology and Management 308:198–206.

DeRose, R. J., and J. N. Long. 2012a. Drought-driven disturbance history characterizes a southern Rocky Mountain subalpine forest. Canadian Journal of Forest Research 42:1649–1660.

DeRose, R. J., and J. N. Long. 2012b. Factors Influencing the Spatial and Temporal Dynamics of Engelmann Spruce Mortality during a Spruce Beetle Outbreak on the Markagunt Plateau, Utah. Forest Science 58:1–14.

Dyer, E. D. A. 1975. Frontalin attractant in stands infested by the spruce beetle, Dendroctonus rufipennis (Coleoptera: Scolytidae). The Canadian Entomologist 107:979–988.

Edburg, S. L., J. A. Hicke, P. D. Brooks, E. G. Pendall, B. E. Ewers, U. Norton, D. Gochis, E. D. Gutmann, and A. J. Meddens. 2012. Cascading impacts of bark beetle-caused tree

mortality on coupled biogeophysical and biogeochemical processes. Frontiers in Ecology and the Environment 10:416–424.

Everham, E. M., and N. V. L. Brokaw. 1996. Forest damage and recovery from catastrophic wind. Botanical Review 62:113–185.

Feng, S., and Q. Fu. 2013. Expansion of global drylands under a warming climate. Atmospheric Chemistry and Physics 13:10081–10094.

Fettig, C. J., R. R. Borys, S. R. McKelvey, and C. P. Dabney. 2008. Blacks Mountain Experimental Forest: Bark beetle responses to differences in forest structure and the application of prescribed fire in interior ponderosa pine. Canadian Journal of Forest Research 38:924–935.

Fettig, C. J., M. L. Reid, B. J. Bentz, S. Sevanto, D. L. Spittlehouse, and T. Wang. 2013. Changing climates, changing forests: a western North American perspective. Journal of Forestry 111:214–228.

Fisher, J. B., M. Sikka, W. C. Oechel, D. N. Huntzinger, J. R. Melton, C. D. Koven, A. Ahlström, M. A. Arain, I. Baker, J. M. Chen, P. Ciais, C. Davidson, M. Dietze, B. El-Masri, D. Hayes, C. Huntingford, A. K. Jain, P. E. Levy, M. R. Lomas, B. Poulter, D. Price, A. K. Sahoo, K. Schaefer, H. Tian, E. Tomelleri, H. Verbeeck, N. Viovy, R. Wania, N. Zeng, and C. E. Miller. 2014. Carbon cycle uncertainty in the Alaskan Arctic. Biogeosciences 11:4271–4288.

Foster, D. R. 1988. Species and stand response to catastrophic wind in central New England, USA. Journal of Ecology 76:135–151.

Frank, J. M., W. J. Massman, B. E. Ewers, L. S. Huckaby, and J. F. Negrón. 2014. Ecosystem CO_2 /H_2O fluxes are explained by hydraulically limited gas exchange during tree

mortality from spruce bark beetles: CO_2 /H_2O FLUX EXPLAINED FROM DISTURBANCE. Journal of Geophysical Research: Biogeosciences 119:1195–1215.

Furniss, M. M., M. D. McGregor, M. W. Foiles, and A. D. Partridge. 1979. Chronology and characteristics of a Douglas-fir beetle outbreak in northern Idaho. USDA Forest Service General Technical Report INT-59. Intermountain Forest and Range Experiment Station, Ogden, UT.:19.

Geiszler, D. R., D. R. Gara, and W. R. Littke. 1984. Bark beetle infestations of lodgepole pine following a fire in south central Oregon. Zitschrift fur Angewandte Entomologie 98:389–394.

Goetz, S. J., B. Bond-Lamberty, B. E. Law, J. A. Hicke, C. Huang, R. A. Houghton, S. McNulty, T. O'Halloran, M. Harmon, A. J. H. Meddens, E. M. Pfeifer, D. Mildrexler, and E. S. Kasischke. 2012. Observations and assessment of forest carbon dynamics following disturbance in North America. Journal of Geophysical Research 117.

Hanberry, B. B., and M. H. Hansen. 2015. Latitudinal range shifts of tree species in the United States across multi-decadal time scales. Basic and Applied Ecology 16:231–238.

Hansen, E. M. 2013. Forest Development and Carbon Dynamics After Mountain Pine Beetle Outbreaks. Forest Science 60.

Hansen, E. M., and B. J. Bentz. 2003. Comparison of reproductive capacity among univoltine, semivoltine, and re-emerged parent spruce beetles (Coleoptera: Scolytidae). The Canadian Entomologist 135:697–712.

Hansen, E. M., B. J. Bentz, J. A. Powell, D. R. Gray, and J. C. Vandygriff. 2011. Prepupal diapause and instar IV developmental rates of the spruce beetle, Dendroctonus rufipennis (Coleoptera: Curculionidae, Scolytinae). Journal of Insect Physiology 57:1347–1357.

Hansen, E. M., B. J. Bentz, and D. L. Turner. 2001a. Physiological basis for flexible voltinism in the spruce beetle (Coleoptera: Scolytidae). The Canadian Entomologist 133:805–817.

Hansen, E. M., B. J. Bentz, and D. L. Turner. 2001b. Temperature-based model for predicting univoltine brood proportions in spruce beetle (Coleoptera: Scolytidae). Canadian Entomologist 133:827–841.

Hansen, E. M., J. F. Negron, A. S. Munson, and J. A. Anhold. 2010. A retrospective assessment of partial cutting to reduce spruce beetle-caused mortality in the southern Rocky Mountains. Western Journal of Applied Forestry 25:81–87.

Hansen, W. D., F. S. Chapin III, H. T. Naughton, S. Rupp, and D. Verbyl. 2016. Forest-landscape structure mediates effects of a spruce bark beetle (Dendroctonus rufipennis) outbreak on subsequent likelihood of burning in Alaskan boreal forest. Forest Ecology and Management 369:38–46.

Hart, S. J., T. Schoennagel, T. T. Veblen, and T. B. Chapman. 2015a. Area burned in the western United States is unaffected by recent mountain pine beetle outbreaks. Proceedings of the National Academy of Sciences 112:4375–4380.

Hart, S. J., T. T. Veblen, K. S. Eisenhart, D. Jarvis, and D. Kulakowski. 2014a. Drought induces spruce beetle (Dendroctonus rufipennis) outbreaks across northwestern Colorado. Ecology 95:930–939.

Hart, S. J., T. T. Veblen, and D. Kulakowski. 2014b. Do tree and stand-level attributes determine susceptibility of spruce-fir forests to spruce beetle outbreak in the early 21st century? Forest Ecology and Management 318:44–53.

Hart, S. J., T. T. Veblen, N. Mietkiewicz, and D. Kulakowski. 2015b. Negative feedbacks on bark beetle outbreaks: widespread and severe spruce beetle infestation restricts subsequent infestation. PLOS ONE.

Hebertson, E. G., and M. J. Jenkins. 2008. Climate factors associated with historic spruce beetle (Coleoptera: Curculionidae) outbreaks in Utah and Colorado. Environmental Entomology 37:281–292.

Hicke, J. A., M. C. Johnson, J. Hayes, and H. K. Preisler. 2012. Effects of bark beetle-caused tree mortality on wildfire. Forest Ecology and Management 271:81–90.

Hood, S., and B. Bentz. 2007. Predicting postfire Douglas-fir beetle attacks and tree mortality in the northern Rocky Mountains. Canadian Journal of Forest Research 37:1058–1069.

Jenkins, M. J., W. G. Page, E. G. Hebertson, and M. E. Alexander. 2012. Fuels and fire behavior dynamics in bark beetle-attacked forests in Western North America and implications for fire management. Forest Ecology and Management 275:23–34.

Jenkins, M. J., J. B. Runyon, C. J. Fettig, W. G. Page, and B. J. Bentz. 2014. Interactions among the mountain pine beetle, fires, and fuels. Forest Science 60.

Jiang, X., S. A. Rauscher, T. D. Ringler, D. M. Lawrence, A. P. Williams, C. D. Allen, A. L. Steiner, D. M. Cai, and N. G. McDowell. 2013. Projected future changes in vegetation in western North America in the twenty-first century. Journal of Climate 26:3671–3687.

Jolly, W. M., M. A. Cochrane, P. H. Freeborn, Z. A. Holden, T. J. Brown, G. J. Williamson, and D. M. J. S. Bowman. 2015. Climate-induced variations in global wildfire danger from 1979 to 2013. Nature Communications 6:7537.

Jolly, W. M., R. A. Parsons, A. M. Hadlow, G. M. Cohn, S. S. McAllister, J. B. Popp, R. M. Hubbard, and J. F. Negron. 2012. Relationships between moisture, chemistry, and

ignition of Pinus contorta needles during the early stages of mountain pine beetle attack. Forest Ecology and Management 269:52–59.

Joyce, L. A., S. W. Running, D. D. Breshears, V. H. Dale, R. W. Malmsheimer, R. N. Sampson, B. Sohngen, and C. W. Woodall. 2014. Ch. 7: Forests. Pages 175–194 Climate Change Impacts in the United States: The Third National Climate Assessment. U.S. Global Change Research Program.

Kalkstein, L. S. 1976. Effects of climatic stress upon outbreaks of the southern pine beetle. Environmental Entomology 5:653–658.

Keane, R. E., R. A. Loehman, and L. M. Holsinger. 2011. The FireBGCv2 Landscape Fire Succession Model: A research simulation platform for exploring fire and vegetation dynamics. USDA Forest Service General Technical Report RMRS-GTR-55:145.

Kulakowski, D., and T. T. Veblen. 2002. Influences of fire history and topography on the pattern of a severe wind blowdown in a Colorado subalpine forest. Journal of Ecology 90:806–819.

Kulakowski, D., and T. T. Veblen. 2006. The effect of fires on susceptibility of subalpine forests to a 19th century spruce beetle outbreak in western Colorado. Canadian Journal of Forest Research 36:2974–2982.

Larsson, S., R. Oren, R. H. Waring, and J. W. Barrett. 1983. Attacks of mountain pine beetle as related to tree vigor of ponderosa pine. Forest Science 29:395–402.

Little, E. L. 1971. Atlas of United States trees, volume 1, conifers and important hardwoods. US Department of Agriculture. RN 1146. 9pp, 200 maps.

Logan, J. A., and J. A. Powell. 2001. Ghost forests, global warming, and the mountain pine beetle (Coleoptera: Scolytidae). American Entomologist 47:160–173.

Malmstrom, C. M., and K. F. Raffa. 2000. Biotic disturbance agents in the boreal forest: considerations for vegetation change models. Global Change Biology 6:35–48.

Mattson, W. J., and R. A. Haack. 1987. The role of drought in outbreaks of plant-eating insects. Bioscience 37:110–118.

McKenzie, D., D. L. Peterson, and J. J. Littell. 2009. Chapter 15 Global Warming and Stress Complexes in Forests of Western North America. Pages 319–337 Developments in Environmental Science. Elsevier.

Mezei, P., W. Grodzki, M. Blazenec, J. Skvarenina, V. Brandysova, and R. Jakus. 2014. Host and site factors affecting tree mortality caused by the spruce bark beetle (Ips typographus) in mountainous conditions. Forest Ecology and Management 331:196–207.

Negron, J. 1998. Probability of infestation and extent of mortality associated with the Douglas-fir beetle in the Colorado Front Range. Forest Ecology and Management 107:71–85.

Notaro, M., A. Mauss, and J. W. Williams. 2012. Projected vegetation changes for the American Southwest: combined dynamics modeling and bioclimatic-envelope approach. Ecological Applications 22:1365–1388.

O'Halloran, T. L., S. A. Acker, V. M. Joerger, J. Kertis, and B. E. Law. 2014. Postfire influences of snag attrition on albedo and radiative forcing: Snag fall dominates post-fire albedo. Geophysical Research Letters 41:9135–9142.

Peet, R. K. 1981. Forest vegetation of the Colorado front range. Vegetatio 45:3–75.

Powell, J. A., and B. J. Bentz. 2009. Connecting phenological predictions with population growth rates for mountain pine beetle, an outbreak insect. Landscape Ecology 24:657–672.

Raffa, K. F., B. H. Aukema, B. J. Bentz, A. L. Carroll, J. A. Hicke, M. G. Turner, and W. H. Romme. 2008. Cross-scale Drivers of Natural Disturbances Prone to Anthropogenic Amplification: The Dynamics of Bark Beetle Eruptions. BioScience 58:501.

Rasmussen, L. A., G. D. Amman, J. C. Vandygriff, R. D. Oakes, A. S. Munson, and K. E. Gibson. 1996. Bark beetle and wood borer infestation in the greater Yellowstone area during four postfire years. USDA Forest Service Research Paper INT-RP-487. Intermountain Research Station, Ogden, UT.

Rehfeldt, G. E., N. L. Crookston, M. V. Warwell, and J. S. Evans. 2006. Empirical analyses of plant-climate relationships for the western United States. International Journal of Plant Sciences 167:1123–1150.

Reicosky, D. C., L. J. Winkelman, J. M. Baker, and D. G. Baker. 1989. Accuracy of houly air temperatures calculted from daily minima and maxima. Agricultural and Forest Meteorology 46:193–209.

Rich, R. L., L. E. Frelich, and P. B. Reich. 2007. Wind-throw mortality in the southern boreal forest: effects of species, diameter and stand age. Journal of Ecology 95:1261–1273.

Rogers, B. M., D. Bachelet, R. J. Drapek, B. E. Law, R. P. Neilson, and J. R. Wells. 2015. Drivers of Future Ecosystem Change in the US Pacific Northwest: The Role of Climate, Fire, and Nitrogen. Global Vegetation Dynamics: Concepts and Applications in the MC1 Model 214:91.

Schmid, J. M., and R. H. Frye. 1976. Stand ratings for spruce beetles. US Dept. of Agriculture, Forest Service, Rocky Mountain Forest and Range Experiment Station.

Schmid, J. M., and R. H. Frye. 1977. Spruce beetle in the Rockies.

Seidl, R., P. Baier, W. Rammer, A. Schopf, and M. J. Lexer. 2007. Modelling tree mortality by bark beetle infestation in Norway spruce forests. Ecological Modelling 206:383–399.

Sherriff, R. L., E. E. Berg, and A. E. Miller. 2011. Climate variability and spruce beetle (Dendroctonus rufipennis) outbreaks in south-central and southwest Alaska. Ecology 92:1459–1470.

Sibold, J. S., T. T. Veblen, K. Chipko, L. Lawson, E. Mathis, and J. Scott. 2007. Influences of secondary disturbances on lodgepole pine stand development in Rocky Mountain National Park. Ecological Applications 17:1638–1655.

Temperli, C., H. Bugmann, and C. Elkin. 2013. Cross-scale interactions among bark beetles, climate change, and wind disturbances: a landscape modeling approach. Ecological Monographs 83:383–402.

Temperli, C., T. T. Veblen, S. J. Hart, D. Kulakowski, and A. J. Tepley. 2015. Interactions among spruce beetle disturbance, climate change and forest dynamics captured by a forest landscape model. Ecosphere 6.

USFS. 2015. Aerial survey highlights for Colorado 2014. http://www.fs.usda.gov/detail/r2/forest-grasslandhealth/?cid=stelprd3827262.

Van Wagner, C. E. 1973. Height of crown scorch in forest fires. Canadian Journal of Forest Research 3:373–378.

Veblen, T. T., K. S. Hadley, E. M. Nel, T. Kitzberger, M. Reid, and R. Villalba. 1994. Disturbance Regime and Disturbance Interactions in a Rocky Mountain Subalpine Forest. The Journal of Ecology 82:125.

Veblen, T. T., K. S. Hadley, M. S. Reid, and A. J. Rebertus. 1991. The Response of Subalpine Forests to Spruce Beetle Outbreak in Colorado. Ecology 72:213.

Veblen, T. T., T. Kitzberger, and J. Donnegan. 2000. Climatic and human influences on fire regmines in ponderosa pine forests in the Colorado Front Range. Ecological Application 10:1178–1195.

Wallin, K. F., and K. F. Raffa. 2004. Feedback between individual host selection behavior and population dynamics in an eruptive herbivore. Ecological Monographs 74:101–116.

Waring, R. H., and G. B. Pitman. 1980. A simple model of host resistance to bark beetles. Page 2. Oregon State University, School of Forestry, Corvallis, OR.

Westerling, R. J., H. G. Hidalgo, D. R. Cayan, and T. W. Swetnam. 2006. Warmer and earlier spring increases western US forest wildfire activity. Science 313:940–943.

Wichmann, L., and H. P. Ravn. 2001. The spread of Ips typographus (L.)(Coleoptera, Scolytidae) attacks following heavy windthrow in Denmark, analysed using GIS. Forest Ecology and Management 148:31–39.

Zhang, J., S. Huang, and F. He. 2015. Half-century evidence from western Canada shows forest dynamics are primarily driven by competition followed by climate. Proceedings of the National Academy of Sciences 112:4009–4014.

Zhang, Q., R. I. Alfaro, and R. J. Hebda. 1999. Dendroecological studies of tree growth, climate and spruce beetle outbreaks in Central British Columbia, Canada. Forest Ecology and Management 121:215–225.

Zolubas, P., J. Negron, and A. S. Munson. 2009. Modelling spruce bark beetle infestation probability. Baltic Forestry 15:23–27.

Chapter 6: Conclusions

Forests of the western US contribute 20 to 40% of total US carbon sequestration (Pacala et al. 2001), making them a valuable part of the US carbon budget in addition to their role in contributing to ecological stability and ecosystem services. While disturbances such as wildfire and insect outbreaks are intrinsic components of western US landscapes, anthropogenic climate change is pushing the frequency and severity of these disturbances away from historical values, threatening the future of these valuable ecosystems (Dale et al. 2001). Within the Rocky Mountains, the complex interactions between vegetation, disturbances, and climate make predicting the future of this region difficult. This dissertation utilized an individual tree-based model, which can capture these multi-scale interactions, to investigate the response of Rocky Mountain vegetation to external drivers such as wildfire, windthrow, spruce beetle infestation, and changing climate.

The initial objective for this project was to parameterize, calibrate, and validate UVAFME to the southern Rocky Mountains landscape. These calibration and validation steps were necessary so that the model could be applied within the region and so that it could be utilized to answer questions about the potential fate of Rocky Mountain vegetation. Chapter 2 outlined the parameterization and calibration conducted and in Chapter 3 it was shown that UVAFME can successfully predict the expected change in species composition with elevation within the southern Rocky Mountains. Model-simulated total biomass at two disparate subalpine sites (one in southern WY, and one in southern CO) was not significantly different from inventory-derived total biomass at those locations. UVAFME was also able to accurately predict relative species dominance and size class distribution, especially in the upper size classes, at both sites. Additionally, successional trajectories predicted by UVAFME compared favorably with

descriptions of succession at all four subalpine study sites. This robust validation with independent inventory data supports the use of UVAFME in future chapters to predict the response of subalpine vegetation to shifting climate and disturbance regimes. These results also indicate that UVAFME can be used for future studies within the Rocky Mountains. Further model development, including the addition of forest management and harvest routines, additional bark beetle infestation routines, and further improvement to the windthrow and wildfire submodels, will allow for this model to be used to answer a wide array of questions regarding vegetation dynamics and interactions among vegetation, disturbances, and climate.

The first objective also involved determining the response of Rocky Mountain vegetation to climate change without concurrent increases in other disturbances. With increasing temperatures alone, UVAFME predicted a decline in subalpine biomass and a shift upwards in elevation in the dominance of ponderosa pine (*Pinus ponderosa*) and Douglas-fir (*Pseudotsuga menziesii*). UVAFME also predicted a shift upwards in Engelmann spruce (*Picea engelmannii*) and subalpine fir (*Abies lasiocarpa*), however the reality of this prediction is dependent on the availability of space for upward migration. These changes in species composition with elevation resulted from only a moderate (2°C) increase in temperature, and were still fairly persistent even 200 years after temperature was cooled back to current values. These results indicate that vegetation of the southern Rocky Mountains is particularly vulnerable to climate- and competition-related mortality arising from climate change. Even if temperature increases are kept to 2°C, as was agreed to in the recent UN Climate Change Conference, we are still likely to see dramatic, potentially lasting changes in biomass and species composition in the Rocky Mountains. With changing species composition and biomass, there may also be an additional shift in wildfire intensity and frequency, as these fire characteristics are greatly affected by the

species composition and size structure of forests (Hood et al. 2007). These changes may also result in feedbacks to climate through changes in albedo, surface roughness, and biogeochemical cycling (Anderson et al. 2011).

The second objective was to investigate the internal dynamics within the Rocky Mountains subalpine zone through long-term simulations without disturbances. Using UVAFME, and the ability to "turn off" disturbances, it was found that the subalpine zone may contain internal cyclic phenomena. The ability to see these underlying cycles was only possible after disturbances were removed, allowing for autogenic succession across all plots to continue unimpeded. By themselves, subalpine fir and Engelmann spruce exhibited a periodicity of about 200 and 300 years, respectively. Together, with interspecies competition, both species exhibited a periodicity of about 300 years. Without disturbances, these cycles were self-perpetuating, and occurred over and over at both the plot and landscape-level. This cyclic behavior suggests that given shifts in disturbance or climate regimes, the initial conditions that set up the cyclic phenomena may change and allow for the cycle to go in a completely different direction.

Ecological modeling, and in particular individual-based modeling, uniquely allows for studies of this nature. Barring incredibly intensive field studies, where rare, practically non-existent plots as old as 1,000 years are found, and every tree on such plots is cut and cored, long-term investigations into internal forest dynamics and the endogenous factors that influence them are possible only through model simulations. Ecological modeling allows us to easily manipulate ecosystems that are characteristically unfeasible to manipulate in the field. Through various model simulations, we are able to discern differences in forest characteristics and dynamics arising from competition, climate change, or shifts in disturbance regimes. Long-term model output also allows us to see large-scale changes in these forest characteristics, which may not be

manifested at the time scale of a single field study. With guidance and new empirical equations from remote sensing and field-based studies, ecological modeling allows us to investigate the future of forested landscapes, under a variety of potential scenarios.

The third objective for this project was to determine the response of spruce beetle infestations, and subsequently subalpine vegetation, to climate change. With both spruce beetle infestations and increasing temperatures, UVAFME predicted a further decline in Engelmann spruce biomass with climate change, and a stronger shift upwards in elevation of Douglas-fir and ponderosa pine. The loss of spruce biomass was greatest for the scenario including both climate change and spruce beetle disturbance, though there was still a dampening effect of climate change on spruce beetle infestations towards the end of the simulations, resulting from a decline in available spruce hosts. In simulations with climate change and spruce beetle disturbance, beetle infestation caused a loss of Engelmann spruce biomass as well as a shift towards smaller spruce stems. This shift allowed for greater competition between Engelmann spruce and lower elevation species (i.e. Douglas-fir and ponderosa pine), and facilitated the invasion of these species into the subalpine zone. These results, along with the results from the climate sensitivity test in Chapter 3, suggest that the subalpine zone of the Rocky Mountains may be subject to drastic changes in the future. These potential negative impacts may be mitigated through forest management treatments, however care must be taken to ensure that such tactics do not result in other unintended consequences.

Within the forested ecosystems of the western US, management practices and fire suppression efforts of the 20th century have led to dense, disturbance-prone forest stands and elevated fuel levels, increasing the probability for high-severity fires and insect outbreaks (Kaufmann et al. 2006, DeRose et al. 2013). Recent efforts have been employed to reduce the

occurrence of these large, damaging fires and outbreaks while also allowing or simulating historical disturbance regimes and ecological conditions (Hansen et al. 2010, Schultz et al. 2012). The effects of management on forest biomass and ecosystem health are becoming increasingly important, as more and more policies are being adopted to increase carbon storage on federal lands in the wake of ongoing climate change (Ellenwood et al. 2012, Kline et al. 2016). However, a full-scale study on the effects of these new management strategies has not yet been conducted.

As agents of environmental and climatological change, many feel that humans have a responsibility to foster ecological sustainability and resilience. At the very least it is thought that we should try to mitigate our negative impacts on the Earth system. But too often the full effects of our actions, however well intentioned, are not realized until late in the game. How can we make management decisions without being paralyzed by the fear of the potential negative consequences? Along with extensive field and remote sensing-based studies, individual-based models such as UVAFME can be used to predict the effects of future climate change, and may also be able to predict the success of various management and climate mitigation techniques. In regions such as the Rocky Mountains, which have complicated, multi-scale interactions among several important drivers, individual-based models may become increasingly important tools for understanding forest dynamics.

Many other ecosystems also contain such complicated interactions across multiple spatiotemporal scales – the North American and Eurasian boreal forests and the Amazonian rainforest, to name only a few (Bonan 1989, Antonarakis et al. 2011). Individual-based models can be used in these systems as well, especially as changing climate and disturbances continue to impact their characteristics and functioning. We conduct these examinations into forest dynamics

and vegetation response, not only for the satisfaction of good scientific inquiry, but also for the potential positive change we may enact. Currently, individual-based modeling at the global- and even continental-scale is incredibly computationally intensive. However, as computing methods and technologies continue to improve, the feat of global-scale individual-based modeling will hopefully become more and more attainable. With such large-scale simulations, important questions and theories pertaining to the future of the Earth system can be tested, and we may be able to earn our positions as environmental stewards.

References

Anderson, R. G., J. G. Canadell, J. T. Randerson, R. B. Jackson, B. A. Hungate, D. D. Baldocchi, G. A. Ban-Weiss, G. B. Bonan, K. Caldeira, L. Cao, N. S. Diffenbaugh, K. R. Gurney, L. M. Kueppers, B. E. Law, S. Luyssaert, and T. L. O'Halloran. 2011. Biophysical considerations in forestry for climate protection. Frontiers in Ecology and the Environment 9:174–182.

Antonarakis, A. S., S. S. Saatchi, R. L. Chazdon, and P. R. Moorcroft. 2011. Using Lidar and Radar measurements to constrain predictions of forest ecosystem structure and function. Ecological Applications 21:1120–1137.

Bonan, B. G. 1989. A computer model of the solar radiation, soil moisture, and soil thermal regimes in boreal forests. Ecological Modelling 45:275–306.

Dale, V. H., L. A. Joyce, S. Mcnulty, R. P. Neilson, M. P. Ayres, M. D. Flannigan, P. J. Hanson, L. C. Irland, A. E. Lugo, C. J. Peterson, D. Simberloff, F. J. Swanson, B. J. Stocks, and B. Michael Wotton. 2001. Climate Change and Forest Disturbances. BioScience 51:723.

DeRose, R. J., B. J. Bentz, J. N. Long, and J. D. Shaw. 2013. Effect of increasing temperatures on the distribution of spruce beetle in Engelmann spruce forests of the Interior West, USA. Forest Ecology and Management 308:198–206.

Ellenwood, M. S., L. Dilling, and J. Milford. 2012. Managing United States public lands in response to climate change: a view from the ground up. Environmental Management.

Hansen, E. M., J. F. Negron, A. S. Munson, and J. A. Anhold. 2010. A retrospective assessment of partial cutting to reduce spruce beetle-caused mortality in the southern Rocky Mountains. Western Journal of Applied Forestry 25:81–87.

Hood, S. M., C. W. McHugh, K. C. Ryan, E. Reinhardt, and S. L. Smith. 2007. Evaluation of a post-fire tree mortality model for western USA conifers. International Journal of Wildland Fire 16:679–689.

Kaufmann, M. R., T. T. Veblen, and W. H. Romme. 2006. Historical fire regimes in ponderosa pine forests of the Colorado Front Range, and recommendations for ecological restoration and fuels management. Front Range Fuels Treatment Partnership Roundtable, findings of the Ecology Workgroup.

Kline, J. D., M. E. Harmon, T. A. Spies, A. T. Morzillo, R. J. Pabst, B. C. McComb, F. Schnekenburger, K. A. Olsen, B. Csuti, and J. C. Vogeler. 2016. Evaluating carbon storage, timber harvest, and potential habitat possibilities for a western Cascades (US) forest landscape. Ecological Applications.

Pacala, S. W., G. C. Hurtt, D. Baker, P. Peylin, R. A. Houghton, R. A. Birdsey, L. Heath, E. T. Sundquist, R. F. Stallard, P. Ciais, P. Moorcroft, J. P. Caspersen, E. Shevliakova, B. Moore, G. Kohlmaier, E. Holland, M. Gloor, M. E. Harmon, S.-M. Fan, J. L. Sarmiento, C. L. Goodale, D. Schimel, and C. B. Field. 2001. Consistent land and atmosphere-based US carbon sink estimates. Science 92:2316–2320.

Schultz, C. A., T. Jedd, and R. D. Beam. 2012. The Collaborative Forest Landscape Restoration Program: a history and overview of the first projects. Journal of Forestry 110:381–391.

University of Virginia Forest Model Enhanced – User's Manual

The University of Virginia Forest Model Enhanced (UVAFME), written in Fortran(90), is an update and extension of the individual-based gap model FAREAST (Yan & Shugart 2005) into an object-oriented flexible structure, allowing easier model modifications and enhancements. UVAFME is an individual-based gap model that simulates the annual establishment, growth, and death of individual trees on independent patches (i.e. plots) of a landscape. An average of several hundred of these patches simulates the average biomass and species composition of a forested landscape through time. Climate is based on inputs of mean monthly precipitation and temperature, derived from the historical data record (see Section A). Soil moisture and soil nutrients are simulated based on a coupled, three-layer soil submodule using inputs on site and soil characteristics (Section B).

Individual tree growth for each year is calculated through optimal diameter increment growth, modified by available resources and species- and tree size-specific tolerances to temperature and light, moisture, and nutrient availability. Individual trees can thus compete with one other for above- and belowground resources. Light availability throughout the canopy is calculated using the Beer-Lambert Law and is dependent on the vertical distribution of LAI within the plot (Section C). Tree growth response to temperature is based on an asymptotic relationship between growth rate and annual growing degree-days. Drought response is based on an index that represents the proportion of the growing season that experiences soil moisture limitation. The final annual increment growth for each tree is determined by multiplying the smallest (i.e. most limiting) growth-limiting factor by the optimal increment growth (Section D). Establishment of seedlings and saplings is based on species-specific resource and environmental tolerances (Section F).

UVAFME also simulates the responses to fire and windthrow disturbance, based on inputs of disturbance return interval and mean intensity (Section E.1). The occurrence of both disturbances is probabilistic, based on the site's disturbance-specific return interval. When fire occurs on a plot, the intensity of the fire as well as species- and size-specific tolerances determine which trees die from fire-related cambial damage. Windthrow is stand-replacing in UVAFME, and as such kills all trees on the plot when it occurs. When high intensity fires or windthrow occurs, there is a five-year delay on seedling and sapling establishment. Trees can also die due to age- or stress-related factors (Section E.2). Trees that die, as well as leaf litter and coarse woody debris are transferred to the soil layers.

Table of Contents

A. Climate

A.1. Temperature and Precipitation

Climate in UVAFME is simulated through distributions of monthly temperature and precipitation. The mean minimum and maximum monthly temperatures (in °C), as well as the standard deviations for these values, for a specific site (averaged from at least 30 years of historical climate data) are used to create the range of possible temperatures for the site in question. Mean monthly precipitation (mm) and the standard deviation of this value for each site (also from 30 years of historical data) are also used. These distributions of climate data are used to generate daily values of maximum temperature (t_{max}), minimum temperature (t_{min}), and precipitation (p) throughout the simulation. Initially, the monthly values of t_{max} and t_{min} are modified with the following equation:

$$t_m = \bar{t}_m + \bar{t}_{std}\, t_f \qquad (A.1)$$

where t_m is the monthly temperature minimum or maximum for a particular simulated month, $\bar{t}_m$ is the input average (minimum or maximum) temperature for that month, $\bar{t}_{std}$ is the input standard deviation, and t_f is a normally distributed random number (mean of 0.0 and a standard deviation of 1.0) between -1.0 and 1.0.

These monthly values are generated anew for each year of the simulation. These values can also be generated separately for each plot, depending on whether or not the user wants climate to be fixed for all plots within a site. Daily values of t_{min} and t_{max} for each year are then created through the following equation:

$$t_d = t_m + \left(\frac{t_{m+1} - t_m}{j_{m+1} - j_m}\right)(j_d - j_m) \qquad (A.2)$$

where t_d is the minimum or maximum temperature for that day, j_m is the Julian Day corresponding to the middle of that particular month, and j_d is the Julian Day corresponding to that day. The daily average temperature is then generated with the following equation (see Figure A.1 for an example):

$$t_{av_d} = \frac{t_{max_d} + t_{min_d}}{2} \quad \text{(A.3)}$$

where t_{av_d} is the daily temperature for that day, t_{max_d} is the maximum temperature for that day, and t_{min_d} is the minimum temperature for that day. In this way, for each daily time step in the simulation, a daily minimum, maximum, and average temperature are generated.

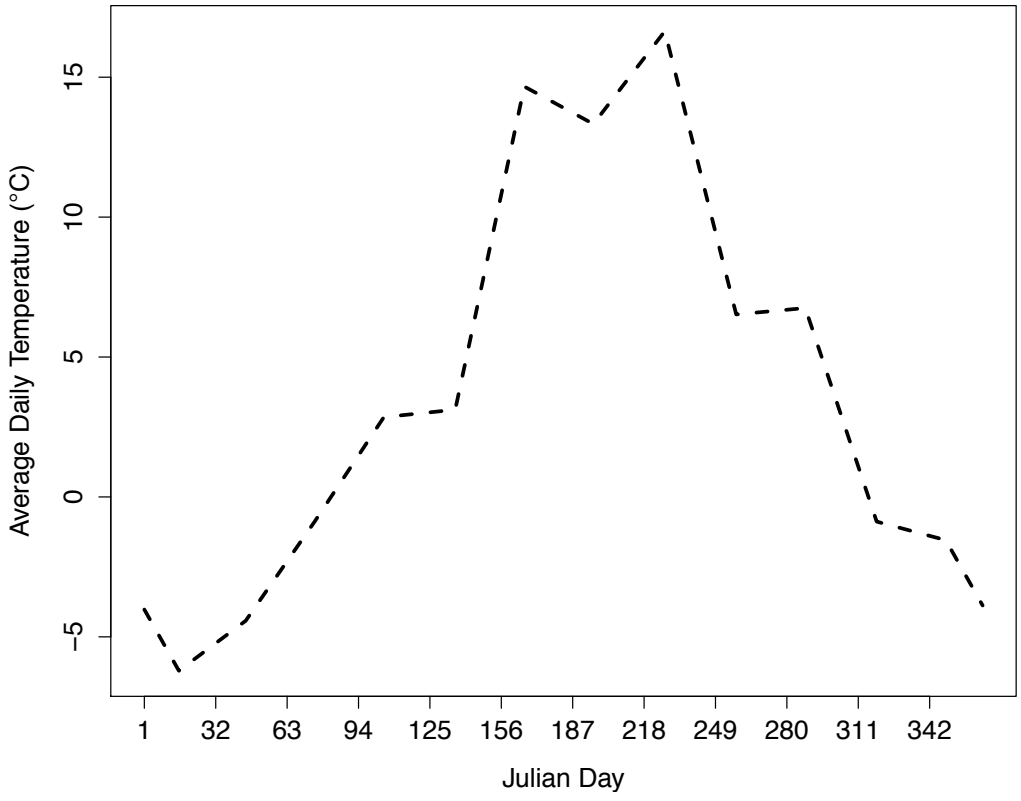

Figure A.1. Example calculation of daily average temperature (°C) for a year for a site in the Colorado Rocky Mountains.

To generate daily precipitation values, the initial monthly values of precipitation are first modified with the following equation:

$$p_m = \max(\bar{p}_m + \bar{p}_{std} p_f, 0.0) \quad \text{(A.4)}$$

where p_m is the average precipitation for a particular month (cm), $\bar{p}_m$ is the input average precipitation for that month (cm), $\bar{p}_{std}$ is the input standard deviation of that precipitation measurement, and p_f is a normally distributed random number (mean of 0.0 and standard deviation of 1.0) between -0.5 and 0.5. These monthly values are generated anew for each year of the simulation, as with the temperature values. These values can also be generated separately for each plot as with the temperature values. Daily values of precipitation for year are then generated through the following equations.

First the number of rain days for each month is generated:

$$r_m = \min(25.0, \frac{p_m}{4.0} + 1.0) \quad \text{(A.5)}$$

where r_m is the amount of rain days for that month (days). In this way, the amount of rainfall per month determines the distribution of rain for that month (Fig. A.2).

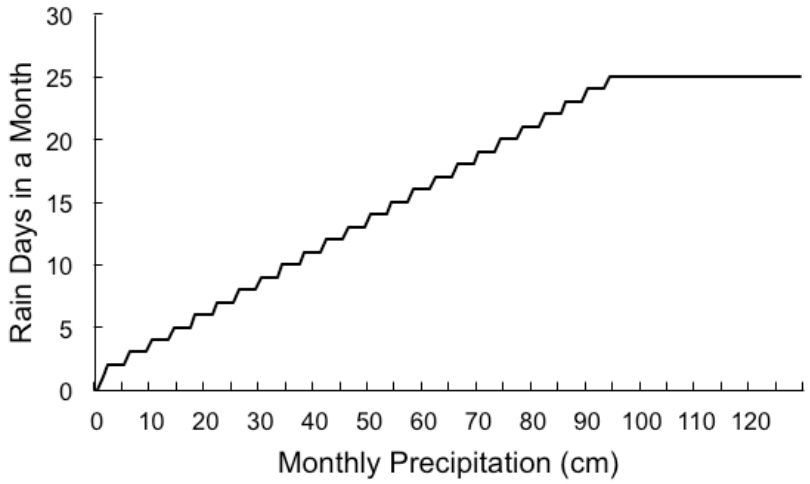

Figure A.2. Number of rain days for a month based on monthly precipitation (cm) for that month.

Then, daily precipitation values are generated through the following:

Starting from the first of each month, for each day in each month, if the number of rain days is greater than 0, (i.e. $r_m > 0$) then a uniformly distributed random number between 0.0 and 1.0 is generated (u_r). If this number is less than or equal to the percent of days in the month on which it rains (i.e. $u_r \leq \frac{r_m}{d_m}$, where r_m is the number of rain days for a particular month, and d_m is the number of days in that month), then the amount of rainfall for that day (p_d, cm) is equal to $\frac{p_m}{r_m}$. If the random number is greater than $\frac{r_m}{d_m}$, then the amount of rainfall for that day is 0.0.

The number of rain days is then subtracted by 1, and the model moves to the next day. This continues until there are no more rain days left in the month, at which point all subsequent days in the month receive no rainfall. In this way, monthly precipitation values are distributed throughout the month to generate daily precipitation values.

A.2. Extraterrestrial Radiation

Daily extraterrestrial radiation, extraterrestrial noon radiation, and day length for each day at a site are calculated based on latitude of the site and day of the year. Extraterrestrial radiation is later used to calculate potential evapotranspiration.

First, the relative distance from the Earth to the Sun for that particular day is calculated:

$$d_r = 1.0 + 0.033 \cos(0.017214 j_d) \quad \text{(A.6)}$$

where d_r is the relative distance from the Earth to the Sun, and j_d is the Julian Day of the year.

Next, the solar declination (δ_d, in radians) for that day is calculated:

$$\delta_d = 0.409 \sin(0.017214\, j_d - 1.39) \quad \text{(A.7)}$$

Finally, sunset hour angle (Ω_d, in radians) for that day is calculated through the following:

$$\omega_d = -\tan(\varphi) \tan(\delta_d) \quad \text{(A.8)}$$

where φ is latitude of the site, in radians. If ω_d is greater than or equal to 1.0, $\Omega_d = 0.0$. If ω_d is less than or equal to -1.0, $\Omega_d = \pi$. Otherwise:

$$\Omega_d = \cos^{-1}(\omega_d) \quad (A.9)$$

Extraterrestrial radiation for that day (R_d, in MJ m^{-2} d^{-1}) is then calculated (see Figure A.3 for an example):

$$R_d = 37.58603 \cos(\varphi) \cos(\delta_d)(\sin(\Omega_d) - \Omega_d \cos(\Omega_d)) \quad (A.10)$$

Day length for that day (l_d, in hrs) is calculated as (see Figure A.4 for an example):

$$l_d = 7.639437\Omega_d \quad (A.11)$$

Extraterrestrial noon radiation for that day (R_{d_n}, in MJ m^{-2} min^{-1}) is calculated as:

$$R_{d_n} = 0.082 d_r \cos(\varphi - \delta_d) \quad (A.12)$$

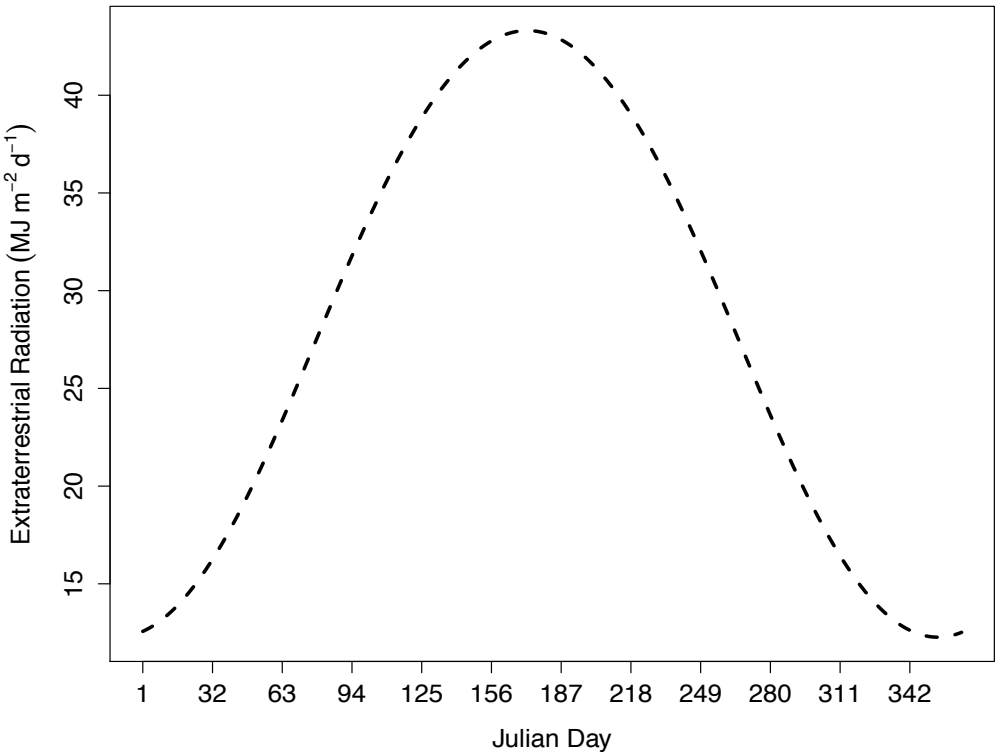

Figure A.3. Example calculation for daily extraterrestrial radiation (MJ m^{-2} d^{-1}) for the year for a site at a latitude of 40°N.

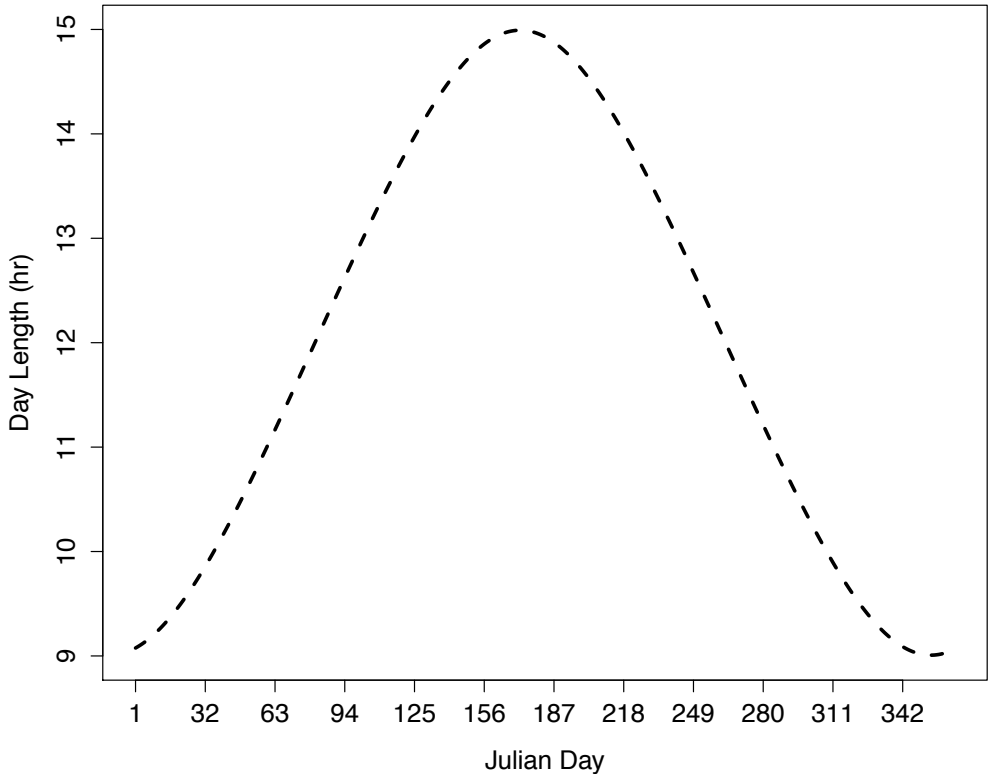

Figure A.4. Example calculation for day length (hr) for the year for a site at a latitude of 40°N.

A.3. Potential Evaporation

Daily potential evaporation is calculated using Hargreaves Evaporation Formulation, with inputs of daily minimum (t_{min_d}, °C), maximum (t_{max_d}, °C), and average temperatures (t_{av_d}, °C), and daily extraterrestrial radiation (R_d, MJ m^{-2} day^{-1}). If the average temperature for that day is less than or equal to 0.0 (i.e. $t_{av_d} \leq 0.0$), then potential evaporation (PET, cm) for that day is 0.0. Otherwise (see Figure A.5 for an example):

$$PET = 9.3876\times10^{-5}\sqrt{\left(t_{max_d} - t_{min_d}\right)}\left(t_{av_d} + 17.8\right)R_d \qquad (A.13)$$

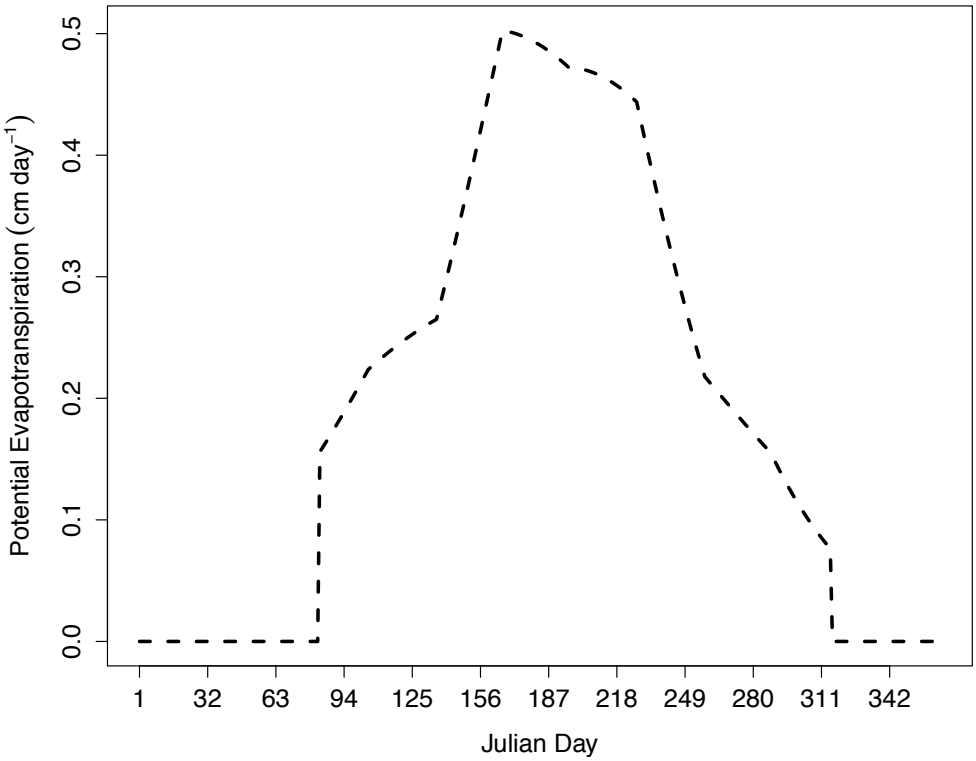

Figure A.5. Example calculation of potential evaporation (cm day^{-1}) for the year for a site in the Colorado Rocky Mountains.

A.4. Climate Change

Linear climate change can be prescribed in UVAFME. This is achieved by modifying the initial values of average minimum and maximum temperatures and precipitation for a particular site. The minimum and maximum temperatures for a site are modified through the following equations:

First the amount of temperature change per year is calculated from input values of total temperature change and duration of change:

$$t' = \frac{t_c}{y_c+1} \quad (A.14)$$

where t' is the amount of temperature change per year once climate change starts (in °C yr^{-1}), t_c is the total amount of temperature change prescribed (in °C), and y_c is the duration of climate

change (in years). When climate change starts in the model, the initial minimum and maximum temperature values are modified each year for the duration of climate change with the following equation:

$$\bar{t}_m = \bar{t}_m + t' \quad \text{(A.15)}$$

where t_m is the average (minimum or maximum) temperature for a particular month and a particular site. This continues for the duration of climate change, at which point the total change in temperature (t_c) will have occurred, and temperature stabilizes at the new value of $\bar{t}_m + t_c$. Average precipitation for a site can be modified through the following:

Again, the amount of precipitation change per year is calculated from input values of total precipitation change (in % yr^{-1}) and duration of change:

$$p' = \frac{p_c}{y_c+1} \quad \text{(A.16)}$$

where p' is the amount of precipitation change per year once climate change starts (in %), p_c is the total amount of temperature change prescribed (in %), and y_c is the duration of climate change (in years). When climate change starts, the initial monthly precipitation values are modified each year for the duration of climate change:

$$\bar{p}_m = \bar{p}_m + \bar{p}_m p' \quad \text{(A.17)}$$

where p_m is the monthly precipitation for a particular month and site (cm). This continues for the duration of climate change, at which point the total change in precipitation (p_c) will have occurred, and precipitation stabilizes at the new value of $\bar{p}_m + \bar{p}_m p_c$.

Climate change can also be generated using a GCM file as an input file. In this way, non-linear changes in temperature and precipitation can be prescribed.

A.5. Altitudinal Change

Often it is beneficial to run the model at the same site, but at a different elevation (such as in studies in complex terrain). Both temperature and precipitation change as altitude/elevation changes. These changes can be generated in UVAFME using input values of the original site elevation, the new elevation (altitude), and temperature and precipitation lapse rates. As with climate change, these changes are made to the initial average minimum and maximum monthly temperatures and precipitation for a particular site. Temperature is modified using the following equation:

$$\bar{t}_m = \bar{t}_m - 0.01(a - e)\, t_l \qquad (A.18)$$

where $\bar{t}_m$ is the average (minimum or maximum) temperature for a particular month, a is the new altitude at which the model is to be run (in meters), e is the original elevation at which the input climate data was generated (in meters), and t_l is temperature lapse rate for the site (in °C km^{-1}). Precipitation is modified using the following equation:

$$\bar{p}_m = \max\left(\bar{p}_m + 0.001 p_l(a - e), 0.0\right) \qquad (A.19)$$

where $\bar{p}_m$ is the average precipitation for a particular month and p_l is the precipitation lapse rate for the site (in cm km^{-1}).

B. Soil Processes

B.1. Soil water

Soil water balance in UVAFME is modeled as a simple bucket model with a daily time step. Outputs are aggregated over the year to influence yearly tree growth. Using this simple model allows for relatively little inputs: slope (in degrees), canopy LAI (in m m^{-1}), A_O layer dry matter content (tonnes ha^{-1}), field capacity of the soil (cm), wilting point of the soil (cm), base soil depth (cm), potential evapotranspiration (cm day^{-1}), and precipitation (cm). These inputs are

received from site input variables and from the Climate module. Variables that are derived and used in the soil water model are A_O layer water content (cm), A layer water content (cm), and base layer water content (cm). Output variables for this model include daily actual evapotranspiration (cm), and daily runoff (cm).

Precipitation (input from the Climate module) is received at the surface. This precipitation is then divided into canopy evapotranspiration, canopy interception, runoff, ground water storage, and evaporation from the soil surface.

B.1.1 If potential evaporation (PET, cm) is less than or equal to 0.0

If PET is less than or equal to 0.0 cm for that day, then precipitation is first partitioned into throughfall and canopy interception:

$$I = \min\left(\max\left((LAI_{wmax} - LAI_{w0}), 0.0\right), p\right) \quad (B.1)$$

where I is the canopy interception (cm), p is precipitation (cm), and LAI_{wmax} is the maximum canopy water content possible, defined as $0.15LAI$, where LAI is the leaf area index (m m^{-1}) of the plot. This maximum value means that each leaf or needle can contain at most a 0.15 cm film of water. Throughfall (T, cm) is then calculated as:

$$T = \max(\mathrm{p} - \mathrm{I}, 0.0) \quad (B.2)$$

The canopy water content is then updated:

$$LAI_w = \mathrm{LAI_{w0}} + I \quad (B.3)$$

where LAI_w is the updated canopy water content (cm). If the snow accumulation and snowmelt routine is being used, the model checks if the throughfall is accumulated in the snowpack. If the air temperature is less than 5°C (i.e. $t_{av_d} < 5.0$) then the throughfall is assumed to be snow and is accumulated in the snowpack ($S_P = S_P + T$). Daily thaw of the snowpack is calculated using a

simple degree-day model, using air temperature. If the air temperature is above the base temperature (t_b, generally 0°C):

$$M = \min\left(0.01 c_m \left(t_{av_d} - t_b\right), S_P\right) \quad \text{(B.4)}$$

where M is the thaw (cm) and f_m is the melt factor, based on site conditions. If the air temperature is below the base temperature, no thawing occurs. If thaw occurs, the snowpack depth is updated as $S_P = S_P - M$, and the thaw is set to the new throughfall value for further soil water modeling.

Next, throughfall (either from the canopy throughfall or indirectly through snowmelt) is partitioned into ground water storage and runoff. Slope runoff is first calculated as:

$$R_S = \left(\frac{\theta}{90.0}\right)^2 T \quad \text{(B.5)}$$

where R_S is the amount of runoff due to slope factors (cm), and θ is the slope of the site (in degrees). The water available for groundwater (GW_{avail}, cm) is then calculated as:

$$GW_{avail} = T - R_S \quad \text{(B.6)}$$

Next, the groundwater in the organic soil layer is updated and infiltration into the A layer is calculated:

$$AO_w = \min\left(AO_{w0} + GW_{avail}, AO_{wmax}\right) \quad \text{(B.7)}$$

$$OtoA = \max\left(GWavail - AO_w + AO_{w0}, 0.0\right) \quad \text{(B.8)}$$

where AO_w is the updated organic layer soil moisture storage (cm), AO_{w0} is the current organic layer soil moisture storage (cm), $OtoA$ is groundwater infiltration from the organic into the A layer (cm), and AO_{wmax} is the maximum possible organic later soil moisture, defined as the organic layer carbon content times 0.25 (i.e., $0.25AO_{C0}$). Next, groundwater in the A layer is updated and infiltration into the base layer is calculated:

$$SA_w = \min\left(SA_{w0} + OtoA, SA_{fc}\right) \quad \text{(B.9)}$$

$$AtoB = \max\left(OtoA - SA_w + SA_{w0}, 0.0\right) \quad \text{(B.10)}$$

where SA_w is the updated A layer soil moisture (cm), SA_{w0} is the current organic layer soil moisture (cm), SA_{fc} is the field capacity of the A layer (cm), and $AtoB$ is the groundwater infiltration from the A layer into the B layer (cm). The base soil layer water storage is then updated as:

$$SB_w = \min\left(SB_{w0} + AtoB, SB_{wmax}\right) \quad \text{(B.11)}$$

where SB_w is the updated base soil moisture (cm), SB_{w0} is the current base soil moisture (cm), and SB_{wmax} is the maximum base soil layer moisture (cm), defined as the base soil depth times 0.6 (i.e., $0.6Z_{SB}$). Finally, groundwater runoff is calculated as whatever groundwater is left over after groundwater storage:

$$R_G = \max\left(AtoB - SB_w + SB_{w0}, 0.0\right) \quad \text{(B.12)}$$

where R_G is the groundwater runoff (cm). Total runoff is then calculated as $R = R_S + R_G$. After these calculations have been completed, the canopy water content, organic layer soil moisture, A layer soil moisture, and base layer soil moisture are updated (i.e. $LAI_{w0} = LAI_w$, $AO_{w0} = AO_w$, $SA_{w0} = SA_w$, and $SB_{w0} = SB_w$).

B.1.2 If PET is greater than 0.0

If potential evapotranspiration is greater than 0.0 cm, evapotranspiration is also considered in the simulation. First, canopy interception, throughfall, snow accumulation and snow melt, and slope runoff are calculated as above. The amount of water available for groundwater infiltration after losses to canopy interception, runoff, and potential evapotranspiration is then calculated:

$$GW_{avail} = T - R_s - PET \quad \text{(B.13)}$$

If available groundwater infiltration is greater than 0.0:

If this available soil moisture (GW_{avail}) is greater than 0.0 cm, then the water will be allocated to different soil layers in descending order (soil organic layer, soil A layer, and base soil layer) as above. As there is greater available water than atmospheric demand, actual evapotranspiration (cm) is equal to potential evapotranspiration ($AET = PET$). Groundwater runoff and total runoff are then calculated as above, and the canopy water content and soil water content of all layers are updated as above.

The figure below (Fig. B.1) shows a schematic of the situation just described. Precipitation is received at the canopy level and some of that is lost to interception. Throughfall is calculated as the amount of precipitation left over after losses to canopy interception. Then some of that water is lost to slope runoff and evapotranspiration (as there is more precipitation than PET, AET = PET), and the rest of the water infiltrates into the soil layers. Any water left over is also lost to runoff.

If available groundwater infiltration is below 0.0:

If precipitation has been depleted, or if GW_{avail} is less than or equal to 0.0, evaporatranspiration will extract water from the following layers, in order: the canopy, the organic layer, the A layer, and then the base soil layer. GW_{avail} should be negative in this scenario, and represents the atmospheric demand that needs to be extracted from the soil layer. As such, the atmospheric demand on the soil and canopy (GW_{demand}) is set equal to GW_{avail}. Next, canopy evapotranspiration is calculated as:

$$E_{LAI} = \min\left(-GW_{demand}, \max(LAI_w - LAI_{wmin}, 0.0)\right) \quad \text{(B.14)}$$

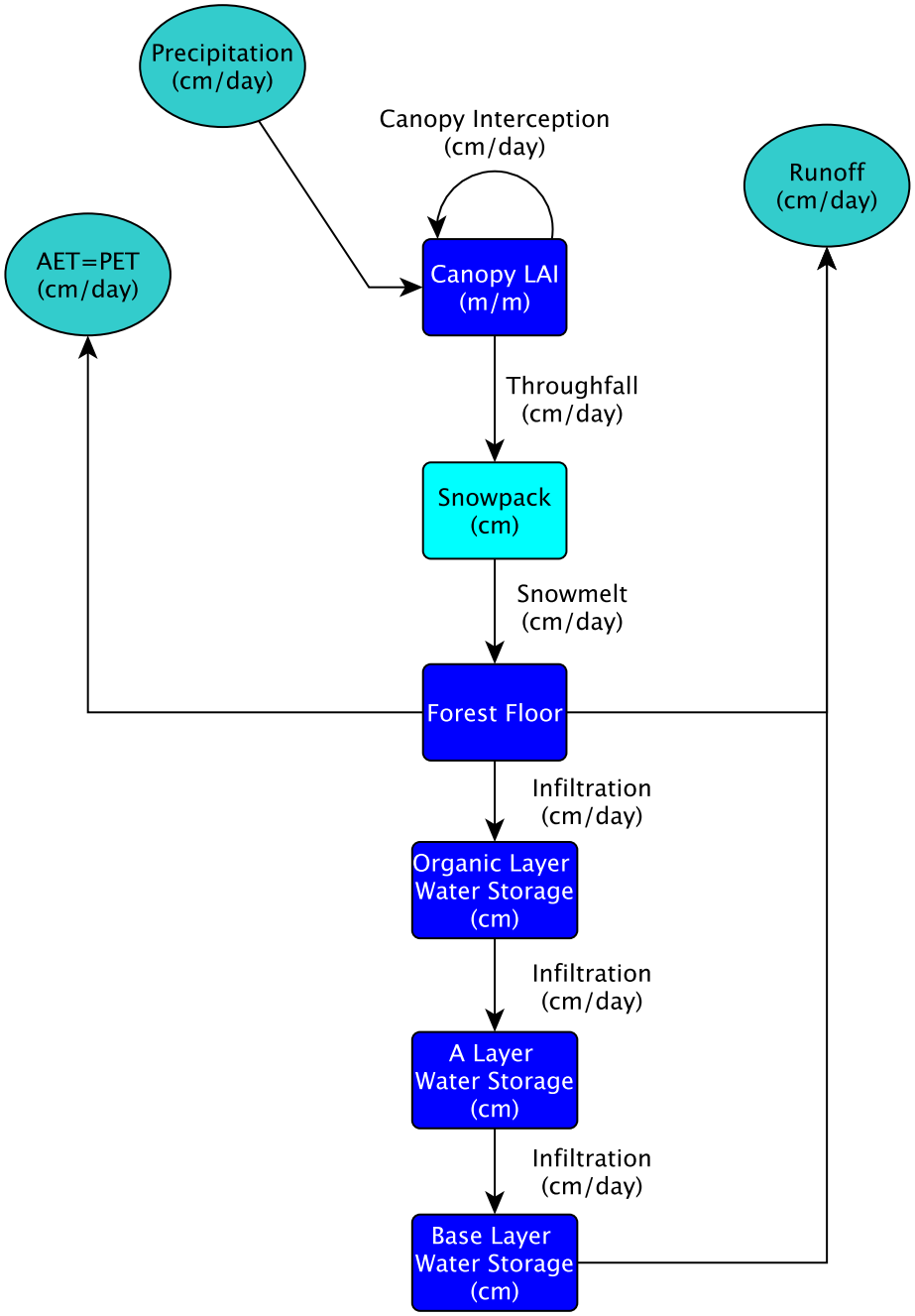

Figure B.1. Schematic of water flow in the soil moisture routine of UVAFME when there is adequate soil moisture and precipitation to meet evaporative demand.

where E_{LAI} is the canopy evapotranspiration (cm day^{-1}), LAI_w is the canopy water content (cm), and LAI_{wmin} is the minimum possible canopy water content, defined as $0.01LAI$. The canopy water content is then reduced:

$$LAI_w = LAI_w - E_{LAI} \quad (B.15)$$

Next, actual evapotranspiration is updated as:

$$AET = AET + E_{LAI} \quad (B.16)$$

The atmospheric demand on the organic layer (AO_{demand}, cm) is then calculated as:

$$AO_{demand} = \min\left(GW_{demand} + E_{LAI}, 0.0\right) \quad (B.17)$$

This water is then extracted from the AO layer and AET is updated:

$$E_{AO} = \min(-AO_{demand}, max(AO_{w0} - AO_{wmin}, 0.0)) \quad (B.18)$$

$$AET = AET + E_{AO} \quad (B.19)$$

where E_{AO} is the evaporation from the organic layer (cm day^{-1}), AO_{w0} is the current organic layer soil moisture (cm), and AO_{wmin} is the minimum possible soil moisture for the organic layer, calculated as the organic layer carbon content times 0.025 (i.e. $0.025AO_{C0}$). The evaporated water is extracted from the organic layer:

$$AO_{w0} = AO_{w0} - E_{AO} \quad (B.20)$$

The atmospheric demand on the A layer (A_{demand}, cm) is then calculated:

$$A_{demand} = \min\left(AO_{demand} + E_{AO}, 0.0\right) \quad (B.21)$$

The amount to be extracted from the soil A layer is then calculated as:

$$E_{SA} = \min\left(-A_{demand}, \max\left(SA_{w0} - SA_{wp}, 0.0\right)\right) \quad (B.22)$$

where E_{SA} is evaporation from the A layer (cm day^{-1}), SA_{w0} is the current A layer soil moisture (cm), and SA_{wp} is the wilting point of the A layer (cm). Actual evapotranspiration is updated again:

$$AET = AET + E_{SA} \quad (B.23)$$

Then the A layer soil moisture is updated:

$$SA_{w0} = SA_{w0} - E_{SA} \quad (B.24)$$

The atmospheric demand on the base layer (B_{demand}, cm) is calculated:

$$B_{demand} = \min\left(A_{demand} + E_{SA}, 0.0\right) \quad \text{(B.25)}$$

The amount of water extracted from the base soil layer is then calculated as:

$$E_{SB} = \min\left(-B_{demand}, \max(SB_{w0} - SB_{wmin}, 0.0)\right) \quad \text{(B.26)}$$

where E_{SB} is the evaporation from the base soil layer (cm day^{-1}), SB_{w0} is the current base soil layer water content (cm), and SB_{wmin} is the minimum possible base soil layer water content (cm), defined as the base soil height times 0.1 (i.e. $0.1Z_{SB}$). Finally, the base layer soil moisture and AET are updated:

$$SB_{w0} = SB_{w0} - E_{SB} \quad \text{(B.27)}$$

$$AET = AET + E_{SB} \quad \text{(B.28)}$$

As there is no left over soil moisture in the soil column for groundwater runoff, total plot runoff is calculated as just runoff due to slope:

$$R = R_s \quad \text{(B.29)}$$

Below is a schematic of the situation described above (Fig. B.2). Precipitation is received at the canopy level and some of that is lost to interception. Throughfall is calculated as the amount of precipitation left over after losses to canopy interception. Then some of that water is lost to slope runoff and evapotranspiration. At this point, PET is greater than the available moisture, and water is extracted from each soil layer until PET is diminished or the soil layers are depleted to their minimum moisture levels or until atmospheric demand is satisfied.

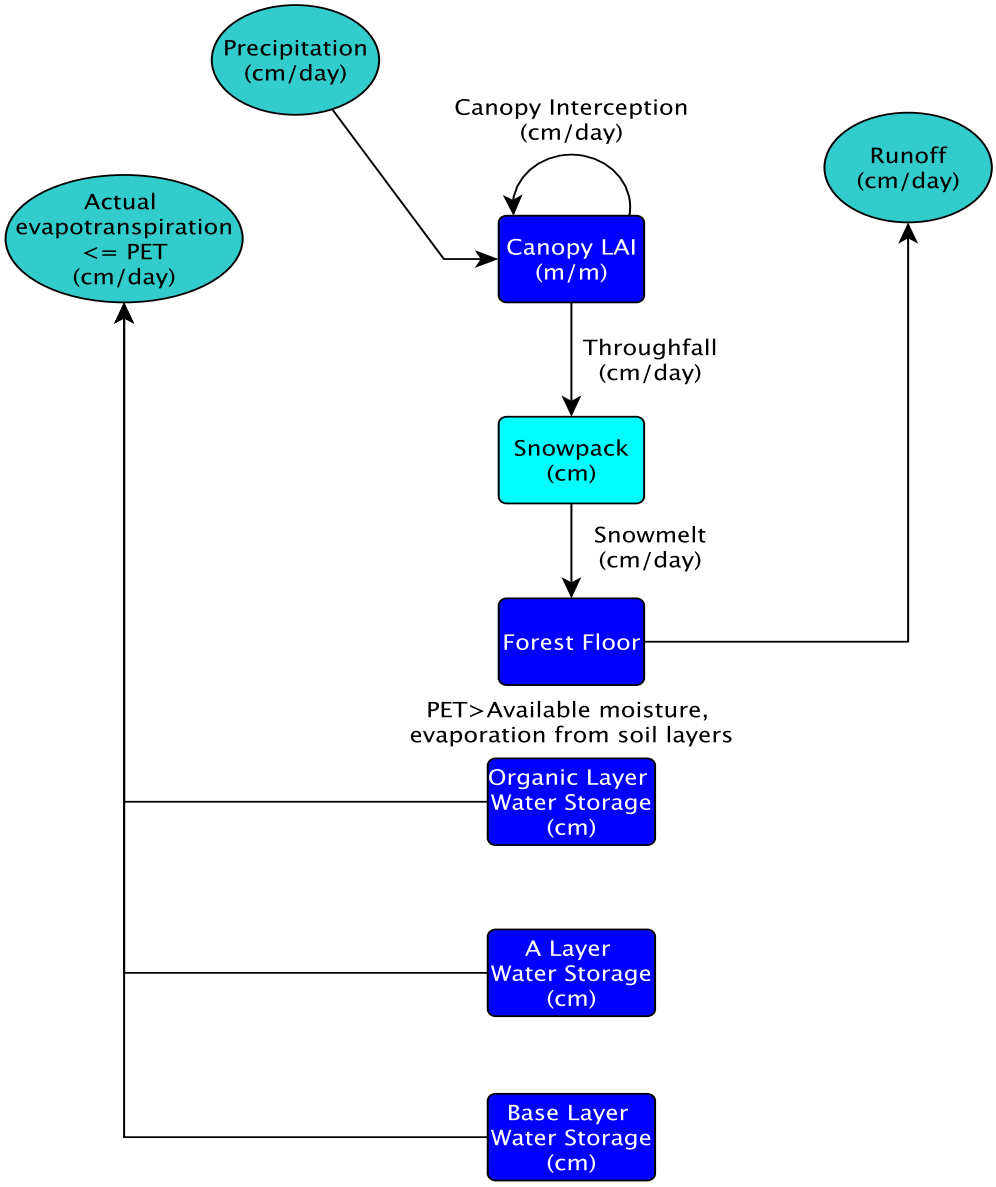

Figure B.2. Schematic of water flow in the soil moisture routine of UVAFME when there is not enough soil moisture or precipitation to meet evaporative demand.

B.2. Soil decomposition

Soil decomposition is also modeled as a three-soil layer model. Inputs for this subroutine are carbon and nitrogen content of the organic and A layers (updated from the Tree Growth and Mortality subroutine), temperature, precipitation, soil moisture (from the Soil Moisture subroutine), and other soil and site input parameters. From this subroutine, plant available nitrogen and carbon in the soil are calculated. Initially, the carbon to nitrogen ratio of the organic layer (AO_{CN}) is calculated:

$$AO_{CN} = \frac{AO_{C0}}{AO_{N0}} \quad \text{(B.30)}$$

where AO_{C0} is the organic layer carbon content (tonnes C ha^{-1}), and AO_{N0} is the organic layer nitrogen content (tonnes N ha^{-1}). Loss of carbon through respiration in the organic layer is calculated as a function of soil moisture, temperature, and current carbon content. First, the effect of soil moisture on organic layer respiration is calculated as:

$$f_{AOw} = \max\left(1.0 - \left(\frac{1.0 - RSWC_{AO}}{0.3}\right)^2, 0.2\right) \quad \text{(B.31)}$$

where $f_{AOw}$is the effect of soil moisture on respiration and $RSWC_{AO}$ is the relative soil water content of the organic layer (cm), defined as:

$$RSWC_{AO} = \min\left(\frac{AO_{w0}}{0.25}, 0.5\right) \quad \text{(B.32)}$$

where AO_{w0} is the organic layer soil moisture (cm). The effect of air temperature on soil respiration is then calculated:

$$f_{t_{AO}} \begin{cases} t_{av_d} \geq -5.0, \; f_{t_{AO}} = 3.0^{0.1\left(t_{av_d} - 1.0\right)} \\ t_{av_d} < -5.0, \; f_{t_{AO}} = 0.0 \end{cases} \quad \text{(B.33)}$$

where $f_{t_{AO}}$ is the effect of air temperature on soil respiration and t_{av_d} is the air temperature (°C). Soil respiration from the organic layer is then calculated:

$$R_{AO} = 5.24E^{-4} f_{Tao} \cdot f_{AOw} \cdot AO_{C0} \quad \text{(B.34)}$$

where R_{AO} is the soil respiration from the organic layer (tonnes C ha^{-1} day^{-1}). The constant 5.24E^{-4} is empirically derived. Next, the amount of nitrogen lost from the organic layer is calculated based on the soil respiration and the C:N ratio of the layer:

$$Nloss_{AO} = \frac{R_{AO}}{AO_{CN}} \quad (B.35)$$

where $Nloss_{AO}$ is the nitrogen loss from the organic layer (tonnes N ha^{-1} day^{-1}). The N content of the organic layer is then updated:

$$AO_{N0} = AO_{N0} - Nloss_{AO} \quad (B.36)$$

Next, the amount of carbon lost due to N immobilization is calculated based on the N loss, and an average C:N ratio for microbes:

$$Closs_{A0N} = 30.0 Nloss_{AON} \quad (B.37)$$

where $Closs_{A0N}$ is the amount of carbon lost to N immobilization. The constant 30.0 is an average C:N ratio of microbial substrate. Finally, the amount of carbon in the organic layer is updated:

$$AO_{C0} = AO_{C0} - Closs_{AON} - R_{AO} \quad (B.38)$$

At this point, the carbon balance for the organic layer is complete, and the subroutine moves on to the A layer. First, the carbon and nitrogen amounts and the C:N ratio of the A layer (SA_{CN}) are calculated:

$$SA_{C0} = SA_{C0} + Closs_{AO} \quad (B.39)$$

$$SA_{N0} = SA_{N0} + Nloss_{AO} \quad (B.40)$$

$$SA_{CN} = \frac{SA_{C0}}{SA_{N0}} \quad (B.41)$$

where SA_{C0} is the carbon content of the A layer (tonnes C ha^{-1}), and SA_{N0} is the nitrogen content of the A layer (tonnes N ha^{-1}). Next, as in the organic layer decomposition simulation, the effect of soil moisture on soil respiration in the A layer is calculated:

$$f_{SAw} = \max\left(1.0 - \left(\frac{1.0 - RSWC_{SA}}{0.8}\right)^2, 0.2\right) \quad \text{(B.42)}$$

where f_{SAw} is the effect of soil moisture on soil respiration in the A layer, and $RSWC_{SA}$ is the relative soil water content of the A layer, defined as:

$$RSWC_{SA} = SA_{w0} SA_{fc} \quad \text{(B.43)}$$

where SA_{w0} is the soil water content of the A layer, and SA_{fc} is the field capacity of the A layer. Next, the effect of air temperature on soil respiration in the A and base layers is calculated:

$$f_t \begin{cases} t_{av_d} \geq -5.0, \; f_t = 2.5^{0.1\left(t_{av_d} - 1.0\right)} \\ t_{av_d} < -5.0, \; f_t = 0.0 \end{cases} \quad \text{(B.44)}$$

where f_t is the effect of air temperature on soil respiration in the A and base soil layers. Soil respiration in the A layer is then calculated:

$$R_{SA} = 1.24E^{-5} f_t \cdot \; f_{SAw} \cdot SA_{CN} \quad \text{(B.45)}$$

where R_{SA} is respiration from the soil A layer (tonnes C ha^{-1} day^{-1}), and the constant 1.24x10^{-5} is an empirically derived constant. Next, the amount of carbon that will go into the B layer is calculated:

$$SB_{Cinput} = R_{SA}/20.0 \quad \text{(B.46)}$$

where SB_{Cinput} is the amount of C from the A layer traveling to the base layer, and the constant 20.0 is the average C:N ratio of the base layer. Next, the amount of nitrogen in the A layer available for plant use is calculated:

$$N_{avail} = \frac{R_A}{SA_{CN} \max\left(0.5, \frac{\left(SA_{CN} - 4.0\right)}{SA_{CN}}\right)} \quad \text{(B.47)}$$

where N_{avail} is the plant available nitrogen in the A layer. Next, C and N values for the A layer are updated:

$$SA_{C0} = SA_{C0} - R_A - SB_{Cinput} \quad \text{(B.48)}$$

$$SA_{N0} = SA_{N0} - N_{avail} \quad \text{(B.49)}$$

At this point, the soil decomposition simulation for the A layer is complete, and the subroutine moves to the final layer, the base layer. First, the amount of carbon in the base layer is updated using the input from the A layer:

$$SB_{C0} = SB_{C0} + SB_{Cinput} \quad \text{(B.50)}$$

where SB_{C0} is the carbon content of the base layer (tonnes C ha^{-1}). Next, respiration from the base layer is calculated:

$$R_{SB} = 2.74E^{-7} \cdot SB_{C0} \cdot f_t \quad \text{(B.51)}$$

where R_{SB} is soil respiration from the base layer (tonnes C ha^{-1} day^{-1}), and 2.74E^{-7} is an empirically derived constant. The carbon content for the base layer is then updated:

$$SB_{C0} = SB_{C0} - R_{SB} \quad \text{(B.52)}$$

Finally, the total soil respiration is calculated as the sum of respiration from all layers:

$$C_{resp} = R_{AO} + R_{SA} + R_{SB} \quad \text{(B.53)}$$

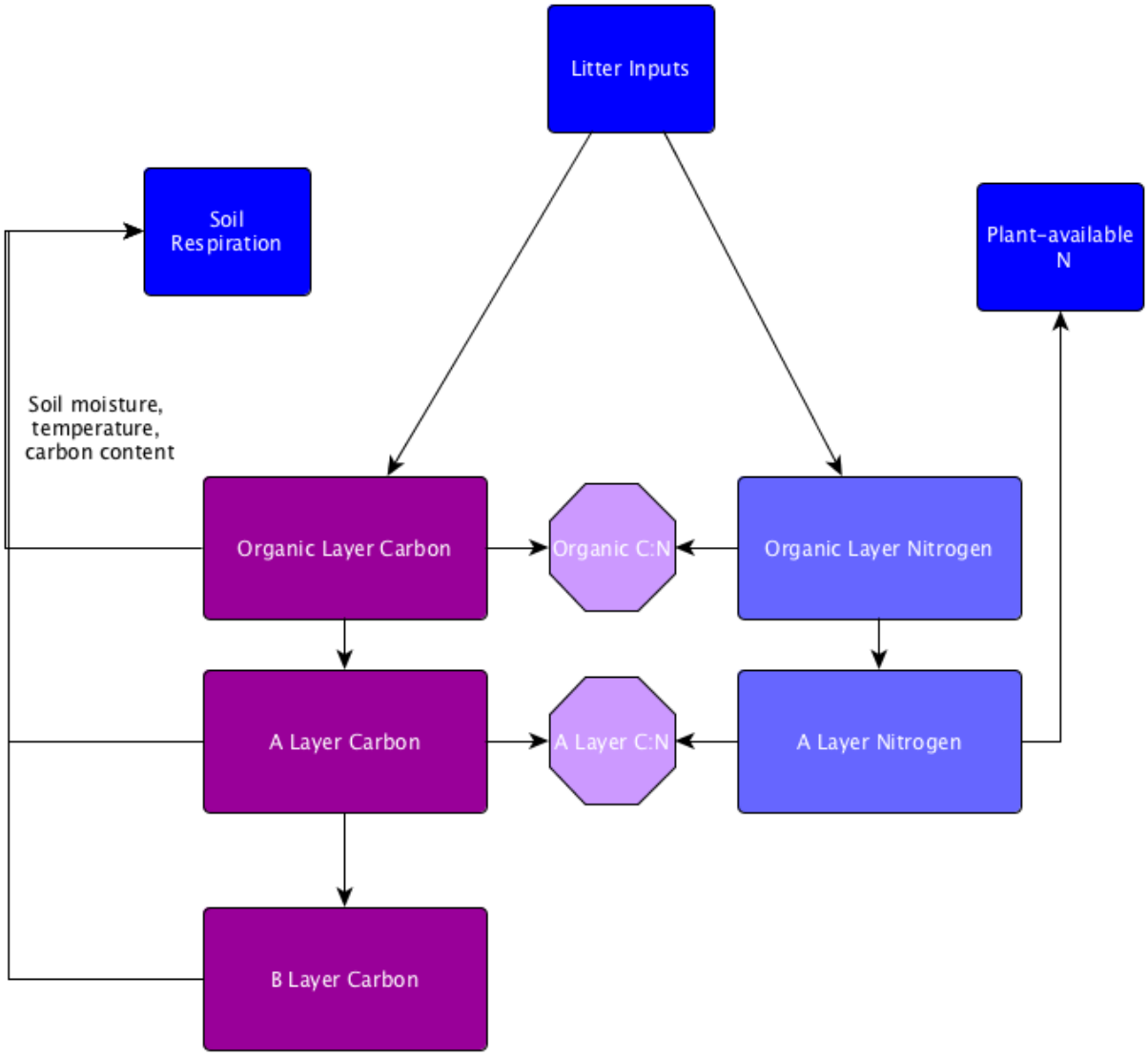

Figure B.3. Schematic of soil nutrient modeling in UVAFME.

C. Tree Canopy Processes

The canopy subroutine is used to calculate light and shading from the canopy, from both deciduous and coniferous trees. If the number of trees on the plot is equal to 0, the model sets the light levels on the plot equal to 1.0: $light_{con} = 1.0$ and $light_{dec} = 1.0$, where $light_{con}$ is an array of light availability at each layer in the canopy for coniferous trees, and $light_{dec}$ is an array of light availability at each layer in the canopy for deciduous trees. If the number of trees on the plot is greater than 0, then the subroutine uses the LAI for each tree on the plot to calculate an overall plot LAI, and then uses this LAI to determine light level at each layer in the canopy. First, the LAI of each tree on the plot is calculated:

$$LAI_{tree} = {D_{bole}}^2 D_L \quad (C.1)$$

where LAI_{tree} is the leaf area index of the individual tree (m m^{-1}), D_{bole} is the diameter of the tree at the bottom of the canopy (i.e. at clear branch bole height) (cm), and D_L is a scalar input parameter of the relationship between leaf area and squared diameter at clear branch bole height of that tree species. Additionally, each tree's LAI is summed to calculate an overall plot LAI:

$$LAI = \sum LAI_{tree} \quad (C.2)$$

Next, the canopy depth (Z_{can}) of each tree is calculated:

$$Z_{can} = \max\left(H_{tree} - H_{bole} + 1, 1\right) \quad (C.3)$$

where Z_{can} is the canopy depth (m), H_{tree} is the total height of the tree (m), and H_{bole} is the clear branch bole height (m). Next, the tree's LAI and the canopy depth are used to calculate the average LAI within a given 1 m layer of the tree's canopy:

$$LAI_{layer} = \frac{LAI_{tree}}{Z_{can}} \quad (C.4)$$

where LAI_{layer} is the LAI in any given 1 m layer of the simulated tree. If the tree in question is coniferous, then for each 1 m layer of the whole plot canopy:

$$LAI_{c1} = LAI_{c1} + LAI_{layer} \quad (C.5)$$

and

$$LAI_{c2} = LAI_{c2} + LAI_{layer} \quad (C.6)$$

where LAI_{c1} and LAI_{c2} are temporary arrays to hold LAI values for each layer in the plot-wide canopy. If the tree is deciduous:

$$LAI_{c1} = LAI_{c1} + LAI_{layer} \quad (C.7)$$

and

$$LAI_{c2} = LAI_{c2} + 0.8LAI_{layer} \quad (C.8)$$

In this way, the LAI for each 1 m layer of each tree is added to overall plot-wide LAI arrays, LAI_{c1} and LAI_{c2}. These two arrays represent overall plot LAI distributed into 1 m sections.

Next, two new arrays (LAI_{c3} and LAI_{c4}) are used to calculate the light level at each layer in the canopy. Initially, the light level at the top of the canopy (i.e. at the maximum height trees in the model are allowed to grow, typically set to 60 m) for each array is set from the previous two arrays:

$$LAI_{c3}(maxH) = LAI_{c1}(maxH) \quad (C.9)$$

and

$$LAI_{c4}(maxH) = LAI_{c2}(maxH) \quad (C.10)$$

Next, the LAI values from the first two arrays are used to calculate cumulative LAI at each layer in the canopy:

$$LAI_{c3}(maxH - ih) = LAI_{c3}(maxH - ih + 1) + LAI_{c1}(maxH - ih) \quad (C.11)$$

and

$$LAI_{c4}(maxH - ih) = LAI_{c4}(maxH - ih + 1) + LAI_{c2}(maxH - ih) \quad (C.12)$$

where ih is the current canopy layer. Using these values, the light availability in each layer of the canopy for both coniferous and deciduous trees ($light_{con}$ and $light_{dec}$, respectively) are calculated using Beer's Law:

$$light_{con}(ih) = e^{\frac{-0.4LAI_{C4}(ih+1)}{plotsize}} \quad (C.13)$$

$$light_{dec}(ih) = e^{\frac{-0.4LAI_{C3}(ih+1)}{plotsize}} \quad (C.14)$$

where $plotsize$ is the user-defined area of each plot (usually set to 500 m^2).

D. Tree Growth

In the tree growth subroutine, the growth of individual trees is calculated based on environmental and allometric factors. For each plot, the model checks to make sure there are trees on the plot. If there are, the model loops through each tree to first calculate the current biomass and height of each tree, and to calculate shading and environmental stressors.

Initially, the variable spp_{avail} is calculated, which represents whether or not a particular species can grow seedlings that year. It is calculated as:

$$spp_{avail} = \max\left(kron(D - D_{max}D_{thresh}), spp_{avail}\right) \quad (D.1)$$

where D is the diameter at breast height of the tree (cm), D_{max} is the average maximum diameter for that species of tree (cm), and D_{thresh} is the minimum annual growth threshold (set to 0.03 cm).

The function $kron(x)$ returns 1.0 if $x > 0.0$ and returns 0.0 otherwise. Thus, if the actual diameter of the tree is less than or equal to the maximum diameter times the growth threshold, the function will return 0.0, otherwise it will return 1.0. In this way, spp_{avail} is either 0 or 1 depending on if that tree is capable of generating seedlings in that plot that year. For example, *Abies lasiocarpa*, or subalpine fir, has a maximum diameter of about 61 cm. In this case, any subalpine fir growing in UVAFME would have to have a diameter at base height

(DBH) greater than 1.83 cm (i.e. 61 cm x 0.03 cm) to be considered "available" for putting out seedlings. Next, the leaf biomass is calculated for each tree as:

$$B_{leafC} = 2.0LAI_{tree} \cdot tree_{LC} \quad (D.2)$$

where B_{leafC} is the leaf biomass of the tree (tonnes C), and $tree_{LC}$ is the average specific leaf area ratio for that species of tree. Next, the maximum diameter increment growth possible for the tree, given optimum environmental conditions is calculated. This is based on allometric equations relating the height and DBH of the tree, calculated using species-specific parameters as well as the current DBH of the tree. It is calculated as follows:

$$D_{opt} = \frac{gD\left(1.0-\frac{D \cdot H_{tree}}{D_{max}H_{max}}\right)}{2.0H_{tree}+s \cdot e^{\frac{-sD}{H_{max}-H_{std}} \cdot D}} \quad (D.3)$$

where D_{opt} is the maximum diameter increment growth possible for that tree, given optimum environmental conditions (cm), g is a species-specific tree growth scalar parameter, D is the current diameter of the tree (cm), H_{tree} is the current height of the tree (m), D_{max} is the average maximum diameter of that tree species, H_{max} is the average maximum height of that tree species, s is the initial height-diameter relationship of that tree species, and H_{std} is the standard height measurement for most tree characteristics (set to 1.3 m in the model).

Next, the shading effects on each tree are calculated. The model uses the available light calculated in the Canopy Processes section (see Section C) and species-specific tolerances to shade to calculate the effect of shading on each tree. If the tree is a conifer, the effect of shading on that tree is calculated as:

$$f_{light} = l_a(1.0 - e^{-l_b(light_{con}-l_c)}) \quad (D.4)$$

where f_{light} is the effect of shading on tree diameter growth, $light_{con}$ is the light available for conifers at the specific tree's height, and l_a, l_b, and l_c are response factors based on species-specific tolerances to shading. If the tree is deciduous, f_{light} is calculated as:

$$f_{light} = l_a(1.0 - e^{-l_b(light_{dec} - l_c)}) \quad (D.5)$$

where $light_{dec}$ is the light available for deciduous trees at the specific tree's height. The shading at the bottom of the canopy is also calculated to determine the effect of shading on the lower branches of the tree. This will later be used to determine if thinning of lower branches will occur. The shade at the bottom of the canopy (f_{can}) is calculated using the same equations as the above two equations, except the $light_{dec}$ and $light_{con}$values are the light level at the clear branch bole height of the tree (i.e. H_{bole}, or height at the bottom of the canopy). Figure D.1 shows the light response of different shade tolerance levels, with 1 being the most shade tolerant, and 5 being the least shade tolerant.

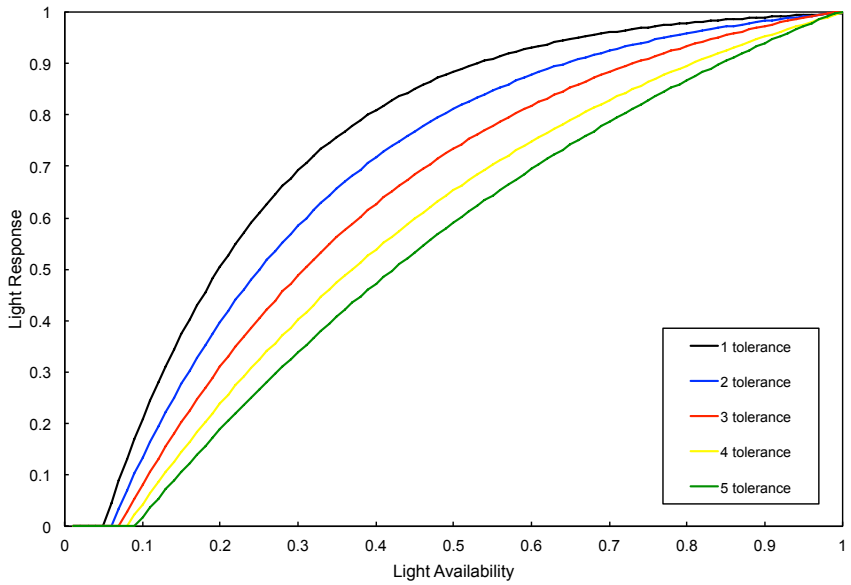

Figure D.1. Tree growth response to light availability for different tolerance levels of trees. A light tolerance of 1 is the most shade tolerant, and a light tolerance of 5 is the least shade tolerant. The light response is used to calculate actual DBH increment growth for the year for each tree.

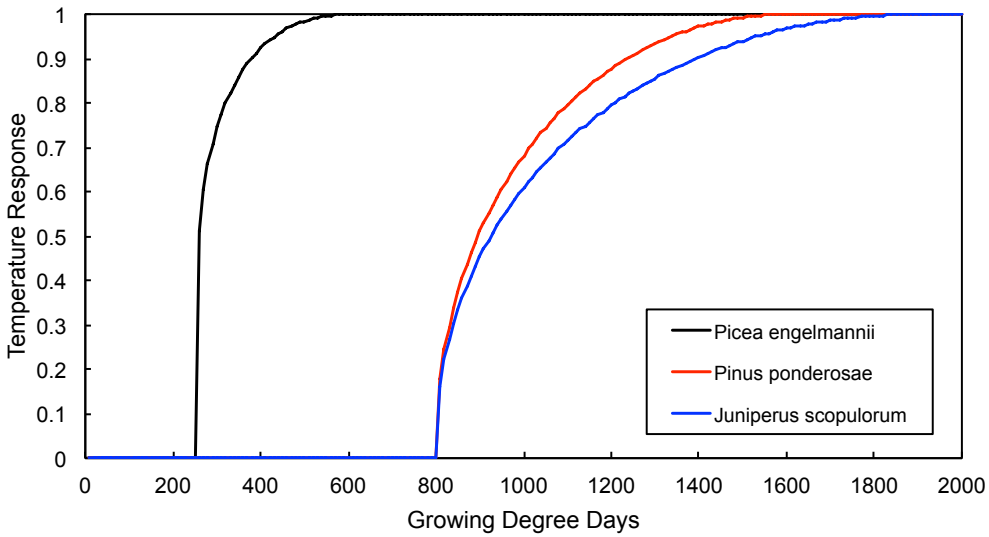

Figure D.2. Tree growth response to growing degree days (proxy for temperature) for three different Rocky Mountain species. *Picea engelmannii* (Engelmann spruce) is a subalpine species, capable of tolerating very low temperatures (DD_{min} = 250, DD_{opt}=600, and DD_{max}=1665). *Pinus ponderosa* is a montane species, existing in the middle elevations of the Rocky Mountains (DD_{min}=800, DD_{opt}=1600, and DD_{max}=2500). *Juniperus scopulorum* is a low-elevation species, capable of tolerating fairly high temperatures (DD_{min}=800, DD_{opt}=1900, and DD_{max}=3200).

Next, other environmental effects on diameter increment growth are calculated. The effect of temperature on growth is calculated using the cumulative number of growing degree days (GDD) in the year. The GDD for the year is defined as the cumulative sum of average daily temperatures above 5°C for the year. The effect of growing degree days on tree growth (f_{temp}) is calculated as:

$$f_{temp} = \left(\frac{GDD - DD_{min}}{DD_{opt} - DD_{min}}\right)^{\frac{DD_{opt} - DD_{min}}{DD_{max} - DD_{min}}} \cdot \left(\frac{DD_{max} - GDD}{DD_{max} - DD_{opt}}\right)^{\frac{DD_{max} - DD_{opt}}{DD_{max} - DD_{min}}} \quad (D.6)$$

where GDD is the growing degree days for the year, DD_{min} is the minimum growing degree days for the tree species, DD_{opt} is the optimum growing degree days for the species, and DD_{max} is the maximum growing degree days for the species. In this function, f_{temp} is equal to 1.0 if $GDD \geq DD_{opt}$, and f_{temp} is 0.0 if $GDD \leq DD_{min}$. Otherwise, the equation above is used to

calculate f_{temp}. Figure D.2 shows the temperature response for three species in the Rocky Mountains.

The effect of drought on tree growth is calculated using the number of "upper dry days" and "base dry days" in the year. The upper dry days are defined as the proportion of growing season days (i.e. days with an average temperature above 5°C) that have a relative A layer soil water and a relative B layer soil water content less than a maximum dry parameter (γ), set to 1.0 in the model. The relative water contents checked against γ are as follows:

$$SA_{RFC} = \frac{SA_{w0}}{SA_{FC}} \quad (D.7)$$

$$SB_{Rmax} = \frac{SB_{w0}}{SB_{wmax}} \quad (D.8)$$

$$SB_{Rmin} = \frac{SB_{w0}}{SB_{wmin}} \quad (D.9)$$

The base dry days for the year are defined as the proportion of growing season days (i.e. days with an average temperature above 5°C) that have a relative A layer water content (relative to the wilting point) less than the maximum dry parameter (γ). This relative water content is calculated as:

$$SA_{Rwp} = \frac{SA_{w0}}{SA_{wp}} \quad (D.10)$$

Once the upper and base dry days for the year are calculated, these, along with species-level drought tolerances, are used to calculate each tree's response to drought for the year:

$$f_{drought} = \sqrt{\frac{\max(dry - drydays, 0.0)}{dry}} \quad (D.11)$$

where $f_{drought}$ is the tree's response to drought, dry is a species-specific parameter based on drought tolerance (ranging from 0.5, most tolerant, to 0.05, least tolerant), and $drydays$ is the

proportion of upper dry days that year. If the tree in question has a drought tolerance of 1 (most tolerant to drought) and it is a conifer, $f_{drought}$ is calculated as:

$$f_{drought} = \max\left(0.33\sqrt{\frac{\max(dry - drydays_{base})}{dry}}, \sqrt{\frac{max(dry - drydays, 0.0)}{dry}}\right) \quad (D.12)$$

where $drydays_{base}$ is the proportion of base dry days that year. If the tree in question has a drought tolerance of 1 and it is deciduous, $f_{drought}$ is calculated as:

$$f_{drought} = \max\left(0.2\sqrt{\frac{\max(dry - drydays_{base})}{dry}}, \sqrt{\frac{max(dry - drydays, 0.0)}{dry}}\right) \quad (D.13)$$

Otherwise, it is calculated using the first drought response equation. Figure D.3 shows the drought response of the 6 different drought tolerances.

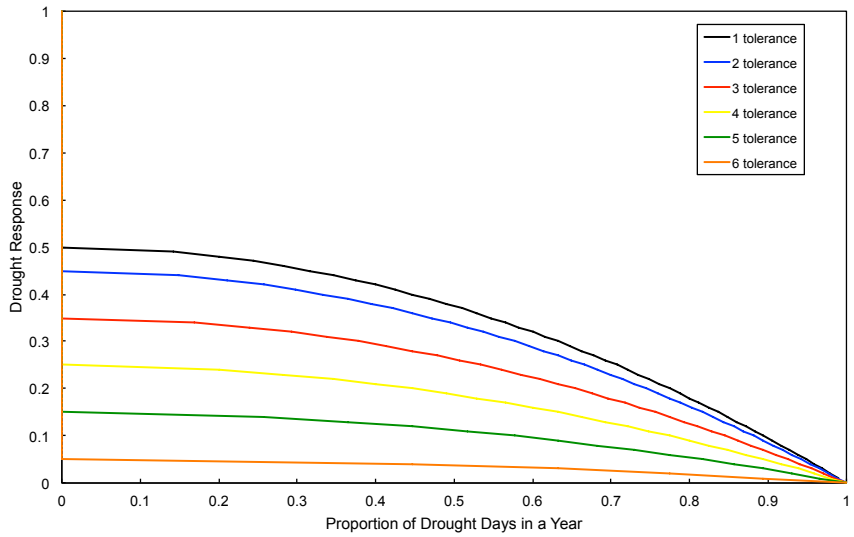

Figure D.3. Tree growth response to drought for the 6 different tolerance levels in the model, 1 being the most drought tolerant, and 6 being the least.

After these three environmental effects are calculated, the overall effect of environmental stressors so far is calculated. UVAFME uses Liebig's Law of the Minimum to calculate

cumulative environmental stress. The tree is only limited by the most limiting environmental factor. Thus, the environmental stress so far is calculated as:

$$f_{env} = \min\left(f_{light}, f_{temp}, f_{drought}\right) \quad \text{(D.14)}$$

where f_{env} is the growth response of the most limiting environmental factor. The model then calculates an intermediate DBH (D', cm) of the tree using the optimum DBH modified by f_{env}:

$$D' = D + D_{opt} f_{env} \quad \text{(D.15)}$$

The model then updates what the height of the tree would be given this calculated diameter using allometric equations relating DBH and height:

$$H'_{tree} = H_{std} + (H_{max} - H_{std})\left(1.0 - \mathrm{e}^{\left(-\frac{sD'}{H_{max} - H_{std}}\right)}\right) \quad \text{(D.16)}$$

Figure D.4 shows DBH-height relationship for four different Rocky Mountain species, each with different maximum heights, maximum diameters, and DBH-height relationships.

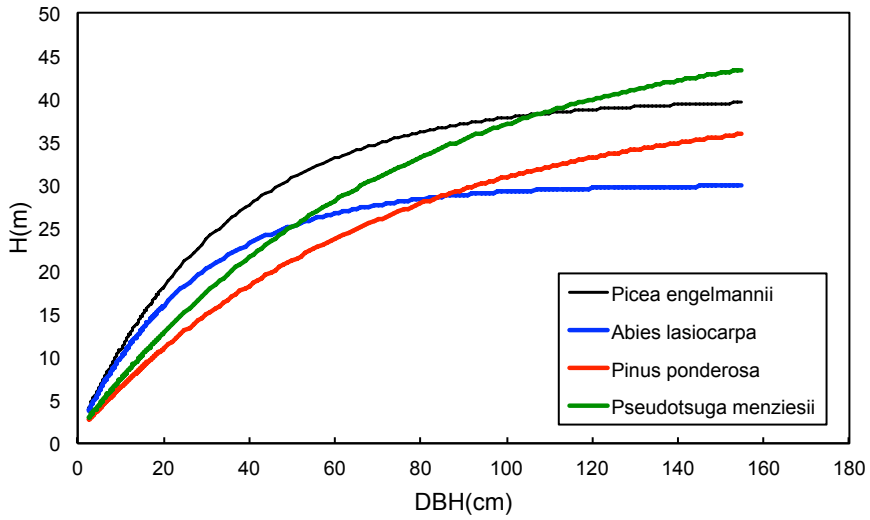

Figure D.4. Height:DBH relationships for four different Rocky Mountain species.

Next, an intermediate value for the diameter at the bottom of the tree's canopy, D'_{bole}, is calculated given these intermediate values. If the total updated height of the tree (H'_{tree}) is less

than last year's value of the height of the bottom of the canopy (H_{bole}) or if $H'_{tree}$is less than 1.3 m, then the diameter at clear bole height is equal to the tree's current DBH:

$$D'_{bole} = D' \quad \text{(D.17)}$$

Otherwise, D'$_{bole}$ is updated as:

$$D'_{bole} = \frac{H'_{tree} - H_{bole}}{H'_{tree} - 1.3}^{D'} \quad \text{(D.18)}$$

Next, the new leaf biomass for each tree is calculated (B'_{leafC}) as in Equation D.2 using the new height and DBH. Using this information, the nitrogen requirement for the plot is calculated. This N requirement is used to calculate the effect of N stress on tree growth for the year. If the tree in question is a conifer, N_{req} for the plot is updated as:

$$N_{req} = N_{req} + (B'_{leafC} - B_{leafC})/leaf_{CNcon} \quad \text{(D.19)}$$

where $leaf_{CNcon}$ is the conifer C:N ratio, set to 60.0 in the model. If the tree is deciduous, N_{req} is updated as:

$$N_{req} = N_{req} + (B'_{leafC})/leaf_{CNdec} \quad \text{(D.20)}$$

where $leaf_{CNdec}$ is the deciduous C:N ratio, set to 40.0 in the model. In this way, the total N requirement for the plot is updated to include nitrogen required for the leaves added on by conifers that year and for the leaves made by deciduous trees that year. Next, the total biomass for carbon is updated for each tree. This is calculated as a sum of stem, twig, and root biomass. Stem biomass is calculated as:

$$B'_{stemC} = \frac{C\rho_{bulk}\beta}{\beta+2.0} \times D'^2 H'_{tree} 0.9 \quad \text{(D.21)}$$

where B'_{stemC} is an intermediate value for stem biomass (tonnes C), C is a carbon parameter, set to 3.92699x10^{-5} in the model, ρ_{bulk} is the average bulk density of the tree species, and β is a parameter, set to 1.0 in the model. The twig biomass (B'_{twigC}, tonnes C) is calculated as:

$$B'_{twigC} = C\rho_{bulk}\left(\frac{2.0}{\beta+2.0} - 0.33\right) {D'_{bole}}^2 (H'_{tree} - H'_{can}) \quad (D.22)$$

The root biomass (B'_{rootC}, tonnes C) is calculated as:

$$B'_{rootC} = B'_{stemC}\frac{r_{depth}}{H'_{tree}} + \frac{B'_{twigC}}{2.0} \quad (D.23)$$

where r_{depth} is the tree's root depth, set to 0.8 m in the model. The total biomass (B'_{treeC}, tonnes C) is then updated as:

$$B'_{treeC} = B'_{stemC} + B'_{twigC} + B'_{rootC} \quad (D.24)$$

After the new biomass has been calculated, the N biomass for each tree is updated as:

$$B'_{treeN} = B'_{treeC}/stem_{CN} \quad (D.25)$$

where B'_{treeN} is the N biomass of the tree, and $stem_{CN}$ is the stem C:N ratio, set to 450.0 in the model. The N requirement for the plot is then updated as:

$$N_{req} = N_{req} + (B_{treeC0} - B'_{treeC})/stem_{CN} \quad (D.26)$$

where B_{treeC0} is the previous year's tree biomass, and B'_{treeC} is the updated biomass using the new DBH. In this way, N_{req} is the total nitrogen required to grow each tree the amount calculated based on the DBH calculated above. The N requirement is then converted to tonnes ha^{-1} and divided by the available nitrogen to get a relative N available for plant growth (N_R):

$$N_{req} = \max\left(\frac{1000N_{req}}{plotsize}, 0.0\right) \quad (D.27)$$

$$N_R = N_{avail}/N_{req} \quad (D.28)$$

Using this relative available nitrogen, the effect of nitrogen availability on tree growth is calculated using species-specific parameters based on nutrient tolerance:

$$f_{poor} = fert_1 + fert_2 N_R + fert_3 {N_R}^2 \quad (D.29)$$

where f_{poor} is a factor based on nitrogen availability, $fert_1$, $fert_2$, and $fert_3$ are values based on species-specific nutrient tolerance. If f_{poor} is calculated to be greater than 1.0, it is set to 1.0.

Likewise, if it is calculated to be less than 0.0, it is set to 0.0. The effect of nutrient availability on tree growth ($f_{nutrient}$) is then calculated as:

$$f_{nutrient} = f_{poor} N_R \quad \text{(D.30)}$$

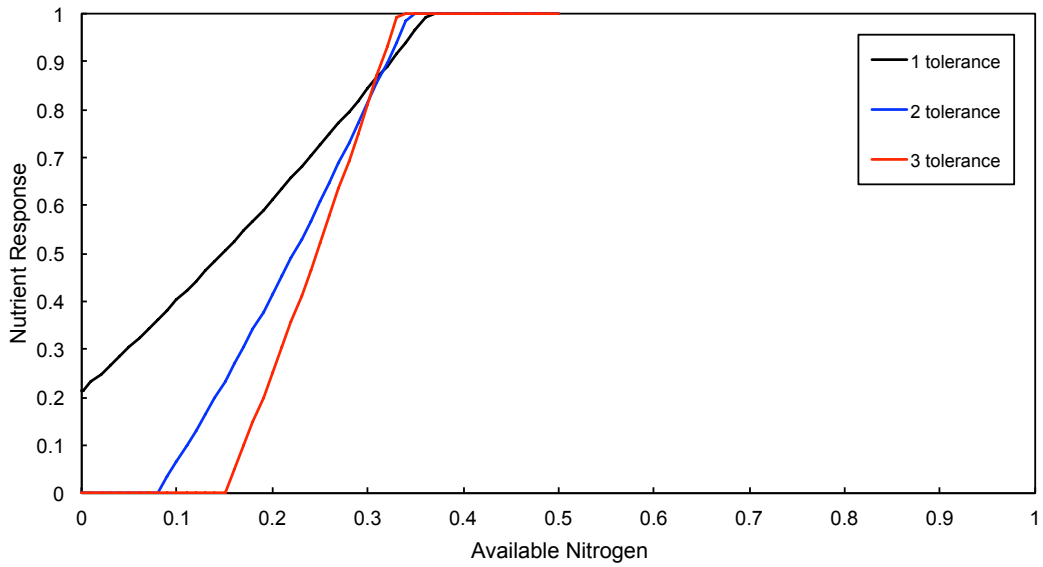

Fig. D.5. Tree growth response to drought for the 3 different tolerance levels in the model, 1 being the most drought tolerant, and 3 being the least.

Figure D.5 shows this nutrient effect for the three different nutrient tolerances. This is used to calculate the actual DBH increment growth for the year. Again, the Law of the Minimum is used the actual DBH growth based on the optimum possible DBH growth, modified by the most limiting factor:

$$D_{incr} = D_{opt}(\min(f_{nutrient}, f_{env})) \quad \text{(D.31)}$$

where D_{incr} is the actual DBH increment growth for the year. Next, the DBH for the tree is updated using last year's value and the actual increment growth:

$$D = D + D_{incr} \quad \text{(D.32)}$$

Using the increment value, a growth check is made to determine if the tree had enough growth that year to survive stress-related death. Two checks are made, one to see if the increment growth for that year is greater than an allometrically-derived growth check, and one to see if the most limiting environmental factor's effect is greater than another growth check. The allometrically-derived growth check is calculated as:

$$C_A = \min\left(\frac{D_{max}}{AGE_{max}0.1}, D_{thresh}\right) \quad \text{(D.33)}$$

where C_A is the growth check, AGE_{max} is that species' average maximum age (yrs) and D_{thresh} is a growth threshold, set to 0.03 cm in the model. The model checks to see if (1) D_{incr} is less than C_A or if (2) the effect of the most limiting environmental factor (i.e. min $(f_{nutrient}, f_{env})$) is less than D_{thresh}. If this is true, and the tree is a conifer, the tree's mortality counter is increased by one. Once this mortality counter reaches 3 (i.e. two consecutive years of low increment growth and/or high stress), the tree's mortality marker is set to true. This mortality marker is used later in the model to determine if the tree dies from stress-related causes. If the tree is a deciduous tree, it can only have one year of low growth, and as such as soon as it does not pass both growth checks, its mortality marker is set to true. If the tree passes both growth checks, the mortality counter is set to 0 and the mortality marker is set to false.

After these checks are made, the actual tree height (H_{tree}), diameter at clear branch bole height (D_{bole}), leaf biomass (B_{leafC}), total carbon and nitrogen biomass (B_{treeC}, B_{treeN}) are calculated using the equations described previously. The change in biomass for each tree from last year's run to this year's (ΔB_{treeC}) is then calculated:

$$\Delta B_{treeC} = B_{treeC} - B_{treeC0} \quad \text{(D.34)}$$

where B_{treeC0} is last year's tree biomass (not including leaves). Using this value, the total net primary production (NPP) for the plot is updated:

$$NPP = NPP + \Delta B_{treeC} \quad (D.35)$$

in this way, the model adds up each tree's change in biomass to calculate a plot-wide NPP value. The nitrogen used on the plot (N_{used}) is also calculated in a similar fashion:

$$N_{used} = N_{used} + \Delta B_{treeC}/stem_{CN} \quad (D.36)$$

Next, leaves are added to the NPP and N_{used}. If the tree is a conifer, the leaf primary production (PP, tonnes C) is calculated as the amount of added leaf biomass for that year:

$$PP = b_l B_{leafC} - B_{leafC0} \quad (D.37)$$

where B_{leafC0} is last year's leaf biomass, and b_l is equal to 1.0 plus the conifer leaf ratio (set to 0.3 in the model). The NPP and N_{used} for the plot are then updated as:

$$NPP = NPP + PP \quad (D.38)$$

$$N_{used} = N_{used} + \frac{PP}{leaf_{CNcon}} \quad (D.39)$$

where $leaf_{CNcon}$ is the conifer leaf C:N ratio, set to 60.0 in the model. The total biomass (B_C, tonnes C) for the plot is then updated as:

$$B_C = B_C + B_{treeC} + B_{leafC} \quad (D.40)$$

In this way, the total biomass for the plot is calculated as a sum of each tree's total biomass. The total nitrogen (B_N, tonnes N) is also calculated in a similar way:

$$B_N = B_N + B_{treeN} + B_{leafC}/leaf_{CNcon} \quad (D.41)$$

If the tree is deciduous, the NPP and N_{used} are updated as:

$$NPP = NPP + B_{leafC} \quad (D.42)$$

$$N_{used} = N_{used} + B_{leafC}/leaf_{CNdec} \quad (D.43)$$

Here, the model adds the total amount of leaf biomass (rather than just the change) because as a deciduous tree, it has grown back all of its leaves that year. The total plot carbon and nitrogen are then updated as:

$$B_C = B_C + B_{treeC} \quad (D.44)$$

$$B_N = B_N + B_{treeN} \quad (D.45)$$

In this case, the model does not add leaf carbon and leaf nitrogen for deciduous trees to the total plot biomass values.

After the individual tree and plot-level biomass values have been calculated, the model updates the height of the bottom of the canopy (clear branch bole height) for each tree. Here, the model checks to see if the environmental stressors are high enough to cause thinning of the lower canopy branches. This is done by checking to see if the effect of the most limiting factor (either from temperature, drought, shading, or nutrient availability) is less than the growth threshold. This check value is calculated as:

$$C_C = \min\left(f_{temp}, f_{drought}, f_{canshade}, f_{nutrient}\right) \quad (D.46)$$

where C_C is the growth check for canopy thinning, and $f_{canshade}$ is the effect of shading at the bottom of the canopy, calculated in the same manner as is f_{light} (Eq. D.4, D.5) but using the light at height of the bottom of the canopy, rather than at the height of the top of the tree. If C_C is less than or equal to D_{thresh} (set to 0.03 in the model), then the branches at the bottom of the canopy are thinned, and the clear bole height increases by 1:

$$H_{bole} = H_{bole} + 1.0 \quad (D.47)$$

If this new clear branch bole height is less than the total tree height (H_{tree}), H_{bole} is incremented by another 0.1 m. Otherwise, no change is made to the tree's clear branch bole

height. If this change is made, the diameter at the height of the canopy (D_{bole}) is updated using the equation previously described (Eq. D.18), and the carbon and nitrogen values for the tree are updated (B_{treeC} and B_{treeN}, Eq. D.24, D.25). These new biomass values are then used to calculate how much thinning occurred:

$$L_{BC} = B_{treeC1} - B_{treeC} \quad (D.48)$$

where L_{BC} is the amount of stem litterfall (tonnes C), and B_{treeC1} is the biomass of the tree before thinning. This litterfall is added to the soil carbon and nitrogen pools:

$$AO_{Cinto} = AO_{Cinto} + L_{BC} \quad (D.49)$$

$$AO_{Ninto} = AO_{Ninto} + L_{BC}/stem_{CN} \quad (D.50)$$

where AO_{Cinto} and AO_{Ninto} are the carbon and nitrogen pools that will be added to the overall C and N pools for the organic layer. Next, the leaf biomass is updated for the new clear branch bole height and the amount of leaf litter from thinning (L_{BL}) is calculated:

$$L_{BL} = B_{leafC1} - B_{leafC} \quad (D.51)$$

where B_{leafC1} is the leaf biomass before thinning. Next, this leaf litter is added to the organic layer input pools. If the tree is a conifer:

$$AO_{Cinto} = AO_{Cinto} + L_{BL}b_l \quad (D.52)$$

$$AO_{Ninto} = AO_{Ninto} + L_{BL}/leaf_{CNcon}b_l \quad (D.53)$$

And if the tree is deciduous:

$$AO_{Cinto} = AO_{Cinto} + L_{BL} \quad (D.54)$$

$$AO_{Ninto} = AO_{Ninto} + L_{BL}/leaf_{CNdec} \quad (D.55)$$

After these calculations are made, the Growth subroutine is complete and the model moves on to the Mortality subroutine.

E. Tree Mortality

Mortality of individual trees can occur through several different pathways Trees may die because of age or growth-related stressors, or through disturbances. Currently, UVAFME has the ability to implement probabilistic fire and wind disturbance. The probability of tree death occurring through any one of these methods is determined by species input parameters such as stress tolerance, maximum age and probability of reaching that age, and fire tolerance, as well as disturbance probabilities and characteristics.

In the Mortality subroutine, the model first checks to determine if fire or wind disturbance occurs that year. This is based on uniform random numbers (between 0.0 and 1.0) for fire and wind probability checked against site-specific fire and wind return intervals (i.e. the number of fires or windthrow events in 1000 years). If the fire probability for that year (f_{prob}) is less than the site-wide probability for fire or if the wind probability for that year (w_{prob}) is less than the site-wide probability for wind, the model enters into the disturbance section of the Mortality subroutine, otherwise it moves on to check for age- and growth-related stressors alone.

E.1. Disturbances

If the number of trees on the plot is greater than 0, then these trees are set to be hit by disturbance. If f_{prob} is less than the site-wide return interval for fire, then fire occurs on that plot that year.

E.1.1. Fire

The model first generates an intensity value for this fire. This is generated using a normally distributed random number between 0.0 and 12.0, with a site-specific mean. This mean fire intensity (f_{int}) corresponds to the site-wide average fire intensity, with 0.0 to 4.0 being low-

level, brush fires, 5.0 to 8.0 being mid-level fires, and 9.0 to 12.0 being high-level, crown fires. Depending on the mean fire intensity, the distribution of possible fire intensities generated by the model can be shifted to be mostly low level, mostly high level, or mostly mid level. The normally distributed random number generated with the mean fire intensity value represents the fire category for that year's fire.

Once the fire category for that year's fire is generated (f_{cat}), the model checks to see if the fire intensity is high enough to cause wholescale tree death. If f_{cat} is greater than or equal to 11.0, there is a five-year wait before seedlings can regenerate. As such, when f_{cat} is greater than or equal to 11.0, the variable f_{count} is set to 5. Otherwise, f_{count} is remains at 0.

Next, the model determines the effect the fire will have on each tree. In UVAFME fire affects both individual tree survival and the seedling bank for each species. The effect of fire on each species seedling bank (f_{fire}) depends exclusively on species-specific fire regeneration tolerances (1-6; 1 being the most tolerant, and 6 being the least tolerant). The variable f_{fire} ranges from 100.0 to 0.001, depending on the species' tolerance to fire. Figure E.1 shows how f_{fire} changes with respect to fire tolerance. The seedling bank for each species is then updated as:

$$Sl_{bank} = 10.0s_i + s_p \cdot spp_{avail} \cdot f_{fire} \quad \text{(E.1)}$$

where Sl_{bank} is that species' seedling bank, s_i is an input parameter that represents the probability of being a seed invader from outside the plot (the highest value, 1, would be for wind-dispersed seeds), and s_p is a parameter representing whether or not that species is capable of sprouting from stumps (1: yes, 0: no).

After the fire response to the seedling bank is calculated, the model determines which trees will be killed by fire. This is based on the species- and tree size-specific fire tolerance as

well as the fire intensity (f_{cat}). All trees less than 12.7 cm in DBH are killed by fire. Trees that are larger than 12.7 cm DBH may be killed by fire based on their species-specific bark thickness coefficient (b_{thick}, cm bark cm DBH^{-1}). First, the crown scorch height (SH, m) is determined based on fire intensity and wind speed.

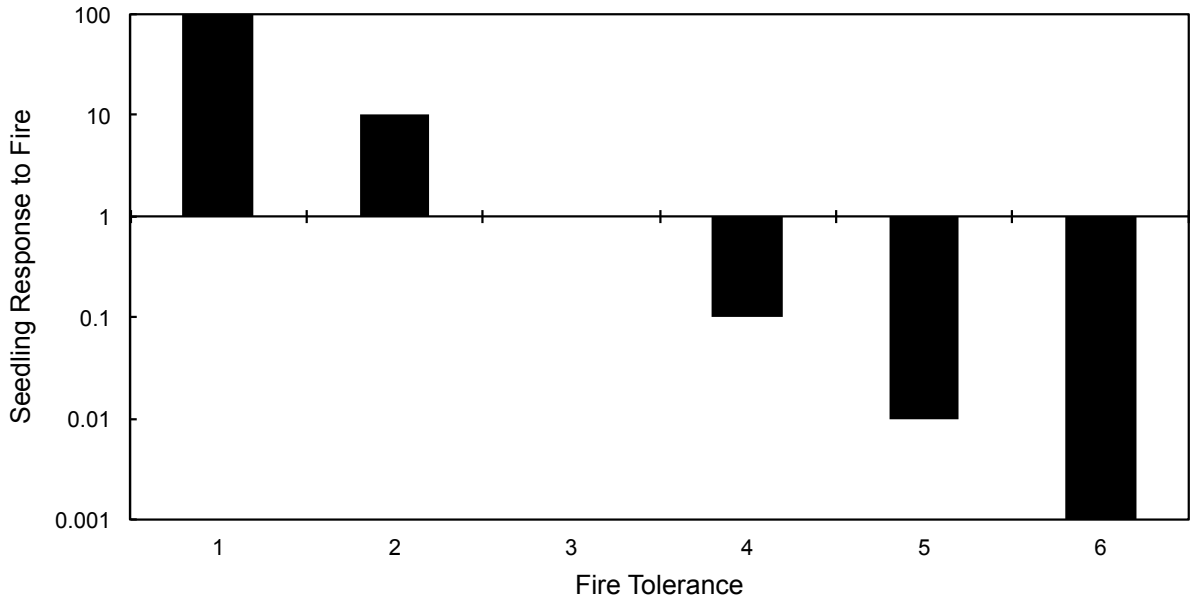

Figure E.1. Seedling bank response to fire for the 6 different fire tolerances. A fire tolerance of 1 corresponds to a high tolerance to fire, and a fire tolerance of 6 corresponds to a low tolerance to fire. In this case, species with a fire tolerance above 3 will benefit from a fire, species with a tolerance below 3 will be hindered by fire, and species with a fire tolerance of 3 will not be affect by fire in terms of their seedling bank size.

$$SH = \frac{a \cdot FI^{1.1667}}{(T_{kill} - T_{amb})[b \cdot FI + c \cdot U^3]^{0.5}} \quad (E.2)$$

where a, b, and c are empirical parameters equal to 0.74183 m °C^{-1}, 0.025574 (kW m^{-1})$^{4/3}$, and 0.021433 km^{-1} hr (kW m^{-1})$^{7/9}$, respectively, T_{kill} is the lethal temperature for tree foliage (set to 60 °C in this model), T_{amb} is the ambient air temperature of a fire (set to 20°C), FI is the fire intensity (kW m^{-1}), set to $1000 f_{cat}$, U is the wind speed (km hr^{-1}), generated as a random value between 0 and 32 km hr^{-1}. This value for wind speed is based on a default wind speed of 32 km

hr^{-1} from Reinhardt & Crookston (2003). The length each tree crown that is scorched (CS, m) is then calculated as:

$$CS = SH - (H_{tree} - Z_{bole}) \quad (E.3)$$

where H_{tree} is the tree height (m), and Z_{bole} is the crown depth (m). Next, the percent of scorched crown volume (CK, %) is calculated for each tree.

$$CK = 100\frac{CS(2CL-CS)}{CL^2} \quad (E.4)$$

Finally, the probability of fire mortality (p_{fire}) is calculated for each tree based on the species-specific bark thickness parameter, DBH, and percent scorched crown volume.

$$p_{fire} = \frac{1}{1+e^{[-1.941+6.32(1-e^{-b_{thick}DBH})-0.00053CK^2]}} \quad (E.5)$$

The equations for scorch height and percent crown volume scorched are based on the fire module from Fire BGCv2 RMRS-GTR-55 (Kean *et al.* 2011) and from Van Wagner (1973). Probability of fire mortality is based on the mortality equation from Ryan & Reinhardt (1988). The parameters a, b, and c, and the values for T_{kill} and T_{amb} are based on Keane *et al.* (2011). Finally, the species-specific bark thickness values are also based on values published by Keane *et al.* (2011).

If the tree in question will be killed by fire that year, its fire mortality marker is set to true. Otherwise, its fire mortality marker is set to false. Next, the model kills trees that die by fire or through natural death, since in this case, there may be a fire that does not kill all the trees on the plot, but some of the trees that survived the fire may die from age- or stress-related issues. Wind disturbance does not occur when a fire occurs that year.

For each tree on the plot, the model checks to see if it survived the fire and if it survived growth- and age-related stressors. To survive growth-related stressors, the tree has to have a mortality marker of false (determined in the Growth subroutine, based on that tree's DBH

increment growth that year) or it has to pass the random check against growth survival, based on the tree's species-specific stress tolerance. In this case, the model generates a uniformly distributed random number between 0.0 and 1.0 and checks to see if it is less than the variable C_G. This variable ranges from 0.31 to 0.43, depending on the tree species' stress tolerance (ranges from 1 to 5; 1 being tolerant, 5 being intolerant to stress). In this way, even if the tree's mortality marker is set to true, it has a 57 to 69% chance of still surviving, depending on its stress tolerance.

In order to survive age-related stressors, the tree must also pass a random check against age survival. Again, the model generates a uniformly distributed random number between 0.0 and 1.0 and checks to see if it is less than the variable C_O. This age-related check is calculated as:

$$C_O = \varepsilon / AGE_{max} \quad \text{(E.6)}$$

where ε is an input parameter based on that tree species propensity to survive to its maximum age. Higher values of ε denote a lower probability of reaching its maximum age.

If the tree survives age- and growth-related stressors as well as fire, the model copies its attributes, increments the number of trees on the plot for next year by one ($nt = nt + 1$) and calculates the amount of non-thinning litterfall for the year and adds it to the organic layer litter pools. If the tree is a conifer:

$$AO_{Cinto} = AO_{Cinto} + B_{leafC}(b_l - 1.0) \quad \text{(E.7)}$$

$$AO_{Ninto} = AO_{Ninto} + B_{leafC}(b_l - 1.0)/leaf_{CNcon} \quad \text{(E.8)}$$

Otherwise, if the tree is deciduous:

$$AO_{Cinto} = AO_{Cinto} + B_{leafC} \quad \text{(E.9)}$$

$$AO_{Ninto} = AO_{Ninto} + B_{leafC}/leaf_{CNdec} \quad \text{(E.10)}$$

If, however, the tree dies, through age, stress, or fire, the model does not copy its attributes and the model calculates how much carbon and nitrogen the tree puts into the soil. If the tree is a conifer:

$$AO_{Cinto} = AO_{Cinto} + B_{treeC} + B_{leafC} \quad (E.11)$$

$$AO_{Ninto} = AO_{Ninto} + B_{treeC}/stem_{CN} + B_{leafC} b_l / leaf_{CNcon} \quad (E.12)$$

Otherwise, if the tree is deciduous:

$$AO_{Cinto} = AO_{Cinto} + B_{treeC} + B_{leafC} \quad (E.13)$$

$$AO_{Ninto} = AO_{Ninto} + B_{treeC}/stem_{CN} + B_{leafC}/leaf_{CNdec} \quad (E.14)$$

Once the model has finished calculating these values, it moves on to the Renewal subroutine and the number of trees on the plot is updated to be the number of trees that survived fire and stressors that year.

E.1.2. Wind

If, instead, wind disturbance occurs that year (i.e. w_{prob} is less than the site-wide wind probability) all trees are killed on the plot. In this case, there is a three-year lag time before regeneration can start. As such the variable w_{count} is set to 3. Again, fire cannot occur in the same year as wind disturbance. The seedling bank is updated to reflect windthrow effects:

$$Sl_{bank} = Sl_{bank} + s_i + s_p \cdot spp_{avail} \quad (E.15)$$

As all the trees on the plot will be killed by windthrow, the model calculates how much carbon and nitrogen will be added to the soil organic layer from these dying trees. The amount of biomass from leaves (B_{LAI}) that go into the soil is first calculated as:

$$B_{LAI} = 2.0 LAI_{tree} sl_c \quad (E.16)$$

where sl_c is the specific leaf area ratio of the tree. Next, the stem and leaf carbon and nitrogen are added into the organic layer. If the tree is a conifer:

$$AO_{Cinto} = AO_{Cinto} + B_{treeC} + B_{LAI} b_l \quad (E.17)$$

$$AO_{Ninto} = AO_{Ninto} + \frac{B_{treeC}}{stem_{CN}} + \frac{B_{LAI} b_l}{leaf_{CNcon}} \quad (E.18)$$

Otherwise, if the tree is deciduous:

$$AO_{Cinto} = AO_{Cinto} + B_{treeC} + B_{LAI} \quad (E.19)$$

$$AO_{Ninto} = AO_{Ninto} + \frac{B_{treeC}}{stem_{CN}} + \frac{B_{LAI}}{leaf_{CNdec}} \quad (E.20)$$

At this point, the number of trees on the plot is set to 0 as they were all killed by windthrow. The seedling number is also set to 1. This is a plot-level, species-specific value that is equal to 1 if that species' seedling bank is greater than 0.0 and set to 0 if it is not. The model is now finished with the Mortality subroutine and moves on to the Renewal subroutine.

E.2. No disturbances

If no disturbances occur in the year, then the model only checks for age- and growth-related stressors. If the number of trees is greater than 0, then the model loops through and checks for growth and age survival, otherwise the model moves directly to the Renewal subroutine. For each tree on the plot, the model checks to see if the tree survives the growth and age-related checks described above (see section E.1.1). If the tree survives, the model copies its attributes, increments the number of trees on the plot by 1 ($nt = nt + 1$), and then calculates the amount of non-thinning litterfall for the year and adds it to the organic layer litter pools. If the tree is a conifer:

$$AO_{Cinto} = AO_{Cinto} + B_{leafC}(b_l - 1.0) \quad (E.21)$$

$$AO_{Ninto} = AO_{Ninto} + B_{leafC}(b_l - 1.0)/leaf_{CNcon} \quad (E.22)$$

Otherwise, if the tree is deciduous:

$$AO_{Cinto} = AO_{Cinto} + B_{leafC} \quad (E.23)$$

$$AO_{Ninto} = AO_{Ninto} + B_{leafC}/leaf_{CNdec} \quad (E.24)$$

If, however, the tree dies, through age or stress, the model does not copy its attributes and the model calculates how much carbon and nitrogen the tree puts into the soil. If the tree is a conifer:

$$AO_{Cinto} = AO_{Cinto} + B_{treeC} + B_{leafC} \quad (E.25)$$

$$AO_{Ninto} = AO_{Ninto} + B_{treeC}/stem_{CN} + B_{leafC}b_l/leaf_{CNcon} \quad (E.26)$$

Otherwise, if the tree is deciduous:

$$AO_{Cinto} = AO_{Cinto} + B_{treeC} + B_{leafC} \quad (E.27)$$

$$AO_{Ninto} = AO_{Ninto} + B_{treeC}/stem_{CN} + B_{leafC}/leaf_{CNdec} \quad (E.28)$$

Once the model has finished calculating these values, it moves on to the Renewal subroutine and the number of trees on the plot is updated to be the number of trees that survived growth and age stressors that year.

F. Tree Renewal

In Renewal subroutine, the seedling and seed banks for each species are updated and new trees are established on the plots. If the available nitrogen the plot is greater than 0.0 then trees can grow on the site, and the model continues with the Renewal subroutine. Otherwise no trees establish and the soil is updated to reflect N and C inputs and outputs for the year.

F.1. Seed and seedling bank calculations

F.1.1. No windthrow or whole-scale fire disturbance

If windthrow did not occur that year and if there was either no fire at all or only a low- to mid-level fire (i.e. $f_{cat} < 11.0$) then the model makes modifications to the current seedling and

seed banks, and calculates how many trees can be renewed on the plot. First the maximum growth for the plot (g_{max}) is set to 0.0. Then, for each species, the growth cap (g_{cap}) is calculated as:

$$g_{cap} = \min\left(f_{temp}, f_{drought}, f_{nutrient}\right) \quad \text{(F.1)}$$

If there are no trees on the plot, then the seedling regrowth potential (g_R) for that species is set to the growth cap. Otherwise, the model also takes the effect of shading from other trees into account when calculating the regrowth potential for that species:

$$g_R = \min\left(g_{cap}, f_{light}\right) \quad \text{(F.2)}$$

Then, the seedling growth max for the plot is updated as:

$$g_{max} = \max\left(g_{max}, g_R\right) \quad \text{(F.3)}$$

In this way, the g_{max} for the plot is updated as the model goes through each species, so that the plot-wide g_{max} is equal to the g_R of the species with the highest seedling regrowth potential. Finally, if a species' regrowth potential is less than the growth threshold (D_{thresh}; set to 0.03 in the model), then its regrowth is set to 0.0.

Next, the N_{rnew} and N_{rmax} are set up as counters for when new trees are established on the plot. N_{rmax}, the maximum number of trees that can be renewed, is calculated as:

$$N_{rmax} = \min\left((plotsize \cdot g_{max}) - nt, 0.5plotsize\right) \quad \text{(F.4)}$$

where $plotsize$ is the area of the plot (set to 500 m^2 in the model), and nt is the number of trees on the plot. Then, N_{rnew} is calculated as:

$$N_{rnew} = \min\left(\max(N_{rmax}, 3), (plotsize - nt)\right) \quad \text{(F.5)}$$

The model then moves on to calculate the seedling and seed banks for each plot.

If the seedling number for the plot is equal to 0.0:

If the seedling number for the plot is equal to 0.0, then the model first updates the seedbank for each species as:

$$S_{bank} = S_{bank} + s_i + s_{num} \cdot spp_{avail} + s_p \cdot spp_{avail} \quad (F.6)$$

where S_{bank} is the number of seeds in that species' seedbank, s_{num} is a species-specific input parameter that represents the seed numbers from inside the plot (1 for cones, 10 for samaras or maple keys, and 100 for wind-dispersed birch or populous). If the regrowth for that species (g_R) is greater than or equal to the growth threshold (D_{thresh}), then the seeds in that species' seed bank are added to the seedling bank, and the seed bank is set back to 0.0:

$$Sl_{bank} = Sl_{bank} + S_{bank} \quad (F.7)$$

$$S_{bank} = 0.0 \quad (F.8)$$

Otherwise, if g_R is less than D_{thresh}, the seeds in the seedbank do not become seedlings, and the seedbank is reduced based on a species-specific seed reduction parameter:

$$S_{bank} = S_{bank} \cdot s_{surv} \quad (F.9)$$

where s_{surv} is the seedling reduction parameter. Next, the effect of fire on the seedling bank is calculated as in Equation E.1, and then the seedling bank for each species is updated.

$$Sl_{bank} = Sl_{bank} + s_p \cdot spp_{avail} \cdot f_{fire} \quad (F.10)$$

If there was no fire that year, f_{fire} is equal to 1.0, and thus has no effect on the seedling bank. The seedling number for each plot (Sl_N) is calculated as:

$$Sl_N = \max\left(kron(Sl_{bank}), Sl_N\right) \quad (F.11)$$

In this way, the model loops through each species and modifies the plot-wide seedling number each time. If the seedling bank for the species in question is greater than 0.0, then Sl_N takes the maximum of either 1.0 or the current value of Sl_N. If the seedling bank for that species

is less than 0.0, Sl_N is the maximum between 0.0 and Sl_N. Thus, the seedling number for each plot is either 1.0 or 0.0, depending on if any species has a seedling bank greater than 0.0. Next the seedling bank for the species is converted from a per m^2 value to a general plot number value through:

$$Sl_{bank} = Sl_{bank} plotsize \quad (F.12)$$

Finally, the value p_{sum} for the plot is calculated as the sum of each species' seedling bank times its regrowth:

$$p_{sum} = \sum Sl_{bank} g_R \quad (F.13)$$

At this point, the model has finished calculating the seed and seedling banks and moves on to the tree regeneration part of the Renewal subroutine.

If the seedling number for the plot is not equal to 0.0:

If, however, there are currently seedlings on the plot, (i.e. the seedling number for the plot is 1.0), then the model first calculates the p_{sum} as in Equation F.13. Next, the model updates the seed bank and seedling bank for each species. It first updates the seed bank as in Equation F.6.

If a species' regrowth value is greater than or equal to the grow threshold (D_{thresh}) then the seeds in the seed bank germinate into seedlings:

$$Sl_{bank} = Sl_{bank} + S_{bank} \quad (F.14)$$

$$S_{bank} = 0.0 \quad (F.15)$$

Otherwise, the seed bank is reduced as in Equation F.9. Next, the effect of fire on the seedling bank is calculated as in Equation E.1 and then the seedling bank for each species is updated. Again, if there was no fire that year, f_{fire} is equal to 1.0, and thus has no effect on the seedling bank. Finally, the seedling bank for the species is converted from a per m^2 value to a

general plot number value and the seedling number for the plot is calculated as in Equations F.11 and F.12. At this point, the model has completed computing the maximum possible trees that can be renewed and has finished updating the seed banks and seedling banks for each species. It then moves on to the part of the Renewal subroutine where new trees are established on the plot.

F.1.2. Windthrow or whole-scale fire disturbance

If there was windthrow or whole-scale fire disturbance (i.e. $f_{cat} \geq 11.0$) then the model waits 3 (for wind) or 5 (for fire) years before starting the regeneration process. This is achieved using the f_{count} and w_{count} variables, set up when fire or wind disturbance is first initiated. Each year the model checks to see if either counter is equal to 1. If it is not, it subtracts 1 from the counter and sets the plot value p_{sum} to 0.0.

Once either counter reaches 1, the model first computes the growth cap for each species as in Equation F.1 and it then computes p_{sum} as in Equation F.13. Finally, it converts the seedling bank number for each species from the per m^2 value and computes the seedling number value for the plot as in Equations F.11 and F.12.

With this, the model has finished all the different scenarios for computing the seed and seedling banks and the number of trees that can be renewed on the plot. UVAFME then moves on to generating new trees on the plot.

F.2. Regenerating new trees

If p_{sum} for the plot is greater than 0.0, then the model updates the p_{sp} for each species (where p_{sp} was first calculated as $p_{sp} = Sl_{bank} \cdot g_{cap}$). Otherwise, it sets the previously calculated N_{rnew} (see Equation F.5) to 0 and moves on. If p_{sum} is greater than 0.0:

$$p_{sp} = \frac{p_{sp}}{p_{sum}} \quad \text{(F.16)}$$

In effect this takes each species' p_{sp}, which in general corresponds to its potential for regeneration on that plot, and then divides it by the plot-wide sum of p_{sp} (i.e. p_{sum}), converting p_{sp} into a relative potential for regeneration. Next, the model modifies p_{sp} again:

$$p_{sp(s)} = p_{sp(s-1)} + p_{sp(s)} \quad \text{(F.17)}$$

where s is an index for species. This in effect converts p_{sp} of each species to a cumulative relative potential for regeneration. Next, the model checks to see if N_{renew} is greater than or equal to 1. If it is, the model moves to regenerate trees on the plot. If it is less than 1, the model does not regenerate new trees and moves to the final step in the modeling process for the year. If N_{renew} is greater than or equal to 1, then the model creates N_{renew} new trees on the plot. This is achieved through a random number calling the species of each new tree (modified by p_{sp} so that species with a higher p_{sp} will contribute more new trees than species with a low p_{sp}), and another random number generating the starting DBH of each new tree.

Once a new tree is set to be placed on the plot, the seedling bank for the species of tree that was called is reduced by one. The DBH for each new tree is determined through a normally distributed random number (with a mean of 0.0 and a standard deviation or 1.0) between 0.5 and 2.5. Once the new diameter of the tree is determined, the clear branch bole height of the tree is set to 1 m, and then the total tree height, diameter at clear branch bole height, C and N biomass, and leaf biomass are determined based on Equations D.16, D.18, D.24, D.25, and D.2. Next, the NPP, N_{used}, and litter inputs for the plot are updated. If the tree is a conifer:

$$NPP = NPP + B_{leafC} \cdot l_B + B_{treeC} \quad \text{(F.18)}$$

$$N_{used} = N_{used} + \frac{B_{leafC}}{leaf_{CNcon}} + B_{treeN} \quad \text{(F.19)}$$

$$AO_{Cinto} = AO_{Cinto} + B_{leafC}(l_B - 1.0) \quad \text{(F.20)}$$

$$AO_{Ninto} = AO_{Ninto} + B_{leafC}(l_B - 1.0)/leaf_{CNcon} \quad (F.21)$$

Otherwise, if the tree is deciduous:

$$NPP = NPP + B_{leafC} + B_{treeC} \quad (F.22)$$

$$N_{used} = N_{used} + \frac{B_{leafC}}{leaf_{CNcdec}} + B_{treeN} \quad (F.23)$$

$$AO_{Cinto} = AO_{Cinto} + B_{leafC} \quad (F.24)$$

$$AO_{Ninto} = AO_{Ninto} + B_{leafC}/leaf_{CNdec} \quad (F.25)$$

With this, the model has completed regenerating new trees and updates the number of trees on the plot to reflect the new trees added. Finally, it updates the seedling bank for each species by multiplying the current number of seedlings by a species-specific input parameter that corresponds to annual seedling percent survival (sl_{surv}). The model also converts the seedling bank back to a per m^2 value.

$$Sl_{bank} = Sl_{bank} \cdot sl_{surv}/plotsize \quad (F.26)$$

Finally, the model calculates the plot-level remaining nitrogen using the N_{used} and N_{avail} variables that were calculated throughout the simulation:

$$N_{remain} = N_{avail} - N_{used} \quad (F.27)$$

If the remaining nitrogen is greater than 0.0, the amount of nitrogen going into the organic layer from the A layer is calculated as

$$AO_{Nflux} = N_{remain}(\min\left(\frac{R}{1000.0}, 0.1\right)) \quad (F.28)$$

where R is the runoff for the plot that year. Next, the model updates the nitrogen content of the A layer:

$$A_{N0} = A_{NO} + N_{remain} - AO_{Nflux} \quad (F.29)$$

If N_{remain} was calculated to be 0.0 or lower, the nitrogen flux into the organic layer is 0.0 and the new nitrogen content for the A layer is:

$$A_{N0} = A_{N0} + N_{remain} \quad (F.30)$$

Next, the nitrogen content of the A layer is modified based on the runoff for that year:

$$A_{N0} = A_{NO} - 0.00002R \quad (F.31)$$

The carbon content of the A layer is also modified using the amount of nitrogen that was transferred to the organic layer.

$$A_{C0} = A_{C0} - 20.0AO_{Nflux} \quad (F.32)$$

Next, carbon and nitrogen for the B layer is updated:

$$B_{C0} = B_{C0} + 20.0AO_{Nflux} \quad (F.33)$$

$$B_{N0} = B_{N0} + AO_{Nflux} \quad (F.34)$$

Finally, the N and C from the litter collected is added to the organic layer:

$$AO_{C0} = AO_{C0} + AO_{Cinto} \quad (F.35)$$

$$AO_{N0} = AO_{N0} + AO_{Ninto} \quad (F.36)$$

With these calculations, the model has finished its simulations for the year and moves on to the next year.

References

Keane, R. E., R. A. Loehman, and L. M. Holsinger. 2011. The FireBGCv2 Landscape Fire Succession Model: A research simulation for exploring fire and vegetation dynamics. USDA Forest Service General Technical Report RMRS-GRR-55:145.

Reinhardt, E., and N. Crookston, editors. 2003. The fire and fuels extension to the forest vegetation simulator. Gen. Tech. Rep. RMRS-GTR-116. Ogden, UT: Department of Agriculture, Forest Service, Rocky Mountain Research Station: 209.

Ryan, K.C., and E.D. Reinhardt. 1988. Predicting Postfire Mortality of Seven Western Conifers. Canadian Journal of Forest Research 18: 1291-1297.

Van Wagner, C. E. 1973. Height of crown scorch in forest fires. Canadian Journal of Forest Research. 3: 373-378.